Electronic Thesis and Dissertation Repository

8-23-2013 12:00 AM

A Micro-CT Analysis of the Hominoid Subnasal Anatomy

Arthur M. Klages
The University of Western Ontario

Supervisor
Dr. Andrew Nelson
The University of Western Ontario

Graduate Program in Anthropology

A thesis submitted in partial fulfillment of the requirements for the degree in Master of Arts

© Arthur M. Klages 2013

Follow this and additional works at: https://ir.lib.uwo.ca/etd

Part of the Biological and Physical Anthropology Commons

A MICRO-CT ANALYSIS OF THE HOMINOID SUBNASAL ANATOMY

Monograph

by

Arthur <u>Klages</u>

Graduate Program in Anthropology

A thesis submitted in partial fulfillment
of the requirements for the degree of
Master of Arts in Bioarchaeology and Archaeology

The School of Graduate and Postdoctoral Studies
The University of Western Ontario
London, Ontario, Canada

Abstract

This thesis conducted a micro-CT analysis of extant hominoid subnasal anatomy and a review of the subnasal anatomy of the Miocene hominoids. This thesis tested the hypothesis that the extant hominoids exhibit diagnostic morphological patterns of the subnasal anatomy that are phylogenetically informative. The terminology of the subnasal anatomy was revised and new measurements were constructed to analyze the morphology of the hominoid subnasal anatomy. It is suggested that previous analyses of the hominoid subnasal anatomy were limited by technological constraints, poorly constructed measurements, and ambiguous terminology. This micro-CT analysis confirmed that the extant hominoids do exhibit diagnostic patterns of their subnasal morphology and that these patterns are indeed phylogenetically informative. A new character state was also discovered that differentiated extant cercopithecoids from extant hominoids. The extant hominids exhibit a shared derived subnasal morphology, while *Pongo* exhibits the most diagnostic and derived morphological pattern among the extant hominoids.

Keywords

Acknowledgments

Table of Contents

List of Figures

1 Introduction, Research Objectives, and Research Questions

1.1 Introduction to the Miocene Hominoids

The extant African and Asian great apes, relict members of the two surviving hominid subfamilies, preserve only a small fraction of the biological and geographic diversity exhibited by the Miocene hominoids (Bilsborough and Rae, 2007; Harrison, 2010). During the Miocene epoch, 23 to 5 mya, hominoids ranged across Eurasia and Africa—from Spain in the west, to Thailand in the east, and to Namibia in the south—while the extant great apes are now restricted to tropical forest refugia in sub-Saharan Africa, and the islands of Borneo and Sumatra (Begun, 2007; Begun et al., 2012; Koufos, 2007).

The past two decades have seen a wealth of fossil Miocene Eurasian hominoid discoveries and major taxonomic revisions of the Miocene hominoids (Begun, 2007; Koufos, 2007; Begun, 2010; Alba, 2012; Begun et al., 2012). (Indeed the taxonomy of the family *Hominidae* has also been revised). However, the phylogenetic relationships of the Miocene hominoids and the origins of the African hominines remain contested in paleoanthropology, in spite of, or perhaps in part due, to these additional fossil discoveries (Pilbeam, 2002; Moyà-Solà et al., 2004; 2009; Begun, 2010; Begun et al., 2012; Alba, 2012). One cause of the uncertainty in hominoid phylogeny is the paucity of the Africa fossil record after 13 mya (Begun, 2010; Begun et al., 2012). While a small number of African hominoid fossils have been discovered recently in the 10 to 9 mya period (see: Kunimatsu et al., 2007; Suwa et al., 2007; Bernor, 2007), the small sample size and the fragmentary nature of the fossils has not adequately resolved the issue of the origin of the African hominines (Begun, 2010; Begun et al., 2012). The dearth of African hominoids has lead researchers to postulate that either a Eurasian Miocene hominoid migrated back to Africa to give rise to the extant African hominines (Begun, 2007; 2010; Begun et al., 2012) or that hominoids have had a continual presence in Africa and their fossils await discovery (Cote, 2004; Bernor, 2007; Harrison, 2010).

1.2   Phylogenetic Systematics

Another reason for the uncertainties surrounding the phylogeny of the Miocene hominoids and the origin of the African hominines arises from conflicting interpretations of fossil material (see: Pilbeam, 2002; Moyà-Solà et al., 2004; 2009; Begun, 2007; 2010; Alba, 2012; Begun et al., 2012; Pérez de los Ríos et al., 2012). Hominoid phylogenies are typically generated following the rules of phylogenetic systematics or cladistics (cf. Wiley and Lieberman, 2011). Clades of related taxa are constructed based on the presence of shared derived characters called synapomorphies and the most parsimonious arrangements of clades are interpreted to represent the most likely evolutionary relationships of these taxa (Wiley and Lieberman, 2011). However, the validity of a phylogeny relies on the proper assessment of the characters and the character states employed in the analysis (Wiley and Lieberman, 2011). It is clear from the literature that even when researchers employ similar characters in their phylogenetic analyses, they do not agree on the interpretations of these characters or their character states (Pilbeam, 2002; Moyà-Solà et al., 2004; 2009; Begun, 2007; 2010; Alba, 2012; Begun et al., 2012; Pérez de los Ríos et al., 2012). Comparative analyses of fossil material are also hindered by the absence of well-defined and consistently applied methodological approaches, terminologies, and measurements (see: Pilbeam, 2002; Brown et al., 2005; Bilsborough and Rae, 2007).

1.3   The Morphology of the Hominoid Subnasal Anatomy

One "character" that is considered by researchers to be reliable, phylogenetically informative, and that is widely employed in the construction of phylogenies is the morphology of the subnasal anatomy (Robinson, 1954; Ward and Kimbel, 1983; McCollum et al., 1993; Brown et al., 2005: Begun, 2007; Bilsborough and Rae, 2007). This "character" is in fact a complex comprised of a number of characters which have been the subject of analysis in both extant and fossil hominoids (Ward and Kimbel, 1983; McCollum et al., 1993; McCollum and Ward, 1997). The morphology of the subnasal anatomy is considered to be highly diagnostic of the extant hominine and pongine subfamilies and its evolution has been observed in the Miocene fossil record (Ward and Kimbel, 1983; McCollum et al., 1993; McCollum and Ward, 1997; Brown et al., 2005; Begun, 2007; Bilsborough and Rae, 2007).

The morphology of the subnasal anatomy and its phylogenetic significance was the focus of studies conducted in the 1980's and 1990's by Ward and Kimbel (1983), McCollum et al., (1993), and McCollum and Ward (1997). However, these studies relied on early CT technology (Ward and Kimbel, 1983) and imprecise radiographic techniques to analyze the largely internal morphology of the subnasal anatomy (McCollum et al., 1993; McCollum and Ward, 1997). It is also apparent that the terminology, measurements, and characters employed in the analysis of the hominoid subnasal anatomy could be substantially improved. A review of the fossil subnasal anatomy of the Miocene hominoids suggested that important aspects of the subnasal anatomy were poorly defined and characters were possibly misunderstood by researchers which could have affected the interpretation of these characters in fossil specimens.

1.4 Micro-CT Analysis of the Hominoid Subnasal Anatomy

This thesis addresses the technological and methodological limitations of previous studies by undertaking a micro-CT analysis of the hominoid subnasal anatomy. Twenty-nine primate crania were scanned with a micro-CT scanner at the Sustainable Archaeology facility in London, Ontario, and their subnasal anatomy was reconstructed for a quantitative analysis.

The advent and availability of micro-CT scanning technology and three-dimensional reconstruction software provided an opportunity to revisit analyses of the subnasal anatomy with unprecedented precision. Micro-CT imaging technology has revolutionized paleoanthropology, facilitating the reconstruction of fragmentary craniofacial material and the generation of three-dimensional models and cross-sectional views of the entire cranium, including the internal anatomy (Zollikofer et al., 1998; Ulhaas, 2007). Micro-CT imaging permits the internal morphology of the hominoid subnasal anatomy to be visualized uninhibited by the surrounding skeletal elements and allows precise measurements and observations to be performed on sections through the subnasal anatomy. As the morphology of the hominoid subnasal anatomy is both largely internal and as it is considered to be a phylogenetically informative "character" in paleoanthropology, the morphology of the hominoid subnasal anatomy is a valid candidate for a micro-CT analysis.

1.5   Research Objectives and Research Questions

This thesis will address a number of research objectives. First, previous analyses of the morphology of the subnasal anatomy will be reviewed in order to identify their limitations due to technology or methodological construction. Second, an extensive review and synthesis of the fossil record of the subnasal anatomy in Miocene hominoids, including clear identifications of fossil specimens, will be provided in order to elucidate what is known about its morphology and evolution in one convenient source. The lack of clear identification of specimens combined with frequent taxonomic revisions complicates the reading of the literature on the Miocene hominoid subnasal anatomy, a problem this synthesis aims to address. Third, it will revise the terminology used to describe the subnasal anatomy in a logical and consistent manner. If the subnasal anatomy is to be analyzed there can be no ambiguity with regard to what aspects are under discussion. It is hoped that this revised terminology will set the standard for future analysis of the hominoid subnasal anatomy. Fourth, it will provide an improved quantitative methodology to capture and analyze the hominoid subnasal anatomy based on the use of micro-CT imaging technology. Finally, this thesis will address the following research question: are the descriptions of the subnasal anatomy and the diagnostic patterns identified in literature accurate?

1.6   Research Hypotheses

This thesis will analyze the morphology of the hominoid subnasal anatomy by utilizing micro-CT imaging in order to examine the characters and morphological patterns of the subnasal anatomy that are used to identify the extant hominoids in paleoanthropology. In doing so, this thesis will test two hypotheses regarding the morphology of the subnasal anatomy. The micro-CT analysis will first test the hypothesis of McCollum et al. (1993) and McCollum and Ward (1997) that the extant hominoids *Hylobates*, *Gorilla*, *Pan*, *Homo*, and *Pongo*, exhibit diagnostic morphological patterns of the subnasal anatomy and that these patterns are phylogenetically informative. Second, the micro-CT analysis will test the hypothesis of McCollum and Ward (1997) that in the earliest stages of ontogeny the morphology of the subnasal anatomy is not phylogenetically informative.

It is hypothesized that a new methodology based on the use of micro-CT imaging technology will refine the analysis of the hominoid subnasal anatomy and by addressing this research

question, this thesis will contribute to an improved, and possibly revised, understanding of the hominoid subnasal anatomy and the phylogeny and evolution of the Miocene hominoids. The methodology outlined will provide a basis for future analyses of the hominoid subnasal anatomy that should include an expansion of the sample size to examine statistically relevant intraspecific comparisons and interspecific variation and the application of this methodology to a reanalysis of the Miocene hominoid fossil record.

1.7   Chapter Outlines

This introductory chapter has defined the objectives and research questions of this thesis. Chapter Two defines the skeletal elements of the hominoid subnasal anatomy and provides a revised, logical, and precise terminology to describe its anatomy. Chapter Three critically examines previous analyses of the hominoid subnasal anatomy, including their methodological and technological limitations. Chapter Four describes and reviews what is known about the subnasal anatomy of the extant hominoids. Chapter Five is an extensive review and synthesis of all Miocene hominoids for which the subnasal anatomy is represented in the fossil record. Chapter Six outlines the material and methods used in this thesis, including the micro-CT scanning methodology, and provides precise definitions of all measurements and ratios employed in this analysis. Chapter Seven outlines the results obtained in the analysis of the hominoid subnasal morphology. Chapter Eight discusses these results and their phylogenetic implications in detail. Chapter Nine summarizes the conclusions reached from this review and micro-CT analysis of the morphology of the hominoid subnasal anatomy and suggests a course for future analyses.

The appendices include full descriptions of the primate individuals employed in this analysis, the raw data generated by the micro-CT analysis, the quantitative results generated in this analysis, the measurements of the primate subnasal anatomy on micro-CT generated sagittal sections, the micro-CT scanning parameters employed in this analysis, the results of intra-observer error testing, and a description of the mounting of individual crania for micro-CT scanning.

2 The Skeletal Elements and Terminology of the Hominoid Subnasal Anatomy

2.1 Terminology of the Subnasal Anatomy

Before undertaking an analysis or a review of the hominoid subnasal anatomy, it is important to properly define and understand the skeletal elements, and the terminology used to describe them. A review of the relevant literature revealed that analyses of subnasal anatomy are complicated by the use of discrepant terminology (see: Ward and Kimbel, 1983; McCollum et al., 1993; McCollum and Ward, 1997; Brown et al., 2005; Begun, 2007; Bilsborough and Rae, 2007). In this thesis an attempt has been made to clearly define appropriate terminology and apply it consistently to the analysis of the morphology of the subnasal anatomy. It should be noted that all images of the primate subnasal anatomy presented in this thesis were taken from micro-CT (μ-CT) reconstructions of primate crania generated using VGStudio MAX imaging software.

In previous discussions, the subnasal anatomy has been referred to as the "subnasal alveolar morphology" (Ward and Kimbel, 1983; Brown et al., 2005), the "subnasal/premaxillary morphology," the "premaxillary morphology," (Ward and Kimbel, 1983) the "subnasal morphology" (Ward and Kimbel, 1983; McCollum and Ward, 1993) and the "subnasoalveolar anatomy" (McCollum and Ward, 1997).

In this thesis, the term "subnasal anatomy" will be used to refer to the skeletal elements that form the floor of the nasal cavity (and the roof of the oral cavity) and those that lie inferiorly and anteriorly to it, excluding the dentition. These elements primarily include the premaxillae (or the anterior alveolar processes of the maxillae), the palatine processes of the maxillae, and the horizontal plates of the palatine bones (see: Figure 1 and Figure 2) (Ward and Kimbel, 1983; McCollum et al., 1993; White and Folkens, 2000; Schwartz, 2007; Lieberman, 2011). The prevomer and vomer may also be considered elements of the subnasal anatomy (White and Folkens, 2000; Schwartz, 2007).
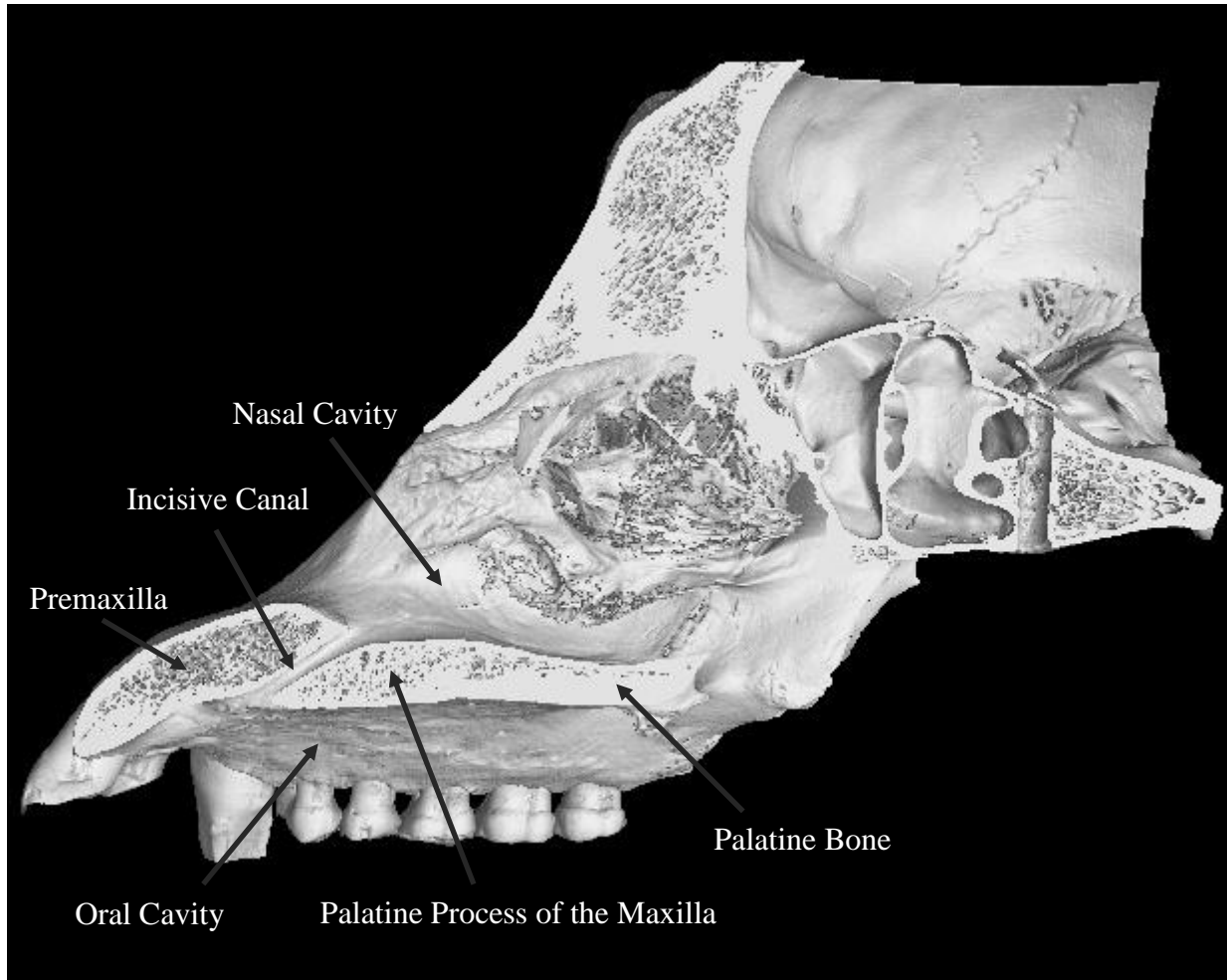
Figure 1 Subnasal Terminology (μ-CT of adult male *G. gorilla*, lateral view)

2.2 The Premaxillae/Anterior Alveolar Processes

The premaxillae in primates are paired elements that form the anterior portion of the hard palate containing the dental alveoli for the incisors and possibly the mesial half of the canine alveoli (see: Figure 1) (Begun, 2007; Lieberman, 2011). Among the non-human primates the premaxillae are typically discrete skeletal elements exhibiting patent premaxillomaxillary sutures throughout adulthood, although the nasal aspect of the premaxillomaxillary sutures tend to fuse during adulthood in hominoids and this fusion can be used as a method of aging individuals (McCollum and Ward, 1997; Swindler and Curtis, 1998; Bilsborough and Rae, 2007; Lieberman, 2011). However, the oral aspects of the premaxillomaxillary sutures are observable into the adult life of most primates (Swindler and Curtis, 1998).
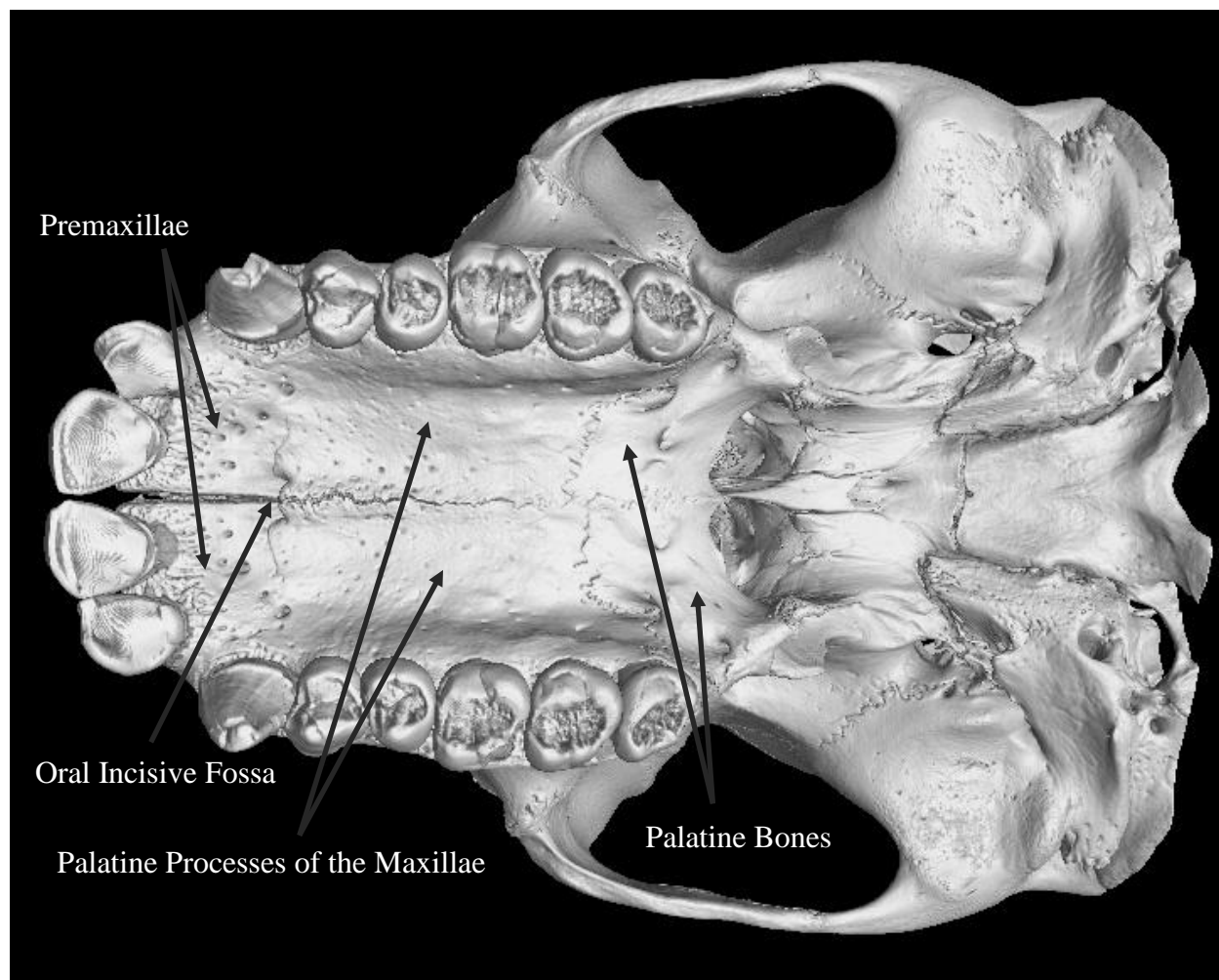
Figure 2 Subnasal Terminology (µ-CT of juvenile male *P. troglodytes*, inferior view)

In *Homo sapiens* the presence or absence of distinct premaxillary skeletal elements has been long debated among skeletal biologists (cf. McCollum and Ward, 1997). The premaxillae are not typically treated as discrete skeletal elements and the equivalent skeletal region is often referred to as the anterior alveolar processes of the maxillae (Ward and Kimbel, 1983; White and Folkens, 2000; Bilsborough and Rae, 2007; Schwartz, 2007; Lieberman, 2011). In fact, Vesalius demonstrated that Galen had studied monkeys when conducting dissections of cranial anatomy as Galen noted the presence of discrete premaxillae elements in humans (Swindler and Curtis, 1998). Studies of nasomaxillary ossification in human embryos revealed the "premaxillae" are generated from the intermaxillary secondary ossification centers of the maxillae (Sperber, 1989; McCollum and Ward, 1997). These "intermaxillae" are homologous to the premaxillae of other primates in that they hold the upper incisors and form the anterior portion of the hard palate

(Sperber, 1989; McCollum and Ward, 1997). The "intermaxilla" generally fuses with the maxilla during ontogeny and superficial evidence of its patency is obliterated (McCollum and Ward, 1997; Swindler and Curtis, 1998). However, the boundary between the "intermaxilla" and maxilla is often discernible at birth and these sutures can be observable up to five years of age (Swindler and Curtis, 1998). The presence of the "intermaxilla" was often distinguishable here from the rest of the maxillae in the micro-CT visualizations used in this thesis. This thesis will use the term "premaxillae" to refer to those elements in the non-human primates and the term "anterior alveolar processes" to refer to the homologous regions of the maxillae in *H. sapiens*.

The literature often refers to a portion of the premaxillae as the nasoalveolar clivus, although this term is typically poorly defined, or even undefined and is not commonly found in anatomical literature (see: Brown et al., 2005; Begun, 2007; Bilsborough and Rae, 2007). The nasoalveolar clivus is defined as the section of the premaxillae/anterior alveolar processes between the inferior margin of the nasal aperture and the alveolar processes of the incisors (Mai et al., 2005; Wood, 2013). In this study the term nasoalveolar clivus is avoided for clarity as it is nearly synonymous with the premaxillae/anterior alveolar processes and is often employed in such a manner (cf: Begun, 2002; 2007; Kelley, 2002; Brown et al., 2005; Bilsborough and Rae, 2007).

2.3   The Palatine Processes of the Maxillae

The term "hard palate" is often misapplied in discussions of the subnasal anatomy (see: Ward and Kimbel, 1983; McCollum et al., 1993; McCollum and Ward, 1997; Brown et al., 2005; Begun, 2007; Bilsborough and Rae, 2007). When authors use hard palate in this context, they are referring to the palatine processes of the maxillae. However, the hard palate refers the bony elements that separate the oral cavity from the nasal cavity and form the roof of the mouth in mouth in most mammals. Thus, the hard palate consists of the premaxillae, the palatine processes of the maxillae, and the horizontal plates of the palatines (see: Figure 1 and Figure 2) (White and Folkens, 2000; Brown et al., 2005; Schwartz, 2007). (Anatomically, the "palate" is separated into the anterior "hard" or bony palate and the posterior "soft" or fleshy palate, although only the hard palate is relevant to this micro-CT analysis [Mai et al. et al., 2005; Schwartz, 2007; Wood, 2013]). Therefore, the use of the term "hard palate" in discussions of the subnasal anatomy is both incorrect and misleading in many contexts. This thesis will use the

term "palatine processes" when referring specifically to the palatine processes of the maxillae to avoid confusion (see: Figure 1 and Figure 2).

2.4   The Nasal and Oral Cavities

The terms "nasal cavity" and "oral cavity" will be used to refer to those cavities that lie superior or inferior to the nasal floor, respectively (see: Figure 1).   A focus of this thesis is the morphology of a passageway found on the midline of the anterior portion of the hard palate that communicates between the oral and nasal cavities, providing passage for blood vessels and nerves (Kimbel, 1983; Mai, 2007; Wood, 2013).

2.5   Terminology of the Anterior Passageway of the Hard Palate/Subnasal Anatomy

As the various terminologies used to describe this anterior passageway through the hard palate in the literature are often misleading or incorrectly applied, this thesis attempts to clarify the description of this passageway by employing a revised and consistent terminology.   The passageway through the anterior hard palate in the nasal cavity floor is variously referred to as an: "incisive canal," "true incisive canal," "incisive foramen," "incisive fenestra," "palatal fenestra," or "incisive fossa" (see: Ward and Kimbel, 1983; McCollum et al., 1993; McCollum and Ward, 1997; Brown et al., 2005; Begun, 2007; Bilsborough and Rae, 2007).   These terms are sometimes used synonymously, sometimes contradictorily, and most often ambiguously.   Herein, these terms will be precisely defined and rigorously applied.   For clarity, this new terminology will be used in the literature review, even if it differs from the original author's usage.

2.6   The Nasal and Oral Incisive Fossae

As mentioned above, the oral and nasal cavities are connected by a passageway that requires an appropriate terminology.   In the majority of primates, this passageway is typically bisected by a bony nasal septum formed by the prevomer and/or vomer resulting in paired openings through the hard palate (cf. Ward and Kimbel, 1983; Bilsborough and Rae, 2007).   In the literature, the superior and inferior ends of these paired openings are sometimes referred to as the "nasal incisive fossae" and "oral incisive fossae" respectively (see: Ward and Kimbel, 1983; McCollum

et al., 1993; McCollum and Ward, 1997; Brown et al., 2005; Begun, 2007; Bilsborough and Rae, 2007). However, the term "incisive fossae" is often used in reference to only the nasal incisive fossae, although this is not made explicit (see: Figure 2 and Figure 3) (see: Ward and Kimbel, 1983; McCollum et al., 1993; McCollum and Ward, 1997; Brown et al., 2005; Begun, 2007; Bilsborough and Rae, 2007). Conversely, the term "incisive fossae" is sometimes employed to describe the entirety of the passageways between the nasal and oral cavities, typically when an individual exhibits a "fenestrated" hard palate (see: Ward and Kimbel, 1983; McCollum et al., 1993; McCollum and Ward, 1997; Brown et al., 2005; Begun, 2007; Bilsborough and Rae, 2007). However, this last instance is a misuse of the term "fossa". By definition, a fossa (plural fossae) is a depression or hollow in the bone ("fossa" comes from *Latin*, meaning "ditch" or "trench") (White and Folkens, 2000; Mai et al., 2005; Schwartz, 2007). Typical fossae in anatomy are the sella turcica, the glenoid fossa, or the mandibular fossa (White and Folkens, 2000; Mai et al., 2005; Schwartz, 2007).
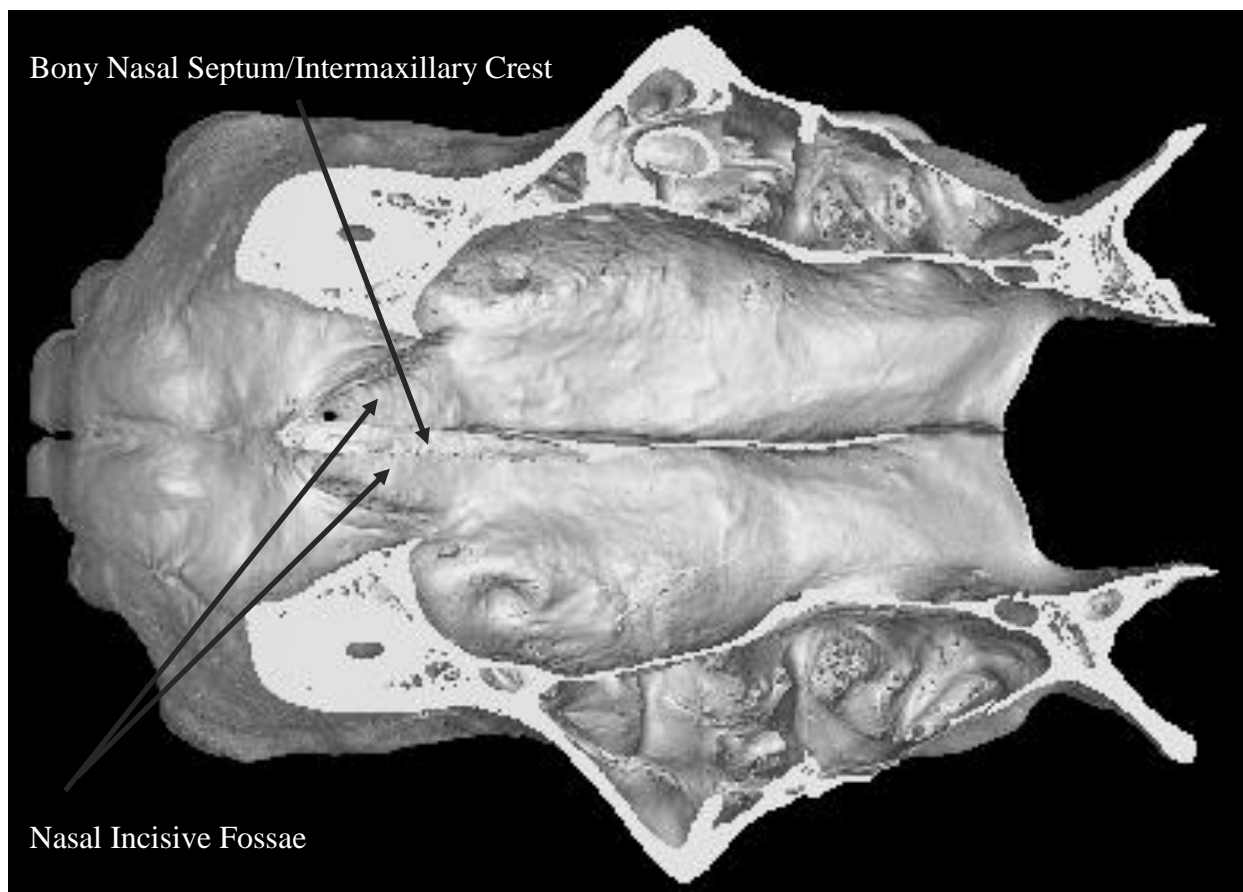
Figure 3 Nasal Incisive Fossae and Bony Nasal Septum (μ-CT of *G. gorilla*, superior view)

By this definition, the term fossa should be used to define only the depression or hollow surrounding the opening of the passageway in the subnasal anatomy. This opening does typically take the shape of a depression, especially in the floor of the nasal cavity. In this thesis the depressions in the floor of the nasal cavity will be referred to as the "nasal incisive fossae" (see: Figure 3) while the corresponding depressions in the oral cavity will be referred to as the "oral incisive fossae" (see: Figure 2).

2.7   The Incisive Foramina

Similar to the misapplication of the term incisive fossae, the literature often refers to the "incisive foramen" to either describe openings of the passageways in the subnasal anatomy or to describe the entirety of the passageway itself (see: Ward and Kimbel, 1983; McCollum et al., 1993; McCollum and Ward, 1997; Brown et al., 2005; Begun, 2007; Bilsborough and Rae, 2007). By definition, a foramen (plural foramina) is a hole, opening, or passage from one part of the body to another, such as the foramen magnum or the obturator foramen (White and Folkens, 2000; Mai et al., 2005; Schwartz, 2007; Wood, 2013). A foramen typically allows the passage of muscles, nerves, veins, or arteries through bone (Mai et al., 2007; Schwartz, 2007; Wood, 2013). In the majority of non-hominid primates and a number of fossil hominoids, a simple incisive foramen connects the oral and nasal cavities (Brown et al., 2005; Begun, 2007; Bilsborough and Rae, 2007). In this case, the incisive foramen can also be referred to as a palatal fenestra, and the hard palate is said to be "fenestrated." As the passageway in the subnasal anatomy is typically partitioned to some degree by a bony nasal septum consisting of the prevomer and/or vomer in most primates, this thesis will refer to these passageways as the "incisive foramina" (see: Figure 4 and Figure 5). The incisive foramina thus terminate superiorly in the nasal incisive fossae and inferiorly in the oral incisive fossae.
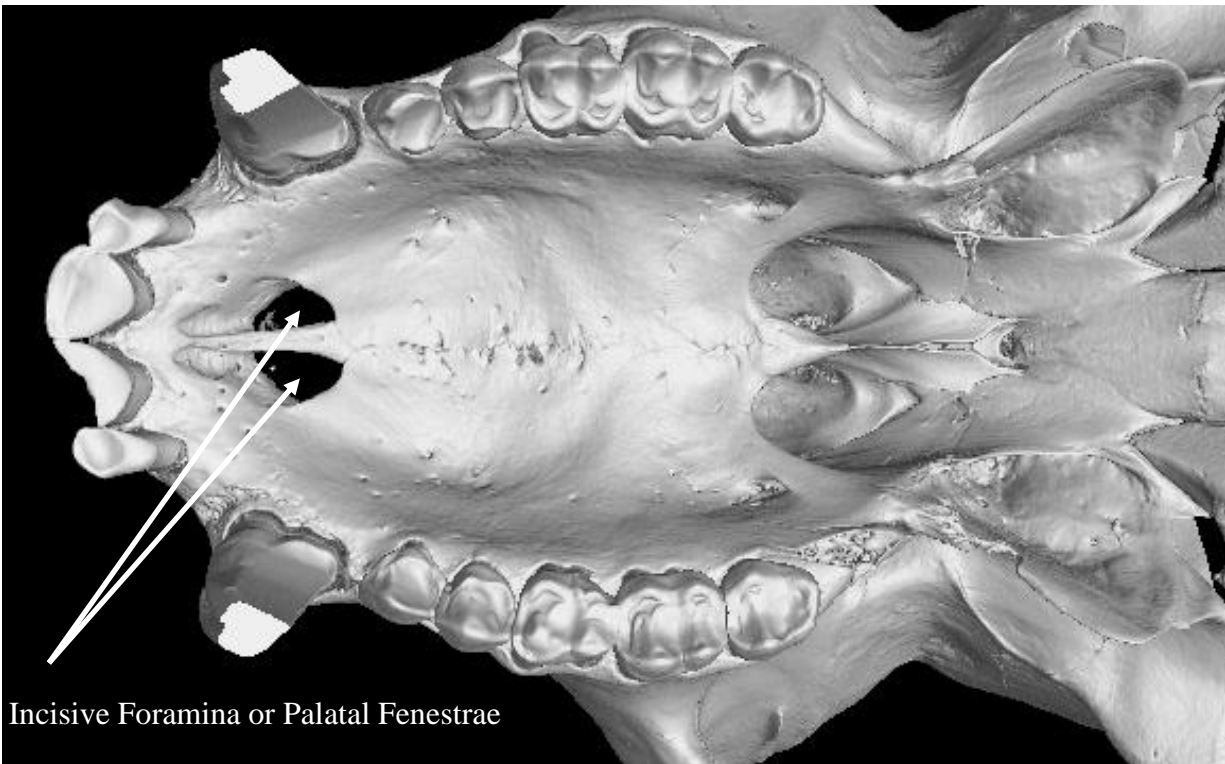
Figure 4 Incisive Foramina/Palatal Fenestrae (µ-CT of male *M. mulatta*, inferior view)
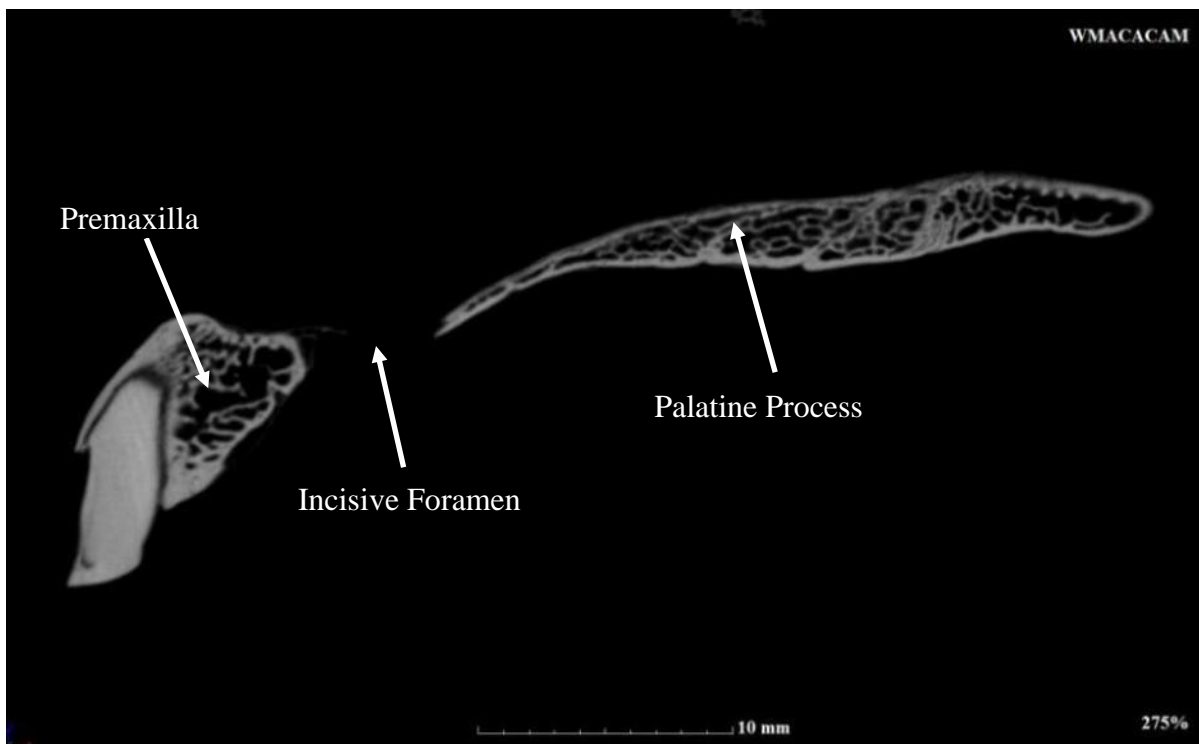
Figure 5 µ-CT Section through an Incisive Foramen (adult male *M. mulatta*, lateral view)

2.8   The Incisive Canal

In the extant hominids and some Middle and Late Miocene hominoids, the literature describes the passageway through the hard palate as an "incisive canal," although the term is never clearly defined (see: Ward and Kimbel, 1983; McCollum et al., 1993; McCollum and Ward, 1997; Brown et al., 2005; Begun, 2007; Bilsborough and Rae, 2007). There is often disagreement whether a particular individual exhibits a "true incisive canal" or not, without mention of what makes an incisive canal "true" (see: Ward and Kimbel, 1983; McCollum et al., 1993; McCollum and Ward, 1997; Brown et al., 2005; Begun, 2007; Bilsborough and Rae, 2007).
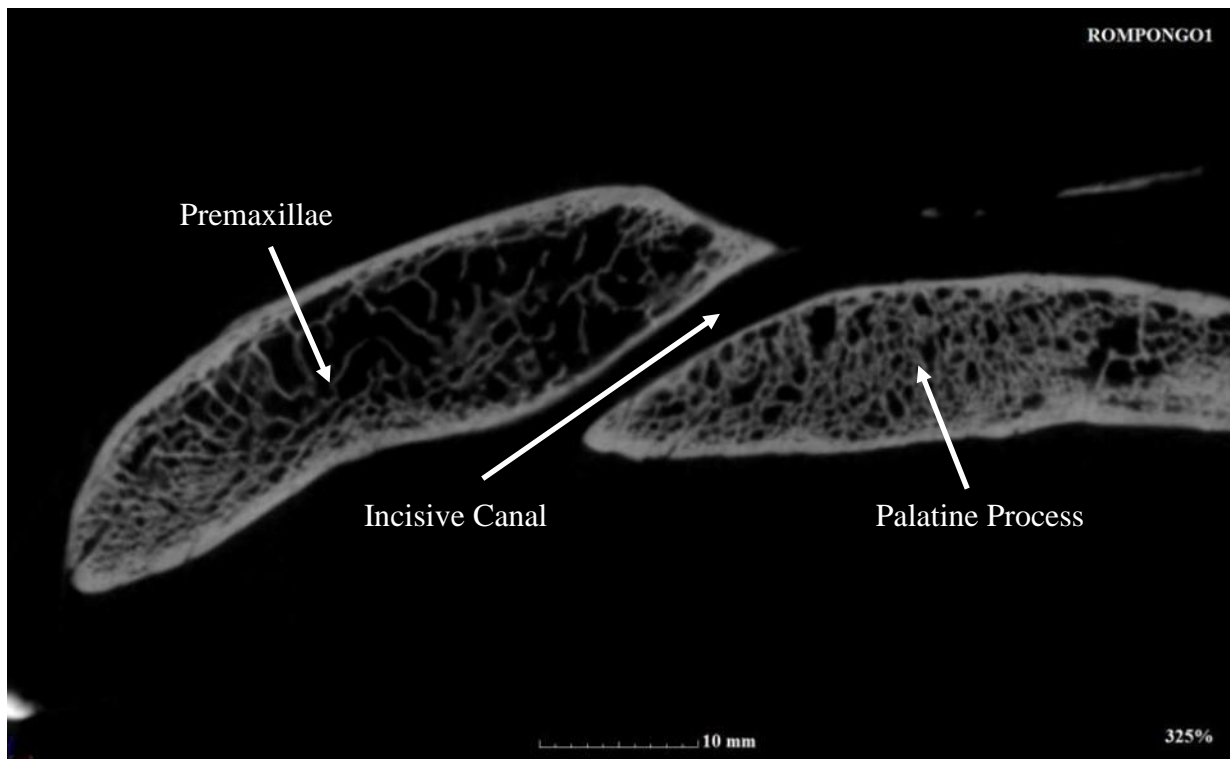
Figure 6 μ-CT Section through an Incisive Canal (adult male *P. abelii*, lateral view)

To avoid further ambiguity regarding the term "incisive canal," this thesis will only apply this term to a particular configuration of the passageway between the nasal and oral cavities (see: Figure 6). Instead of simple incisive foramina communicating between the two cavities, the extant hominids are said to exhibit an "overlap" of the palatine processes by the premaxillae resulting in an angled "canal" connecting the two cavities (McCollum et al., 1993; McCollum

and Ward, 1997). Only those individuals that exhibit an "overlap" of the palatine process by the posterior pole of the premaxilla (or anterior alveolar process) will be said to exhibit an "incisive canal" or "incisive canals" (see: Figure 6). The passageways in those individuals that do not exhibit an overlap of palatine processes by the premaxillae will be referred to as "incisive foramina," or "palatal fenestrae" (see: Figure 4 and Figure 5) ("fenestra" from *Latin*, meaning "window"). The "palatal fenestrae" would be recognizable as a pair of distinct holes through the hard palate in an inferior view of a cranium oriented in the Frankfurt Horizontal Plane (see: Figure 4).

2.9   The Intermaxillary Crest and the Bony Nasal Septum

The intermaxillary crest (see: Figure 3) is formed by a combination of the premaxilla/anterior alveolar process, the prevomer and vomer and runs anteroposteriorly along the midline of the nasal cavity floor partially partitioning the nasal cavity (McCollum and Ward, 1997). The base of the intermaxillary crest is also partly formed from portions of the superior surface of the palatine processes of the maxillae and horizontal plates of the palatines (McCollum and Ward, 1997).

As mentioned, the incisive foramen is often partitioned by components of the bony nasal septum, consisting of the anterior portion of the intermaxillary crest, typically formed by components of the prevomer, vomer, and the premaxillary/anterior alveolar processes in many primate taxa (see: Figure 3) (McCollum and Ward, 1997). The bony nasal septum may invade into the incisive foramen or incisive canal, fully partitioning them into two distinctive channels, resulting in two incisive foramina or "incisive canals", or the bony nasal septum may not invade or partition the incisive foramen or incisive canal, as is often observed in *Pongo* (Ward and Kimbel, 1983; McCollum and Ward, 1997).

It should be apparent that the understanding of the hominoid subnasal anatomy will be improved by the utilization of a standardized terminology, which this thesis attempts to provide. Using the terminology and understanding of the subnasal anatomy outlined in this chapter, this thesis will now undertake a critical review of the previous analyses of the hominoid subnasal anatomy.

3 Previous Analyses of the Hominoid Subnasal Anatomy

Previous analyses of the hominoid subnasal anatomy by Robinson (1953; 1954), Ward and Kimbel (1983), McCollum et al. (1993), and McCollum and Ward (1997) are summarized and critically assessed below. These analyses serve as a starting point for the micro-CT analysis undertaken herein. A number of limitations in both the technology and the methodology in the previous analyses of the hominoid subnasal anatomy are identified in this review, with the hope that they will be rectified in this thesis. For clarity, this review of previous analyses of the hominoid subnasal anatomy will follow the terminology outlined in the previous chapter, even if it differs from the original author's usage, unless noted.

3.1 Robinson, 1953; 1954

The first morphological analyses of the hominoid subnasal anatomy were conducted by Robinson (1953; 1954) who suggested that characters of the subnasal anatomy were valuable in the evaluation of hominin systematics (McCollum et al., 1993) (for the taxonomy employed in this thesis see: Chapter 4.1, The Extant Hominoid and the Family *Hominidae*). Robinson (1953; 1954) was examining hominin remains from South Africa and indentified three different morphological patterns of the subnasal anatomy in specimens of *Australopithecus africanus*, *Paranthropus robustus*, and *Homo erectus*.

3.2 Ward and Kimbel, 1983

The first analysis of the non-human hominoid subnasal anatomy was undertaken by Ward and Kimbel (1983). It was the discovery of maxillary specimens attributed to *Sivapithecus* and their morphological similarities to *Pongo* (Pilbeam et al., 1980; Pilbeam, 1982; Andrews and Tekkaya, 1980; Andrews and Cronin, 1982; Andrews, 1982) that triggered a re-examination of the hominoid subnasal anatomy and its phylogenetic significance.

Ward and Kimbel (1983) identified and analyzed qualitative morphological differences in the extant hominoid subnasal anatomy to assess whether there were diagnostic morphological "patterns" of the hominoid subnasal anatomy that could be utilized as phylogenetically valid indicators. Ward and Kimbel (1983) employed standard radiographs in lateral and frontal

projections to obtain cranial images of aspects of the subnasal anatomy, although it is unclear what role the radiographs played in their analysis. Ward and Kimbel (1983) also utilized computerized tomography (CT) to image midsagittal sections and transverse slices through the incisive foramen of *Australopithecus* specimens and a sample of five adult *Pongo pygmaeus*, six *Pan troglodytes*, and six *Gorilla gorilla* individuals. Slice thickness obtained for CT was either 2 or 4 mm (Ward and Kimbel, 1983).

In addition to imaging the skeletal anatomy, Ward and Kimbel (1983) also performed dissections of the soft-tissues of the subnasal anatomy and incisive fossae on two adult female *Pan*, an adult and juvenile *Gorilla*, and a juvenile *Pongo*. Preserved heads were frozen and sectioned in a sagittal plane a few millimetres to one side of the nasal septum to examine if the differences in the hominoid skeletal subnasal anatomy could be explained by the anatomy of the soft-tissues. Perhaps the most interesting result of Ward and Kimbel (1983) was the conclusion that the differences in the skeletal subnasal anatomy, including the size of the incisive foramina in extant African and Asian hominids, are due to differences in soft tissue anatomy, namely the extent of the neurovascular bundles that pass through the subnasal skeletal elements.

With regard to the skeletal anatomy of the extant hominids, Ward and Kimbel (1983) found distinct "Asian" and "African" morphological patterns of the subnasal anatomy that could be used to distinguish these hominids. The "Asian" morphological pattern of the subnasal anatomy was characterized by the extant hominid *Pongo* which exhibited a large "overlap" of the palatine processes by the elongated premaxillae, resulting in a long, narrow, and shallowly inclined "incisive canal" and a "smooth" nasal cavity floor (Ward and Kimbel, 1983). The "African" morphological pattern was characterized by broad incisive fossae and the presence of a "step-down" in the nasal cavity floor from the premaxillae to the palatine processes, resulting from the elevation of premaxillae above the level of the palatine processes as exhibited by *Gorilla* and *Pan*, although *H. sapiens* exhibited some variation on this pattern (Ward and Kimbel, 1983).

With regard to the Miocene hominoids, it was found that specimens of *Sivapithecus* (and specimens that have since been reassigned to *Ankarapithecus*) shared the "Asian" subnasal pattern with *Pongo* (Ward and Kimbel, 1983). The Miocene hominoid *Rudapithecus* and the Pliocene hominin *Australopithecus* exhibited subsets of the "African" nasal pattern (Ward and

Kimbel, 1983). Ward and Kimbel (1983) also identified an unnamed "cluster" of Early Miocene hominoids that exhibited a primitive morphology of the subnasal anatomy similar those of extant cercopithecoids and hylobatids.

Ward and Kimbel (1983) concluded that characters of the hominoid subnasal anatomy were indeed valid taxonomic indicators, and all hominoids could be sorted into one of two morphological patterns.

3.3   McCollum et al., 1993

McCollum, Grine, Ward, and Kimbel revisited the morphology of the hominoid subnasal anatomy in McCollum et al. (1993). McCollum et al. (1993) revisited Robinson's (1953; 1954) conclusions regarding the phylogenetic validity of the characters in the hominoid subnasal anatomy. As the hominin fossil record had expanded significantly since the original analyses, a reappraisal of the hominoid subnasal anatomy was warranted.

McCollum et al. (1993) differed from Ward and Kimbel (1983) as it aimed to both quantify characters of the hominoid subnasal anatomy and expand the sample size of the analysis to examine intraspecific variation in extant hominoids. The results of this analysis were then applied to the hominin fossil record. The focus on character analysis and the development of quantitative characters followed a new emphasis on cladistics in paleoanthropology (McCollum et al., 1993; Wiley and Lieberman, 2011).

McCollum et al., (1993) examined large samples of extant hominoid crania to provide a statistically relevant basis for the examination of intraspecific variation. As the goal of their analysis was to address the validity of the characters of the subnasal anatomy in hominins, all available African hominin specimens belonging to the genera *Australopithecus*, *Paranthropus*, and the species *H. habilis* and *H. erectus* were also included in the analysis (McCollum et al., 1993).

McCollum et al. (1993) examined male and female adult crania of *Pan* (n=31), *Gorilla* (n=32), *Pongo* (n=20), and *Homo sapiens* (n=40). Only specimens where the third molar was either in

the process of erupting or fully erupted were used, and thus the focus of the analysis was on the morphology of the subnasal anatomy in adult hominoids (McCollum et al., 1993).

With regard to the analysis of the hominoid subnasal morphology, of primary interest in the analysis of McCollum et al. (1993) was the relationship between the premaxillae/anterior alveolar processes and the palatine processes, as this relationship determines the topography of the nasal cavity floor and the morphology of the incisive fossae, incisive foramina, and incisive canals. The degree of the "separation" and the "overlap" of the subnasal elements were used to estimate the length of the palatal fenestrae and the canal length, respectively (McCollum et al., 1993).

The measurement of the "separation" or "overlap" of the subnasal elements was made relative to the occlusal plane in which individuals were oriented, although no definition of the occlusal plane is given in any of the analyses of the hominoid subnasal anatomy (McCollum et al., 1993; see: McCollum and Ward, 1997). Elsewhere, Mai et al. (2005) defined the occlusal plane as the level at which opposing teeth make contact. However, the failure to define the plane upon which the crucial measurements of the analysis depended was problematic. A cursory examination of the dentition of the primates in this analysis suggests that the occlusal "plane" is not a true plane, as is the definition of the Frankfurt Horizontal Plane, and the orientation of an individual in an occlusal plane precisely and consistently would be challenging.

While a number of observations and measurements were made directly on the cranial specimens, the relationship of the premaxillae/anterior alveolar processes to the palatine processes required the generation of sagittal sections through the subnasal anatomy (McCollum et al., 1993). Sagittal sections of the subnasal anatomy were obtained by delineating the skeletal elements on lateral radiographs of the crania (McCollum et al., 1993). In order to make the subnasal anatomy visible on the two-dimensional radiographs, thin metal wires were inserted into the incisive foramina or incisive canals and wrapped tightly around each skeletal element prior to radiography (McCollum et al., 1993). These wires would appear on the radiographs where they were traced and measured for analysis (McCollum et al., 1993). Schematics of the morphologies of the hominoid subnasal anatomy that appear in McCollum et al. (1993) were taken from these tracings.

However, no mention was made as to placement or location of the wires within the incisive foramina or incisive canals. As this micro-CT analysis of the hominoid subnasal anatomy will reveal, the morphology of the subnasal anatomy varies considerably when moving through sagittal sections of the crania and the placement of the wires would have greatly affected the morphology generated by their analysis. McCollum et al. (1993) did not indicate if the wires were kept in the same sagittal section or if the wires were allowed to deviate either medially or laterally as they travelled around the skeletal elements, nor was the thickness of the wire given. As the diameter and the morphology of the incisive foramina or incisive canals varied greatly in the hominoid taxa analyzed the placement of the wires should have been noted by McCollum et al. (1993). All of the aforementioned considerations could have affected the results of their analysis and it is likely that the tracings and schematics depicted in McCollum et al., (1993) are not accurate representations of true midsagittal sections.

While McCollum et al. (1993) attempted to quantify characters of the hominoid subnasal anatomy, the construction of some of the characters and their measurements are questionable in light of information gathered in this micro-CT analysis of the hominoid subnasal anatomy. A number of quantitative measurements are not clearly defined by McCollum et al. (1993).

For example, the breadth of the (nasal) incisive fossae was defined as the breadth immediately behind the posterior pole of the premaxilla/anterior alveolar process (McCollum et al., 1993). However, it is unclear as to precisely what they are measuring. As the posterior pole of the premaxilla/anterior alveolar process is typically elevated above the palatine process, the measurement must angle inferoposteriorly to a point on the surface of the palatine processes, but this point is not defined. It is assumed that McCollum et al. (1993) were measuring to the posterior edge or margin of the nasal incisive fossae, but this micro-CT analysis will reveal that there is often no clearly demarcated edge to the nasal incisive fossa. This micro-CT analysis had intended to include a similar measurement of nasal incisive fossa breadth, but micro-CT images of the hominoid subnasal anatomy reveal that the superior surface of the palatine typically exhibits a smooth and slightly convex surface as it retreats from the incisive foramina, exhibiting no definable edge or margin to the nasal incisive fossae (see: Figure 7 as an example of the absence of a definable margin to the nasal incisive fossae). As such, the breadth of the nasal

incisive fossa was not included as a quantitative measurement in this micro-CT analysis of the hominoid subnasal anatomy as it could not be measured in an accurate and consistent fashion.

The measurement of palatal thickness in McCollum et al. (1993) is equally problematic as it is defined as a measurement of the vertical thickness of the hard palate immediately behind the incisive fossae. Thus, the same problems of definition and placement as the measurement of the (nasal) incisive fossae breadth are encountered, as the margin of the nasal incisive fossae is often indeterminate (see again: Figure 7).

In addition to quantitative measures, a number of qualitative characters were scored by McCollum et al. (1993). The most significant to the analysis of the hominoid subnasal anatomy were the qualitative descriptions of the topography of the nasal cavity floor. The topography of the nasal cavity floor is a character that was described in the previous analysis of the hominoid subnasal anatomy by Ward and Kimbel (1983) and is widely employed in analyses of fossil Miocene hominoids and Pliocene/Pleistocene hominins (cf: Ward and Kimbel, 1983; Begun, 1992; 1994; 2007; Brown et al., 2005; Bilsborough and Rae, 2007). The topography of the nasal cavity floor is typically described in the literature as "stepped" if the premaxillae are elevated above the level of the palatine processes, or "smooth" if there is a smooth transition from the premaxillae to the palatine processes in the nasal cavity floor (Ward and Kimbel, 1983).

However, McCollum et al. (1993) modified the character describing the topography of the nasal cavity floor. The topography of the nasal entrance was now scored as "stepped" or "smooth" at the "lateral aspect of the nasal cavity entrance" (McCollum et al., 1993). McCollum and Ward (1997) would later clarify the meaning of "lateral aspect" as lateral to the (nasal) incisive fossa, and thus McCollum et al. (1993) were scoring the topography of the nasal cavity floor lateral to the incisive fossae.

This approach differed from that of Ward and Kimbel (1983) who examined the change in the vertical relief of the topography of the nasal cavity floor in a midsagittal section through the incisive foramen, not lateral to it (McCollum et al., 1993). The reason given for changing the measurement of the topography of the nasal cavity floor was that the new approach would generate an easily scored qualitative character that did not necessitate the construction of sagittal sections for evaluation (McCollum and Ward, 1997). McCollum and Ward (1997) also argued

that a "step-down" in the subnasal anatomy would always be present in a midsagittal section due to the presence of the incisive foramina of incisive canals, and as such, the character should not be scored in a midsagittal section.

However, this micro-CT analysis reveals that when traversing laterally away from the midsagittal section through the subnasal anatomy the degree of "step-down" from the premaxillae/anterior alveolar processes to the palatine processes in hominoids may diminish to the point where a significant "step-down" in the midsagittal plane transitions into a "smooth" nasal cavity floor lateral to the nasal incisive fossa. In addition, it is apparent that the breadth of the incisive fossae varies greatly in primate taxa, resulting in the scoring of the topography of the nasal cavity floor near the midline of the cranium in *Pongo* to near the nasal cavity wall in *Gorilla*.

The decision to score the topography of the nasal cavity floor lateral to the incisive fossae was problematic for other reasons. As McCollum et al. (1993) describe, *Pan* often exhibits maxillary sinus invasion of the palatine processes, which affects the topography of the nasal cavity floor, especially at the lateral margins of the nasal aperture. However, this is precisely where the topography of the nasal cavity floor was to be scored. Almost a third of *Pan* individuals were scored by McCollum et al. (1993) as exhibiting a "smooth" topography of the nasal cavity floor, but there is a possibility this is a result of maxillary inflation in *Pan*, which does not cause the "smoothness" in the topography of the nasal cavity floor as exhibited by *Pongo* (McCollum et al., 1993). In essence, this is an example of a homoplasy in *Pan* and *Pongo* being treated as a homologous character because of the location where the character was evaluated.

McCollum et al. (1993) go on to note that *Pongo* differs from *Pan* in that the "smooth" nasal floor topography is evident lateral to the incisive fossa, but also in the region of the incisive fossa itself in order to stress the significance of this topography in *Pongo*. This begs the question as to why the topography of the nasal cavity floor was not evaluated in the region of the incisive fossae, where vertical relief may be of more taxonomic significance.

In this thesis, the topography of the nasal cavity floor is measured quantitatively in a section through the long-axis of an incisive foramen or "incisive canal," in part to avoid the inflation of

the palatine processes by the maxillary sinus in *Pan,* and to measure the topography at a point where the relief is more marked, and thus may be more taxonomically significant.

The scoring of the topography of the nasal cavity floor in McCollum et al. (1993) was also limited by it being a qualitative yes/no character, while the amount of "step-down" exhibited by a taxa may have phylogenetic significance.

Ultimately, McCollum et al. (1993) verified the earlier studies of Robinson (1954), and Ward and Kimbel (1983), indicating there is phylogenetic utility in the characters of the subnasal anatomy. However, they modified the conclusions of Ward and Kimbel (1983) which recognized an "African" and "Asian" morphological pattern of the hominoid subnasal anatomy by recognizing diagnostic patterns for each of the extant hominid genera (McCollum et al., 1993). Thus, *Gorilla*, *Pan*, *Homo* and *Pongo* were said to exhibit morphological "patterns" that were diagnostic of each taxon (McCollum et al., 1993). In brief, the extant non-human hominids all exhibited an "overlap" of the palatine processes by the premaxillae, although *Pongo* exhibited the greatest degree of "overlap" (McCollum et al., 1993). 96% of *Gorilla* and 69% of *Pan* individuals exhibited a "stepped" topography of the nasal cavity floor, while conversely 75% of *Pongo* and 96% of *H. sapiens* individuals exhibited a "smooth" nasal cavity floor (McCollum et al., 1993). The identification of these species-specific morphological patterns indicated that the characters of the subnasal anatomy are of phylogenetic significance, validating Robinson's initial discovery (McCollum et al., 1993).

Although outside the focus of this thesis, it is interesting that no consistent morphological pattern was exhibited by fossils typically assigned to early *Homo*, *H. habilis*, and *H. erectus*, suggesting either a high degree of morphological variation within these species or that multiple species are present in the fossil samples (McCollum et al., 1993).

3.4   McCollum and Ward, 1997

McCollum and Ward (1997) published a logical extension of their previous analysis of the adult hominoid subnasal anatomy (McCollum et al., 1993) by examining evidence from comparative ontogeny. By this time most researchers were in general agreement that the subnasal anatomy contained phylogenetically valid characters that could be used to discriminate hominoid taxa.

However, there were still concerns about intraspecific and ontogenetic variation among the hominoids and about the interpretation of the polarities of characters (McCollum and Ward, 1997). McCollum and Ward (1997) attempted to address these concerns by analyzing both quantitative and qualitative characters of the subnasal anatomy to investigate any possible intraspecific variation exhibited during the course of development to maturity. McCollum and Ward (1997) also attempted to ascertain the developmental or functional causes that affected the morphogenesis of the hominoid subnasal anatomy

McCollum and Ward (1997) examined a large number of samples to represent an ontogenetic series of extant hominoids. Individuals of *Pongo pygmaeus* (n=71), *Gorilla gorilla* (n=93), *Pan troglodytes* (n=68), *Homo sapiens* (n=72), and *Hylobates* (n=69) were analyzed. McCollum and Ward (1997) grouped these individuals into five age categories based on the eruption of the first, second, and third molar, and beyond the third molar eruption, based on the patency or fusion of the basilar suture. For *Hylobates*, the last two categories were based on the emergence and full eruption of the canine teeth (McCollum and Ward, 1997).

Measurements for McCollum and Ward (1997) followed the same methodology as the previous analysis of the subnasal anatomy by McCollum et al. (1993) (see above). As such, the same critiques of McCollum et al. (1993) apply to McCollum and Ward (1997).

However, additional concerns were identified in McCollum and Ward (1997), once again with regard to the scoring of the topography of the nasal cavity floor. McCollum and Ward (1997) reiterated that the scoring of the topography was altered in McCollum et al. (1993), in that the topography of the nasal cavity floor was scored as "stepped" or "smooth" lateral to the (nasal) incisive fossae and not in a midsagittal section. McCollum and Ward (1997:381) felt the need to clarify the scoring of this character as the topography of the nasal cavity floor was "virtually always" discussed concurrently with the morphology of the nasal incisive fossa and the incisive foramina or the incisive canal in McCollum et al. (1993). McCollum and Ward (1997) believed this may have led to the assumption that the topography they were describing was in the region of the nasal incisive fossae and "incisive canal", and not adjacent to it, as it had been scored. In the case of this author, they were correct, as it seemed logical that this would be so. McCollum et al. (1993) and McCollum and Ward (1997) are partially responsible for this error, as neither

analysis included any illustrations identifying the location where the topography of the nasal cavity floor was scored, nor did they include any illustrations showing comparisons of the topography of the nasal cavity floor between the hominoid taxa under analysis.

However, McCollum et al. (1993) and McCollum and Ward (1997) did include numerous schematic illustrations and radiographs that depicted the subnasal anatomy of the various taxa discussed in a midsagittal section through an incisive foramen or an "incisive canal". The apparent differences in the "stepped" morphology of the nasal cavity floor in *Gorilla* to the "smooth" morphology exhibited by *Pongo* depicted in these midsagittal sections could have been easily mistaken for the frequent discussions of "stepped" and "smooth" topographies in the accompanying text, if one overlooked the definition of the character in the text.

A reader of the paleoanthropological literature could be forgiven for making this mistake, as midsagittal sections depicting the comparative morphology of the subnasal hominoid anatomy based on Ward and Kimbel (1983), McCollum et al. (1993), and McCollum and Ward, (1997) are ubiquitous in any discussion of the hominoid subnasal anatomy (see: Begun, 1994; 2007; 2010 Brown et al., 2005; Bilsborough and Rae, 2007; Begun et al., 2012). Typically, no definition of this character being scored laterally to the incisive fossae is found in the accompanying text, leaving the reader to assume the diagrams are depicting the descriptions of the "stepped" and "smooth" nasal floor topographies that are found in the text. The fact that the scoring of this character lateral to the incisive fossa is not typically mentioned in the paleoanthropological literature, although the topography of the nasal cavity floor is mentioned frequently in both descriptions of fossils specimens and reviews of the literature, suggests that it is misunderstood by many researchers, despite their frequent references to McCollum et al., (1993) and McCollum and Ward (1997). I suggest that McCollum and Ward were correct when they noted that previous analyses by Ward and Kimbel (1983) and McCollum and Ward (1993) "had the unfortunate effect of implying the nasal floor topography is scored more medially, in the immediate vicinity of the incisive fossa" (1997:381). A reading of the more recent literature suggests that this may still be the case.

In an effort to avoid the confusion regarding the scoring of the topography of the nasal cavity floor, this thesis will analyze the topography of the nasal cavity floor as a quantitative

measurement of the relationship between the premaxilla/anterior alveolar process and the palatine process in a sagittal section through the long-axis of an incisive foramen or "incisive canal."

Unfortunately, one other issue must be addressed regarding the schematics of the hominoid subnasal anatomy depicted in both McCollum et al., (1993) and McCollum and Ward (1997). These schematics are misleading in that they claim to depict midsagittal sections through the hominoid subnasal anatomy, but they are not representative of the midsagittal sections generated from the micro-CT reconstructions performed in this analysis.
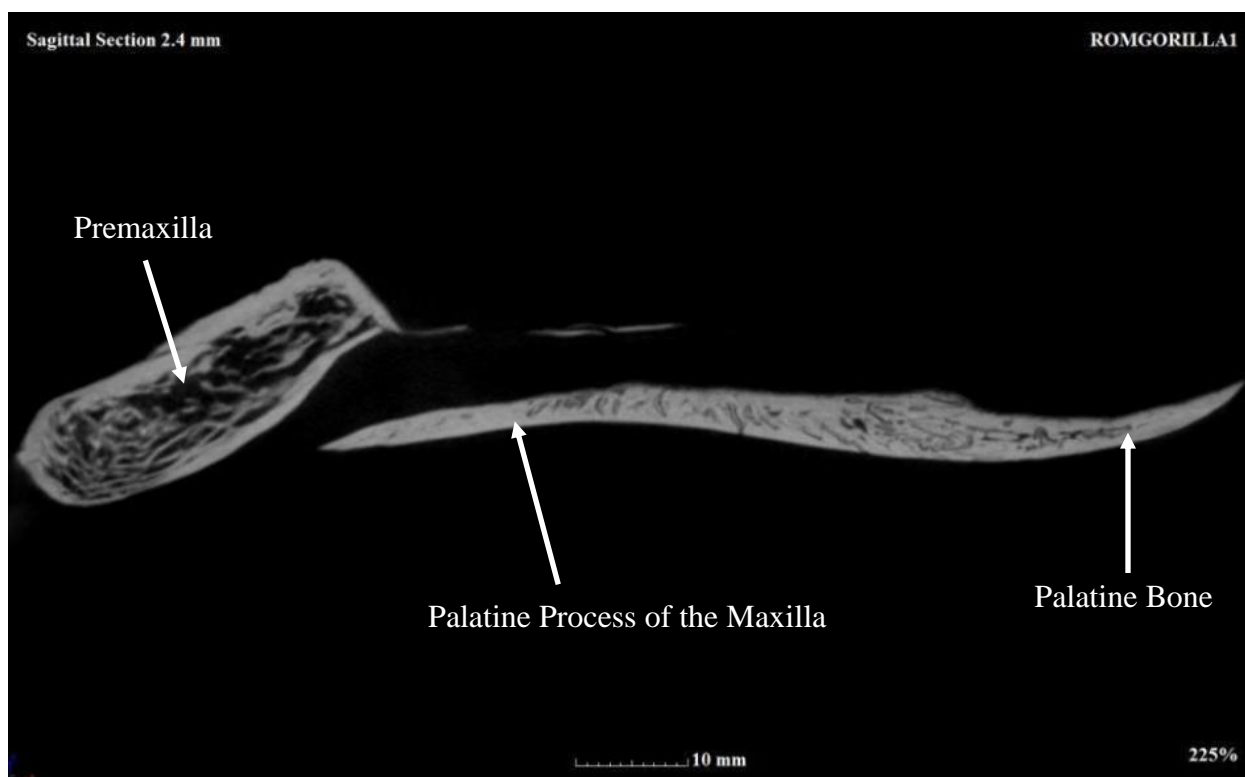
Figure 7 µ-CT Section through the Long-Axis of an Incisive Foramen (male *G. gorilla*)

The midsagittal sections of the subnasal anatomy in McCollum et al. (1993) and McCollum and Ward (1997) depict the nasal sill, prevomer, vomer, and bony nasal septum, similar to how they appear in midsagittal micro-CT sections through the subnasal anatomy (see: Figure 8). However, details of the subnasal anatomy, including the morphology of alveolar process and palatine process, and the incisive foramen or incisive canal are shown as they would appear on a sagittal section through the long-axis of an incisive foramen (see Figure 7). For taxa other than

Pongo or *H. sapiens*, a section through the long-axis of an incisive foramen would lay a considerable distance away from the midline of the cranium, and as such, the details of the prevomer, vomer, incisors would not appear as they are depicted by McCollum et al. (1993) and McCollum and Ward (1997) (compare: Figure 7 and Figure 8).
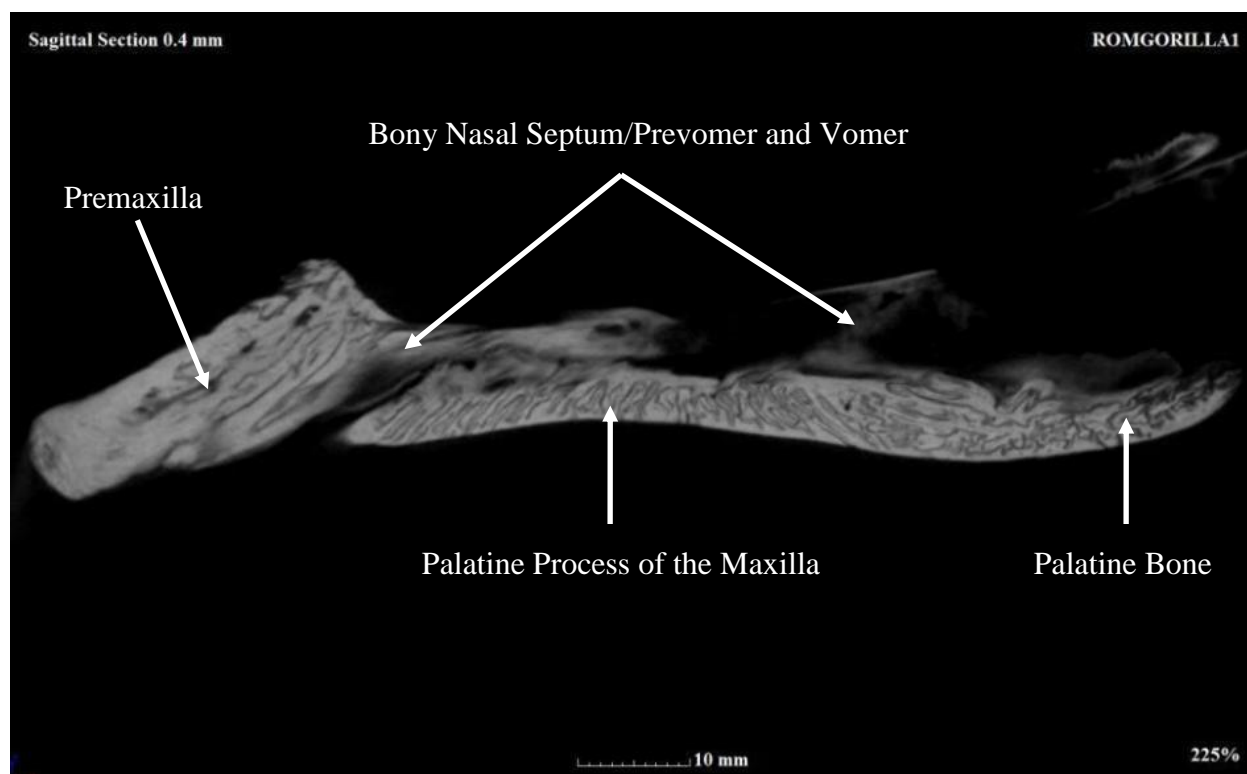
Figure 8 μ-CT Section through the Midsagittal Plane (adult male *G. gorilla*)

Similarly, the morphology and relationship of the premaxilla/anterior alveolar process and the size and orientation of the incisive foramen or "incisive canal" as seen in a micro-CT midsagittal section do not appear as depicted by McCollum et al. (1993) and McCollum and Ward (1997). In a micro-CT midsagittal section, some combination of the prevomer, vomer or bony nasal septum typically partitions the incisive foramina or incisive canals in most taxa and thus a true midsagittal section is not as depicted in their schematics (see: Figure 8). The morphology or topography of the surface of the skeletal elements of the subnasal anatomy was also found to be more complicated that the rather simple oblong or ovoid sections depicted in McCollum et al. (1993) and McCollum and Ward (1997). While described as "schematics" or representation of

the subnasal anatomy, the depictions found in Ward and Kimbel (1983), McCollum et al., (1993), and McCollum and Ward (1997) are nevertheless misleading as to its actual morphology.

Ultimately, McCollum and Ward (1997) concluded that the qualitative characters used to discriminate extant taxa based on the subnasal anatomy did not vary appreciably with sex or age, with the exception of individuals in the earliest stages of ontogeny (McCollum and Ward, 1997). Quantitative characters, with minor exceptions, were also said not to vary with age, again with the exception of individuals in the earliest stages of ontogeny (McCollum and Ward, 1997).

However, it appeared that during the earliest stages of ontogeny the nasal cavity floor is free of substantial topographic relief that is diagnostic of many extant hominoid taxa (McCollum and Ward, 1997). The anterior portion of the maxilla rotates upwardly during development, altering the angulation of the premaxillae/anterior alveolar processes and the palatine processes and the relationship between the two elements (McCollum and Ward, 1997). This rotation is accompanied by an extensive resorption of the floor of the anterior nasal cavity, ultimately leading to an increase in the topographic relief in many adult hominoids (McCollum and Ward, 1997). McCollum and Ward (1997) concluded that only at this early stage of ontogeny did the morphology of the subnasal anatomy cease to discriminate between extant hominoid taxon.

Differences in craniofacial orientation, the size and inclination of the incisors and the vascular anatomy were found to be the major influences on variation in the subnasal anatomy and as such, McCollum and Ward (1997) conclude that the subnasal anatomy of *Pongo* is highly derived relative to the other extant hominoids. However, they argue there is no evidence that the morphology exhibited by *Gorilla* represents the primitive "hominoid pattern" as argued by some researchers (see: Chapter 4, The Subnasal Anatomy of the Extant Hominoids) (McCollum and Ward, 1997; contra Begun, 1992; 1994). Differences in the subnasal anatomy due to sexual dimorphism were found only in *Pongo* and *Gorilla*, and were a result of the differences in development due to delayed sexual maturation in males (McCollum and Ward, 1997).

3.5   Conclusions

The technological and methodological limitations of these previous analyses of the hominoid subnasal anatomy suggest that a re-analysis is required. By employing a micro-CT scanner and a

new methodology, limitations of previous analyses can be circumvented and a more accurate and precise understanding of the hominoids subnasal anatomy can presented. The research objective of this thesis is to test the hypothesis of McCollum et al., (1993) and McCollum and Ward (1997) that the extant hominoids *Hylobates*, *Gorilla*, *Pan*, *Homo*, and *Pongo*, exhibit diagnostic morphological patterns of their subnasal anatomies and that these patterns are phylogenetically informative. The following chapter will review what is currently hypothesized about the morphological patterns of the extant hominoid subnasal anatomy.

4 The Subnasal Anatomy of the Extant Hominoids

This chapter will discuss the subnasal anatomy of the extant hominoids, outlining the hypothesized morphological pattern (or patterns) each taxon is thought to exhibit.

4.1 The Extant Hominoids and the Family *Hominidae*
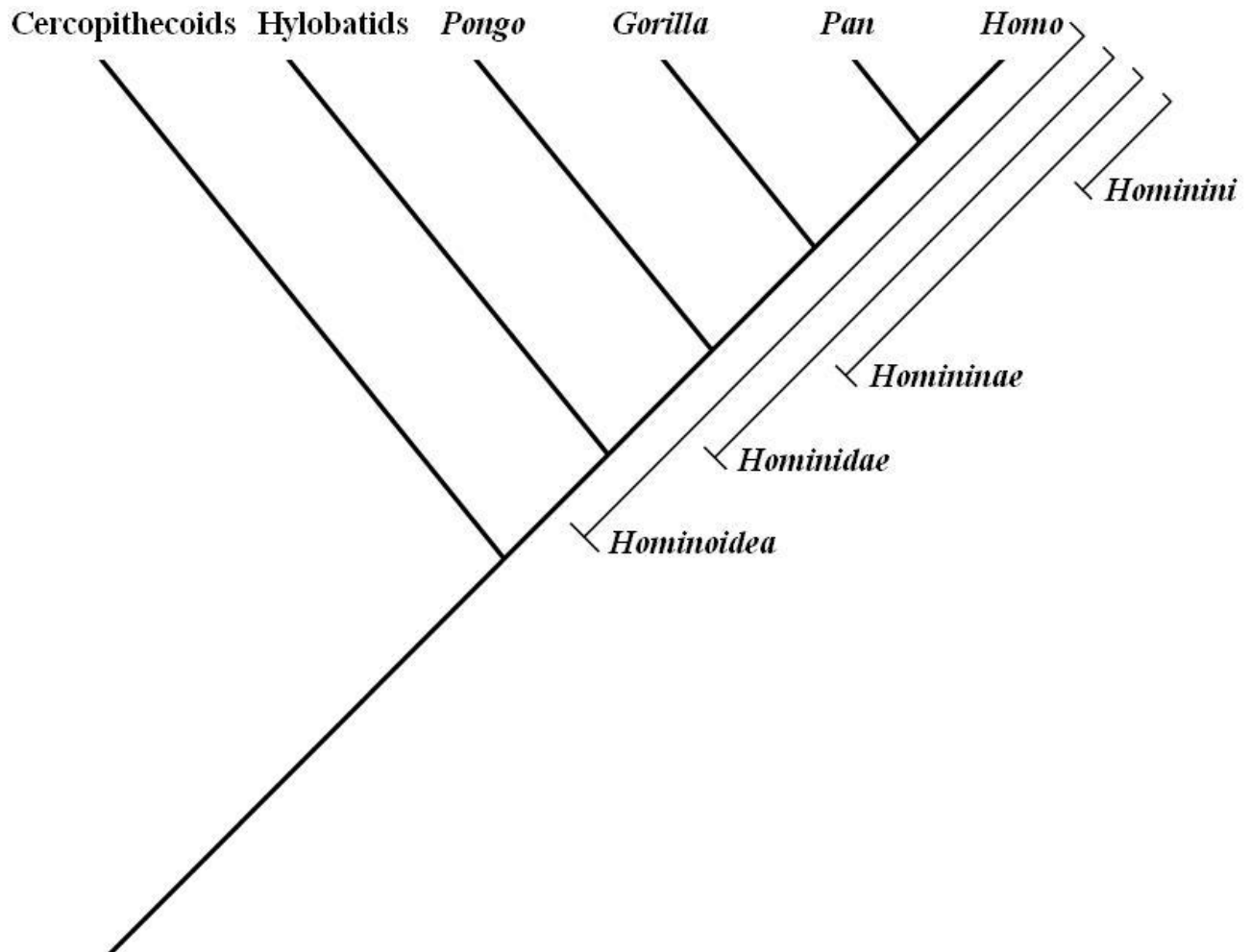
Figure 9 Primate Cladogram

The extant hominoids (Superfamily *Hominoidea*) include the large-bodied great apes (*Pongo*, *Gorilla*, and *Pan*), humans (*H. sapiens*), and the small-bodied lesser apes (*Hylobatidae*) (see: Figure 9) (Bilsborough and Rae, 2007; Harrison, 2010).

The extant lesser apes are assigned to the family *Hylobatidae* (the hylobatids) (Bilsborough and Rae, 2007). This thesis follows a taxonomy that assigns the extant large-bodied hominoids *Pongo*, *Gorilla*, *Pan*, and *Homo* to the family *Hominidae*, following recent taxonomic practices that categorize taxa based exclusively on phylogenetic relationships informed by cladistic analysis (see: Figure 9) (Begun, 1992; Harrison, 2010; Wiley and Lieberman, 2011). Thus, *Pongo*, *Gorilla*, *Pan*, and *Homo* will be referred to as hominids throughout.

The extant Asian hominid *Pongo* is assigned to the subfamily *Ponginae* (the pongines) which includes all taxa that evolved since the lineage diverged from a hominid Last Common Ancestor (LCA) (Harrison, 2010). The extant African hominids, *Gorilla*, *Pan*, and *Homo*, are assigned to the subfamily *Homininae* (the hominines) that also includes all taxa which evolved since the lineage diverged from the hominid LCA (see: Figure 9) (Harrison, 2010). Humans and their immediate ancestors—those taxa that evolved after the divergence of the human lineage from a shared LCA with the chimpanzees—are assigned to the tribe *Hominini* (the hominins) (Harrison, 2010). Hominins are those taxa traditionally referred to as hominids. The use of a revised taxonomy of the *Hominidae*, while expanding the traditional definition of the term "hominid," has the benefit of emphasizing the phylogenetic relationships of the taxa under study, which is the basis of cladistic taxonomy, and is already commonly employed throughout the discipline (Harrison, 2010; Wiley and Lieberman, 2011).

For clarity, the terminology used to describe the subnasal anatomy of the extant hominoids will follow the conventions outlined in this thesis, even if it differs from the original author's usage. The following sections discuss what is hypothesized about the morphology of the extant hominoid subnasal anatomy. Although *Pongo* diverged from the hominid lineage before the emergence of the hominines (see: Figure 9), *Pongo* is discussed after the hominines in this thesis as *Pongo* exhibits the most derived characters of the subnasal anatomy (cf. Ward and Kimbel, 1983; McCollum et al. 1993).

4.2   The Extant Hylobatids

The extant hylobatids are a radiation of small-bodied hominoids from Southeast Asia that exhibit derived postcranial adaptations for suspension and brachiation (Bilsborough and Rae, 2007).

Hylobatids are largely frugivorous, with the exception of the more folivorous siamang (*Symphalangus syndactylus*) (Groves, 2001; Bilsborough and Rae, 2007). Four genera of hylobatids are currently recognized based on genetic studies that consistently reveal four deep-time lineages in the family *Hylobatidae* (Thinh et al., 2010). The genera *Hylobates*, *Nomascus*, and *Hoolock* differ largely in coloration and geographic distribution, while the genus *Symphalangus* is markedly larger and more robust than the other hylobatids (Groves, 2001; Bilsborough and Rae, 2007; Thinh et al., 2010).

4.2.1 *Hylobatidae*

In some aspects of their cranial morphology the hylobatids are primitive among extant hominoids, sharing characters with the short-faced ceboids (Superfamily *Ceboidea*) and the cercopithecoids (Superfamily *Cercopithecoidea*) and the fossil hominoid genus *Proconsul* (Begun, 2007). However, their short and globular neurocrania and their reduced midfacial prognathism are thought to be highly derived relative to the last common ancestor (LCA) of the hominoids and cercopithecoids (Bilsborough and Rae, 2007).

With the exception of dental specimens from the Quaternary of China and Indonesia, no fossil hylobatids are known and their phylogenetic relationship to other hominoids remains obscure (Bilsborough and Rae, 2007).

Subnasal anatomy: The hard palate of *Hylobates* is long for its size and broad anteriorly, reflecting the frugivorous diet (Bilsborough and Rae, 2007). The hard palate of *S. syndactylus* is also broad anteriorly, despite its folivorous diet (Bilsborough and Rae, 2007).

Brown et al. (2005) and Bilsborough and Rae (2007) argued the premaxillae are relatively short and gracile and are level in height with the palatine processes. However, McCollum and Ward (1997) argued that *Hylobates* consistently display a "step-down" in the nasal cavity floor from the premaxillae to the palatine processes. McCollum and Ward (1997) noted that the posterior pole of the premaxilla is depressed along the midline but the posterior edge rises as it approaches the lateral aspect of the nasal cavity, and thus the premaxillae are elevated lateral to the incisive fossae, where this character was scored. It is possible McCollum and Ward's (1997) approach to scoring the topography of the nasal cavity floor accounts for the discrepancies in the scoring of

the nasal cavity floor in *Hylobates* from that of Brown et al. (2005) and Bilsborough and Rae (2007), although the latter refer to McCollum and Ward (1997) in their discussions of the hominoid subnasal anatomy.

The premaxillae are "separated" from the palatine processes by large incisive foramina that link the nasal and oral cavities (Bilsborough and Rae, 2007). The nasal and oral incisive fossae are broad and deep, resulting in large incisive foramina and a "fenestrated" hard palate (Bilsborough and Rae, 2007; Brown et al., 2005). The vomer extends anteriorly to the incisive foramina where it articulates with the posteriorly protruding prevomer, forming a bony nasal septum that partitions the incisive foramen, forming the two distinct incisive foramina (Bilsborough and Rae, 2007). This bony nasal septum is found in all species of *Hylobates*, except for *H. klossii*, the smallest hylobatid (McCollum and Ward, 1997; Bilsborough and Rae, 2007). An incisive crest, a distinctive crest in the midsagittal plane anterior to the nasal incisive fossae and derived from the prevomer, is also exhibited in *Hylobates* (McCollum and Ward, 1997).

The hylobatid "pattern" of a "separation" in the subnasal elements forming large palatal fenestrae is found in many mammals and the majority of non-hominoid primates, and as such is considered to be the primitive pattern of the extant hominoid subnasal anatomy (McCollum et al., 1993; Brown et al., 2005; McCollum and Ward, 1997; Begun, 2007; Bilsborough and Rae, 2007).

4.3   The Hominines

The extant hominines are represented by members of *H. sapiens* and the relict African populations of the hominids *Gorilla* and *Pan* (Begun, 2007; Bernor, 2010). The extant hominines exhibit a number of cranial synapomorphies including a frontoethmoidal sinus and a klinorhynchous face (Brown et al., 2005; Begun, 2007; Bilsborough and Rae, 2007). Among the hominines, *Gorilla* and *Pan* share a number of craniodental similarities and a similar cranial blauplan (Bilsborough and Rae, 2007). *Gorilla* and *Pan* exhibit a long and low neurocranium, a continuous supraorbital torus and thin occlusal dental enamel (Begun, 1992; 2007; Bilsborough and Rae, 2007).

4.3.1 *Gorilla*

Gorilla is a large-bodied, knuckle-walking, frugivorous hominine, although folivory may make up a large-component of its diet, especially as a fallback strategy (Bilsborough and Rae, 2007). *Gorilla* is the largest of the extant hominids and exhibits the most marked degree of sexual dimorphism (Begun, 2007; Bilsborough and Rae, 2007). *Gorilla* taxonomy has been the subject of many revisions, based on both morphological and genetic studies, with subspecies being elevated to the species-level and the reorganization of subspecies (Bilsborough and Rae, 2007; Scally et al., 2012). Two species (*Gorilla beringei* and *Gorilla gorilla*) are now recognized based on an East/West population divide (Bilsborough and Rae, 2007; Scally et al., 2012). Commonly recognized as distinct subspecies are the highly-folivorous Eastern Mountain gorilla (*Gorilla beringei beringei*) and the Eastern Lowland gorilla (*G. b. graueri*), the largest of the gorillas (Bilsborough and Rae, 2007; Scally et al., 2012). Also recognized as subspecies are the Western Lowland gorilla (*Gorilla gorilla gorilla*), the most frugivorous subspecies, and the Cross River gorilla (*G. g. diehli*), an isolated population of the Western Lowland gorilla (Bilsborough and Rae, 2007; Scally et al., 2012).

Subnasal anatomy: The hard palate is long and the inferior surface of the hard palate is anteriorly shallow, but it deepens past the postcanine dentition (Bilsborough and Rae, 2007). Populations of *Gorilla* exhibit variation in the general morphology of the hard palate (Bilsborough and Rae, 2007). *G. g. gorilla* exhibits the shortest hard palate among the gorillas, *G. g. graueri* exhibits a longer hard palate, and *G. beringei* the longest hard palate, while *G. g. diehli* exhibits the narrowest hard palate (Bilsborough and Rae, 2007). The palatine processes are substantially thinner than the premaxillae in *Gorilla* (McCollum et al., 1993).

The premaxillae are more elongated, robust, and vertically oriented than *Hylobates*, although shorter than those of other hominids (Begun, 2007; Begun et al., 2012). The premaxillae are typically truncated in outline in a midsagittal section, especially in males (McCollum et al., 1993). The premaxilla is biconvex—convex in both the sagittal and transverse planes—a derived hominid character (Begun, 2007). The nasal and oral incisive fossae of *Gorilla* are deep and broad in diameter, resulting in bowl-shaped depressions, especially in the nasal cavity floor (McCollum et al., 1993; Begun, 2007; Bilsborough and Rae, 2007; Begun et al., 2012). A long

prevomer is present, articulating with the vomer and the premaxillae (Bilsborough and Rae, 2007). The prevomer and vomer form a bony nasal septum that typically descends into the nasal incisive fossae and bisects the incisive foramen, forming two distinct incisive foramina (McCollum et al., 1993; Bilsborough and Rae, 2007). The resulting incisive foramina are typically very broad in diameter (Begun, 2007; Bilsborough and Rae, 2007).

However, *Gorilla* individuals are thought to vary in other aspects of the subnasal anatomy. In some individuals the posterior poles of the premaxillae are elevated about the palatine process, resulting in a "step-down" in the floor of the nasal cavity lateral to the nasal incisive fossae (McCollum et al., 1993; Begun, 2007; Bilsborough and Rae, 2007). A "step-down" in the nasal cavity floor from the premaxillae to the palatine processes is often considered to be a derived hominid character in discussions of hominoid evolution (Brown et al., 2005; Begun, 2007; Bilsborough and Rae, 2007). In some of these individuals the elevated premaxillae "overlap" the palatine process to varying degrees, resulting in an "incisive canal" (Ward and Kimbel, 1983; McCollum et al., 1993; Brown et al., 2005; Begun, 2002; 2007; Bilsborough and Rae, 2007). The "incisive canal" of *Gorilla* is typically broader, shorter, and more steeply inclined than those exhibited by *Pan* or *Pongo* (Ward and Kimbel, 1983; Begun, 1994; 2007; Bilsborough and Rae, 2007; Begun et al., 2012).

In other *Gorilla* individuals, the premaxillae are thought not to "overlap" the palatine processes, resulting in large incisive foramina and a "fenestrated" hard palate, similar to the primitive "hominoid pattern" exhibited by *Hylobates* (Begun, 1992; 1994; 2007; Bilsborough and Rae, 2007). The resulting palatal fenestrae are typically very wide, significantly broader than those exhibited by *Pan* (Begun, 1992; 1994; 2007; Bilsborough and Rae, 2007).

While McCollum et al. (1993) and Bilsborough and Rae (2007) argue that 65% of adult *Gorilla* individuals exhibit a "step-down" in the topography of the nasal cavity floor lateral to the nasal incisive fossae, Begun (1992; 1994; 2002; 2007) suggests that in some *Gorilla* individuals the posterior poles of the premaxillae are not elevated above the level of the palatine processes. In these individuals the premaxillae do not "overlap" the palatine processes, resulting in a "fenestrated" hard palate (Begun, 2007).

In summary, *Gorilla* individuals are thought to exhibit one of three "patterns" of the subnasal anatomy: a "step-down" in the nasal cavity floor with a "incisive canal," a "step-down" in the nasal cavity floor and a "fenestrated" hard palate, or the absence of a "step-down" in the nasal cavity floor and a "fenestrated" hard palate, although this raises the question of the utility of characters of the subnasal morphology in diagnosing *Gorilla*. These hypothesized patterns of the *Gorilla* subnasal anatomy will be tested in this thesis.

4.3.2   *Pan*

Pan is a large-bodied, largely frugivorous, knuckle-walking hominine (Bilsborough and Rae, 2007). *Pan* is smaller than *Gorilla* and exhibits less sexual dimorphism (Bilsborough and Rae, 2007). *Pan* is also more frugivorous than *Gorilla* (Bilsborough and Rae, 2007). Two species of *Pan* are typically recognized: the chimpanzee (*Pan troglodytes*) and the bonobo (*Pan paniscus*) (Bilsborough and Rae, 2007). *P. paniscus* is typically more gracile in its facial anatomy and exhibits more-limited sexual dimorphism in the cranium and canines (Bilsborough and Rae, 2007). Up to four subspecies of *Pan troglodytes* may be recognized in the literature: *P. t. troglodytes*; *P. t. verus*; *P. t. schweinfurthii*; and *P. t. ellioti* (Bilsborough and Rae, 2007; Oates et al., 2009).

Pan differs from *Pongo* and *Gorilla* in exhibiting less midfacial prognathism, which is likely a result of reduced canine dimorphism in *Pan* (Bilsborough and Rae, 2007). While there is no significant reorganization of the face in *Pan* relative to *Gorilla*, there are significant differences in their subnasal anatomies (Shea, 1984; Bilsborough and Rae, 2007).

Subnasal anatomy: The hard palate is long and its inferior surface is anteriorly shallow, but deepens posteriorly to the postcanine dentition (Bilsborough and Rae, 2007). The premaxillae of *Pan* are more elongated, robust, and horizontally oriented than *Gorilla* and are similar to *Australopithecus* (Begun, 1992; 1994; 2007; Brown et al., 2005; Bilsborough and Rae, 2007). The premaxillae are characteristically ovoid in outline in a midsagittal section, also similar to *Australopithecus* (McCollum et al., 1993). The premaxillae of *Pan* are biconvex, convex in both the sagittal and transverse planes, similar to *Gorilla*. This is a derived hominid character (Bilsborough and Rae, 2007). The palatine processes are substantially thinner than the premaxillae in *Pan* (McCollum et al., 1993).

The nasal and oral incisive fossae of *Pan* are deep and broad in diameter, resulting in bowl-shaped depressions, especially in the nasal incisive fossae, and are similar to the configuration exhibited by *Gorilla*, although the fossae are relatively smaller in *Pan* (Begun, 1992; 1994; 2007; McCollum et al., 1993; Bilsborough and Rae, 2007). The vomer is long and articulates with the prevomer and premaxillae, although the prevomer is smaller than that of *Gorilla* (Bilsborough and Rae, 2007). The prevomer and vomer form a bony nasal septum that descends into the nasal incisive fossae in 54% of *Pan* individuals, where it partitions the incisive foramen into two distinct incisive foramina (McCollum et al., 1993; Bilsborough and Rae, 2007). There is a lower frequency of full partitioning of the incisive foramen in *Pan* than *Gorilla* (Bilsborough and Rae, 2007).

In 69% of *Pan* individuals the posterior poles of the premaxillae are elevated above the palatine processes, resulting in a "step-down" in the floor of the nasal cavity lateral to the nasal incisive fossae, although this "step-down" is less marked than that exhibited by *Gorilla* (Ward and Kimbel, 1983; Begun, 1992; 2007; McCollum et al., 1997; Brown et al., 2005; Bilsborough and Rae, 2007).

Unlike *Gorilla*, the premaxillae extensively "overlap" the palatine processes, resulting in an "incisive canal" (Ward and Kimbel, 1983; McCollum and Ward, 1993; Bilsborough and Rae, 2007). According to Bilsborough and Rae (2007) the premaxillae "overlap" the palatine processes to a similar extant as that of *Pongo*, although McCollum et al. (1993) describe the "overlap" as moderate. The "incisive canal" is typically narrower, longer, and oriented more horizontally than that of *Gorilla*, but is broader and more vertically oriented than the "incisive canal" of *Pongo* (Ward and Kimbel, 1983; McCollum et al., 1993; Bilsborough and Rae, 2007). Bilsborough and Rae (2007) argue that the "incisive canal" of *Pan* is similar in length to *Australopithecus* and *Pongo*, although Brown et al. (2005) suggest it is relatively shorter in length than *Pongo*.

However, in 31% of *Pan* individuals the "step-down" in the nasal cavity floor is altogether absent and the premaxillae transition smoothly into the palatine processes resulting in a "smooth" nasal cavity floor lateral to the nasal incisive fossae and similar the configuration exhibited by *Pongo* (McCollum et al., 1993; Bilsborough and Rae, 2007). The differences in the

topography of the nasal cavity floor in *Pan* do not appear to result from sexual dimorphism (McCollum et al., 1993). The smooth transition partially results from the elongation and more horizontal orientation of the premaxillae relative to *Gorilla*, in combination with the tapering of the posterior pole of the premaxillae and anterior pole of the palatine processes, although *Pan* exhibits a superoinferiorly thicker palatine process than *Gorilla* (Ward and Kimbel, 1983; Bilsborough and Rae, 2007).

However, there is a possibility that the "smooth" topography of the nasal cavity floor in these individuals is largely a result of maxillary sinus invasion of the palatine processes (McCollum et al., 1993). Thus, the "smooth" topography of the nasal cavity floor in *Pan* is a homoplasy and is not homologous with the "smooth" topography exhibited by *Pongo*.

In summary, *Pan* individuals are thought to exhibit one of two "patterns" of the subnasal anatomy: a "step-down" in the nasal cavity floor with an "incisive canal" that is similar to individuals of *Gorilla* or a "smooth" nasal cavity floor with an "incisive canal" more similar to *Pongo*, although this raises the question of the utility of characters of the subnasal morphology in classifying *Pan*. These hypothesized patterns of the *Pan* subnasal anatomy will be tested in this thesis. *Pan* is thus thought to be more derived in the morphological pattern of its subnasal anatomy relative to *Gorilla*, particularly in the relationship between the premaxillae and palatine processes and the length and breadth of the "incisive canal." *Pan* is thought to always exhibit an incisive canal. The degree to which the premaxillae "overlap" the palatine processes in *Pan* is similar to that of *Pongo*, and it is considered to be a derived character relative to *Gorilla* (Begun, 2007; Bilsborough and Rae, 2007). However, the superficial similarities between *Pan* and *Pongo* are not likely homologous with *Pongo*, but rather are homoplasies in the two genera (Bilsborough and Rae, 2007).

4.3.3   *Homo*

Homo is a large-bodied, omnivorous and obligate bipedal hominine that is represented by one extant species, *H. sapiens*. *H. sapiens* is highly derived relative to the other extant hominids in the encephalization of the neurocranium (Bräuer, 2007). The subnasal anatomy of *H. sapiens* is derived relative to other extant hominines, largely due to the extreme reduction of the dentition

and subnasal prognathism, and the highly klinorhynchous facial profile (Ward and Kimbel, 1983; McCollum et al., 1993; Ross and Henneberg, 1995).

Subnasal anatomy: The anterior alveolar processes of *H. sapiens* are significantly more vertically oriented and shorter in length than those of the other extant hominoids (McCollum et al., 1993). The vertical orientation of the anterior alveolar processes results in a nasoalveolar "clivus" that is strongly "flexed" around the anterior nasal spine (Ward and Kimbel, 1983; McCollum et al., 1993). There are two components to the anterior alveolar processes: the vertically oriented "intermaxillary plate" and a horizontally oriented "superior plate" that bears the nasal crest and which articulates with the anterior end of the vomer (Ward and Kimbel, 1983). In some *H. sapiens* individuals these two components form a distinctive "inverted-L" shape in a midsagittal section, unlike other the other extant hominoids (Ward and Kimbel, 1983).

Similar to the anterior alveolar processes, the anterior portion of the palatine processes are "flexed," exhibiting a marked inferior deflection under the "superior plate" of the anterior alveolar processes (Ward and Kimbel, 1983; McCollum et al., 1993). This downward deflection of the palatine processes in *H. sapiens* is unique among the extant hominoids (Ward and Kimbel, 1983; McCollum et al., 1993; McCollum and Ward, 1997).

In 95% of adult *H. sapiens* individuals the floor of the nasal cavity is "smooth" lateral to the nasal incisive fossae, similar to *Pongo* (McCollum et al., 1993; McCollum et al., 1997). However, a "step-down" in the nasal cavity floor lateral to the nasal incisive fossae occurs at a higher frequency in juveniles prior to the complete eruption of the anterior dentition (McCollum and Ward, 1997). The diameter of the nasal incisive fossa is between that exhibited by the other extant hominines and that of *Pongo* (McCollum et al., 1993).

H. sapiens is characterized by a small "overlap" of the subnasal elements as the anterior alveolar processes overlap the palatine processes to a lesser degree than other extant hominoids, due to the near-vertical orientation of the anterior alveolar processes (McCollum et al., 1993, McCollum and Ward, 1997). *H. sapiens* exhibits a long incisive foramen that is a result of the palatine processes being "flexed" against the vertically oriented anterior alveolar processes, rather than being a function of the "overlap" of the two elements, as is the case in the other extant hominoids (McCollum et al., 1997).

The diameter of the long and vertically oriented incisive foramen is only marginally greater than that of *Pongo* (McCollum and Ward, 1997). The incisive foramen is rarely partitioned by the bony nasal septum into distinct foramina (McCollum et al., 1993; McCollum and Ward, 1997).

In *H. sapiens* the bony nasal septum is comprised of prevomeral and vomeral elements (McCollum and Ward, 1997). The prevomer not only articulates with the posteroinferior surface of the anterior alveolar processes, it also extends superiorly to articulate along the superior surface of the nasal sill posterior to the anterior nasal spine (McCollum and Ward, 1997). A pair of other nasal crests (lateral and turbinal) is also found in the nasal cavity and appear to be coincident and co-joining (McCollum et al., 1993).

It is noteworthy that in both *H. sapiens* and non-human infant hominids the anterior portion of the palatine processes are often vertically "flexed" against the premaxillae (McCollum and Ward, 1997). That adult *H. sapiens* and infant hominids share a similar morphological pattern of the subnasal anatomy is evidence of a possible paedomophism in *H. sapiens* (McCollum and Ward, 1997).

4.4 The Pongines

4.4.1 *Pongo*

The relict Southeast Asian populations of the hominid *Pongo* are the only remaining members of the geographically and morphologically diverse Miocene Asian hominoids. *Pongo* is a large-bodied, sexually dimorphic, and predominantly frugivorous hominid (Bilsborough and Rae, 2007). The two allopatric populations of *Pongo pygmaeus* are more frequently being recognized as two distinct species: *P. pygmaeus* from Borneo and *P. abelii* from the island of Sumatra (Groves, 2001; Bilsborough and Rae, 2007). With the elevation of *P. abelii* to species status, care must be taken to ascertain which population of *Pongo* is being discussed in the literature as individuals of both populations were formerly assigned to *P. pygmaeus*. While the two populations exhibit differences in their craniofacial morphology, individuals of both populations can exhibit marked individual variation (Bilsborough and Rae, 2007). Specimens analyzed in this thesis most likely belong to *P. abelii*, the Sumatran orangutan, previously identified as *P. pygmaeus abelii*.

Pongo has a distinctive morphology of the cranium among the extant hominids, including a short neurocranium, a more vertically oriented frontal bone, supraorbital costae, a narrow interorbital distance, absence of a frontoethmoidal sinus, a concave facial profile, an extremely airorhynchous face, long nasals, marked subnasal prognathism, thick and crenulated occlusal molar enamel, and a highly derived subnasal anatomy (Ward and Kimbel, 1983; Ross and Ravosa, 1993; Brown et al., 2005; Begun, 2007; Bilsborough and Rae, 2007). *Pongo* is unique among the extant hominids in lacking digastric fossae on the mandibular symphysis, markings for the anterior digastric muscles; a synapomorphy shared only with the Late Asian Miocene hominoid *Khoratpithecus* (Chaimanee et al., 2006; Bilsborough and Rae, 2007).

Subnasal anatomy: *Pongo* is distinctive among the extant hominids for its marked subnasal prognathism (Bilsborough and Rae, 2007). The subnasal prognathism is due to the hyper-elongation and almost horizontal orientation of the premaxillae, although *P. pygmaeus* typically exhibits more prognathic premaxillae than *P. abelii* (Ward and Kimbel, 1983; Brown et al., 2005; Begun, 2007; Bilsborough and Rae, 2007). The premaxillae are robust and extremely convex in the sagittal plane, more convex than the premaxillae of the African hominines, but it is flat in the transverse plane, unlike the extant hominines (Begun, 2007).

The posterior poles of the premaxillae extensively "overlap" the palatine processes and transition smoothly into the palatine processes in 75% of individuals, resulting in a "smooth" nasal cavity floor lateral to the incisive fossae and the absence of the pronounced "step-down" in the floor of the nasal cavity that is often exhibited by extant hominines (Ward and Kimbel, 1983; McCollum et al., 1993; McCollum and Ward., 1997; Brown et al., 2005; Begun, 2007; Bilsborough and Rae, 2007). The "smooth" transition of the nasal cavity floor results from the hyper-elongation and almost horizontal orientation of the premaxillae in combination with tapering of the posterior pole of the premaxillae and anterior pole of the palatine process (Ward and Kimbel, 1983). *Pongo* is the only extant non-human hominid to consistently exhibit a "smooth" nasal cavity floor and this character is considered to be highly diagnostic of the genus (Ward and Kimbel, 1983; McCollum et al., 1993; McCollum and Ward, 1997; Brown et al., 2005; Bilsborough and Rae, 2007). *Homo* also exhibits a "smooth" nasal cavity floor (McCollum et al., 1993; McCollum and Ward, 1997), but it does not result from an extensive "overlap" of the palatine

processes as in *Pongo* and thus, the similarities in the topography of the nasal cavity floor are not evidence of a homology.

Bilsborough and Rae (2007) describe the palatine processes as superoinferiorly thin in the region of premaxillary "overlap". However, McCollum et al. (1993) claim the premaxillae and the palatine processes are more similar in thickness when viewed in a midsagittal section, due to an increase in the thickness of the palatine processes relative to the African hominines.

The nasal and oral incisive fossae are very narrow and in some individuals nearly indistinct, there being no trace of a depression at the opening into the incisive foramina (Ward and Kimbel, 1983; Brown et al., 2005; Bilsborough and Rae, 2007).

Bilsborough and Rae (2007) have argued that the vomer typically extends partially into the nasal incisive fossae and partitions the opening into the incisive foramen and a prevomer is often present in those individuals that do not exhibit this extension of the vomer into the nasal incisive fossae. However, McCollum et al. (1993) argued that the incisive foramen is not partitioned by a bony structure and the anterior attachment of the vomer is typically located well-posterior to the nasal incisive fossa. However, McCollum and Ward (1997) later argued the vomer typically extends partially into the incisive fossae and only in some individuals does the vomer terminate posterior to the nasal incisive fossae.

Due to the extensive "overlap" of the palatine processes by the premaxillae, the incisive foramina take the configuration of "incisive canals", which are very narrow, elongated, and shallowly inclined relative to the extant hominines (Ward and Kimbel, 1983; McCollum et al., 1993; Brown et al., 2005; Begun, 2007; Bilsborough and Rae, 2007). The degree of "overlap" of the palatine processes by the premaxillae exceeds that of the African hominines (McCollum et al., 1993). The angle and length of the "incisive canals" result from the elongation and the almost horizontal orientation of the premaxillae and the reduction of its "separation" from the palatine processes (McCollum et al., 1993).

The morphological "*Pongo* pattern" of the subnasal anatomy in *Pongo*, including the hyper-elongation of the premaxilla, the extensive "overlap" of the palatine processes, and the resulting

"smooth" nasal cavity floor are considered to be derived pongine characters and significant phylogenetic indicators (Ward and Kimbel, 1983; McCollum et al., 1993; Begun, 2007).

4.5   Soft Tissue Physiology of the Hominoid Subnasal Anatomy

The passageways in the bony elements of the subnasal anatomy are reflective of the soft tissue anatomy and physiology of hominoids (Ward and Kimbel, 1983; Mai, 2007; Schwartz, 2007; Wood, 2013). The incisive foramina or incisive canals provide passage for blood vessels and nerves (Kimbel, 1983; Mai, 2007; Wood, 2013). The terminal branch of the descending palatine artery (or sphenopalatine artery) and the right and left branches of the nasopalatine nerve pass through the incisive foramina or incisive canals into the oral cavity (Ward and Kimbel, 1983; Mai, 2007).

In *Gorilla* and *Pan* the nasopalatine nerves travel through the nasal cavity and pass down into the incisive foramina on either side of the vomer (Ward and Kimbel, 1983). The same is true of a recurrent branch of the greater palatine artery and some smaller veins (Ward and Kimbel, 1983). In *Homo*, a recurrent branch of the greater palatine artery and some smaller veins occupy the incisive foramina or incisive canals (Ward and Kimbel, 1983). However, in *Pongo*, while a large nasopalatine nerve also travels through the incisive canal, there are no arteries or veins occupying the incisive canal (Ward and Kimbel, 1983). Thus, there is a difference in the vascular patterns in the subnasal anatomy of African and Asian hominoids, and it is probable that *Pongo* is derived in its soft-tissue anatomy (Ward and Kimbel, 1983). The absence of arterial or venous structures in the incisive canal in *Pongo* is an explanation for its narrowness. Based on the subnasal skeletal anatomy of *Sivapithecus* it is likely they exhibited the same soft tissue anatomy as *Pongo*. The premaxillary and palatal vascularisation in hominines involves septal branches originating from the sphenopalatine artery (Ward and Kimbel, 1983). The information gleaned from soft tissue examinations strengthens the notion that differences in the skeletal elements of the subnasal anatomy are indicative of real phylogenetic indicators and different evolutionary lineages.

5   The Subnasal Anatomy of the Miocene Hominoids

There has been a rapid expansion of the Miocene hominoid fossil record over the past two decades, leading to reanalysis of hominoid craniofacial characters and the phylogenetic relationships of the Miocene hominoids, in particular their relationships with the extant hominids (Pilbeam, 1997; Pilbeam and Young, 2004; Begun, 2007; 2010; Bernor, 2007; Moyà-Solà et al., 2009a; 2009b; Harrison, 2010; Alba, 2012; Begun et al., 2012). In light of these discoveries, this chapter examines all the fossil Miocene hominoid taxa for which evidence of the subnasal anatomy has been recovered. A number of important Miocene hominoid taxa are not included as their subnasal anatomy is currently unknown. Taxa are identified by their most current and widely used nomenclature. However, as the Miocene hominoids undergo frequent taxonomic revisions some effort has been made to note the historic nomenclature of specimens. In reviewing the literature, and in light of the frequency of taxonomic revision in paleoanthropology, it was realized that relying on generic or specific nomen to identify specimens can be problematic to future identification of the specimens in question.

As the genus *Dryopithecus* has recently undergone a major taxonomic revision it can be used to highlight the problems of specimen identification in the literature (see: Moyà-Solà et al., 2009a; 2009b; Begun, 2010; Begun et al., 2012). While four species of *Dryopithecus* had been recognized, specimens from Spain and Hungary were removed from the genus *Dryopithecus* and assigned to both new genera and species (Moyà-Solà et al., 2009b; Begun, 2010; Begun et al., 2012). Previous analyses of the subnasal anatomy of *Dryopithecus* in the literature (see: Brown et al., 2005; Bilsborough and Rae, 2007) referred to specimens that no longer belong to *Dryopithecus*. Without a clear indication of what specific specimens are being discussed or analyzed, taxonomic revisions, while necessary, can complicate a reading of the literature.

Effort was made in this thesis to identify which specimens were being discussed in the literature and the accession numbers of the specimens are provided whenever possible. This makes it clear which specimens are discussed and ensures that specimens can still be identified following inevitable future taxonomic revisions. For clarity, the terminology used to describe the subnasal anatomy of the Miocene fossil record will follow the conventions outlined in this thesis, even if it differs from the original author's usage.

5.1   Early Miocene African Hominoids (~23.5 to ~17.5 Ma)

5.1.1   *Proconsul*

Proconsul was a mid- to large-sized sexually dimorphic hominoid known from an abundance of craniodental and postcranial elements from East Africa (Begun, 2007; Bilsborough and Rae, 2007; Koufos, 2007). The subnasal anatomy is known from specimens of *P. heseloni* and *P. nyanzae* (Harrison, 2002). *P. heseloni* includes material originally assigned to *P. africanus* and is known from an abundance of specimens (including a partial skeleton similar in size to *S. syndactylus*) from Rusinga Island and Mfangano, Kenya, dated to 17.5 Ma (Le Gros Clark and Leakey, 1950; Walker and Teaford, 1989; Walker et al., 1993; Harrison, 2002; Begun, 2007; Koufos, 2007). The morphologically similar *P. nyanzae* was larger than *P. heseloni*, and also dates to 17.5 Ma (Ward et al., 1993; Harrison, 2002; Begun, 2007). The postcranial elements of *Proconsul* are suggestive of an above-branch arboreal quadruped, similar to other Miocene catarrhines, but with some hominoid attributes in the elbow, wrist, hip, and foot joints (Walker, 1997; Ward, 1997a; Begun, 2007).

Specimens: The subnasal anatomy of *P. heseloni* is represented by the holotype (KNM-RU 7290), a partial skull (KNM-RU 2036), and a male hard palate and lower face (KNM-RU 16000) from Rusinga Island (Walker et al., 1983; 1993; Teaford et al., 1988; Harrison, 2002; Begun, 2007). The subnasal anatomy of *P. nyanzae* is represented by the holotype (BMNH 16647), a lower face and palate (Teaford, 1988; Ward et al., 1993; Harrison, 2002).

Subnasal anatomy: The hard palates of *P. heseloni* and *P. nyanzae* are long, rectangular, and relatively shallow (Harrison, 2002). The premaxillae are relatively short and gracile and do not "overlap" the palatine processes, nor are the premaxillae elevated above the level of the palatine processes (McCollum and Ward, 1997; Harrison, 2002; Brown et al., 2005; Bilsborough and Rae, 2007; contra: Ward and Kimbel, 1983; Koufos, 2007). As the palatine processes are "retracted" so far from the premaxillae, the nasal and oral incisive fossae are deep and broad in diameter, resulting in large incisive foramina and a "fenestrated" hard palate (Ward and Kimbel, 1983; McCollum and Ward, 1997; Harrison, 2002; Brown et al., 2005; Bilsborough and Rae, 2007). Thus, *P. heseloni* and *P. nyanzae* exhibited the primitive "mammalian pattern" of a

"fenestrated" hard palate, which was likely the primitive "hominoid pattern" of the subnasal anatomy (Brown et al., 2005; Bilsborough and Rae, 2007; Koufos, 2007).

5.1.2   *Morotopithecus*

Morotopithecus bishopi was a *Pan*-sized, markedly sexually dimorphic hominoid known from craniodental and postcranial material originally assigned to *Proconsul* from Moroto, Uganda, although there is uncertainty about its age (Walker and Rose, 1968; Harrison, 2002; Pickford et al., 2003; Begun, 2007; Bilsborough and Rae, 2007; Koufos, 2007). Ar/Ar dating indicates and age of 20 to 21 Ma (Gebo et al., 1997), while faunal correlation suggests an age of 14 to 17 Ma (Harrison, 2002; Pickford et al., 2003), which is consistent with initial K/Ar dates of 14 Ma (Harrison, 2002). *M. bishopi* differs postcranially from *Afropithecus* and *Proconsul* in exhibiting derived hominid-like characters in the shoulder, hip, and knee joints, and in the vertebrae which are indicative of the large range of motion used in suspension (Walker and Rose, 1968; MacLatchy, 2000; 2004; Begun, 2007; Bilsborough and Rae, 2007).

Specimens: The subnasal anatomy of *M. bishopi* is represented by the holotype (UMP 62-11), a lower face and hard palate from Moroto, Uganda (Gebo, 1997; Harrison, 2002; Begun, 2007; Bilsborough and Rae, 2007).

Subnasal anatomy: The hard palate of *M. bishopi* is broad anteriorly (Harrison, 2002). The premaxillae are short and gracile, but are more projecting than in *P. heseloni* and *P. nyanzae* (Gebo et al., 1997; Harrison, 2002; Young and MacLatchy, 2004; Begun, 2007). The premaxillae do not "overlap" the palatine processes (Gebo et al., 1997; Young and MacLatchy, 2004; Begun, 2007). The nasal and oral incisive fossae are deep and broad in diameter, resulting in large incisive foramina and a "fenestrated" hard palate, similar to *P. heseloni* and *P. nyanzae* (Harrison, 2002; Young and MacLatchy, 2004; Brown et al., 2005; Begun, 2007). However, the premaxillae are elevated above the level of the palatine processes in *M. bishopi* resulting in a "drop" in the floor of the nasal cavity lateral to the nasal incisive fossae, a derived hominoid character (Brown et al., 2005).

5.1.3   *Afropithecus*

Afropithecus turkanensis was a medium-bodied hominoid known from craniodental specimens, including a partial cranium, and postcranial elements from Kalodirr, Kenya, dated to 17.5 Ma, and contemporaneous with *P. heseloni* and *P. nyanzae* (Leakey and Leakey, 1986a; Leakey et al., 1988a; Leakey and Walker, 1997; Harrison, 2002; Brown et al., 2005; Begun, 2007; Bilsborough and Rae, 2007; Koufos, 2007). *A. turkanensis* is similar in size to *P. nyanzae*, but differs markedly from *P. heseloni* in craniofacial anatomy, evidence of mosaic evolution and an Early Miocene hominoid radiation (Leakey and Leakey, 1986a; Leakey and Walker, 1997; Harrison, 2002; Begun, 2007; Bilsborough and Rae, 2007; Koufos, 2007).

The Oligocene catarrhines *Aegyptopithecus zeuxis* and *Saadanius hijazensis*, the Early Miocene hominoid *Afropithecus turkanensis*, and the Middle Miocene catarrhine *Victoriapithecus macinnesi*, all exhibit a similar cranial morphology, including a long and low neurocranium and a long and prognathic mid-face (Leakey and Leakey, 1986; Benefit and McCrossin 1991; 1997; 2002; Bilsborough and Rae, 2007; Koufos, 2007; Zalmout et al., 2010). Benefit and McCrossin (1991) argued that the similarities between *A. turkanensis* and *Aegyptopithecus zeuxis* indicate the persistence of this cranial form into the Early Miocene (Bilsborough and Rae, 2007; Koufos, 2007). Cranial similarities with *A. zeuxis*, *Victoriapithecus macinnesi*, and *Saadanius hijazensis* are strong evidence that *A. turkanensis* exhibited the primitive hominoid morphology and that the extant hylobatids are highly-derived from earlier hominoids (Benefit and McCrossin, 1991; 1997; 2002; Bilsborough and Rae, 2007; Koufos, 2007; Zalmout et al., 2010).

Specimens: The subnasal anatomy of *A. turkanensis* is represented by the holotype (KNM-WK 16999), an almost complete face and partial cranium from Kalodirr, Kenya (Leakey and Leakey, 1986a; Leakey et al., 1988a; Harrison, 2002; Begun, 2007).

Subnasal anatomy: The hard palate of *A. turkanensis* is long, narrow, and shallow (Harrison, 2002). The premaxillae are more elongated, projecting, and robust than in *Proconsul* or *M. bishopi* (Leakey and Leakey, 1986a; Leakey and Walker, 1997; Harrison, 2002; Begun, 2007; Bilsborough and Rae, 2007). The elongation of the premaxillae and its increased robusticity are functionally linked to the large, procumbent and mesially inclined incisors (Bilsborough and Rae, 2007). A traditional CT scan suggests the posterior pole of the premaxillae approximates

the anterior pole of the palatine processes (cf. Brown et al., 2005). The same pattern appears in a badly damaged partial maxilla also attributed to *A. turkanensis* (Brown et al., 2005). The narrowing of the incisive foramina would be evidence of a derived hominoid subnasal anatomy (Brown et al., 2005). However, Harrison (2002) and Bilsborough and Rae (2007) stated that the nasal and oral incisive fossae are deep and broad in diameter, suggestive of the primitive "hominoid pattern." The subnasal anatomy of *A. turkanensis* has been difficult to assess due to matrix infilling of the nasal cavity of the type specimen (Brown et al., 2005). This precluded the use of then current radiographic imaging (cf. Brown et al., 2005), but is a case amenable to micro-CT exploration. As of writing, this analysis has not been undertaken.

5.1.4   *Rangwapithecus*

Rangwapithecus gordoni was a medium-bodied hominoid from Songhor, Kenya that dates from 19 to 20 Ma (Andrews, 1974; Andrews, 1978; Harrison, 1986; 1988; 2002; Brown et al., 2005; Bilsborough and Rae, 2007). *R. gordoni* was similar in size to *P. heseloni*, but exhibited craniodental adaptations indicative of folivory (Kay and Unger, 1997; Bilsborough and Rae, 2007).

Specimens: The subnasal anatomy of *R. gordoni* is represented by a lower face and hard palate (KNM-RU 700) (Andrews, 1974; Harrison, 2002).

Subnasal anatomy: The hard palate of *R. gordoni* is long and narrows anteriorly (Harrison, 2002; Bilsborough and Rae, 2007). The premaxillae are relatively short (Harrison, 2002; Bilsborough and Rae, 2007). While there is damage to the incisive fossae, they appear to have been broad in diameter (Harrison, 2002). What remains of the subnasal anatomy of *R. gordoni* is indicative of the primitive "hominoid pattern" of a "fenestrated" hard palate (Harrison, 2002; Brown et al., 2005).

5.1.5   *Nyanzapithecus*

Three species of *Nyanzapithecus*, small to medium-bodied hominoids, are known from dental and gnathic fragments from various locales in Kenya (Bilsborough and Rae, 2007). The subnasal anatomy is known from specimens of *N. vancouveringorum*, dated from 17 to 18.5 Ma

and the younger *N. pickfordi*, dated from 15 to 16 Ma (Harrison, 1986; 2002; Bilsborough and Rae, 2007).

Specimens: *N. vancouveringorum* and *N. pickfordi* are known from fragmentary maxillae and premaxillae (Harrison, 1986; 2002).

Subnasal anatomy: The premaxillae of *N. vancouveringorum* and *N. pickfordi* are more robust than *Afropithecus* and other Early Miocene hominoids (Harrison, 2002; Bilsborough and Rae, 2007). An increase in the robusticity of the premaxilla is a derived character of later Miocene hominoids (Brown et al., 2005; Begun, 2007).

5.1.6   *Turkanapithecus*

Turkanapithecus kalakolensis was a medium-bodied hominoid, similar in size to *Rangwapithecus*, and known from a partial cranium, from Kalodirr, Kenya, dated from 16.6 to 17.7 Ma (Leakey and Leakey, 1986b; Leakey et al., 1988b; Manser and Harrison, 1999; Harrison, 2002; Bilsborough and Rae, 2007). The neurocranium is noteworthy in being absolutely and relatively small, even for an Early Miocene hominoid (Manser and Harrison, 1999; Bilsborough and Rae, 2007).

Specimens: The subnasal anatomy of *T. kalakolensis* is known from the holotype (KNM-WK 16950A), a partial cranium from Kalodirr, Kenya (Leakey and Leakey, 1986b; Leakey et al., 1988b; Harrison, 2002)

Subnasal anatomy: The hard palate of *T. kalakolensis* is narrow, similar to *Rangwapithecus*, but the tooth rows converge posteriorly, unusual for a hominoid (Bilsborough and Rae, 2007). Unfortunately, a large portion of the premaxillae and maxillae are missing, including the region around the incisive fossae (Harrison, 2002).

5.1.7   *Dendropithecus*

Dendropithecus is the best known of a group of small-bodied Early Miocene catarrhines from Kenya, including *Micropithecus*, *Limnopithecus*, and *Kalepithecus* that are often referred to collectively as dendropithecoids (Bilsborough and Rae, 2007). The affiliation of the

dendropithecoids is uncertain as genera have been considered to be hominoids (Fleagle and Simons, 1978; Bilsborough and Rae, 2007), placed in their own superfamily, *Dendropithecoidea* (Harrison, 2002; Bilsborough and Rae, 2007), or referred to as catarrhines (Harrison, 2002; Begun, 2007). The dendropithecoids have also been considered to be hominoids (Begun, 2007; Bilsborough and Rae, 2007), a convention followed here as they share some dental similarities with other hominoids and may be informative of the evolution of the subnasal anatomy (Begun, 2007; Bilsborough and Rae, 2007).

Dendropithecus macinnesi was a sexually dimorphic hominoid, similar in size to *S. syndactylus*, known from Rusinga Island, Kenya, and Uganda, dated from 17 to 20 Ma (Andrews and Simons, 1977; Harrison, 2002; Bilsborough and Rae, 2007). *D. macinnesi* had the least well-developed molar shearing crests of any Early Miocene hominoid, highly indicative of soft-fruit frugivory (Kay and Unger, 1997; Bilsborough and Rae, 2007).

Subnasal anatomy: The hard palate of *D. macinnesi* is long and narrow and the nasal and oral incisive fossae are large (Andrews and Simons, 1977; Harrison, 1981; 1988; 2002). The subnasal anatomy of *D. macinnesi* is indicative of the primitive "hominoid pattern" of a "fenestrated" hard palate (Harrison, 2002).

5.1.8   *Micropithecus*

Micropithecus clarki was a small and markedly sexually dimorphic hominoid from Kenya and Uganda, dated from 19 to 20 Ma (Fleagle and Simons, 1978; Harrison, 1981; 1988; 1989; 2002; Begun, 2007; Bilsborough and Rae, 2007). *M. clarki* exhibited shearing crests and dental enamel pitting indicative of folivory (Bilsborough and Rae, 2007).

Specimens: The holotype of *M. clarki* (UMP 64-02) includes a hard palate and lower face (Fleagle and Simons, 1978; Harrison, 2002).

Subnasal anatomy: The hard palate of *M. clarki* is broader and shallower than *Dendropithecus* (Harrison, 2002; Bilsborough and Rae, 2007). The premaxillae are short and gracile while the nasal and oral incisive fossae are large (Harrison, 2002). The subnasal anatomy of *M. clarki* is indicative of the primitive "hominoid pattern" of a "fenestrated" hard palate (Harrison, 2002).

5.1.9 *Limnopithecus*

Limnopithecus was a small, short-faced hominoid from Kenya and Uganda (Harrison, 2002; Bilsborough and Rae, 2007). The subnasal anatomy is known from palatal fragments of the dentally primitive *L. legetet*, dated from 17 to 21 Ma, and the more derived *L. evansi*, dated from 19 to 20 Ma (Harrison, 2002). The mandible was lightly built and the postcanine dentition exhibited shearing crests indicative of folivory (Bilsborough and Rae, 2007).

Subnasal anatomy: Palatal fragments suggest that the hard palate is short and the premaxillae are short and gracile, primitive hominoid characters (Harrison, 1981; 1982; 1988; 2002; Bilsborough and Rae, 2007).

5.1.10 *Kalepithecus*

Kalepithecus songhorensis was a small-bodied hominoid similar in size, and contemporaneous with, *L. legetet* (Harrison, 1988; 2002; Bilsborough and Rae, 2007). *K. songhorensis* differed from the other dendropithecoids in exhibiting a wider anterior face, large anterior teeth, and low-cusped molars indicative of soft-fruit frugivory (Bilsborough and Rae, 2007).

Subnasal anatomy: Unlike other small-bodied Early Miocene hominoids the premaxillae are elongated and robust, a derived hominid character (Harrison, 1981; 1982; 1988; 2002; Bilsborough and Rae, 2007).

5.2 Middle Miocene African Hominoids (~17.5 to ~10.5 Ma)

Kenyapithecus and *Equatorius* are well known genera from East Africa in the Middle Miocene and may have played a significant role in the evolution of the African Miocene hominoids and the initial radiation of Eurasian hominoids but the subnasal anatomy is not known for either genera (Ward et al., 1999; Kelley et al., 2000; Ward and Duren, 2002; Brown et al., 2005; Begun, 2007; Bilsborough and Rae, 2007).

5.2.1 *Nacholapithecus*

Nacholapithecus kerioi was a large-bodied, sexually dimorphic hominoid known from a mostly complete skeleton from Samburu, Kenya, dated to 15 Ma (Nakatsukasa et al., 1998; Ward and Duren, 2002; Begun, 2007; Bilsborough and Rae, 2007). *N. kerioi* was similar to *Afropithecus* in body-size and molar enamel thickness, suggesting it may belong to an afropithecine clade (Brown et al., 2005; Bilsborough and Rae, 2007). The forelimbs of *N. kerioi* are elongated and more robust than *Proconsul* or *Afropithecus* indicating that *N. kerioi* had enhanced forelimb grasping and climbing abilities (Ishida et al., 2004; Begun, 2007).

Specimens: The subnasal anatomy of *N. kerioi* is known from a partial skeleton (KNM-BG 35250) and lower face (KNM-BG 14700A) from Nachola, Kenya (Ward and Duren, 2002; Kunimatsu et al., 2004; Begun, 2007).

Subnasal anatomy: The premaxillae of *N. kerioi* are more elongated than in *Proconsul* or *M. bishopi* (Begun, 2007). The premaxillae are elevated above the palatine processes resulting in a "step-down" in the floor of the nasal cavity lateral to the nasal incisive fossae (Kunimatsu et al., 2004; Brown et al., 2005; Begun, 2007; Bilsborough and Rae, 2007). The posterior pole of the premaxillae also "overlap" the palatine processes, resulting in the formation of an "incisive canal" (Ward and Duren, 2002; Kunimatsu et al., 2004; Brown et al., 2005; Begun, 2007; Bilsborough and Rae, 2007). The nasal and oral incisive fossae are also smaller than those of Early Miocene hominoids (Ward and Duren, 2002; Bilsborough and Rae, 2007). The subnasal anatomy of *N. kerioi* is derived relative to those of Early Miocene hominoids and it may represent the derived "hominid morphological pattern" (Kunimatsu et al., 2004; Brown et al., 2005).

5.3   Middle Miocene European Hominoids (~17.5 to ~10.5 Ma)

5.3.1 *Griphopithecus*

Griphopithecus was a medium to large-bodied hominoid that is noteworthy for being the oldest known European hominoid genus, based on a molar tooth from the site of Engelswies, Germany,

dated to 16.5 to 17 Ma (Heizmann and Begun, 2001; Begun, 2002; 2007; Bilsborough and Rae, 2007). The genus is represented by over 1000 craniodental specimens assigned to *Griphopithecus alpani*, from Paşalar and Çandir, Turkey, from Děvínská Nová Ves, Slovakia, and from Klein Hadersdorf, Austria, all dating from 13.5 to 16 Ma (Alpagut et al., 1990; Kelley and Alpagut, 1999; Heizmann and Begun, 2001; Begun, 2002; 2007; Begun et al., 2003; Bilsborough and Rae, 2007).

The Turkish specimens of *G. alpani* exhibit thick occlusal molar enamel, low dentine penetrance, and robust mandibles, similar to *Afropithecus* (Alpagut et al., 1990; Kelley and Alpagut, 1999; Kelley et al., 2000; Heizmann and Begun, 2001; Kelley 2002; Begun, 2002; Begun et al., 2003; Bilsborough and Rae, 2007). The increased robusticity of the masticatory apparatus may have been a crucial adaptation that allowed hominoids to process tougher diets and expand into the more seasonal and temperate climates of Eurasia, triggering the Middle Miocene Eurasian hominoid radiation (Andrews, 1992; Begun et al., 1997; 2003; 2012; Begun and Nargolwalla, 2004; Begun, 2007; 2010).

Specimens: The subnasal anatomy of *G. alpani* is represented by two maxillary fragments from Paşalar, Turkey (Alpagut et al, 1990; Kappelman et al., 2003; Begun and Nargolwalla, 2004; Brown et al., 2005). The fragmentary nature of the specimens makes interpretations of the subnasal anatomy difficult (Brown et al., 2005).

Subnasal anatomy: The premaxillae of *G. alpani* are short but more vertically inclined (Begun and Nargolwalla, 2004; Brown et al., 2005). Brown et al. (2005) and Begun (2007) argue that the specimens are too fragmentary to accurately assess the subnasal anatomy, although they suggest that the nasal and oral incisive fossae are broad in diameter and the hard palate may be "fenestrated," the primitive "hominoid pattern" (Begun and Nargolwalla, 2004). Conversely, Kelley suggested the posterior poles of the premaxillae approach or slightly "overlap" the palatine processes, a derived configuration more similar to *Afropithecus* or *Nacholapithecus* (cf. Brown et al., 2005).

5.3.2   *Pierolapithecus*

Pierolapithecus catalaunicus was a large-bodied hominoid and is known from a remarkable partial skeleton, including a near complete face, from El Hostalets de Pierola, Barcelona, Spain, dated to 12.5 to 13 Ma, although magnetostratigraphic dating indicates a date of 11.9 Ma (Moyà-Solà, 2004; Brown et al., 2005; Begun, 2007; Bilsborough and Rae, 2007; Casanovas-Vilar, 2011; Alba, 2012).   The mid-face of *P. catalaunicus* was markedly prognathic, similar to the primitive hominoid *Afropithecus*, but unlike the Eurasian hominoids (Bilsborough and Rae, 2007).   *P. catalaunicus* is known postcranially from lumbar vertebrae, ribs, and hand and foot bones that are noteworthy in exhibiting a number of derived hominid characters (Moyà-Solà et al., 2004; Begun, 2007; Bilsborough and Rae, 2007).

Specimens: The subnasal anatomy of *P. catalaunicus* is represented by a face and partial skeleton (IPS 21350) from Baranc de Can Vila 1, Hostalets de Pierola, Spain (Moyà-Solà, 2004; Bilsborough and Rae, 2007).

Subnasal anatomy: The subnasal anatomy of *P. catalaunicus* is incompletely preserved and it may have suffered taphonomic distortion (Brown et al., 2005; Begun, 2007).   The hard palate of *P. catalaunicus* is short, broad, and deep (Bilsborough and Rae, 2007; Alba, 2012).   The premaxillae are noteworthy for being elongated, horizontally oriented, and markedly projecting, similar to those of *Afropithecus*, but unlike those of Miocene Eurasian hominoids (Moyà-Solà et al., 2004; Bilsborough and Rae, 2007).   The premaxillae are biconvex (convex in both the sagittal and transverse planes) an extant hominine character (Begun, 2007; Bilsborough and Rae, 2007).   Parasagittal CT images of the cranium suggest that the posterior poles of the premaxillae are elevated above and slightly "overlap" the palatine processes, resulting in a "step-down" in the floor of the nasal cavity lateral to the nasal incisive fossae and the formation of an "incisive canal" (Moyà-Solà et al., 2004; Brown et al., 2005).   However, Begun (2007) and Begun and Ward (2005) argued that taphonomic distortion displaced the premaxillae anteriorly, exaggerating the degree of facial prognathism, thereby creating artificial similarities with *Afropithecus*.   Begun (2007) also argued that taphonomic distortion altered the relationship between the premaxillae and the palatine processes, increasing the "overlap" of the palatine processes and artificially creating a more derived configuration of the subnasal anatomy.   Begun

(2007) suggests the subnasal anatomy of *Pierolapithecus* was probably similar to the later European hominoid *Rudapithecus*.

5.3.3   *Dryopithecus*

Dryopithecus was a medium-bodied hominoid, originally known from sites across Europe, but the taxon has undergone a major taxonomic revision where the more recent specimens from Spain and Hungary have been removed from the genus (cf. Begun, 2010; Alba, 2012). All specimens of *Dryopithecus*, and those now assigned to *Hispanopithecus* and *Rudapithecus*, exhibit thin occlusal molar enamel, and frequent dentine exposure, indicative of soft-fruit frugivory and similar to primitive Early Miocene hominoids (Begun, 2007; Bilsborough and Rae, 2007).

The subnasal anatomy of *Dryopithecus* is known for only *D. fontani* (Moyà-Solà et al., 2009b; Alba, 2012).   *D. fontani* is known from craniodental and postcranial material, including a male partial face from the Vallès-Penedès Basin, Spain dated to 11.9 Ma, and three male mandibles and a humerus from St. Gaudens, France, and a female mandible from Austria, dated from 11 to 12 Ma, making it the oldest species of *Dryopithecus* and a near contemporary of *Pierolapithecus* (Begun, 2002; 2007; Bilsborough and Rae, 2007; Moyà-Solà et al., 2009b; Casanovas-Vilar, 2011).

Specimens: The subnasal anatomy of *D*. fontani is represented by a partial face (IPS 35026) from the Vallès-Penedès Basin, Spain (Moyà-Solà et al., 2009b; Alba, 2012).

Subnasal anatomy: The hard palate is wide (Alba, 2012).   The premaxillae appear to be elongated and more robust relative to Early Miocene hominoids (Moyà-Solà et al., 2009b; Alba, 2012). The premaxillae are elevated above the palatine processes but the posterior pole of the premaxillae does not "overlap" the palatine processes resulting in the formation of large incisive foramina and a "fenestrated" hard palate, similar to the primitive "hominoid pattern" (Moyà-Solà et al., 2009b; Alba, 2012).

5.3.4   *Anoiapithecus*

Anoiapithecus brevirostris, represented by a cranium (IPS 43000) from El Abocador de Can Mata, Spain, dated to 11.9 Ma, similar in age to *P. catalaunicus* (Moyà-Solà et al., 2009a; Casanovas-Vilar, 2011). *A. brevirostris* has the most orthognathic face of any Eurasian Miocene hominoid, greatly expanding their range of cranial morphologies, and there is no evidence that marked reduction of facial prognathism was due to taphonomic distortion (Moyà-Solà et al., 2009a; Alba, 2012; contra Begun et al., 2012). *A. brevirostris* also exhibits thick molar occlusal enamel and low dentine penetrance, unlike *Pierolapithecus* or *Dryopithecus*—further evidence in support of a new nomen (Moyà-Solà et al., 2009a; 2009b; Alba, 2012).

Specimens: The subnasal anatomy of *A. brevirostris* is represented by the partially preserved premaxillae of the male cranium IPS 43000 (Moyà-Solà et al., 2009a).

Subnasal anatomy: The hard palate of *A. brevirostris* is short, wide, and deep (Moyà-Solà et al., 2009a). The premaxillae are very short, similar to *Proconsul* (Moyà-Solà et al., 2009a). The incisive foramina were large in diameter (Moyà-Solà et al., 2009a). The premaxillae of *A. brevirostris* do not "overlap" the palatine processes, resulting in large nasal and oral incisive fossae and a "fenestrated" hard palate, similar to the primitive "hominoid pattern" of *Proconsul* (Moyà-Solà et al., 2009a).

5.4   Late Miocene European Hominoids (~10.5 to ~5.2 Ma)

5.4.1   *Rudapithecus*

Specimens once assigned to *Dryopithecus brancoi* have been reassigned to *Rudapithecus hungaricus*, a highly sexually dimorphic medium-bodied hominoid from Rudabánya, Hungary, dated 10 Ma (Begun and Kordos, 1993; Kordos and Begun, 1997; 2001; 2002; Bilsborough and Rae, 2007; Begun, 2010). *R. hungaricus* is known from craniodental specimens, including a partial and nearly-complete partial cranium and postcrania, making the taxon one of the best represented Eurasian hominoids (Begun, 2007; Bilsborough and Rae, 2007). *R. hungaricus* exhibits derived African hominine characters of the crania and the postcrania that are indicative

of derived extant hominid-like suspensory behaviours (Begun and Kordos, 1993; Begun, 2002; 2007; 2010; Bilsborough and Rae, 2007; Begun et al., 2012).

Specimens: The subnasal anatomy of *R. hungaricus* is represented by a female partial cranium (RUD 200) and by female and male hard palates (RUD 12 and RUD44/47) (Begun, 2002; Kordos and Begun, 2001).

Subnasal anatomy: The hard palate of *Rudapithecus* is longer and narrower than *Pierolapithecus* (Bilsborough and Rae, 2007). Brown et al., (2005) describe the premaxillae as being relatively short, while Kordos and Begun (2001) and Begun (2002; 2007) describe an increase in the elongation and robusticity of the premaxilla from those of Early Miocene hominoids. The premaxillae are biconvex, similar to *P. catalaunicus*, but oriented more vertically than in earlier hominoids (Begun, 2007; Brown et al., 2005). The premaxillae are elevated above the palatine processes, resulting in a "step-down" in the floor of the nasal cavity lateral to the nasal incisive fossae (Begun, 2007; Bilsborough and Rae, 2007). The nasal and oral incisive fossae are relatively deep and broad in diameter, but reduced in size relative to Early Miocene hominoids (Begun, 1994; 2002; 2007).

In one individual of *R. hungaricus* (RUD 12) the posterior pole of the premaxillae modestly "overlaps" the palatine processes, resulting in the formation of a short and broad, but "true" "incisive canal", similar to *Pierolapithecus* (Kordos and Begun, 2001; 2002; Begun and Nargolwalla, 2004; Brown et al., 2005; Begun 2007; Bilsborough and Rae, 2007; contra: McCollum and Ward, 1997). However, the premaxillae of this specimen do not appear to be very elongated relative to Early Miocene hominoids (Kordos and Begun, 2001; 2002).

However, a second individual of *R. hungaricus* (RUD 44/47) exhibits variation in its morphology of the subnasal anatomy (McCollum and Ward, 1997; Brown et al., 2005; Bilsborough and Rae, 2007). The premaxillae are elevated above the palatine processes but the posterior pole of the premaxillae do not "overlap" the palatine processes, resulting in the formation of large incisive foramina and a "fenestrated" hard palate, similar to the primitive "hominoid pattern" (McCollum and Ward, 1997; Brown et al., 2005; Bilsborough and Rae, 2007). However, in this specimen the premaxillae appear to be more elongated and robust than those of RUD 12 (Kordos and Begun, 2001; 2002).

5.4.2 *Hispanopithecus*

Specimens once assigned to *Dryopithecus laietanus* have been reassigned to *Hispanopithecus laietanus*, a sexually dimorphic medium-bodied hominoid from El Vallès Penedès, Can Llobateres, Spain, best known from a partial skeleton and cranium (CLl-18800) dated from 9.5 to 10 Ma and contemporaneous with *Rudapithecus* (Moyà-Solà and Köhler, 1995; 1996; Begun, 2002; 2007; 2010; Bilsborough and Rae, 2007; Casanovas-Vilar, 2011). *H. laietanus* is craniodentally similar to *R. hungaricus* and the postcrania of *H. laietanus* exhibits derived hominid suspensory characters (Moyà-Solà and Köhler, 1995; 1996; Begun, 2002; 2007; Moyà-Solà et al. 2004; Bilsborough and Rae, 2007).

Specimens: The subnasal anatomy of *H. laietanus* is represented by a cranium (CLl-18000) from Can Llobateres, Spain (Moyà-Solà and Köhler, 1995; 1996).

Subnasal anatomy: The subnasal anatomy of *H. laietanus* is incompletely preserved due to taphonomic damage, but *H. laietanus* appears broadly similar to specimens of *R. hungaricus* (see above) (Moyà-Solà and Köhler, 1995; Begun 2007). The premaxillae were likely elongated and robust, similar to *Pierolapithecus* (Moyà-Solà and Köhler, 1995; Begun, 2007). The premaxillae are markedly biconvex, more so than *Rudapithecus* (Bilsborough and Rae, 2007). Begun (2002; 2007) argued the posterior pole of the premaxillae are elevated above and "overlap" the palatine processes, resulting in a "step-down" in the floor of the nasal cavity and the formation of an "incisive canal", similar to *Pierolapithecus* and specimens of *Rudapithecus*. However, Moyà-Solà and Köhler (1995) and Alba (2012) have argued that the premaxillae do not "overlap" the palatine processes.

5.4.3 *Ankarapithecus*

Ankarapithecus meteai was a large-bodied hominoid known from cranial specimens, including a male and female face, from the Sinap Formation of Anatolia, Turkey, dated to 10 Ma (Alpagut et al., 1996; Andrews, 1996; Begun and Güleç, 1998; Begun, 2002; 2007; Kelley, 2002; Brown et al., 2005; Bilsborough and Rae, 2007). Specimens once attributed to *Sivapithecus* were reassigned to *A. meteai* based on a re-evaluation of the subnasal anatomy (Begun and Güleç, 1995; 1998; Begun, 2007). The cranium of *A. meteai* exhibits a mosaic of hominid, hominine,

and pongine characters and it may represent the primitive pongine cranial morphology (Alpagut et al., 1996; Begun and Güleç, 1998; Begun, 2007; Bilsborough and Rae, 2007).

Specimens: The subnasal anatomy of *A. meteai* is represented by a male lower-face, including the hard palate (MTA 2125) (Kelley, 2002; Brown et al., 2005). Begun and Güleç (1998) restored the face to remove taphonomic distortion, revising the interpretation of the subnasal anatomy. Previous to their reconstruction, it was thought that *A. meteai* exhibited a morphological pattern of the subnasal anatomy similar to *Sivapithecus* (Begun and Güleç 1995; 1998; Brown et al., 2005).

Subnasal anatomy: The maxillae of *A. meteai* are massive and the hard palate is deep (Alpagut et al., 1996; Begun, 2002; Bilsborough and Rae, 2007). The premaxillae are more elongated, robust, and vertically oriented than those of Early Miocene hominoids (Begun and Güleç, 1998; Begun, 2002; 2007; Bilsborough and Rae, 2007). The premaxillae are biconvex and similar to *Hispanopithecus* (Begun and Güleç, 1998; Begun, 2007; Bilsborough and Rae, 2007). The posterior poles of the premaxillae are elevated above the palatine processes, resulting in a "drop" in the floor of the nasal cavity lateral to the nasal incisive fossae (Begun and Güleç, 1998; Bilsborough and Rae, 2007). Begun (2002) and Bilsborough and Rae (2007) indicate the nasal and oral incisive fossae are large, while Brown et al., (2005) suggests they are reduced but reduced in size relative to earlier Miocene hominoids or extant African hominines. The premaxillae do not appear to "overlap" the palatine processes, similar to specimens of *Rudapithecus* (Begun and Güleç, 1998; Brown et al., 2005; Begun, 2007; Bilsborough and Rae, 2007; Begun et al., 2012). Begun and Güleç (1998) argue that the "step-down" in the nasal cavity floor, relatively large incisive fossae, and the resulting incisive foramina as exhibited by *A. meteai*, are derived hominid characters that are indicative of the primitive "hominid pattern" of the subnasal anatomy, contrary to the definition of the "hominid pattern" based on an "overlap" of the subnasal elements as exhibited by *N. kerioi* (Kunimatsu et al., 2004).

5.4.4   *Ouranopithecus*

Ouranopithecus macedoniensis was the largest of the European hominoids—male individuals were the size of female *Gorilla*—and is known from craniodental specimens, including a complete face, from the Ravin de la Pluie, Xirochori, and Nikiti 1, Greece, dated to 9.5 Ma

(Bonis and Koufos, 1993; Koufos, 1995; Andrews, 1996; Andrews et al., 1997; Begun, 2002; 2007; Brown et al., 2005; Bilsborough and Rae, 2007). The face of *O. macedoniensis* is noteworthy for its hyper-robust masticatory adaptations and superficial similarities to the robust australopithecines (Dean and Delson, 1992; Bonis and Koufos, 1993; Begun, 2002; 2007; Bilsborough and Rae, 2007).

Specimens: *O. macedoniensis* is represented by a male cranium (XIR 1) from the Ravin de la Pluie, Greece (Bonis and Koufos, 1993; Begun et al., 2012).

Subnasal anatomy: The hard palate of *O. macedoniensis* is broad anteriorly and deep, with parallel tooth rows (Begun, 1994; 2002; Begun and Güleç, 1998; Bilsborough and Rae, 2007). The premaxillae are more elongated, robust, and vertically oriented than those of earlier Miocene hominoids (Begun, 1994; 2002; 2007; Begun and Güleç, 1998; Brown et al., 2005; Bilsborough and Rae, 2007). The premaxillae are biconvex (Bilsborough and Rae, 2007). The nasal and oral incisive fossae are relatively deep and broad in diameter, but reduced in size relative to Early Miocene hominoids (Begun, 1994; 2002). The posterior poles of the premaxillae are elevated above and "overlap" the palatine processes, resulting in a "step-down" in the floor of the nasal cavity and the formation of an "incisive canal", similar to *Hispanopithecus* and specimens of *Rudapithecus* (Begun and Kordos, 1997; Begun, 2002; 2007; Brown et al., 2005; Bilsborough and Rae, 2007).

5.4.5   *Oreopithecus*

Oreopithecus bambolii was a large-bodied hominoid known from a number of specimens, including a near-complete but distorted skeleton, from Baccinello and Monte Bamboli, Italy, dated from 6 to 7 Ma (Begun, 2002; 2007; Bilsborough and Rae, 2007). *O. bambolii* is noteworthy for being the last surviving and best known European hominoid although its phylogenetic relationships to other hominoids remain contested (Bilsborough and Rae, 2007). At this time the Italian peninsula was separated from mainland Europe and *O. bambolii* exhibits the mosaic of primitive and derived traits typically found in an insular lineage, including supernumerary dental crests and cusps (Kay and Unger, 1997; Begun, 2007; Bilsborough and Rae, 2007). It has also been suggested that the pelvis of *O. bambolii* exhibits evidence of

bipedalism (Moyà-Solà and Köhler, 1996; Harrison and Rook, 1997; Moyà-Solà et al., 1997; Rook et al., 1999).

Specimens: The subnasal anatomy of *O. bambolii* is represented by a nearly complete skeleton recovered from Italy (Hürzeler, 1960; Begun, 2002). The hard palate of *O. bambolii* is damaged, complicating interpretations of the subnasal anatomy (Harrison, 1986; Begun, 2002).

Subnasal anatomy: The hard palate of *O. bambolii* is long and narrow (Begun et al., 1997; Harrison and Rook, 1997; Begun, 2002). The premaxillae are very short, gracile, and vertically oriented (Harrison, 1986; Begun, 2002; 2007). The nasal and oral incisive fossae are deep and broad in diameter, resulting in large incisive foramina and a "fenestrated" hard palate, similar to *Proconsul* and *Hylobates* (Begun, 2002; 2007; Bilsborough and Rae, 2007).

5.5 Late Miocene Asian Hominoids (~10.5 to ~5.2 Ma)

5.5.1 *Sivapithecus*

Sivapithecus was a large-bodied hominoid known from an abundance of craniodental and postcranial elements assigned to three species (Brown et al., 2005; Begun, 2007; Bilsborough and Rae, 2007). The genus is the best known of the Miocene hominoids, with an abundance of craniodental and postcranial specimens recovered from the Siwalik Hills of India and Pakistan, dated between 7.5 and 12.7 Ma (Ward and Pilbeam, 1983; Kappelman et al., 1991; Ward, 1997b; Brown et al., 2005; Begun, 2007; Bilsborough and Rae, 2007).

S. indicus, which likely includes 12 Myr-old unassigned specimens from the Middle Chinji Formation of Pakistan, is known from craniodental specimens dated from 10 to 12.5 Ma (Raza et al., 1983; Rose, 1984; Kappelman et al., 1991; Kelley, 2002; Begun, 2007). *S. indicus* is the oldest, smallest, and craniodentally most primitive species of *Sivapithecus* (Begun, 2007). *S. parvada* is the largest species, up to twice the size of the other *Sivapithecus*, and is known from craniodental specimens from the Nagri formation, Pakistan, dated to 10 Ma (Kelley, 2002; Begun, 2007; Bilsborough and Rae, 2007). *S. sivalensis*, the best known species, is dated from 8.5 to 9.5 Ma (Pilbeam, 1982; Kelley, 2002; Begun, 2007). *S. sivalensis* is represented cranially by a partial skull (GSP 15000), similar in size to female *Pongo* and exhibiting a number of

derived pongine characters including supraorbital costae, a narrow interorbital distance, tall and narrow orbits, the absence of a frontoethmoidal sinus, and an extremely airorhynchous or dorsally deflected face (Pilbeam, 1982; Ward and Kimbel, 1983; Ward and Brown, 1986; Ward, 1997b; Kelley, 2002; Begun, 2007; Bilsborough and Rae, 2007). However, *S. sivalensis* exhibits thicker occlusal molar enamel than *Pongo* and exhibits digastric fossae, markings for the anterior digastric muscles, when the absence of these fossae are considered an autapomorphy of *Pongo* among the extant hominids (Brown et al., 2005; Begun, 2007; Bilsborough and Rae, 2007). *S. sivalensis* lacks the prominent crenulations of the molar enamel exhibited by *Pongo* (Brown et al., 2005; Begun, 2007; Bilsborough and Rae, 2007). Humeri from *S. indicus* and *S. sivalensis* are more similar to primitive Early Miocene arboreal quadrupeds than they are to those of the extant suspensory orthograde hominids (Pilbeam, 1996; 1997; 2002; Rose, 1997; Madar et al., 2002; Begun, 2007). The morphology and size of the humerus in *S. parvada* is suggestive of a terrestrial quadruped that does not have a living hominoid analogue (Begun, 2007).

Specimens: The subnasal anatomy of *S. sivalensis* is represented by the holotype (GSI D-1), a hard palate from the Siwaliks of Pakistan (Kelley, 2002), a maxillary fragment (GSI D-196) from Haritalyangar, India (Kelley, 2002), and a partial cranium (GSP 15000) from the Potwar Plateau, Pakistan (Pilbeam, 1982; Ward, 1997b; Kelley, 2002; Brown et al., 2005; Begun, 2007; Bilsborough and Rae, 2007).

The subnasal anatomy is also represented by a lower face and hard palate (GSP 16075) not yet assigned to a species—but likely belonging to *S. indicus*—from the Chinji Formation, Pakistan (Kelley, 2002; Begun, 2007).

Subnasal anatomy: The premaxillae of *S. sivalensis* are very elongated and oriented nearly horizontally, similar to *Pongo* (Ward and Kimbel, 1983; Begun, 2007; Bilsborough and Rae, 2007). The premaxillae are convex only in the sagittal plane, as the premaxillae are flat in the transverse plane, similar to *Pongo*, but unlike other Middle and Late Miocene hominoids (Kelley, 2002; Begun, 2007). The premaxillae extensively "overlap" the palatine processes and transitions smoothly into the palatine processes, resulting in the absence of a pronounced "step-down" in the floor of the nasal cavity lateral to the nasal incisive fossae and a "smooth" nasal cavity floor (Kelley, 2002; Brown et al,. 2005; Begun, 2007; Bilsborough and Rae, 2007). The

nasal and oral incisive fossae are very narrow, almost slit-like to indistinct in appearance, and are connected by an "incisive canal" (Kelley, 2002; Brown et al., 2005; Bilsborough and Rae, 2007). The "incisive canal" is very long and narrow relative to all other Miocene hominoids, but similar to *Pongo* (Kelley, 2002; Brown et al., 2005). The subnasal anatomy of *S. sivalensis* is noteworthy for its synapomorphies with *Pongo* to the exclusion of all other genera of Miocene hominoids (Ward and Kimbel, 1983; McCollum et al., 1993; Begun, 2002; 2007).

The subnasal anatomy of the older *S. indicus* from the Chinji Formation is more primitive than that of *S. sivalensis* (Begun, 2007). The shape of the hard palate is similar to *Pongo* and *S. sivalensis* (Raza et al., 1983; Ward, 1997b; Kelley, 2002; Begun, 2007). The premaxillae are elongated, robust and oriented horizontally, relative to earlier Miocene hominoids but the premaxillae are short relative to *S. sivalensis* (Kelley, 2002; Begun, 2007). The premaxillae "overlap" the palatine processes and there is a smoother transition into the palatine processes than in other Miocene hominoids (Begun, 2007). However, the incisive fossae and the incisive foramina are not preserved and thus, a definite diagnosis of the presence of a *Pongo*-like "incisive canal" cannot be made (Begun, 2007). It is not surprising that the older *S. indicus* might exhibit a more primitive form of the subnasal anatomy than *S. sivalensis*.

5.5.2   *Lufengpithecus*

Lufengpithecus was a large-bodied sexually dimorphic Asian hominoid, known from thousands of craniodental specimens, including several crania from Lufeng, Yunnan province, China, dated from 8 to 9 Ma (Kelley, 2002; Brown et al., 2005; Begun, 2007; Bilsborough and Rae, 2007). *Lufengpithecus* is notable among hominoids in having a marked degree of sexual dimorphism – greater than that exhibited by extant hominoids (Kelley and Qinghua, 1991; Bilsborough and Rae, 2007). Three species of *Lufengpithecus* are recognized, distinguished by size and geography – each is known from a specific locale (Begun, 2007; Bilsborough and Rae, 2007). *L. lufengensis* from Shihuiba is the best known species and is represented by a number of partial crania, while *L. keiyuanensis* is known from Yuanmou (Harrison et al., 2002; Brown et al., 2005; Begun, 2007). *L. lufengensis* exhibits thick and crenulated molar enamel and a robust mandibular morphology and is considered to be closely affiliated with *Pongo* based on dental similarities, although unlike *Pongo*, *L. lufengensis* exhibits digastric fossae, markings for the

anterior digastric muscles (Ward, 1997b; Begun, 2007; Bilsborough and Rae, 2007). The postcrania of *Lufengpithecus* are suggestive of extant hominid suspensory behaviour, unlike *Sivapithecus* (Begun, 2007).

Specimens: The subnasal anatomy of *L. lufengensis* is represented by a fragmentary partial cranium (PA 644) from Shihuiba, Lufeng, China, and that of *L. keiyuanensis* from a juvenile partial cranium (YV0999) from Hudie Liangzi, Yuanmou Basin, China (Kelley, 2002; Brown et al., 2005).

Subnasal anatomy: The premaxillae of *L. lufengensis* are relatively short and oriented vertically (Kelley, 2002; Brown et al., 2005; Begun, 2007). The premaxillae of the *L. keiyuanensis* juvenile (YV0999) are shorter than *Pan* at an equivalent stage of development (Brown et al., 2005). The posterior poles of the premaxillae are elevated above the palatine processes, resulting in a "step-down" in the floor of the nasal cavity, similar to *Ankarapithecus*, but unlike *Sivapithecus* (Brown et al, 2005; Begun, 2007). The nasal and oral incisive fossae of *L. keiyuanensis* are relatively deep and broad in diameter, but reduced in size relative to Early Miocene hominoids (Brown et al., 2005). Brown et al. (2005) suggest that the adult crania of *L. lufengensis*, though superoinferiorly crushed, may exhibit a similar morphological pattern of the subnasal anatomy as the juvenile *L. keiyuanensis*.

5.6 Late Miocene African Hominoids (~10.5 to ~5.2 Ma)

Little is known of the Late Miocene African hominoids, with the exception of the purported hominin taxa *Sahelanthropus*, *Orrorin*, and *Ardipithecus* (Harrison, 2010). However, while maxillary and palatal fragments are known for these genera, the configurations of the subnasal anatomy have yet to be reported in the literature (Senut et al., 2001; Brunet et al., 2002; White et al., 2009). A number of genera are identified between 9 and 10 Ma, including *Samburupithecus*, *Chororapithecus*, and *Nakalipithecus* (Bernor, 2007; Kunimatsu et al., 2007; Suwa et al., 2007). Unfortunately, these genera are only represented by isolated teeth, or maxillary and mandibular fragments (Bernor, 2007; Kunimatsu et al., 2007; Suwa et al., 2007). The next non-hominin hominoid genus recognized is *Pan*, represented in the fossil record by four individual teeth from the Kapthurin Formation of the Tugen Hills, Kenya, dated 0.5 Ma (McBrearty and Jablonski,

2005; Bilsborough and Rae, 2007). The teeth are clearly affiliated with *Pan*, and all exhibit thin occlusal molar enamel (McBrearty and Jablonski, 2005; Bilsborough and Rae, 2007). The teeth were recovered near fossil localities where *Homo erectus* mandibles have also been recovered, suggesting sympatry between *Pan* and hominins at this time (McBrearty and Jablonski, 2005; Bilsborough and Rae, 2007). No other fossil evidence of *Pan* or any *Gorilla* fossils have been recognized (Bilsborough and Rae, 2007).

5.7   Discussion and Conclusions

There are a number of morphological patterns of the subnasal anatomy identifiable in the Miocene fossil record, indicative of evolutionary trends of subnasal characters. It should be noted that the literature is typically unclear as to whether the scoring of the topography of the nasal cavity floor (the elevation of the premaxillae and the degree of "step-down") is occurring at the nasal incisive fossae or lateral to them, due to confusion surrounding this character in the literature. This may have affected the scoring and interpretation of these characters and could affect the understanding of the evolution of the subnasal anatomy. The topography of the hominoid nasal cavity floor in this review relies on the information presented in the literature out of necessity, although it is suggested here that a reanalysis of all subnasal fossil material be undertaken to clarify the topography.
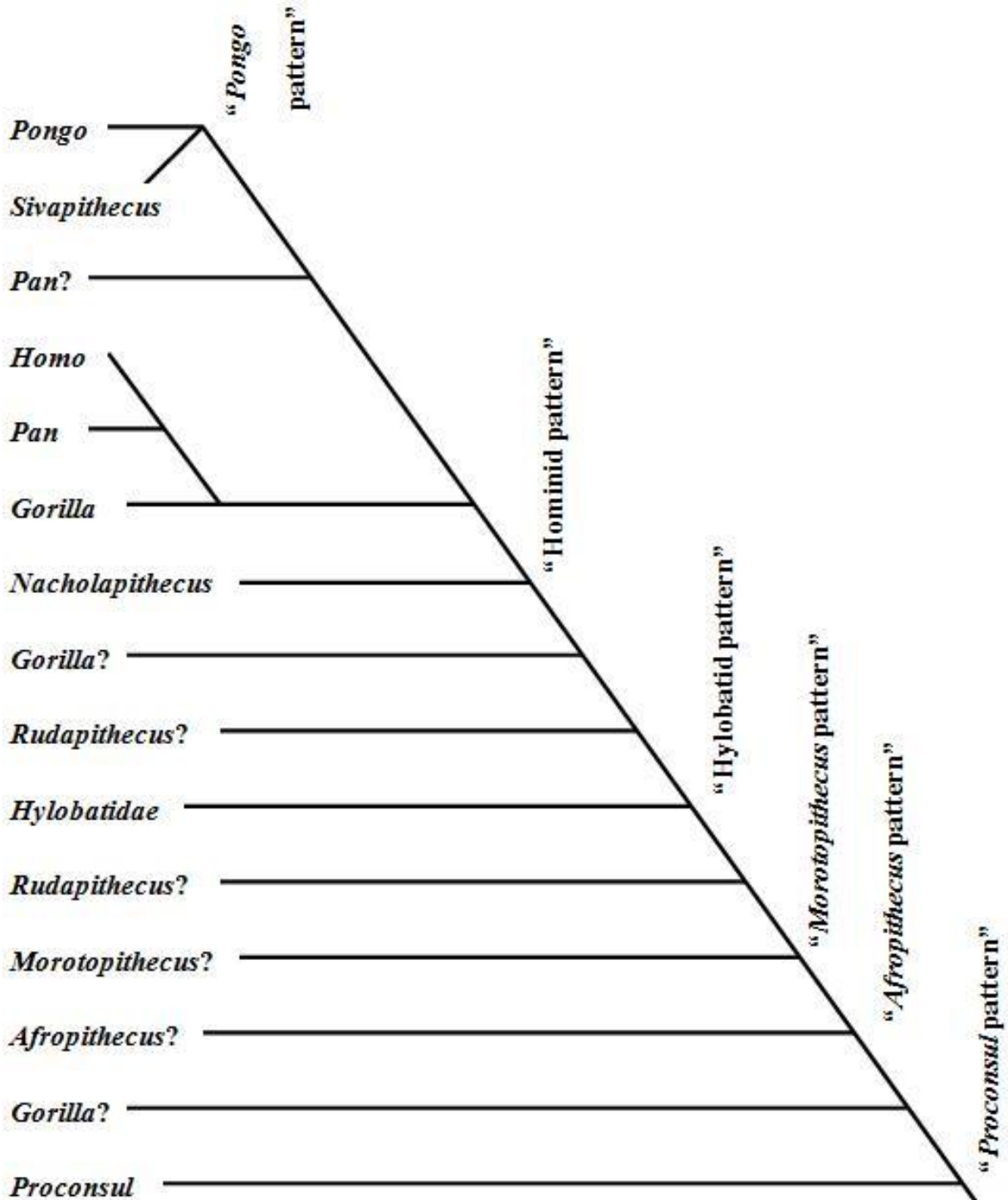
Figure 10 Cladogram of Hominoid Subnasal Morphology Based on Literature Review (question marks [?] denote the multiple interpretations of morphological patterns hypothesized in the literature)

The earliest hominoids exhibited a primitive "mammalian pattern" of the subnasal anatomy, characterized by short and gracile premaxillae, large palatal fenestrae, and no elevation of the premaxillae above the level of the palatine processes. The Early Miocene hominoids *Proconsul heseloni* and *P. nyanzae* typify this pattern of the subnasal anatomy, which will be referred to as the "*Proconsul* pattern". A number of other Early Miocene hominoids may exhibit the "*Proconsul* pattern", including *Rangwapithecus gordoni* and the dendropithecoids *Dendropithecus macinnesi*, *Micropithecus clarki*, *Limnopithecus legetet*, and *L. evansi*. However, the subnasal anatomy is not fully known in these taxa due to the fragmentary nature of these fossils, and the only characters of the "*Proconsul* pattern" they clearly exhibit are the short and gracile premaxillae and the large palatal fenestrae. The height of the premaxillae relative to the palatine processes is not known for these taxa. In should also be noted that the "*Proconsul* pattern" is based on shared primitive characters, or symplesiomorphies, which can only be used to group taxa into a clade, but are not informative of evolutionary relationships within the clade (see: Figure 10) (Wiley and Lieberman, 2011).

Derived characters, or apomorphies, are required to trace the evolution the hominoid subnasal anatomy (Wiley and Lieberman, 2011). *Morotopithecus bishopi* possibly exhibits the first derived character of the hominoid subnasal anatomy. While *M. bishopi* exhibits short and gracile premaxillae and large palatal fenestrae, it also exhibits an elevation of the premaxillae above the palatine processes, resulting in a "drop" in the topography of the nasal cavity floor. This morphology is derived relative to *Proconsul* and will be referred to as the "*Morotopithecus* pattern" (see: Figure 10). As it is unclear as to whether *R. gordoni* or the dendropithecoids mentioned above exhibit a "drop" in the nasal cavity floor, it is possible they could exhibit the "*Morotopithecus* pattern" as well.

Afropithecus turkanensis does not appear to exhibit a "drop" in the nasal cavity floor, but the premaxillae are derived relative to *Proconsul*, being more robust and elongated. This "*Afropithecus* pattern" may also be exhibited by *Nyanzapithecus* and the dendropithecoids *Kalepithecus*, which exhibit elongation and increase in robusticity of the premaxillae (see: Figure 10). However, *A. turkanensis* may exhibit another derived character of the subnasal anatomy as Brown et al. (2005) suggest it exhibits a marked narrowing of the palatal fenestrae relative to *Proconsul*, although matrix infilling of the nasal cavity complicates the interpretation of this

character. A micro-CT analysis of the *A. turkanensis* cranium could resolve this issue and help to elucidate the evolutionary pathway of the extant hominid subnasal anatomy and the relationship of the Early Miocene African hominoids to the Middle Miocene African hominoid *Nacholapithecus kerioi*.

N. kerioi exhibits an elongation of the premaxillae, a "step-down" in the nasal cavity floor, a reduction in the size of the incisive foramina and an "overlap" of the subnasal elements. *N. kerioi* could be equally derived from either the "*Morotopithecus*" or "*Afropithecus* pattern" of subnasal anatomy. *N. kerioi* is noteworthy in being the first taxon to exhibit an "overlap" of the subnasal elements, a character exhibited by the all extant adult hominids, and *N. kerioi* has been said to exhibit a "hominid pattern" of the subnasal anatomy as it will be referred to here (see: Figure 10) (Kunimatsu et al., 2004; Brown et al., 2005).

The Middle Miocene hominoid *Griphopithecus alpani* exhibits short premaxillae and broad nasal and oral incisive fossae and may exhibit palatal fenestrae similar to the "*Proconsul* pattern", although Kelley suggests the posterior pole of the premaxillae may "overlap" the palatine process (Brown et al., 2005).

Pierolapithecus catalaunicus appears to exhibit an elongation of the premaxillae, an elevation of the premaxillae above the palatine processes and an "overlap" of the subnasal elements, which are indicative of the "hominid pattern" of the subnasal anatomy. *P. catalaunicus* is also the first taxon to exhibit a biconvex premaxilla, which is a derived character found in extant hominines but not in *Pongo*, indicative of a "hominine" pattern.

Unlike *P. catalaunicus*, *Anoiapithecus brevirostris* exhibits the hallmarks of the "*Proconsul*" pattern, including short gracile premaxillae and palatal fenestrae, although it is not known if the premaxillae are elevated above the palatine processes. The differences in the subnasal anatomy of *A. brevirostris* relative to *P. catalaunicus* is also further evidence in support of a new nomen for this material.

Interpretation of the subnasal anatomy becomes more complicated with the Late Miocene hominoids. *Hispanopithecus laietanus* and *Rudapithecus hungaricus* exhibit an increase in the robusticity of the premaxillae, a reduction of the nasal incisive fossae, and a "drop" in the floor

of the nasal cavity, combining derived characters of the "*Morotopithecus*" and "*Afropithecus* patterns" (see: Figure 10). At least one specimen of *R. hungaricus* exhibits an "overlap" of the subnasal elements, although another exhibits palatal fenestrae, indicative of variation in the taxon. Although not all specimens of *R. hungaricus* and *H. laietanus* exhibit the "hominid pattern" of the subnasal anatomy, both taxa exhibit biconvex premaxillae, although this is considered to be a derived character of the extant hominines. It can be said that *H. laietanus* and *R. hungaricus* are derived in their subnasal anatomies relative to *G. alpani* and *A. brevirostris*.

The interpretations of *Ankarapithecus meteai* and *Ouranopithecus macedoniensis* are more straightforward as both taxa exhibit elongated, robust and biconvex premaxillae, elevated palatine processes, "overlap" of the subnasal elements. Thus, *A. meteai* and *O. macedoniensis* exhibit the derived "hominine pattern" of the subnasal anatomy.

The Late Miocene European hominid *Oreopithecus bambolii* exhibits aspects of the primitive "*Proconsul* pattern" of the subnasal anatomy, including very short and gracile premaxillae and large palatal fenestrae, although it is unknown if *O. bambolii* exhibits a "drop" in the nasal cavity floor, due to the taphonomic distortion in the skeleton.

The Late Miocene Asian hominoid *Sivapithecus sivalensis* exhibits derived characters of the subnasal anatomy not found in other Miocene hominoids, including the hyper-elongation of the premaxillae, a more marked "overlap" of the subnasal elements, and a very long and shallowly inclined "incisive canal" and a "smooth" nasal cavity floor. All of these derived characters are exhibited by *Pongo*, and *S. sivalensis* is said to exhibit the "*Pongo* pattern" of the subnasal anatomy (see: Figure 10). The "*Pongo* pattern" is derived relative to the "hominid pattern", although it is noteworthy that both *S. sivalensis* and *Pongo* exhibit premaxillae that are convex in only the sagittal plane, and not biconvex as in the extant hominines. The older *S. indicus* exhibits the same "*Pongo* pattern" of the subnasal anatomy as *S. sivalensis*, although it is more primitive in exhibiting less elongation of the premaxillae and less "overlap" of the subnasal elements, as would be expected in an earlier member of the lineage. The characters of the subnasal anatomy are strong evidence linking *Sivapithecus* to the pongine clade.

However, it is interesting that the Late Miocene hominoids *Lufengpithecus lufengensis* and *L. keiyuanensis* are thought to be more closely related to *Pongo* due to similarities of the dentition

as the subnasal anatomy of *Lufengensis* is markedly different from *Pongo*. *Lufengensis* does not exhibit the hyper-elongation of the premaxillae found in *Pongo*, and it exhibits a "step-down" in the nasal cavity floor, rather than a "smooth" nasal cavity floor. *Lufengensis* thus exhibits the "hominid pattern" of the subnasal anatomy. If *Lufengensis* is more closely related to *Pongo* than *Sivapithecus*, then all of the synapomorphies of the "*Pongo* pattern" in *Sivapithecus* are due to convergent evolution, and had to have been evolved separately in a *Lufengensis-Pongo* lineage.

The Miocene fossil record does contain evidence of trends in the evolution of the subnasal anatomy from the primitive hominoid "*Proconsul* pattern", although its evolution was not linear in nature. A number of taxa exhibit a mosaic of derived characters, and taxa that exhibit derived subnasal anatomies are primitive in other aspects of the skeletal morphology. In general, there is an elongation of the premaxillae, a narrowing of the incisive foramina and an elevation of the premaxillae relative to the palatine processes over time, although it is uncertain whether the evolution of one character preceded the other, or if they occurred in concert. The derived "hominid pattern" appears first in *N. kerioi*, when "overlap" of the subnasal elements occurs. A number of other Middle and Late Miocene taxa exhibit the "hominid pattern", including *P. catalaunicus* and *Lufengpithecus*. Two patterns may have evolved from this "hominid pattern", each exhibiting unique derived characters. *A. meteai* and *O. macedoniensis* may exhibit a derived "hominine pattern", defined by the biconvexity of the premaxillae, while *Sivapithecus* is the only genus of Miocene hominoid that exhibits the derived "*Pongo* pattern" of the subnasal anatomy.

Having completed reviews of the morphology of the extant and Miocene hominoid subnasal anatomy, the following chapter outlines the materials and methods employed in a micro-CT analysis to test hypothesis regarding the morphological patterns exhibited by the extant hominoids.

6   Materials and Methods

6.1   A Micro-CT Analysis of the Hominoid Subnasal Anatomy

This thesis will analyze the morphology of the hominoid subnasal anatomy by utilizing micro-CT imaging technology to test two hypotheses regarding the morphology of the subnasal anatomy and its phylogenetic utility in paleoanthropology. First, this analysis will test the hypothesis put forward in McCollum et al. (1993) and McCollum and Ward (1997) that the extant hominoids *Hylobates*, *Gorilla*, *Pan*, *Homo*, and *Pongo*, exhibit diagnostic morphological "patterns" of their subnasal anatomy and that these "patterns" are phylogenetically informative. Second, this analysis will test the hypothesis put forward in McCollum and Ward (1997) that in the earliest stages of ontogeny the morphology of the hominoid subnasal anatomy is not phylogenetically informative.

This micro-CT analysis will also attempt to confirm or refute contradictory observations of the morphology of the hominoid subnasal anatomy outline in the preceding chapters (cf. Ward and Kimbel, 1983; Begun, 1992; 1994; 2007; McCollum et al., 1993; McCollum and Ward, 1997; Brown et al., 2005; Bilsborough and Rae, 2007). The materials used and the methodology employed in this micro-CT analysis are outlined below.

6.2   Materials

Twenty-nine hominoid crania were borrowed from collections at Western University, University of Toronto, University of Toronto Scarborough, and The Royal Ontario Museum. Seventeen non-human primate and twelve human crania were micro-CT scanned to investigate the morphology of their subnasal anatomy (for a complete list of primates, see: Appendix E). Specimens included individuals at various stages of development. Of the non-human primates, thirteen hominoids were scanned to investigate intrageneric differences and four cercopithecoids were used as an outgroup. Access to collections limited the number of non-human primates that were investigated.

The non-human primates were borrowed from collections at the Biology Department and Western University, the Anthropology Departments at the University of Toronto and the University of Toronto, Scarborough, and the Department of Vertebrate Paleontology at the Royal Ontario Museum. The lesser apes were represented by two adult hylobatids. *Gorilla* was represented by two adult males and an infant. *Pan* was represented by an adult female and four juveniles. *Pongo* was represented by an adult male, a juvenile male, and an infant. The cercopithecoid outgroup was represented by an adult male and female of *Papio* and *Macaca*. Generic and specific identifications were based on information provided from the collections and verified by descriptions in the literature. Age was based on limited information provided from the collections and dental eruption patterns identified using the micro-CT reconstructions. Sex was identified largely on descriptions in the literature for adult specimens. The sex of juvenile specimens is not given, based on the difficulties of identifying sex during ontogeny and the lack of a comparative developmental sequence, to avoid misidentification of sex and consequent errors in the analysis.

Human crania were taken from The Odd Fellows Series (cf. Ginter, 2001), The Stirrup Court Series (cf. Parrish, 2000), and from the teaching collections of the Bioarchaeology Laboratory at the Anthropology Department at Western University. Six adult male and two adult female and one juvenile male and three juvenile females were scanned. Juveniles were included to investigate ontogenetic changes as a number of juveniles were included in the hominoid sample. The human juveniles did not have a fully erupted upper third molar.

6.3   Species and Sex Determination

Whitehead et al. (2005) and Bilsborough and Rae (2007) were used to determine to confirm the species of the non-human primate individuals in this analysis (for a complete list of specimens, see: Appendix E). The same sources were also used to confirm sex determination in adult individuals. The age and sex for the majority of *H. sapiens* individuals were taken from previous analyses by Parrish (2000) and Ginter (2001). The sex of the oldest *Pan* juvenile (UTPAN1) was estimated based on differences in its subnasal morphology metrics from that of the adult female *Pan* (WPAN1), following McCollum and Ward (1997).

6.4   Age Determination

Age was determined by the stage of dental eruption following Smith (1994) and Smith et al. (1994). Full descriptions of each individual's stage of dental development and eruption are given in the appendices (see: Appendix E). Smith (1994) and Smith et al., (1994) provide estimates of the times when each tooth begins eruption. The particular patterns of which teeth are erupting are used to estimate the age of the individuals for juvenile specimens (Smith, 1994; Smith et al., 1994). The micro-CT three-dimensional visualization software permitted accurate determination of the stages of dental development and eruption. Individuals with fully erupted upper third molars were considered to be adults (Smith, 1994; Smith et al., 1994). For *Hylobates* those individuals with fully erupted upper canines were considered to be adults (Smith et al., 1994; McCollum and Ward., 1997). Dental development is tightly canalized in primates and the mean age of eruption does not vary to a large degree between individuals of a species (Smith, 1994; Smith et al., 1994)

6.5   Micro-CT Scanning

Analysis and quantification of the subnasal anatomy, including the degree of "overlap" of the premaxilla and palatine processes required the use of sagittal sections through the crania. These sections were obtained from three-dimensional micro-CT reconstructions of the specimens. A Nikon X-Tek XT H 225 ST Industrial micro-CT scanner at Sustainable Archaeology in London, Ontario was used to scan all crania. The utilization of a micro-CT scanner offered considerable advantages over older CT technology including increased resolution of the image through the reduction of voxel size and the isotropic nature of the voxels (Reinhart, 2008; Volume Graphics, 2012). The reduction of the voxel size resulted in a better image-to-noise (or signal-to-noise) ratio, a more precise determination of an object's surface, and a reduction of image artifacts (Reinhart, 2008; Volume Graphics, 2012).

Scans were obtained using a frame rate of two frames and an exposure time of 500 milliseconds. The number of images was set to "optimize" and typically resulted in 3142 images taken in one complete rotation of the crania. Scanning time for each specimen was approximately 53 minutes. These settings were chosen to balance the quality of the micro-CT reconstructions

versus the scanning time. Kilovoltage was 130-140 KV for all specimens and the intensity varied between 35-45 microamps (for scanning parameters, see: Appendix D). A 0.5 mm aluminum filter was used for all scans. Resolution varied from approximately 75 microns for small crania to 163 microns for adult male hominoids (see: Appendix D).

Specimens were mounted in specially constructed Styrofoam mounting boxes that held the specimen face-up, and at an angle that maximized the theoretically attainable resolution while minimizing beam hardening artifacts (for specimen mounting, see: Appendix G). The mounting boxes also held the specimens securely to minimize displacement of the cranium due to the rotation of the manipulator during scanning.

6.6   Reconstruction Software

After scanning, the individual micro-CT radiographs were reconstructed using CT-Pro reconstruction software. The images of the crania were cropped to reduce the file size and speed processing. The crania were cropped to remove the posterior portion of the cranium, either posterior to the external auditory meatus or posterior to basion, whichever point was more posteriorly located on the individual specimen. In some specimens, the top of the crania was cropped down to the level of the supraorbital torus. In some specimens, the bottom of the crania was cropped up to the level of the external auditory meatus or the occlusal surface of the postcanine dentition. In all specimens the external auditory meatus and basion were preserved as points of reference. While trying to minimize the size of the file, the facial skeleton was kept intact in order to facilitate specimen and taxonomic identification. After cropping a specimen, the file was reconstructed at a reduced resolution, 75% of the original images, to speed up file processing and later storage and analysis of the files. After cropping and reduction, the reconstructed three-dimensional volumes ranged from 2.2 to 5.8 GB in size (for scanning parameters, see: Appendix D).

6.7   Imaging Software

The reconstructed CT Pro files were visualized using VGStudio MAX imaging software. All analyses of the crania were completed using this program. VGStudio MAX utilizes a "local adaptive edge detection algorithm" to minimize measurement uncertainty when computing the

surface determination which improves the accuracy in the determination of an objects surface over clinical CT scanners, while minimizing the "partial volume effect" (Volume Graphics, 2012) The "partial volume effect" results in a "blurring" of the cranial surface as voxels near the surface will often contain both "background" and "material" within the voxel, resulting in the assignment of an "intermediate gray value" to the voxel that causes a "blurring" of the cranial surfaces (Reinhart, 2008; Volume Graphics, 2012). Micro-CT imaging using VGStudio MAX reduced the "partial volume effect" due to the use of high-resolution isotropic voxels and the utilization of an advanced "local adaptive edge detection" algorithm, resulting in more precise surface determination of the crania, and thus, more accurate cranial reconstructions and measurements (Reinhart, 2008; Volume Graphics, 2012).

VGStudio MAX also allowed the reconstructed micro-CT images of a cranium to be visualized in three dimensions. VGStudio MAX provides the user with four views of the reconstructed specimen, a three-dimensional reconstruction of the skull and multiplane reformatted sections through the specimen in the three perpendicular planes. VGStudio MAX allowed the crania to be "registered," or reoriented in the appropriate planes for further analysis. The specimen can be reoriented in each of the three perpendicular planes to achieve the desired orientation to a high precision. Once registered, "slices", or "sections" through the crania could be obtained to image the internal anatomy. It this analysis, the crania were oriented in the Frankfurt Horizontal Plane and sections could be obtained through the sagittal, coronal, or transverse planes. Voxel resolution of the specimens was in the 75 to 163 micron range, or approximately 0.1 to 0.2 mm, compared to slice thicknesses of 2 or 4 mm obtained in a previous analysis of the hominoid subnasal anatomy by Ward and Kimbel (1983) using traditional CT technology (see: Appendix D). Measurements in this micro-CT analysis were thus recorded to the nearest 0.1 mm for consistency with the resolution. All measurements used in this thesis are in millimetres (mm).

6.8   Orientation

When conducting this analysis, it was found that the varied morphologies of the taxa under study made it difficult to construct measurements or identify anatomical landmarks that performed adequately and consistently for all taxa. To solve this problem, measurements capturing the morphology of the subnasal anatomy were made relative to an external reference plane by

placing all individual crania in the same orientation for comparative analysis. Previous analyses of the subnasal anatomy encountered similar difficulties in constructing measurements and also resorted to using an external reference plane to orient specimens and conduct measurements (see: Ward and Kimbel, 1983; McCollum et al., 1993; McCollum and Ward, 1997).

6.8.1   The Frankfurt Horizontal Plane

In this analysis, all individuals were oriented in the Frankfurt Horizontal Plane (FHP) for comparisons and all measurements performed in this analysis were taken relative to the position of the cranium in this reference plane (see: Figure 11). The FHP is a plane defined by three anatomical landmarks—the right and left porion points and the left orbitale (White and Folkens, 2000; Schwartz, 2007). Porion is most superior point on the superior margin of the external auditory meatus (White and Folkens, 2000). The left orbitale is the most inferior point on the inferior margin of the left orbit (White and Folkens, 2000; Schwartz, 2007). The resulting plane, the FHP, is nearly parallel to the surface of the Earth and approximates the natural orientation of the human head in a normal bipedal stance (White and Folkens, 2000; Schwartz, 2007; Lieberman, 2011).

6.8.2   The Frankfurt Horizontal Plane vs. the Occlusal Plane

The FHP is widely used in human skeletal biology for orienting the skull, as it defines the anatomical position of the skull for comparative craniometric measurements (White and Folkens, 2000; Schwartz, 2007). Hominoid skulls are also often placed in the FHP for comparative purposes, although it is not considered to be the standard anatomical position for non-human primate taxa (White and Folkens, 2000; Lieberman, 2011). However, the natural orientation of the skull in non-human hominoids is comparable to that of humans because of the shift of the foramen magnum to the rear of the skull in non-human hominoids (Lieberman, 2011). The FHP was utilized in this thesis as it has a number of advantages as a reference plane over the occlusal plane, which was chosen for previous analyses of subnasal anatomy, although it was not explicitly defined (see: Ward and Kimbel, 1983; McCollum et al., 1993; McCollum and Ward, 1997). As previously noted, the occlusal plane (OP) was defined elsewhere as the level at which opposing teeth make contact (Mai, 2005). The VGStudio Max software permits the precise and

accurate placement of the cranium in the FHP, yielding consistent orientations for all individuals in the analysis. Great care was taken to place the specimen as near to the FHP as possible, as deviations from this orientation would affect all measurements and ratios utilized.
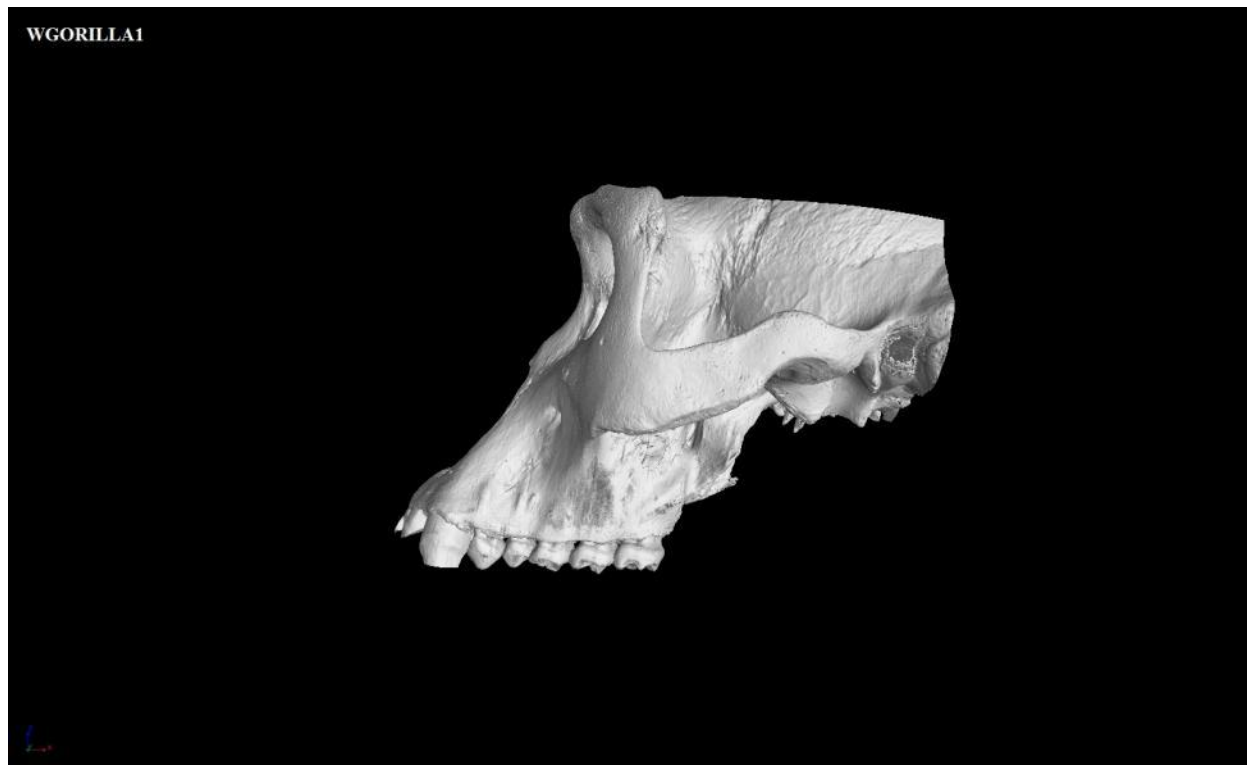
Figure 11 *G. gorilla* **(WGORILLA1) oriented in FHP (μ-CT of adult male, lateral view)**

Unlike the OP, the FHP also more accurately depicts the natural orientation of the cranium. An orientation in the OP places the dentition, and to a lesser degree the hard palate, in the same plane (Ward and Kimbel, 1983; McCollum et al., 1993). However, the angle of the hard palate relative to the cranial base varies both between the hominoid taxa analyzed and during ontogeny of each taxon (Ross and Ravosa, 1993; Ross and Henneberg, 1995). When utilizing the OP to orient individuals for comparison the gross morphological appearance of the subnasal anatomy appears artificially similar; i.e. they all appear to have the hard palate oriented horizontally. A cursory examination of the micro-CT reconstructions of the individuals in this study reveals these differences, which are often of great phylogenetic relevance, in the orientation of the palate and facial anatomy between primate taxa (Shea, 1985; Ross and Ravosa, 1993; Ross and Henneberg, 1995). When oriented in the FHP, comparison of adult and juvenile specimens also

allows the assessment ontogenetic changes in the subnasal anatomy between the different age categories within a taxon.

One disadvantage of using the FHP for the analysis of the subnasal anatomy is that it requires a larger portion of the cranium to orient the individual, while fossil specimens are typically fragmentary. However, even if the OP was employed as a reference plane for a micro-CT analysis of the subnasal anatomy, the same measurements and methodology followed in this thesis could be applied to an orientation in the OP, retaining all the advantages of this methodology over previous analyses. Regardless of the approach selected to analyze the subnasal anatomy, the orientation and measurements utilized should be clearly elucidated, for accurate comparisons to both previous studies and for future analyses.

6.9   Measurements and Ratios

A series of measurements on the subnasal anatomy were performed in order to test the hypothesized morphological patterns of the extant hominoid subnasal anatomy outlined in McCollum et al. (1993) and McCollum and Ward (1997). Measurements were designed to take advantage of the precision offered by the micro-CT imaging technology and to overcome inadequacies in the designs of previous analyses of the hominoid subnasal anatomy.

The following section outlines all measurements used in this thesis. All measurements were performed using VGStudio Max and are presented in millimeters (mm). For analysis of the subnasal anatomy, the majority of measurements were taken on a sagittal section through the long-axis of an incisive foramen. As the scanner resolution for all individuals in the study fell between 100 and 200 microns (0.1 and 0.2 mm) the long-axis of the incisive fossa could be determined to a high degree of precision. In line with the scanning resolution, all measurements were given to a tenth of a millimeter (0.1mm). In comparison, the previous study of the subnasal anatomy by Ward and Kimbel (1983) employed CT technology that was limited by a slice thickness—or resolution—of 2 to 4 mm. Measurements of the various elements of the subnasal anatomy obtained in this thesis were often smaller than the slice thicknesses obtained by Ward and Kimbel (1983).

6.9.1 Sagittal Sections through the Long-Axis of an Incisive Foramen

All measurements were taken with the specimens oriented in the FHP. All measurements, with the exception of Palatal Length, were performed on a sagittal section through the long-axis of an incisive foramen (see: Figure 12). For those individuals that exhibit paired incisive foramina, the right incisive foramen was selected for measurement, for consistency. Some individuals exhibited damage to, or pathology in, the right incisive foramen and in those individuals the left incisive foramen was substituted for measurements, as noted (see: Appendix C).

The long-axis of an incisive foramen was defined to be the greatest anteroposterior length of an incisive foramen. The long-axis was thus parallel to the FHP. The long-axis was determined using superior views of transverse sections through the subnasal anatomy.

In some individuals the incisive foramen angled away from the vertical as seen in posterior views in coronal sections through the subnasal anatomy. In these individuals, the long-axis was determined to be at the midpoint of the superoinferior height of the incisive foramen.
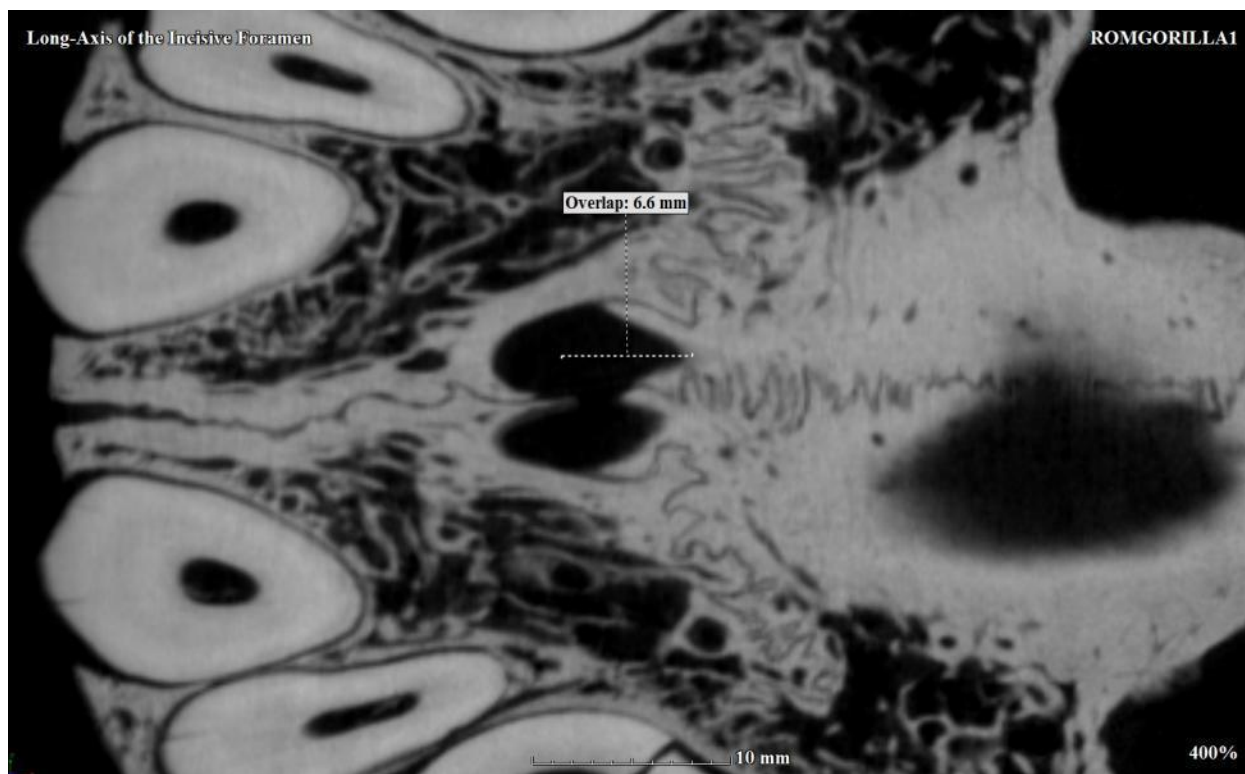
Figure 12 Long-Axis of the Incisive Foramen (μ-CT of adult male *G. gorilla*, superior view)

Investigations of the micro-CT reconstructions revealed that the morphology of the subnasal anatomy could change rapidly when traversing through the sagittal sections of the reconstruction. As a result, all measurements of the subnasal anatomy are sensitive to the selection of the sagittal section being analyzed. If measurements were performed in a sagittal section away from the long-axis of the incisive canal then different measurements would result, possibly affecting the analysis of the subnasal morphology (see: Figure 7 and Figure 8). Thus, great care was taken to ensure that all measurements were performed as near to the long-axis of the incisive foramen as possible in all individuals.

6.9.2   Anatomical Landmarks

The following anatomical landmarks were used to determine the placement of the measurements utilized in this analysis. The following definitions of anatomical landmarks are in reference to a cranium oriented in the FHP.
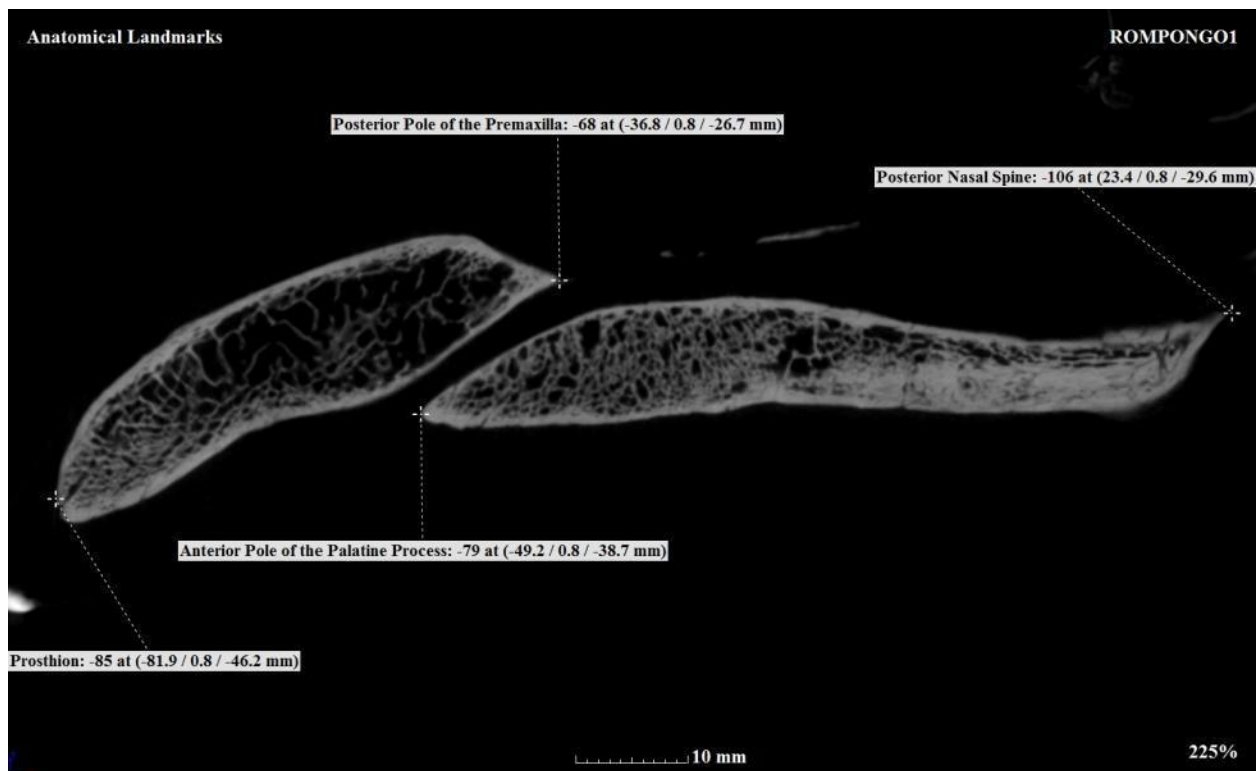
Figure 13 Anatomical Landmarks (note: Prosthion and Posterior Nasal Spine are located off slightly off of this sagittal section) (μ-CT of adult male *P. abelii*, lateral view)

Prosthion: The most anterior midline point on the premaxilla/anterior alveolar process (see: Figure 13) (White and Folkens, 2000; Schwartz, 2007).

Posterior Nasal Spine: The most posterior midline point of the abutting horizontal processes of the palatine bones (see: Figure 13) (Schwartz, 2007).

The following definitions of anatomical landmarks are in reference to a sagittal section through the long-axis of an incisive foramen of a cranium oriented in the FHP.

Anterior Pole of the Palatine Process: The most anterior point of the palatine process (see: Figure 13) (cf. Ward and Kimbel, 1983; McCollum et al., 1993; Ward and McCollum, 1997).

Posterior Pole of the Premaxilla: The most posterior point of the premaxilla/anterior alveolar process (see: Figure 13) (cf. Ward and Kimbel, 1983; McCollum et al., 1993; Ward and McCollum, 1997).

6.9.3   Anatomical Measurements of the Subnasal Anatomy

The following anatomical measurements were used to analyze the morphology of the subnasal anatomy. The following definitions of anatomical measurements refer to a cranium oriented in the FHP. All measurements were performed using the "caliper tool" in VGStudio Max. All linear measurements are in millimeters (mm).

Intra-observer error testing was performed on a cranium of *Hylobates lar* (ROMHYLO1) in order to verify the validity of the results in this study (see: Appendix F). The cranium was oriented in the FHP and measurements of the subnasal anatomy utilized in this analysis were taken on three different occasions: April 16, July 24, and August 9, 2013. There were minimal discrepancies in the measurements of the subnasal anatomy, suggesting that the methodology utilized in this thesis permits accurate and precise measurements of the subnasal anatomy. It is suggested that intra or inter-observer error is most likely to occur during the orientation of the cranium in the FHP or in the determination of the long-axis of an incisive foramen or canal.

Palate Length: Palate Length (see: Figure 14) was a modification of the measurement External Palate Length or Maxilloalveolar Length − the distance from Prosthion to Alveolon (Schwartz,

2007). Alveolon is typically defined as the point on the hard palate where a line drawn between the distal margins of the maxillary alveolar processes intersects the midsagittal plane (White and Folkens, 2007; Schwartz, 2007). However, as this analysis noted that Alveolon typically approximated the Posterior Nasal Spine, Palate Length was defined as the distance from Prosthion to the Posterior Nasal Spine. Thus, Palate Length was utilized as a measurement of the overall length of the hard palate. This definition simplified measurements as the distal margins of the maxillary alveolar process were often hard to define and utilizing Alveolon for Palate Length would have required two additional sets of measurements to precisely identify Alveolon.
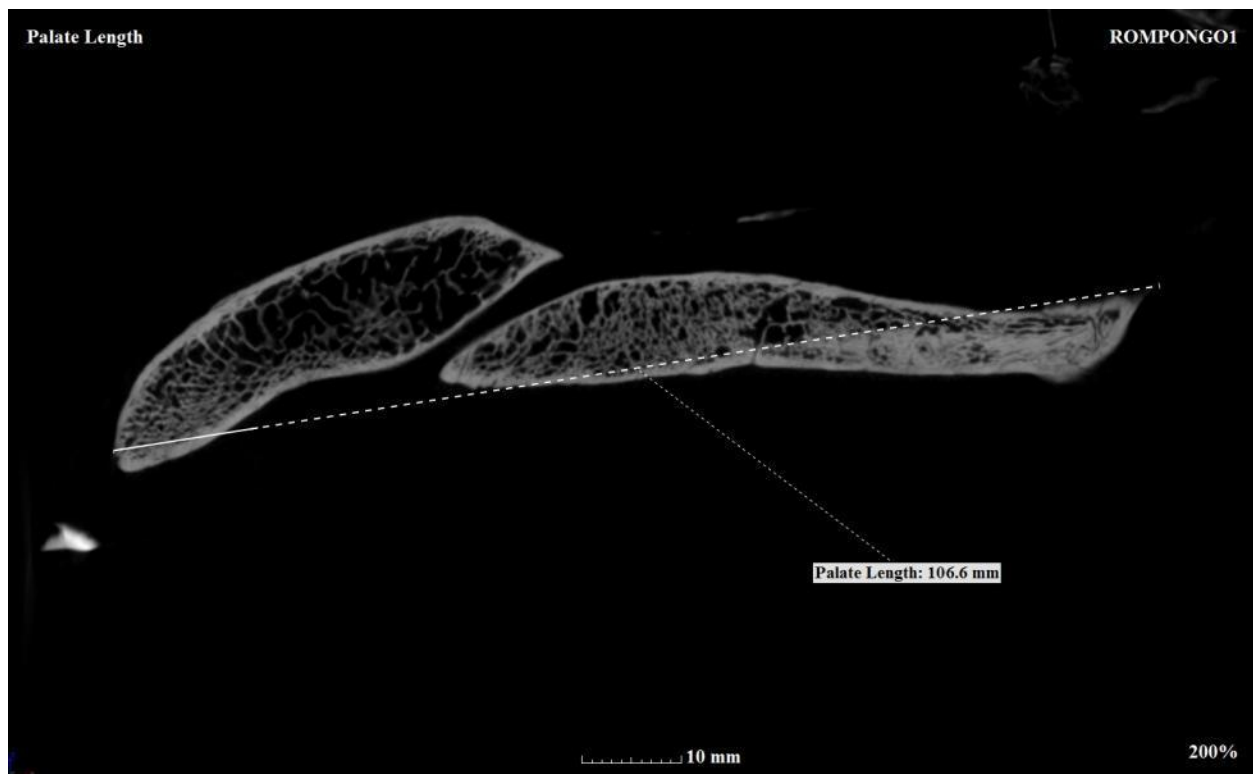
Figure 14 Palate Length (note: The measurement is not fully contained on this sagittal section, as indicated by the dashed line) (μ-CT of adult male *P. abelii*, lateral view)

Premax Length (Premax L): The overall length of the premaxilla/anterior alveolar process measured along its long-axis (see: Figure 15).

Premax Width (Premax W): The overall width of the premaxilla/anterior alveolar process measured at its greatest breadth along an axis approximately perpendicular to the long-axis used for Premax Length (see: Figure 15).
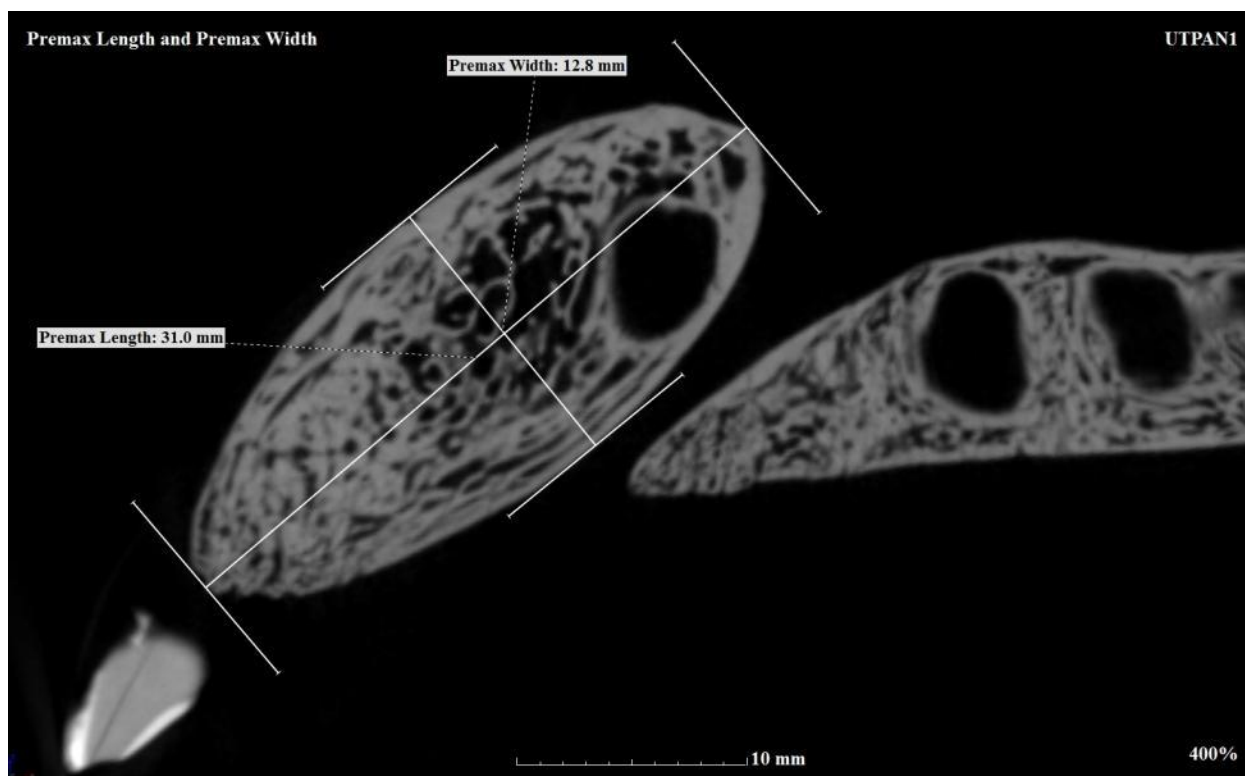
Figure 15 Premax Length and Premax Width (μ-CT of adult male *P. troglodytes*, lateral view)

The measurements of the premaxilla/anterior alveolar process are less precise than the other measurements utilized in this analysis as they are based on estimations of the direction of the long-axis of that element and are not based on well-defined anatomical landmarks. However, as the literature makes frequent reference and assigns phylogenetic significance to the elongation and robusticity of the premaxilla/anterior alveolar process, measurements of these characters were considered vital to this analysis. The Premax Length and Premax Width were also useful in the construction of ratios for comparative analyses of the primate taxa.

6.9.4 Anatomical Measurements of the Incisive Foramen and Incisive Canal

The following anatomical measurements were used to analyze the morphology of the incisive foramen. The following definitions of anatomical measurements refer to a sagittal section through the long-axis of an incisive foramen with the cranium oriented in the FHP. All

measurements were performed using the caliper tool in VGStudio Max. All linear measurements are in millimeters (mm) and all angular measurements are in degrees.

Drop Angle: A right-angle formed by the perpendicular lines connecting the Anterior Pole of the Palatine Process and the Posterior Pole of the Premaxilla (see: Figure 16). The horizontal line that connects the Anterior Pole of the Palatine Process and the fulcrum of the Drop Angle (Overlap) is precisely parallel to the FHP. The Drop Angle is not utilized as a measurement for analysis, but rather was used to orient other measurement. All other measurements of the incisive foramen were performed relative to the Drop Angle to the ensure accuracy and precision of the measurements.
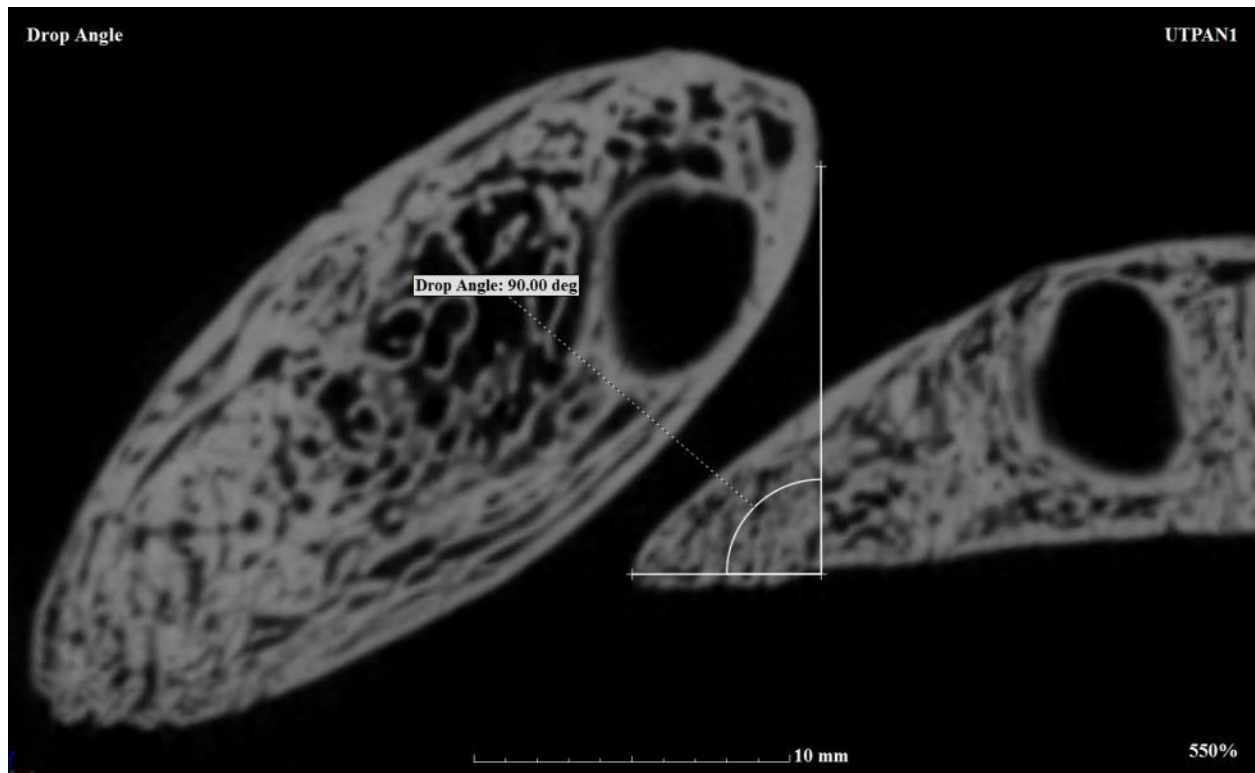
Figure 16 Drop Angle (μ-CT of adult male *P. troglodytes*, lateral view)

Drop: The vertical distance from the Posterior Pole of the Premaxilla to the Anterior Pole of Palatine Process in those individuals that do not exhibit an "overlap" of the palatine process by the premaxilla/anterior alveolar process (see: Figure 17). (For those individual that exhibit an "overlap" of the palatine process by the premaxilla/anterior alveolar process see: Palate Drop). The measurement Drop is perpendicular to the FHP. Drop is a quantitative measure of the

topography of the nasal cavity floor at the incisive foramen, or the "drop" to the nasal cavity floor.
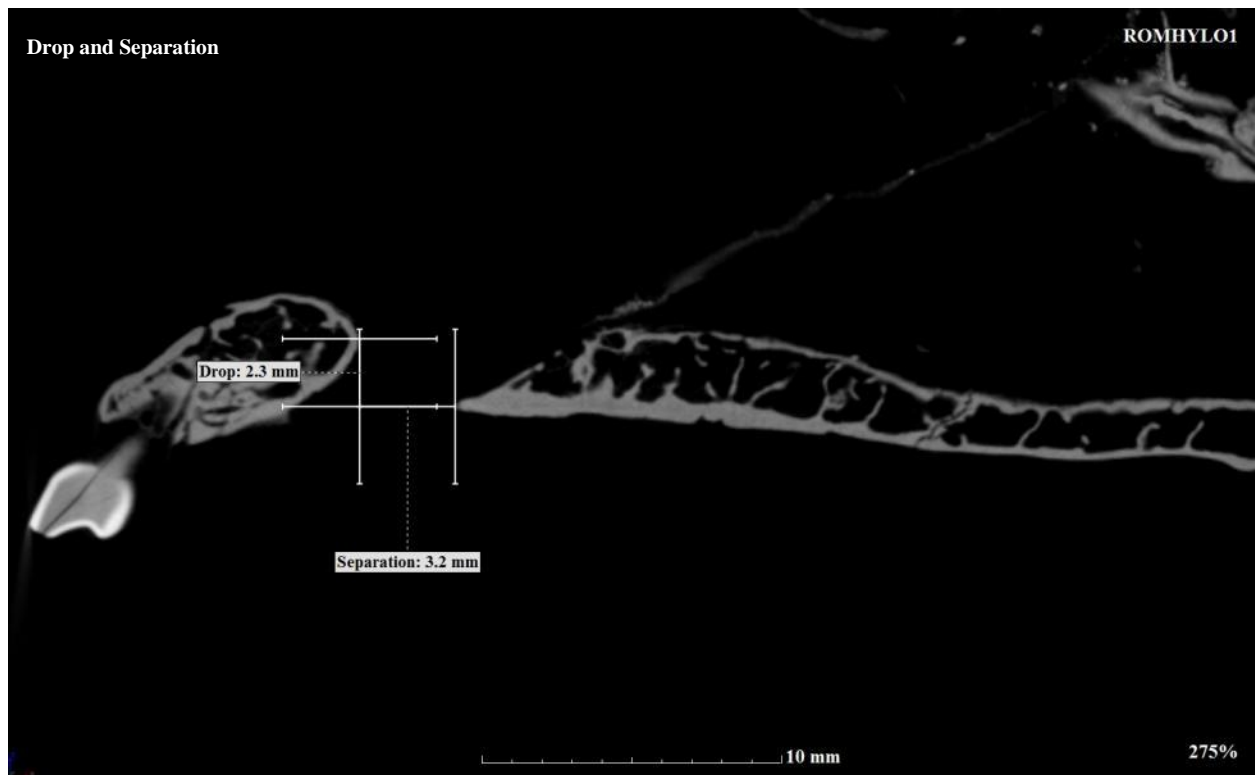
Figure 17 Drop and Separation (µ-CT of adult *H. lar*, lateral view)

Palate Drop: The vertical distance from the Posterior Pole of the Premaxilla to the superior surface of the palatine process in those individuals that exhibit an "overlap" of the palatine process by the premaxilla/anterior alveolar process (see: Figure 18). The measurement Palate Drop is perpendicular to the FHP. Palate Drop is a quantitative measure of the topography of the nasal cavity floor at the incisive foramen. While Drop is a measurement of the vertical distance from the Posterior Pole of the Premaxilla to the Anterior Pole of the Palatine Process, or the degree of "step-down" in the floor of the nasal cavity at the incisive fossa, Palate Drop measures the vertical distance to the superior surface of the palatine process. Palate Drop is analogous to Drop in measuring the degree of "step-down" in the floor of the nasal cavity, but Palate Drop is not directly comparable as the superior surface of the palatine process is typically elevated markedly above the Anterior Pole of the Palatine Process in these specimens.
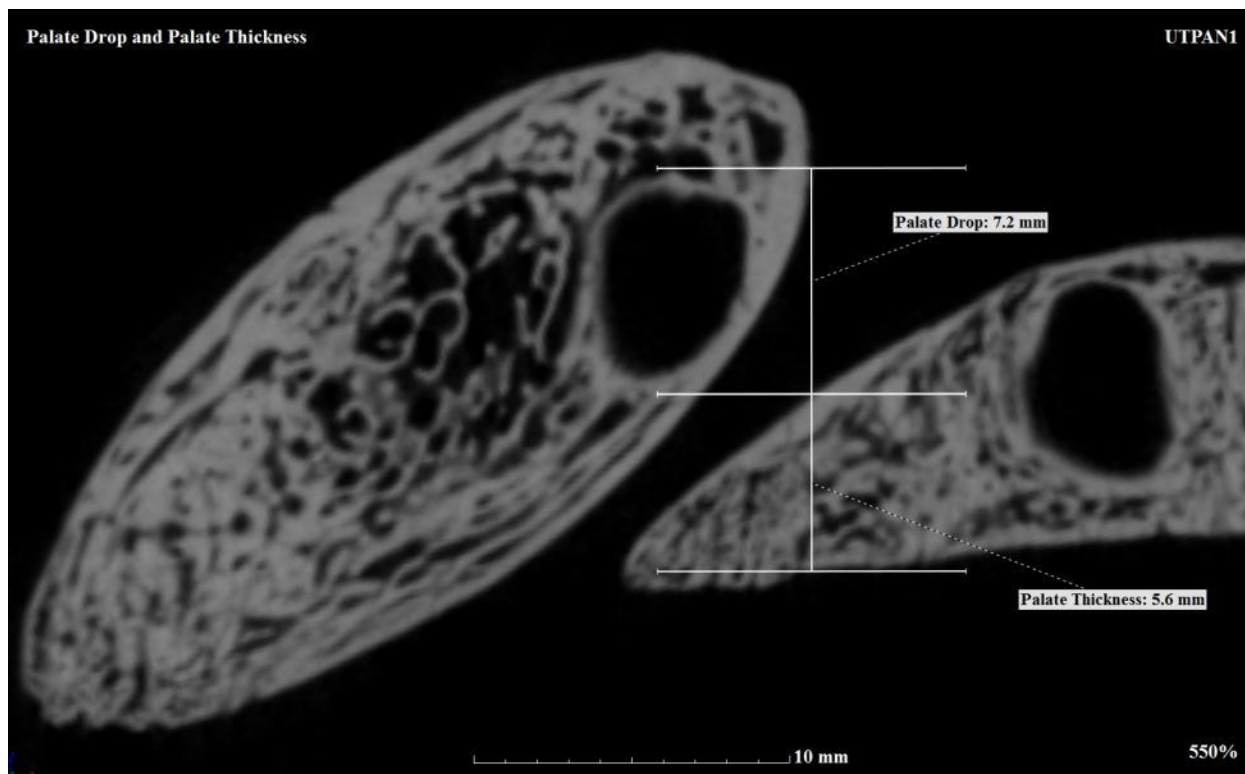
Figure 18 Palate Drop and Palate Thickness (µ-CT of juvenile male *P. troglodytes*, lateral view)

Palate Thickness: The superoinferior (or vertical) thickness of the palatine process directly below the Posterior Pole of the Premaxilla in those individuals that exhibit a positive value of Overlap (see: Figure 18). The line Palate Thickness is collinear with the vertical line forming the Drop Angle. This location was chosen for consistency as the thickness of the palatine process varies considerably in some primate taxa. It was decided not to measure the maximum thickness of the hard palate for analysis as the thickest portion of the hard palate typically lays a large distance posterior to the incisive foramen and does not contribute to the topography of the subnasal anatomy in the region of the incisive foramen. Palate Thickness is a quantitative measure of the thickness of the palatine process directly below the Posterior Pole of the Premaxilla. Palate Thickness was also utilized in the construction of ratios to evaluate the topography of the subnasal anatomy.

Overlap: The horizontal distance from the Posterior Pole of the Premaxilla and the Anterior Pole of the Palatine Process (cf. Ward and Kimbel, 1983; McCollum et al., 1993; Ward and

McCollum, 1997). The measurement Overlap is parallel to the FHP. Overlap is a quantitative measure of the relationship between the premaxilla/anterior alveolar process and the palatine process. A negative value of Overlap indicates a "separation" between the two skeletal elements. Those individuals exhibiting a negative value (or "separation") of Overlap are said to exhibit a "fenestrated" hard palate (see: Figure 17). A positive value of Overlap indicated an "overlap" of the palatine process by the premaxilla/anterior alveolar process (see: Figure 19). Those individuals exhibiting a positive value of Overlap are said to exhibit an "incisive canal".
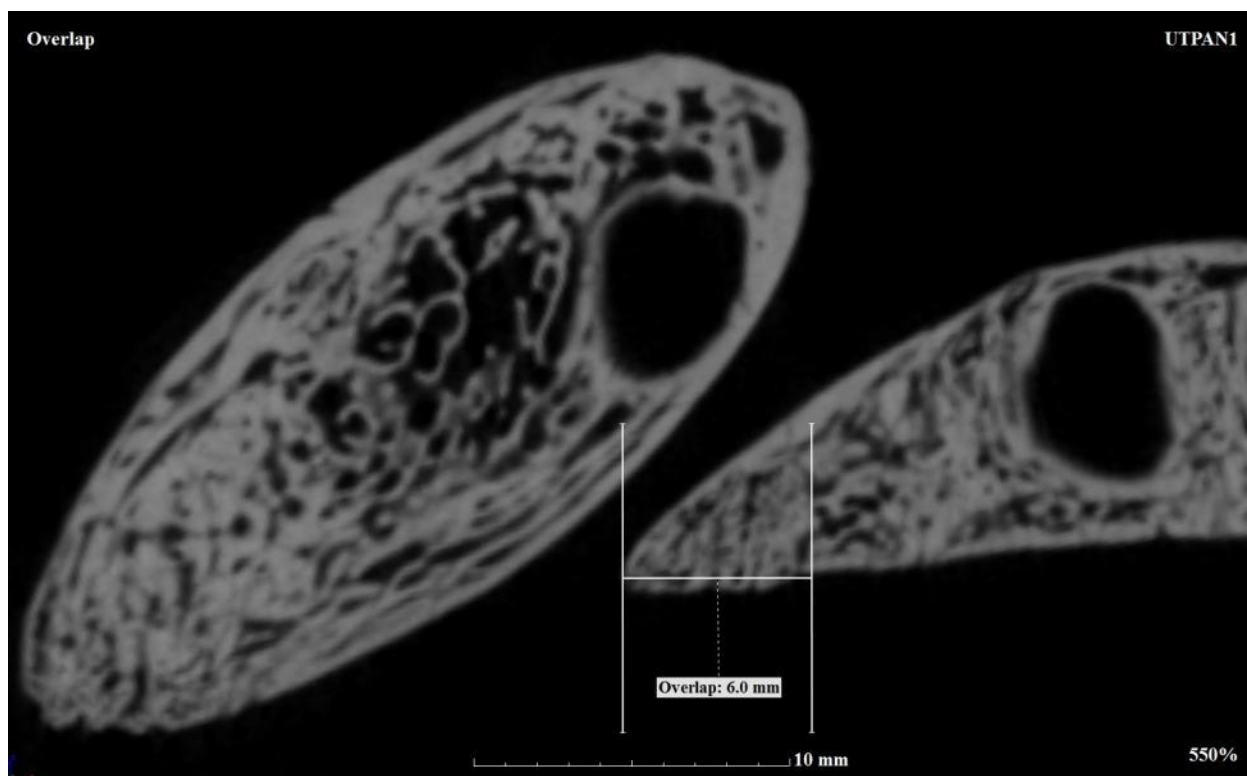
Figure 19 Overlap (μ-CT of juvenile male *P. troglodytes*, lateral view)

Palate Rise: The vertical distance from the Anterior Pole of the Palatine Process to the inferior surface of the premaxilla/anterior alveolar process in those individuals that exhibit a positive value of Overlap (not illustrated). The measurement Palate Rise is perpendicular to the FHP and is analogous Palate Drop. Palate Rise was not utilized as a measurement for analysis, but rather was used in the construction of the Canal Angle (see below).

Half-Palate Drop: The midpoint of the line Palate Drop (see: Figure 20). Half-Palate Drop defines the superoposterior terminus of the incisive canal. Half-Palate Drop was not utilized as a

measurement for analysis, but rather was used in the construction of the Canal Angle and to define Canal Length.

Half-Palate Rise: The midpoint of the line Palate Rise (see: Figure 20). Half-Palate Rise defines the inferoanterior terminus of the incisive canal. Half-Palate Rise was not utilized as a measurement for analysis, but rather was used in the construction of the Canal Angle and to define Canal Length.
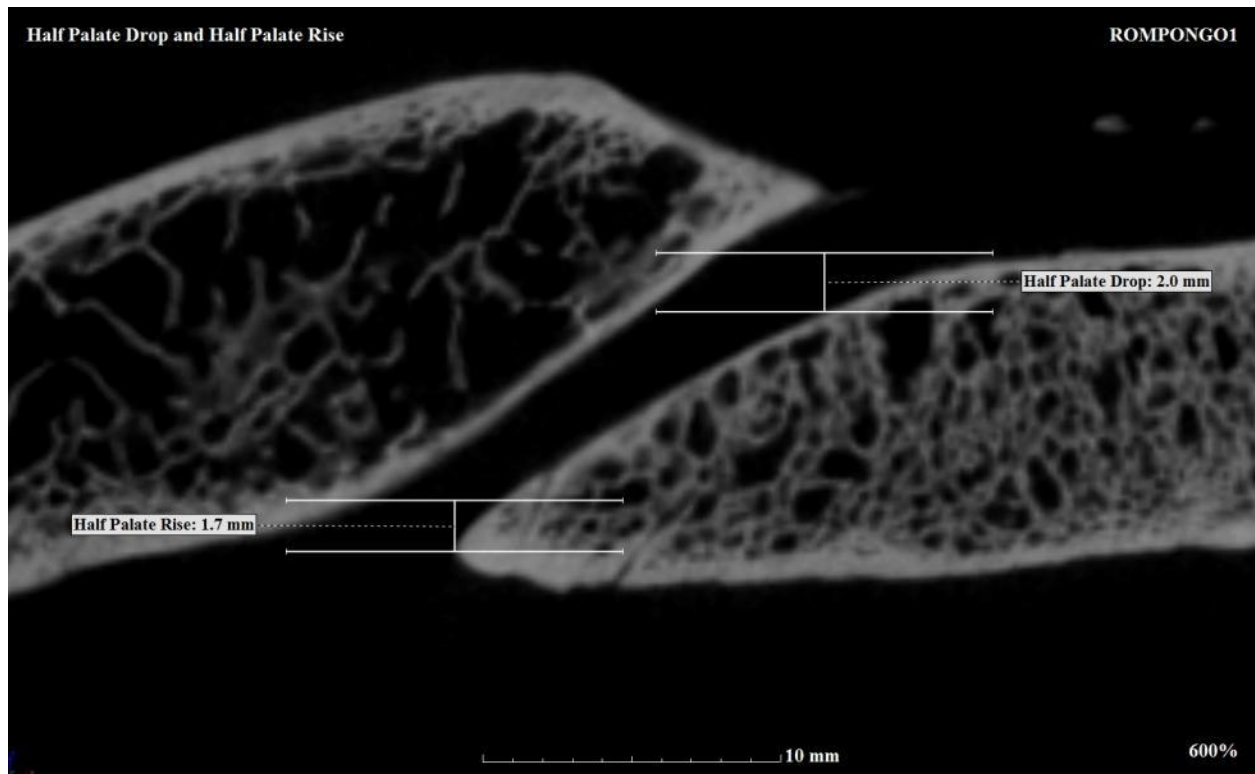
Figure 20 Half-Palate Drop and Half-Palate Rise (μ-CT of adult male *P. abelii*, lateral view)

Canal Angle: The angle formed between the lines Overlap and the line joining the points Half-Palate Rise and Half-Palate Drop (see: Figure 21). Canal Angle is an estimate of the angle of the incisive canal relative to the FHP in those individuals that exhibit a positive value of Overlap. By formally defining Canal Angle in this manner, intra- and inter-observer error in measuring the angle of the incisive canal is thought to be minimized.

Canal Length: The distance between the points Half-Palate Rise and Half-Palate Drop (see: Figure 21). The Canal Length is an estimate of the overall length of the incisive canal in those

individuals that exhibit a positive value of Overlap. The line Canal Length is collinear with the line that defines the Canal Angle.
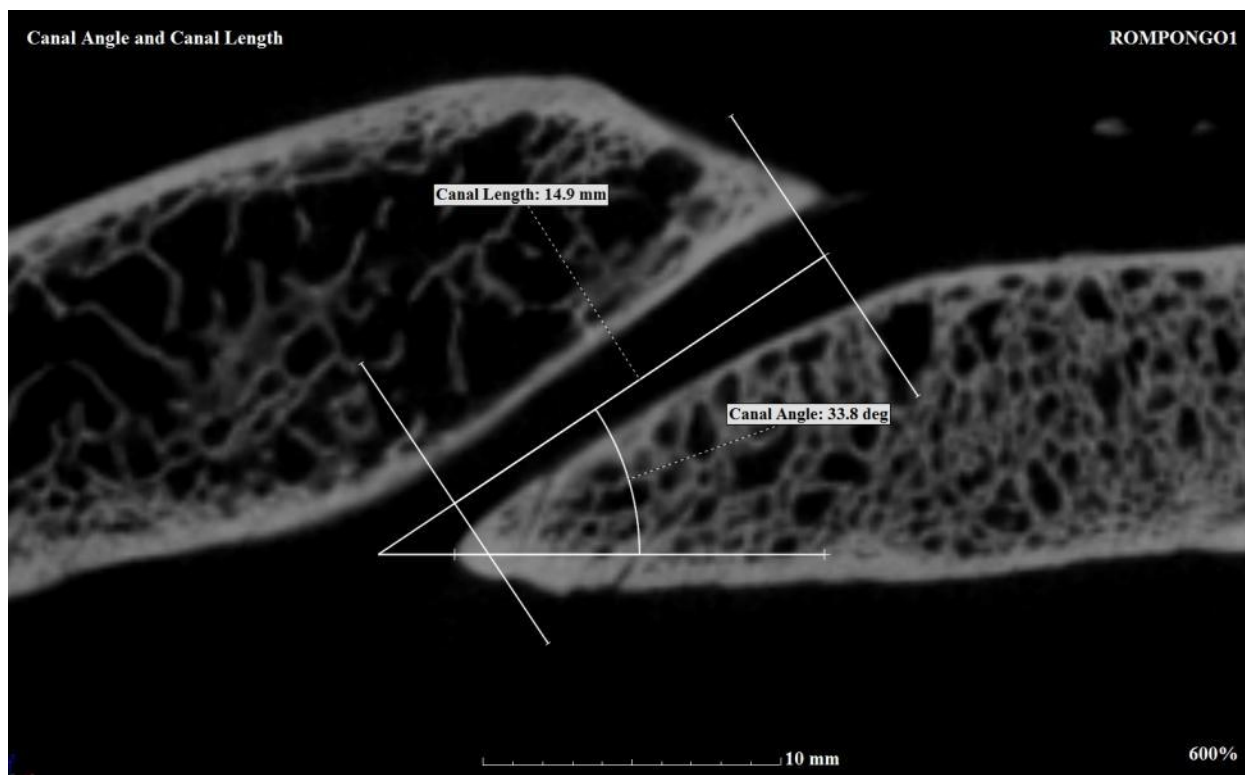
Figure 21 Canal Angle and Canal Length (μ-CT of adult male *P. abelii*, lateral view)

6.10   Ratios

As individuals in this analysis varied by size, due to taxonomic and ontogenetic differences, ratios of relevant measurements were calculated for comparative analyses. A number of ratios were calculated relative to both the Premax Length and the Palate Length to investigate which measurement was more useful for comparisons. Differences in the elongation of the Premaxilla during ontogeny or between taxa may be indicated by differences in the ratio comparing a measurement to Palate Length verse Premax Length.

Premax Length/Premax Width (Premax L/Premax W): Ratio used to evaluate the elongation of the premaxilla relative to the Premax Width.

Premax Length/Palate Length (Premax L/Palate L): Ratio used to evaluate the elongation of the premaxilla relative to the Palate Length.

Overlap/Palate Length (Overlap/Palate L): Ratio used to evaluate the Overlap of the palatine process by the premaxilla relative to the Palate Length. A negative value of the ratio indicates a "separation" between the elements. A positive value of the ratio indicates an "overlap" of the elements.

Overlap/Premax Length (Overlap/Premax L): Ratio used to evaluate the Overlap of the palatine process by the premaxilla relative to the Premax Length. A negative value of the ratio indicates a "separation" between the elements. A positive value of the ratio indicates an "overlap" of the elements.

Drop/Palate Length (Drop/Palate L): Ratio used to evaluate the degree of the "drop" from the Posterior Pole of the Premaxilla to the Anterior Pole of the Palatine Process relative to the Palate Length in those individuals that exhibit a "separation" of the premaxilla/anterior alveolar process from the palatine process.

Drop/Premax Length (Drop/Premax L): Ratio used to evaluate the degree of the "drop" from the Posterior Pole of the Premaxilla to the Anterior Pole of the Palatine Process relative to the Premax Length in those individuals that exhibit a "separation" of the premaxilla/anterior alveolar process from the palatine process.

Palate Drop/Premax Length (Palate D/Premax L): Ratio used to evaluate the degree of the "step-down" from the Posterior Pole of the Premaxilla to the surface of the palatine process relative to the Premax Length in those individuals that exhibit an "overlap" of the palatine process by the premaxilla/anterior alveolar process.

Palate Drop/Palate Thickness (Palate D/Palate T): Ratio used to evaluate the degree of the "step-down" from the Posterior Pole of the Premaxilla to the surface of the palatine process relative to the Palate Thickness in those individuals that exhibit an "overlap" of the palatine process by the premaxilla/anterior alveolar process. As the amount of "step-down" in the subnasal anatomy is influenced by both the height of the Posterior Pole of the Premaxilla above the superior surface of the palatine process (Palate Drop) and the location of the superior surface

of the palatine process itself, which is related to the thickness of the palatine process (Palate Thickness), this ratio was constructed to evaluate the relationship between these two measurements.

Palate Thickness/Palate Length (Palate T/Palate L): Ratio used to evaluate the Palate Thickness relative to the Palate Length in those individuals that exhibit an "overlap" of the palatine process by the premaxilla/anterior alveolar process. This ratio is used to evaluate the thickness or robusticity of the palatine processes.

6.11   Statistical Methods

Access to extant hominoid collections limited the sample sizes available for study. As a result, the small sample sizes of non-human hominoids limited the use of statistical analyses, although the mean ($\bar{x}$) and standard deviation (s) were calculated for each taxon using Microsoft Excel (see: Appendices). A future analysis following the same methodological techniques outlined in this thesis which expands the sample sizes could calculate statistically significant results of all the measurements of the subnasal anatomy. The larger sample of *H. sapiens* crania (n=12) was used to make an initial estimate of intraspecific variation in a hominoid taxon using the mean ($\bar{x}$) and standard deviation (s). The results generated from these measurements and ratios of the hominoid subnasal anatomy are discussed in the following chapter.

7   Results

The following section discusses the results of the micro-CT analysis of the subnasal anatomy for each taxon.

7.1.1   Cercopithecoids

7.1.1.1   *Macaca* and *Papio*

An adult male and an adult female cranium of *Macaca* and *Papio* were analyzed (see: Appendix A). The adult cercopithecoids *Macaca* (-0.95 mm average) and *Papio* (-2.10 mm average) were the only taxa to exhibit negative values of Drop, indicating the premaxillae are depressed below the level of the palatine processes, resulting in "step-up" in the topography of the nasal cavity floor at the incisive foramina (see: Figure 22). Interestingly, the adult *Macaca* (-0.02) and *Papio* (-0.02) exhibited a similar "step-up" in the nasal cavity floor relative to the hard palate length, despite of the discrepancies in the length of the hard palate in these taxa.

However, the adult male *Macaca* (1.4 mm) and *Papio* (3.0 mm) exhibited markedly greater amounts of "step-up" than the adult females (0.6 mm; 1.2 mm, respectively). The adult male *Macaca* (-0.03) and *Papio* (-0.03) also exhibited a markedly greater "step-up" in the nasal cavity floor than the adult females (-0.01; -0.01) relative to the hard palate length. The adult male *Macaca* (-0.14; -0.14) and *Papio* also exhibited larger ratios of ""step-up"" relative to the premaxillary length than the adult females (-0.07; -0.08), suggestive of sexual dimorphism in this character in adult cercopithecoids.

The cercopithecoids *Macaca* (-4.9 mm average) and *Papio* (-8.80 mm average) also exhibited the largest negative values of Overlap, resulting in a large "separation" between the premaxillae and the palatine processes, indicative of large palatal fenestrae (see: Figure 22). While the adult male (-4.9 mm) and female *Macaca* (-5.0 mm) exhibited a similar amount of "separation", the adult male *Papio* (-12.1 mm) exhibited over twice the "separation" of the adult female (-5.5 mm), indicating sexual dimorphism in this character in *Papio*. The "separation" of the subnasal elements relative to the hard palate length was similar in the adult male (-0.11) and female *Macaca* (-0.10 average), and in the adult male *Papio* (-0.11 average), even though the adult male

Papio exhibited the longest hard palate in this analysis. *Papio* males exhibit an extreme elongation of the face, due to their large, sexually dimorphic canines (Swindler and Curtis, 1998). In contrast, the adult female *Papio* (-0.06) exhibited a much smaller ratio of "separation" relative to the hard palate length.
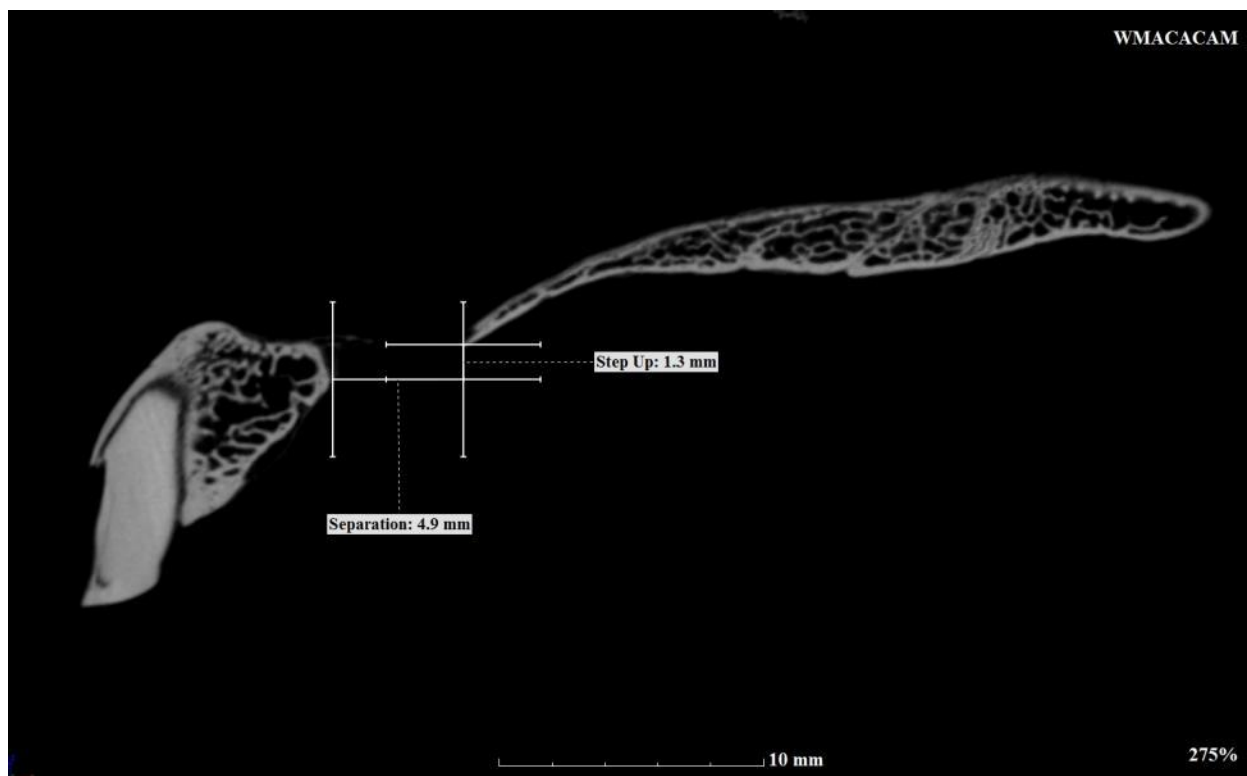
Figure 22 "Cercopithecoid Pattern" of the Subnasal Anatomy (μ-CT of adult male *M. mulatta*, lateral view)

Similar relationships were demonstrated when comparing the "separation" relative to the premaxillary length in the adult male (-0.55) and female *Papio* (-0.60) and the male and female *Macaca* (-0.54; -0.60). While these ratios verify the sexual dimorphism in the size of the palatal fenestrae in *Papio*, they also suggest that *Macaca* exhibits relatively larger fenestrae than *Papio*, as the larger fenestrae in the *Papio* male are likely due to the sexually dimorphic elongation of the face.

Macaca exhibited the smallest elongation of the premaxillae relative to premaxillary width (1.55 average) in the analysis, suggestive of gracile premaxillae. While the adult male (22.0 mm) and female *Papio* (15.5 mm) exhibited marked differences in the premaxillary length, suggestive of

sexual dimorphism, the adult male (2.46) and female (2.32) exhibited similar ratios of premaxillae length relative to the hard palate length. In is noteworthy that while adult *Papio* exhibited an elongation of the premaxillae relative to the premaxillary width compared to the adult *Macaca*, *Papio* (0.19 average) and *Macaca* adults (0.19 average) exhibited similar ratios of the premaxillary length relative to the hard palate length. These ratios indicate that the cercopithecoid premaxillae are relatively gracile and do not exhibit sexual dimorphism, although the premaxillae of *Macaca* are possibly more robust than those of *Papio*.

7.1.2   Hylobatids

7.1.2.1   *Hylobates lar* and *Symphalangus syndactylus*

Two adult hylobatid crania were analyzed (see: Appendix A). The hylobatids *H. lar* (2.3 mm) and *S. syndactylus* (1.5 mm) exhibited small positive values of Drop, indicating the premaxillae are elevated slightly above the level of the palatine processes, resulting in a "drop" in the topography of the nasal cavity floor at the incisive foramina (see: Figure 23). Recall that the measurement Drop is only exhibited by those individuals that also exhibit a "separation" of the premaxilla/anterior alveolar process from the palatine process. Interestingly, the smaller *H. lar* (2.3 mm) exhibited a markedly larger "drop" in the nasal cavity floor than *S. syndactylus* (1.5 mm). *H. lar* also exhibited a larger "drop" relative to the hard palate length (0.06) and premaxillary length (0.26) than *S. syndactylus* (0.03; 0.17, respectively).

The hylobatids exhibited a smaller negative value of Overlap (-3.55 mm average) and thus exhibited a relatively smaller "separation" between the premaxillae and the palatine processes than the cercopithecoids (see: Figure 23). The larger *S. syndactylus* (3.9 mm) exhibited a slightly larger "separation" than *H. lar* (-3.2 mm).   The hylobatids exhibited a smaller ratio of "separation" relative to the premaxillary length (-0.40 average) than the adult *Macaca* (-0.57 average) and the adult male *Papio* (-0.55 average), although the adult female *Papio* (-0.35) exhibited a similar ratio. While *S. syndactylus* (-0.44) exhibited a larger "separation" relative to the premaxillary length than *H. lar* (0.36), they exhibited similar ratios of "separation" relative to the hard palate length (-0.08; -0.07).
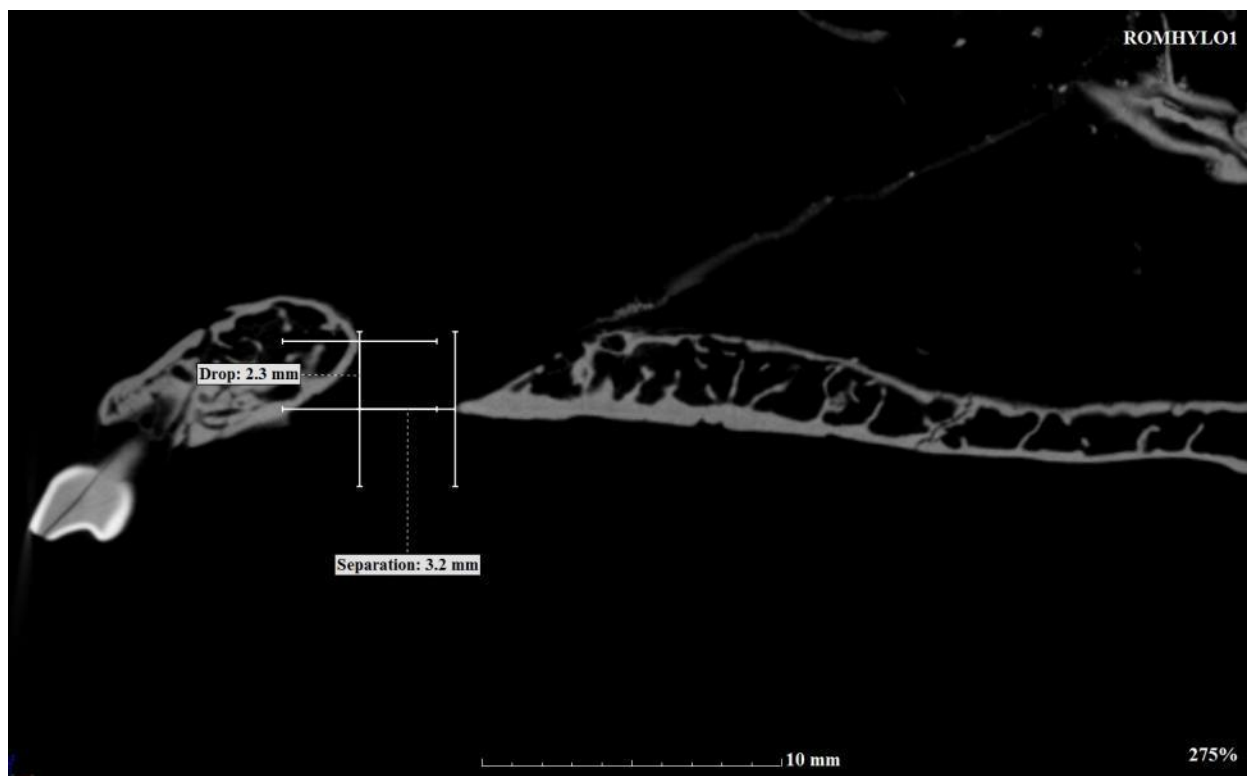
Figure 23 "Hylobatid Pattern" of the Subnasal Anatomy (µ-CT of adult _H. lar_, lateral view)

H. lar (2.20) exhibited a similar relationship of the premaxillary length to the hard palate length as the adult _Papio_ (2.39 average), while _S. syndactylus_ (1.17) exhibited a ratio more similar to the adult _Macaca_ (1.55), indicating there is no increase in the elongation of the premaxillae in the hylobatids. However, _H. lar_ exhibited a marked elongation of the premaxillae relative to the premaxillary width, and the length of the hard palate (0.23; 0.16). However, _S. syndactylus_ also exhibited a markedly longer hard palate (57.0 mm) and wider premaxillae (7.6 mm) than _H. lar_ (40.0 mm; 4.1 mm), contributing to the discrepancies in the ratios between the two taxa. It does appear that the premaxillae of _H. lar_ are elongated relative to _S. syndactylus_, while _S. syndactylus_ exhibits an increase in the robusticity of the premaxillae over _H. lar_.

7.1.3   Hominids

7.1.3.1   Infant and juvenile hominids

Among the non-human hominids, only infants and young juveniles exhibited a Drop measurement as they were the only hominids to also exhibit a "separation" of the premaxilla from the palatine process (see: Figure 24). The *Gorilla* (0.7 mm) and *Pongo* (1.5 mm) infants exhibited small positive values of Drop, indicating that the premaxillae are elevated above the level of the palatine processes, resulting in a "drop" in the topography of the nasal cavity floor at the incisive foramina (see: Figure 24). The *Gorilla* and *Pongo* infant hominids exhibited smaller "drops" than the hylobatids (1.9 mm average). The infant *Gorilla* exhibited smaller ratios of "drop" relative to the hard palate length (0.2) and the premaxillary length (0.08) than the hylobatids (0.04 average; 0.21 average, respectively), as did the infant *Pongo* (0.04; 0.11). The youngest *Pan* juvenile (UTPAN2) exhibited a much larger "drop" (7.3 mm) in the nasal cavity floor.

The *Gorilla* (-2.0 mm) and *Pongo* (-2.0 mm) infants and the youngest *Pan* juvenile (UTPAN2; -0.2 mm) exhibited negative values of Overlap and thus exhibited smaller "separations" between the premaxillae and the palatine processes than the cercopithecoids or hylobatids. The infant *Gorilla* also exhibited smaller "separations" relative the hard palate length (-0.06) and premaxillary length (-0.22) than the hylobatids (-0.07; -0.40), as did the infant *Pongo* (-0.05; -0.15), and the juvenile *Pan* (UTPAN2, -0.00; -0.01). Although a *Pan* infant was not available for analysis, it would be interesting to see if *Pan* also exhibited similar sized palatal fenestrae at a similar stage of ontogeny.

The *Gorilla* (1.11; 0.30) and *Pongo* (1.14; 0.32) infants exhibited very similar relationships in the length of the premaxillae relative to the premaxillary width and the hard palate length, even though the adults of these taxa exhibit significant differences in their premaxillary morphology (compare: infant *Gorilla* Figure 24 and adult male *Gorilla* Figure 25).
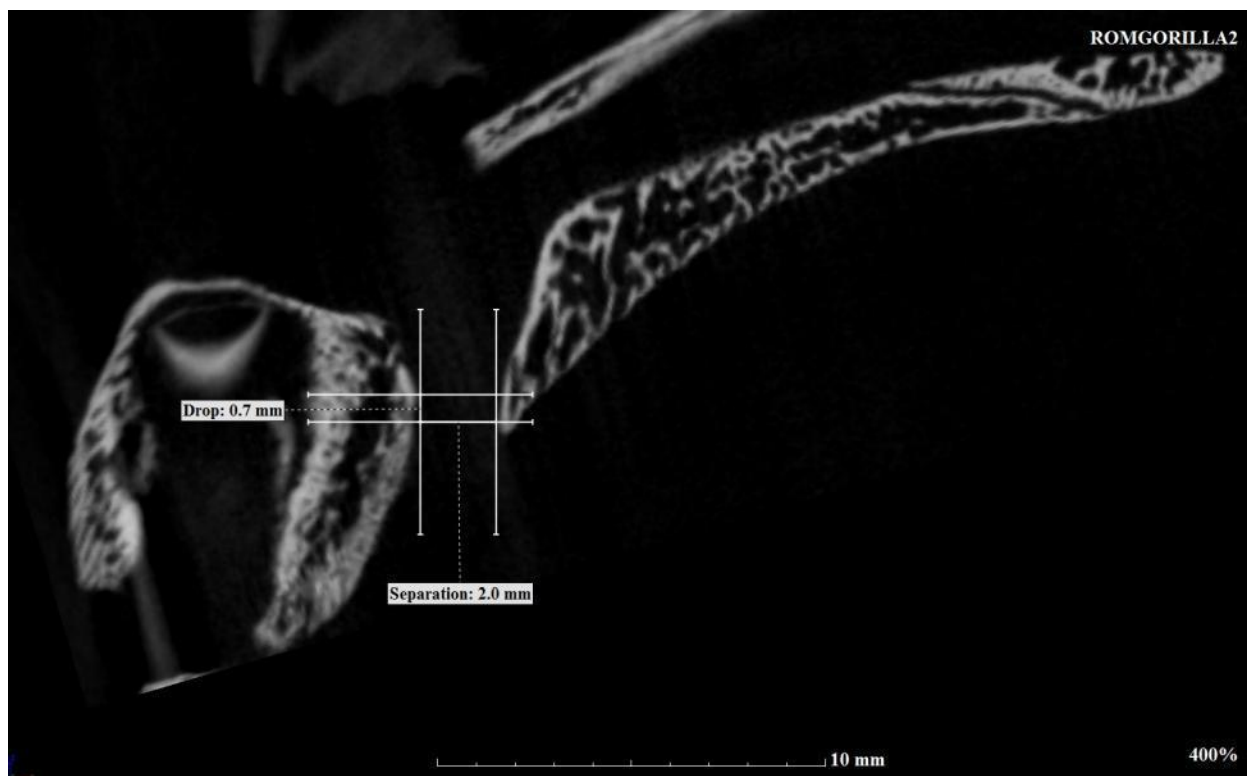
Figure 24 Infant Hominid Subnasal Anatomy (µ-CT of infant *G. gorilla*, lateral view)

7.1.3.2   Hominines

7.1.3.2.1   *Gorilla*

It should be reiterated that the measurement Palate Drop was analogous to Drop in measuring the topography of the nasal cavity floor in those individuals that exhibit an "overlap" of the premaxilla/anterior alveolar processes by the palatine process. In those individuals that exhibit a Drop measurement the term "drop" is used to discuss the topography of the nasal cavity floor, while in those individuals that exhibit a Palate Drop measurement the term "step-down" is used to describe the topography, in order to avoid confusion.

Two adult male and an infant *Gorilla* crania were analyzed (see: Appendix A). The adult male *Gorilla* exhibited large values of Palate Drop (7.15 mm average), indicating that the premaxillae are elevated above the level of the palatine processes, resulting in a ""step-down"" in the topography of the nasal cavity floor at the incisive foramina (see: Figure 25). However, there was marked variation between the amount of "step-down" in *Gorilla* individuals

(ROMGORILLA1, 8.9 mm; WGORILLA1, 5.4 mm, respectively). The adult male *Gorilla* exhibited an absolutely larger "step-down" in the nasal cavity floor than the hylobatids, indicative of deep nasal incisive fossae at the incisive foramen. The adult male *Gorilla* also exhibited a large "step-down" in the nasal cavity floor relative to the premaxillary length (0.20), although there was, again, marked variation between the two individuals (ROMGORILLA1, 0.20; WGORILLA1, 0.16).
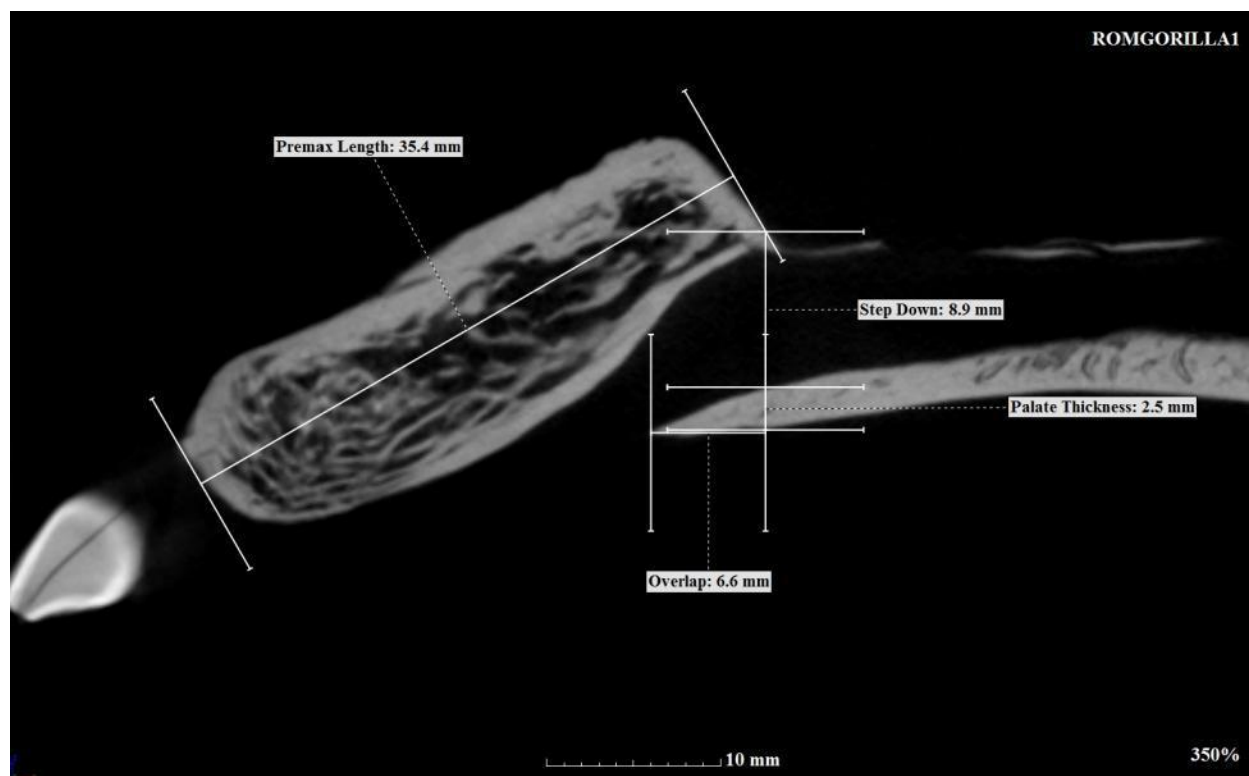
Figure 25 "*Gorilla* Pattern" of the Subnasal Anatomy (μ-CT of adult male *G. gorilla*, lateral view)

Unlike the hylobatids, cercopithecoids, or infant hominids, the adult male *Gorilla* exhibited large positive values of Overlap (4.55 mm average), indicative of a large "overlap" of the palatine processes by the premaxillae, although there was also a marked variation between the two individuals (ROMGORILLA1, 6.66 mm; WGORILA1, 2.5 mm) (see: Figure 25). The adult male *Gorilla* also exhibited large ratios of "overlap" relative to the hard palate length (0.04, average) and the premaxillary length (0.13, average).

The large individual variation in the "step-down" and "overlap" in *Gorilla* were caused by variance in the location of the Posterior Pole of the Premaxilla, due to morphological differences in the premaxillae. McCollum and Ward (1997) also noted that the morphology of the subnasal anatomy in *Gorilla* caused some difficulties in the construction of measurements in their analyses.

Among the hominids the adult male *Gorilla* exhibited extreme ratios of Palate Drop relative to Palate Thickness (7.18 average), the largest ratio in the analysis, even taking into account the marked variation between the two individuals (ROMGORILLA1, 10.80; WGORILLA1, 3.56). This was largely due to the thinness of the palatine process in *Gorilla*.

The adult male *Gorilla* (1.50 mm average) exhibited the smallest values of Palate Thickness among the adult hominids, although there was a marked degree of individual variation in the thickness of the palatine process (ROMGORILLA1, 2.5 mm; WGORILLA1, 0.5 mm) (see: Figure 25). The adult male *Gorilla* also exhibited the thinnest palatine processes to the hard palate length (0.01), although there was a marked degree of individual variation in these ratios. The thinness of the palatine processes was noteworthy as the adult male *Gorilla* also exhibited the longest values of Palate Length in the analysis (107.45 mm average).

As the adult male *Gorilla* exhibited an "overlap" of the subnasal elements, their configuration of the subnasal anatomy is described as an "incisive canal". The adult males exhibited similar angles of the "incisive canal" (ROMGORILLA1, 32.2 degrees; WGORILLA1, 34.1 degrees). However, the lengths of their canal differed markedly (ROMGORILLA1, 7.8 mm; WGORILLA1, 3.0 mm), again due to the variation in the morphology of the premaxillae and the location of the Posterior Pole.

The premaxillae of the adult male *Gorilla* are elongated relative to the premaxillary width (2.73 average) and the hard palate length (0.32 average) compared with *H. lar* (2.20; 0.23) and *S. syndactylus* (1.17; 0.16) (see: Figure 25). This suggests that hominid premaxillae are elongated relative to the hylobatids.

While the adult male *Gorilla* exhibited markedly longer premaxillae relative to their width (2.73 average) than the infant *Gorilla* (1.11), the adult males exhibited a similar ratio of the

premaxillae relative to the hard palate length (0.32 average) as the infant (0.30). This indicates that the premaxilla elongates isometrically relative to its width during ontogeny, scales with positive allometry relative to overall hard palate length during growth.

7.1.3.2.2   *Pan*

An adult female and four juvenile *Pan* crania were analyzed (see: Appendix A). The adult female (6.7 mm) and the older *Pan* juveniles (6.40 mm average) exhibited large values of Palate Drop indicating that the premaxillae are elevated above the level of the palatine processes, resulting in a "step-down" in the topography of the nasal cavity floor at the incisive foramina (see: Figure 26). The adult female *Pan* exhibited a similar degree of "step-down" to the nasal cavity floor as the adult male *Gorilla*, indicative of deep nasal incisive fossae at the incisive foramen. There was an increase in the degree of the "step-down" in the nasal cavity floor with age among *Pan* juveniles, with the oldest juvenile (UTPAN1) exhibiting a larger "step-down" (7.2 mm) than the adult female, although the degree of "step-down" relative to the premaxillary length was similar in the adult female (0.29) and juveniles (0.27 average). The adult female (0.29) and the older *Pan* juveniles (0.27 average) exhibited a slightly larger "step-down" in the nasal cavity floor relative to the premaxillary length than the adult male *Gorilla* (0.20 average).

The adult female *Pan* (4.4 mm) exhibited a large positive value of Overlap, similar to those of the adult male *Gorilla* (4.55 mm average), and indicative of a large "overlap" of the palatine processes by the premaxillae (see: Figure 26). The oldest *Pan* juvenile (UTPAN1) exhibited an even larger "overlap" (6.0 mm) of the subnasal elements. The adult female and oldest *Pan* juvenile also exhibited larger ratios of "overlap" relative to the hard palate length (0.06; 0.08, respectively) and the premaxillary length (0.19; 0.19), than the adult male *Gorilla* (0.13, average). The ratios of "overlap" to both the hard palate length and the premaxillary length increased with age among the *Pan* juveniles.

The adult female *Pan* exhibited a large ratio of Palate Drop relative to Palate Thickness (1.81) compared to other hominids, although much smaller than those of the adult male *Gorilla*, due to the increase in thickness of palatine processes in *Pan*. The degree of "step-down" relative to the thickness of the palatine processes in *Pan* juveniles decreased with age. The oldest *Pan* juvenile

(UTPAN1) had a smaller ratio of "step-down" to palatine process thickness (1.29) than the adult female (1.81).
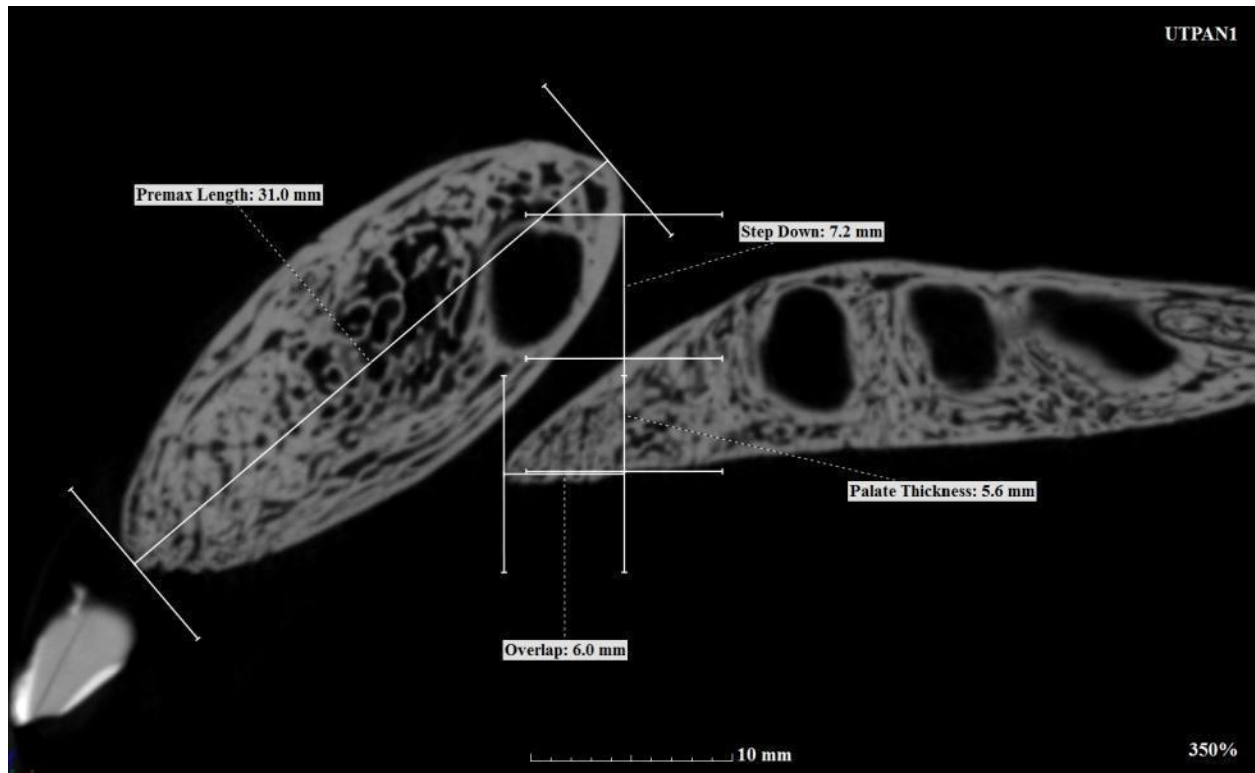
Figure 26 "*Pan* Pattern" of the Subnasal Anatomy (μ-CT of juvenile male *P. troglodytes*, lateral view)

The adult female (3.7 mm) and juvenile *Pan* (3.67 mm average) exhibited greater values absolute values of Palate Thickness than *Gorilla* (see: Figure 26). The thickness of the palatine processes increased with age among *Pan* juveniles. The oldest *Pan* juvenile (UTPAN1, 5.6 mm) exhibited a markedly thicker palatine processes than the adult female (3.7 mm).

The adult female (0.05) and juvenile *Pan* (0.06 average) also exhibited thicker palatine processes relative to the hard palate length than the adult male *Gorilla* (0.01), indicating an increase in the palatine processes in *Pan*. The thickness of the palatine processes relative to the hard palate length increases with age among *Pan* juveniles suggesting an increase in the thickness of the palatine processes during ontogeny. The oldest *Pan* juvenile (UTPAN1) exhibited a markedly thicker palatine processes relative to the hard palate length than the adult female (0.08).

As the adult female and juvenile *Pan* exhibited an "overlap" of the subnasal elements, their configuration of subnasal anatomy is described as an "incisive canal". The adult female (52.3 degrees) and juvenile *Pan* (65.07 degrees average) exhibited markedly steeper angles of the "incisive canal" than *Gorilla* (33.15 degrees average). There is a trend of a decrease in the angle of the "incisive canal" with age among in *Pan*. The length of the "incisive canal" generally increased with age among the *Pan* juveniles, although the oldest *Pan* juvenile (UTPAN1) exhibited a longer "incisive canal" (9.9 mm) than the adult female (7.2 mm), or the adult male *Gorilla* (5.40 mm average).

The hard palate length of the oldest *Pan* juvenile (UTPAN1, 74.4 mm) was longer than that of the adult female (WPAN1, 71.9 mm). While the differences in hard palate length may have been due to individual variation, UTPAN1 could be have been a large female individual, UTPAN1 also exhibited a larger "step-down" in the nasal cavity floor, "overlap" of the subnasal elements, elongation of the premaxillae, length of the "incisive canal", and an increase in palatal thickness relative to the adult female (WPAN1), suggesting that UTPAN1 may have been a male and that there male be morphological differences in the proportions of the subnasal anatomy due to sexual dimorphism in *Pan*.

The oldest *Pan* juvenile (UTPAN1) exhibited a markedly longer premaxilla (31.0 mm) than the adult female (WPAN1, 23.0 mm), although they both exhibited similar premaxillary widths (12.8 mm; 12.9 mm) (see: Figure 26). The length of premaxillae of the adult female (0.32) and juvenile *Pan* (0.41) relative to the hard palate length were similar or larger than that of the adult male *Gorilla* (0.32). However, the premaxilla of the adult female (1.78) *Pan* was less elongated relative to the premaxillary width than those of the *Pan* juveniles (2.24 average) or adult male *Gorilla* (2.73 average). The premaxillae of the adult female *Pan* are relatively elongated in comparison to the cercopithecoids and the hylobatids, similar to the adult male *Gorilla*, but the premaxillae are elongated to a greater degree than *Gorilla*.

The relationship between the premaxillary length and premaxillary width appeared to be fairly constant among the *Pan* juveniles. *Pan* juveniles exhibit a large ovoid shape of the premaxillae in sagittal sections through the incisive foramen, unlike the more rectangular morphology exhibited by the adult female *Pan* and adult male *Gorilla*. It is uncertain whether the differences

in the morphology of adult female and juvenile *Pan* premaxillae are due to ontogeny, sexual dimorphism, or individual variation, and this warrants further study.

7.1.3.2.3   *Homo sapiens*

Three adult female, six adult male, and three juvenile female *H. sapiens* crania were analyzed (see: Appendix A). *H. sapiens* was the only taxon in the analysis that exhibited both a "separation" and an "overlap" of the subnasal elements, and measurements of Drop and Palate Drop, respectively.

Those *H. sapiens* individuals that exhibited a "separation" of the subnasal elements exhibited a morphology of the anterior alveolar process that was similar to the premaxillae of the other adult hominines, although more vertically oriented, resulting in steeply inclined incisive foramina (see: Figure 27).
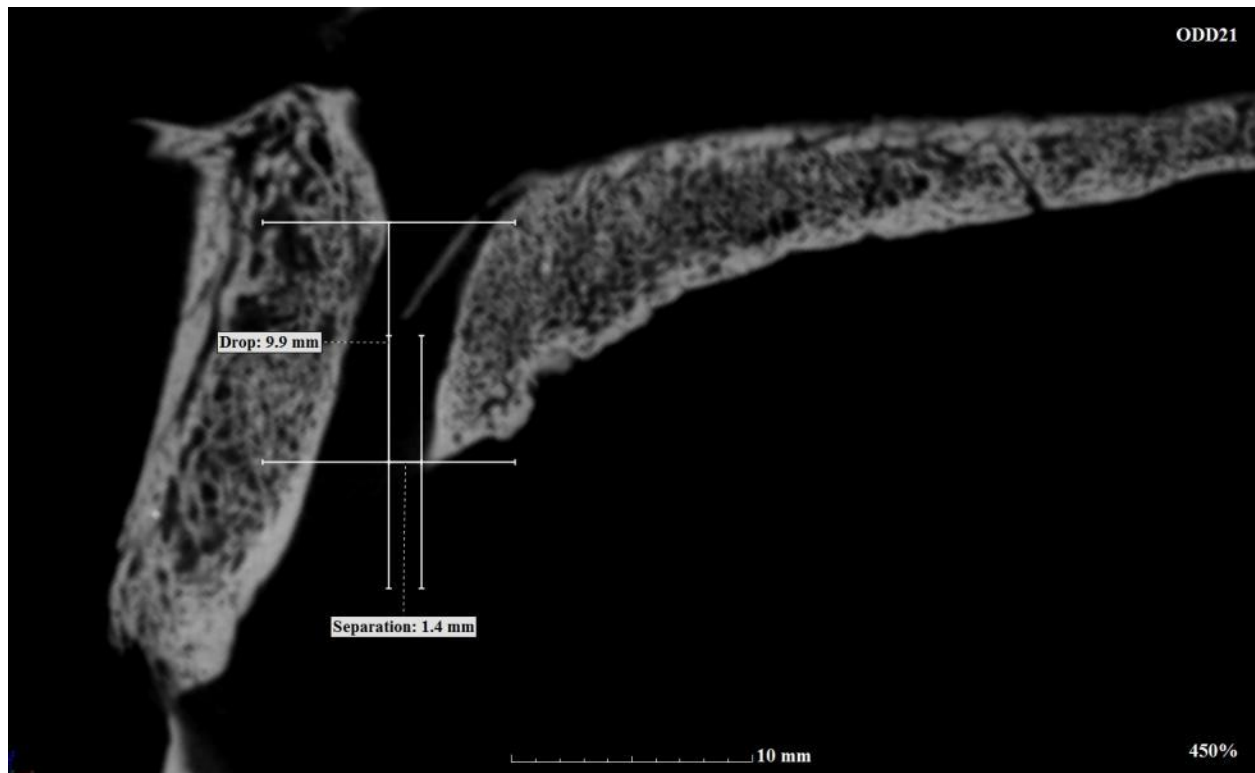
Figure 27 Separation of the Subnasal Elements in *H. sapiens* (µ-CT of adult male, lateral view)

While a number of individuals exhibited the distinctive "inverted-L pattern" of the anterior alveolar processes, in only one individual (ODD 2) did the "superior plate" of the anterior alveolar process contribute to the formation of this "inverted-L pattern" and an "overlap" of the subnasal elements (see: Figure 28) (cf. McCollum et al., 1993; McCollum and Ward, 1997). The "inverted-L pattern" was most typically formed by the bony nasal septum (the prevomer/vomer) which articulated with the anterior alveolar process, and not from a posterior extension of the anterior alveolar process. While the "superior plate" was formed partially by the anterior alveolar processes, it appeared that the bony nasal septum was most responsible for its formation.
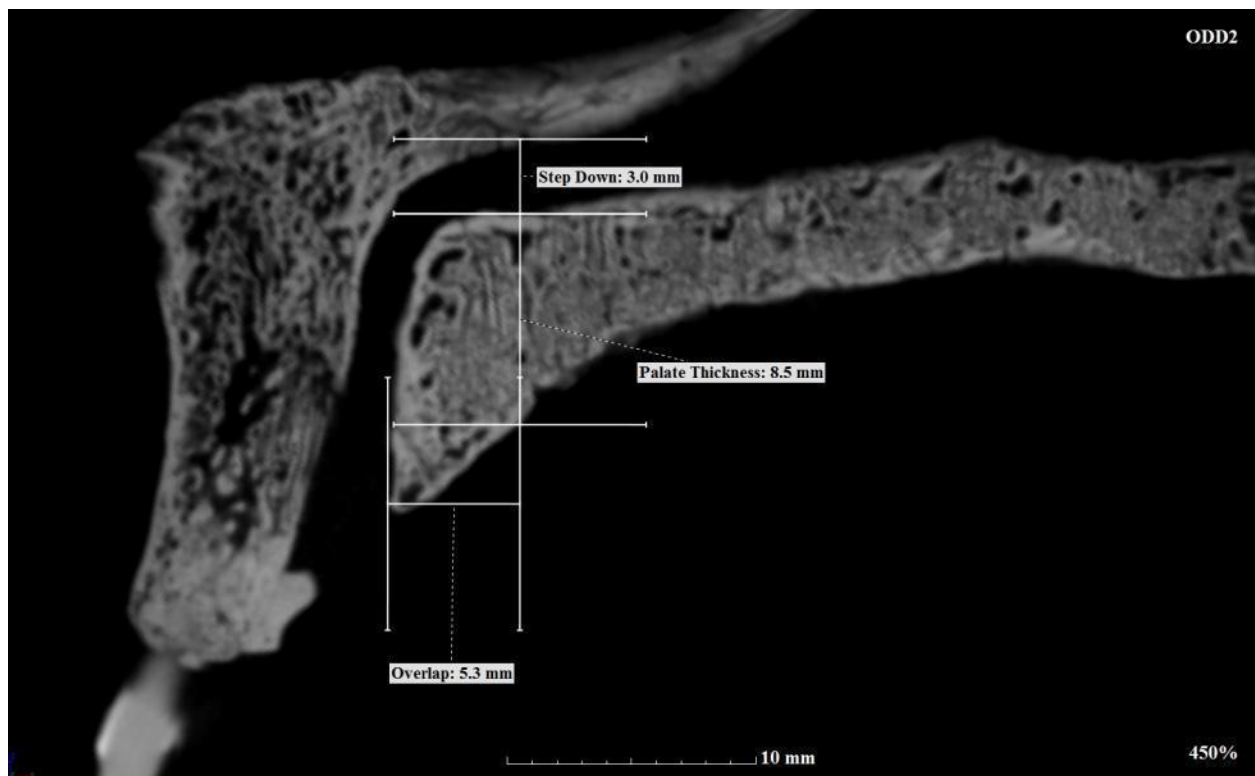
Figure 28 Overlap of the Subnasal Elements in *H. sapiens* (μ-CT of adult female, lateral view)

It should be noted that while the micro-CT images could generally distinguish between the "intermaxillary plate," the "superior plate," and the bony nasal septum, in some individuals bone remodelling obliterated the articulations between the elements, resulting in some difficultly indentifying the Posterior Pole. Recall that the Posterior Pole should be located on the anterior alveolar process. Thus, it was found that the contributions of the bony nasal septum to the

formation of the "superior plate" complicated the interpretation of the subnasal anatomy in *H. sapiens*.

Three of the six adult males (8.83 mm average) and two of the three juvenile females *H. sapiens* (5.75 mm average) exhibit large positive values of Drop, indicating the premaxillae are elevated above the level of the palatine processes, resulting in a "drop" in the topography of the nasal cavity floor at the incisive foramina (see: Figure 27). It should be noted that the juvenile females exhibit a marked variation of "drop" (ODD16, 8.9 mm; ODD17, 2.6 mm). The "drop" in the adult male *H. sapiens* was the largest in the analysis, although similar in size to that exhibited by the youngest *Pan* juvenile (UTPAN2, 7.3 mm).

The three adult males (0.40 average) and the juvenile female (ODD16, 0.37) exhibited the largest "drops" relative to the premaxillary length in the analysis, although similar to the ratio exhibited by the youngest *Pan* juvenile (UTPAN2, 0.36). The three adult male (0.16 average), the juvenile female (ODD16, 0.17) *H. sapiens*, and the youngest *Pan* juvenile (UTPAN2, 0.16) also exhibited similar large ratios of the "drop" relative to the hard palate length. The oldest juvenile female *H. sapiens* (ODD17) exhibited markedly smaller ratios of "drop" relative to the premaxillary length (0.15) and hard palate length (0.05) compared to these individuals, although it should be noted that the upper adult third molars have just begun to erupt and ODD17 has nearly reached the adult stage of ontogeny.

Recall that individuals that exhibit an "overlap" of the subnasal elements also exhibit a "step-down" in the nasal cavity floor. Three of the six adult males (4.37 mm average), all three of the adult females (3.60 mm average), and the youngest juvenile female (ANLAB, 2.7 mm) exhibited moderate values of Palate Drop, indicating that the premaxillae are elevated above the level of the palatine processes, resulting in a "step-down" in the topography of the nasal cavity floor at the incisive foramina (see: Figure 28). While the adult males exhibited a larger average "step-down" than the adult females, there was a large degree of individual variation among the females. The adult *H. sapiens* (3.98 mm) exhibited a smaller amount of "step-down" in the nasal cavity floor than other adult hominines, but similar to the adult male *Pongo* (3.9 mm), indicative of a smoother nasal cavity floor at the incisive foramen.

The adult female *H. sapiens* exhibited a smaller degree of "step-down" relative to the premaxillary length (0.14 average) than the adult males (0.19 average). The adult *H. sapiens* exhibited smaller ratios of "step-down" relative to the premaxillary length than the other adult hominines, indicative of a smoother nasal cavity floor, but the adult *H. sapiens* exhibited a larger ratio than the adult male *Pongo* (0.08).

The adult female *H. sapiens* also exhibited a smaller degree of "step-down" relative to the palatine process thickness (0.51 average) than the adult males (0.75), although male and female *H. sapiens* exhibited smaller ratios of "step-down" to hard palate length than the other adult hominines, but larger ratios than the adult male *Pongo* (0.43), due to the increase in the thickness of the palatine processes in *H. sapiens*.

Three adult male and two juvenile female *H. sapiens* exhibited small negative values of Overlap, or a small "separation" between the premaxillae and the palatine processes (see: Figure 27). The "separation" exhibited by *H. sapiens* was markedly smaller than those exhibited by the hylobatids. However, three adult males and all the adult females exhibited large positive values of Overlap, indicative of an "overlap" in the subnasal elements. *H. sapiens* was the only taxon that exhibited both a "separation" and an "overlap" of the subnasal elements.

The adult female *H. sapiens* exhibited a much larger "overlap" (5.27 mm average) than the adult males (0.32 mm) or the juvenile females (0.33 mm average), due to the negative values in the male and juvenile measurements affecting the averages (see: Figure 28). The adult males and juveniles thus exhibited a large variation in Overlap. However, female *H. sapiens* exhibited larger values of "overlap" than those males that exhibited an "overlap" measurement. The adult female *H. sapiens* exhibited larger ratios of "overlap" relative to the premaxillary length (0.20 average) and the hard palate length (0.10 average) than the adult males (0.01 average; 0.00 average) or juveniles (0.02 average; 0.01 average). Adult female *H. sapiens* exhibited a slightly larger degree of "overlap" relative to the premaxillary length (0.20 average) and the hard palate length (0.10 average) than the adult female *Pan* (0.19; 0.06), but smaller than the adult male *Pongo* (0.25; 0.12).

Adult *H. sapiens* exhibited a thicker palatine process (6.65 mm average) than the other adult hominines, but a thinner palatine process than the adult male (9.0 mm) or juvenile *Pongo* (7.6

mm) (see: Figure 28). The adult female *H. sapiens* exhibited a thicker palatine process (7.10 mm average) than the adult males (6.20 mm average) although there was a large degree of variation in the thickness of the palatine processes in *H. sapiens*. Adult *H. sapiens* (0.12 average) also exhibited thicker palatine processes relative to the hard palate length than the other hominines. The adult female *H. sapiens* (0.13) also exhibited a larger ratio of palatine process thickness to hard palate length than the adult males (0.10).

The adult *H. sapiens* that exhibited an "overlap" of the subnasal elements can be described as having an "incisive canal". These adult *H. sapiens* exhibited markedly steeper angles of the "incisive canal" (62.33 degrees average) than those of the other adult hominids. Male *H. sapiens* (66.70 degrees average) exhibited a steeper "incisive canals" than females (57.97 degrees average). Interestingly, the canal angles of adult *H. sapiens* were most similar to juvenile *Pan* (65.07 degrees average). There was considerable variation in the length of the "incisive canal" in *H. sapiens*, with adult females exhibiting markedly longer incisive canals (10.03 mm) than the adult males (5.40 mm).

The adult male *H. sapiens* (58.00 mm average) exhibited a longer hard palate than the adult females (54.23 mm average), suggestive of sexual dimorphism. The adult female *H. sapiens* exhibited a longer hard palate length than the juvenile females (50.17 mm average).

The width of the premaxillae varied considerably in *H. sapiens*, more so than in other hominoid taxa. The adult female *H. sapiens* exhibited longer premaxillae (26.10 mm average) than the adult males (22.92 mm average) or the juvenile females (20.17 mm average). The adult *H. sapiens* exhibited an elongation of the premaxilla relative to the premaxillary width (3.03 average) compared with other hominines, with some *H. sapiens* exhibiting similar ratios as *Pongo*. However, *H. sapiens* exhibited a marked variation in the elongation of the premaxillae relative to the premaxillary width, with adult females exhibiting a marked larger ratio (3.47 average) than the adult males (2.81 average) or the juvenile females (2.34 average). This suggests that females have elongated premaxillae relative to males and there is a marked increase in the elongation during ontogeny. However, while adult females exhibited longer premaxillae relative to the hard palate length (0.48) than males (0.40 average), the ratios were more similar, while the juvenile females exhibited a similar ratio of the premaxillae relative to the hard palate

length as the adult males (0.40), suggesting that the adult males have more robust premaxillae than females. Adult *H. sapiens* (0.43) also exhibit an elongation of the premaxillae relative to the hard palate length compared with other hominines, with some *H. sapiens* exhibiting similar or larger ratios than *Pongo*.

7.1.3.3   Pongines

7.1.3.3.1   *Pongo*

An adult male, a juvenile male, and an infant *Pongo* cranium were analyzed (see: Appendix A). The adult male (3.9 mm) and juvenile *Pongo* (1.8 mm) exhibited smaller values of Palate Drop than the other non-human hominids, indicating that the premaxillae are elevated above the level of the palatine processes, resulting in a "step-down" in the topography of the nasal cavity floor at the incisive foramina (see: Figure 29). The measurement Palate Drop was analogous to Drop in measuring the topography of the nasal cavity floor in those individuals that exhibit an "overlap" of the premaxilla/anterior alveolar processes by the palatine process. The adult male and juvenile *Pongo* exhibited a small degree of "step-down" to the nasal cavity floor, indicative of smaller nasal incisive fossae at the incisive foramen. The juvenile male *Pongo* did not exhibit a partitioning of the incisive foramen, resulting in a single incisive fossa. The adult male *Pongo* exhibited partitioning of the superior portion of the incisive foramen only, resulting in two small nasal incisive fossae. The adult male (0.08) and juvenile *Pongo* (0.06) exhibited a similar degree of "step-down" relative to the premaxillary length, and the smallest ratios in the analysis, indicative of a smoother floor of the nasal cavity compared to other hominoids.

The adult male (12.4 mm) and juvenile *Pongo* (9.4 mm) exhibited the largest positive value of Overlap in this analysis, indicative of an extreme "overlap" of the palatine processes by the premaxillae (see: Figure 29). The adult male and juvenile *Pongo* also exhibited the largest ratios of "overlap" relative to the hard palate length (0.12; 0.15, respectively) and the premaxillary length (0.25; 0.33) in this analysis. It is interesting that the juvenile exhibited a larger degree of "overlap" than the adult, which could be due to ontogeny or individual variation. An extreme "overlap" of the subnasal elements may be diagnostic of *Pongo*, and this character is likely derived relative to the other hominoids.
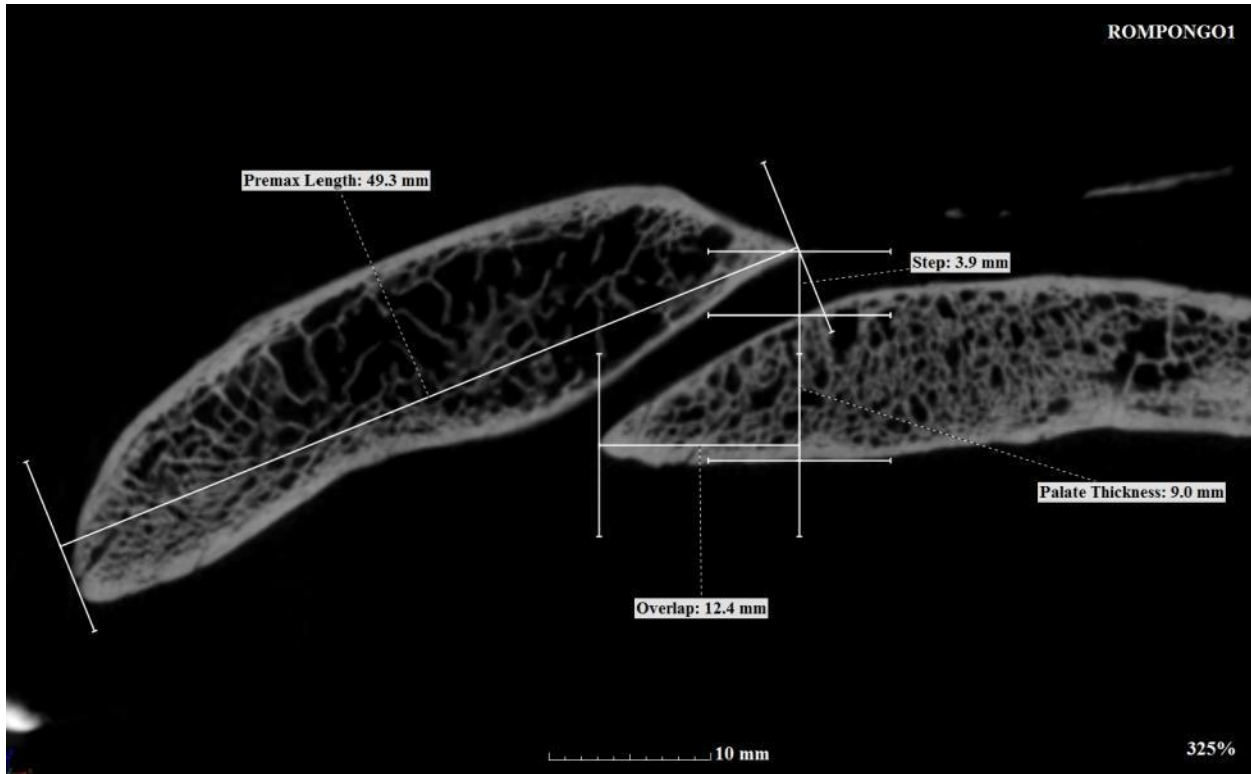
Figure 29 "*Pongo* Pattern" of the Subnasal Anatomy (µ-CT of adult male *P. abelii*, lateral view)

The adult male (0.43) and juvenile *Pongo* (0.24) exhibited the smallest ratio of Palate Drop relative to the palatine process thickness among the non-human hominids, due to the increase in the thickness of the palatine processes in *Pongo*. The differences in the ratio between the adult and juvenile males are due to the larger degree of "step-down" in the adult.

The adult male (9.0 mm) and juvenile *Pongo* (7.6 mm) exhibited the largest values of Palate Thickness among the non-human hominoids (see: Figure 29). The adult (0.08) and juvenile male *Pongo* (0.12) also exhibited the slightly thicker palatine processes relative to the hard palate length than the other non-human hominoids. While the absolute thickness of the palatine processes increased with age in *Pongo* males, the relative thickness of the palatine processes decreased with age, likely due to the elongation of the lower face during development.

As the adult male and juvenile *Pongo* exhibited an "overlap" of the subnasal elements, their configuration of subnasal anatomy is described as an "incisive canal". The adult male (33.8 degrees) and juvenile *Pongo* (42.3) exhibited similar canal angles to adult male *Gorilla*, and

markedly shallower angles than *Pan*. There was a small decrease in angle of the "incisive canals" with age in *Pongo*. The adult male (14.9 mm) and juvenile (12.7 mm) *Pongo* exhibited marked longer "incisive canal" than other hominids, suggesting that a long "incisive canal" may be a derived character and diagnostic of *Pongo*.

The adult male *Pongo* (49.3 mm) exhibited the longest premaxilla in the analysis, markedly longer than the adult male *Gorilla* (34.75 mm average) (see: Figure 29). The adult male and juvenile *Pongo* also exhibited a marked elongation of the premaxillae relative to the premaxillary width (3.76; 3.38) and hard palate length (0.46; 0.47) compared to other non-human hominids. There is a marked elongation of the premaxilla relative to the premaxillary width from the infant (0.32) to juvenile stage of ontogeny (0.47).

8   Discussion of the Primate Subnasal Anatomy

The micro-CT analysis was designed to test two hypotheses regarding morphology of the extant hominoid subnasal anatomy. First, it was to test hypothesis that the extant hominoids *Hylobates*, *Gorilla*, *Pan*, *Homo*, and *Pongo* exhibit the diagnostic morphological patterns of the subnasal anatomy as described by McCollum et al. (1993) and McCollum and Ward (1997), and that these patterns are phylogenetically informative. Second, the micro-CT analysis was to test the hypothesis of McCollum and Ward (1997) that in the earliest stages of ontogeny the morphology of the subnasal anatomy is not phylogenetically informative. Each taxon is examined in turn to determine whether it exhibited the hypothesized morphological "pattern."

8.1.1   Cercopithecoids

An unexpected result of this analysis was the discovery of a diagnostic "step-up" in the nasal cavity floor in the adult cercopithecoids due to the depression of the posterior poles of the premaxillae below the level of the palatine processes, differentiating the cercopithecoids from the hylobatids and hominids that exhibit a "drop" or "step-down" from the premaxillae to the palatine processes (see: Figure 22 and Figure 30). The cercopithecoids and primitive hominoids had been described in the literature as having a similar relationship of the subnasal elements, with no elevation of the premaxillae above the level of the palatine processes (Brown et al., 2005; Bilsborough and Rae, 2007).

The exhibition of a "step-up" in the subnasal anatomy of the cercopithecoids may be of phylogenetic utility and it is possible that this character state is primitive relative to the extant hominoids, as the non-hominoid primates are thought to exhibit the primitive "mammalian pattern" of the subnasal anatomy (Brown et al., 2005; Bilsborough and Rae, 2007; Koufos, 2007). The demonstration of a "step-up" in the subnasal anatomy of the cercopithecoids is likely due orientation of the cranium in the FHP, which is more reflective of the natural position of the crania than the more commonly used occlusal plane, and yielded diagnostic differences in this character. Further analysis of primate subnasal anatomy, perhaps utilizing ceboids or prosimians as an outgroup to the cercopithecoids, could verify whether the "step-up" exhibited by the cercopithecoids is primitive relative to "drop" exhibited by the hylobatids. Both the *Macaca* and

Papio exhibited sexual dimorphism in the "step-up" of the subnasal anatomy, with males exhibiting a more marked "step-up" than females.

The adult cercopithecoids also exhibited larger palatal fenestrae, both absolutely and relatively, than hominoids, suggesting that larger palatal fenestrae are diagnostic of the cercopithecoids and that they may also be primitive relative to hominoids. *Papio* exhibited sexual dimorphism in the size of the palatal fenestrae, with the male exhibiting larger fenestrae and a longer hard palate than female. With the exception of the "step-up" up to the palatine processes in the subnasal anatomy, there was no other evidence of sexual dimorphism in the subnasal anatomy of *Macaca*.

With the exception of the discovery of the "step-up" in the subnasal anatomy, the cercopithecoids exhibited the primitive "mammalian pattern" that was described in the literature (cf. Ward and Kimbel, 1983; Brown et al., 2005; Begun, 2007; Bilsborough and Rae, 2007). Although the overall "pattern" of the cercopithecoid subnasal anatomy was similar in males and females, there were marked quantitative differences between the sexes, possibly due to sexual dimorphism in cercopithecoids.

8.1.2   Hylobatids

The adult hylobatids exhibited a diagnostic "drop" in the nasal cavity floor at the incisive foramina, due to the elevation of the posterior pole of the premaxillae above the level of the palatine processes, unlike the "step-up" exhibited by the adult cercopithecoids (see: Figure 23 and Figure 30). This result confirmed the hypothesis of McCollum and Ward (1997) that the premaxillae of hylobatids were elevated above the level of the palatine processes, contrary to the observations of Brown et al. (2005) and Bilsborough and Rae (2007), who argued the hylobatids and early hominoids exhibited premaxillae that were not elevated above the palatine processes. However, it must be reiterated that previous analyses by McCollum et al. (1993) and McCollum and Ward (1997) scored the topography of the nasal cavity floor lateral to the nasal incisive fossae and not through the long-axis of an incisive foramen, as in this analysis, while it is unclear how Brown et al. (2005) and Bilsborough and Rae (2007) estimated the topography of the nasal cavity floor. If the "step-up" in the subnasal anatomy exhibited by the cercopithecoids is representative of the primitive character state, then the "drop" in the hylobatid nasal cavity floor is likely a derived hominoid character.

The hylobatids also exhibited a reduction in the size of the palatal fenestrae relative to the cercopithecoids, suggesting that a reduction in the palatal fenestrae may be a diagnostic of the hylobatids and possibly a derived hominoid character. However, there did not appear to be evidence of an elongation of the premaxillae in the hylobatids, confirming previous observations that the premaxillae are gracile in the hylobatids (cf. Ward and Kimbel, 1983; McCollum and Ward, 1997; Brown et al., 2005; Begun, 2007; Bilsborough and Rae, 2007). There were taxonomic differences in the morphology of the subnasal anatomy of the hylobatids as *H. lar* exhibited smaller palatal fenestrae but a larger "drop" in the nasal cavity floor than *S. syndactylus*. *S. syndactylus* exhibited shorter but wider premaxillae and a longer hard palate than *H. lar*. It is possible that the difference in the subnasal morphologies exhibited by the highly frugivorous *H. lar* and the more folivorous *S. syndactylus* are reflective of their dietary adaptations (cf. Bilsborough and Rae, 2007).

8.1.3   Infant Hominids and Ontogeny

Like the hylobatids, the infant *Gorilla* and *Pongo* hominids exhibited a "drop" in the nasal cavity floor, although smaller in size than those exhibited by hylobatids. Among the non-human hominids, only the infants and the young juvenile exhibited a "separation" of the subnasal elements, as the older juveniles and adult non-human hominids all exhibited an "overlap" of the subnasal anatomy. In this respect, the morphology of hominid subnasal anatomy at early stages of ontogeny resembled the "primitive hominoid" or hylobatid pattern. However, the infant hominids exhibited smaller palatal fenestrae than the cercopithecoids and hylobatids and palatal fenestrae are altogether absent in older juvenile hominids. The *Gorilla* and *Pongo* infants exhibited many similarities in their subnasal anatomy, including the degree of "separation" and "drop", and the size of the premaxillae, and these infants were morphologically more similar to each other than they were to the adults of their own taxon. The youngest *Pan* juvenile in the analysis exhibited similarities to these infants, suggesting that the morphology of the subnasal anatomy undergoes significant ontogenetic changes and that during the earliest periods of ontogeny the subnasal anatomy may not be of phylogenetic value, confirming the hypothesis of McCollum and Ward (1997).
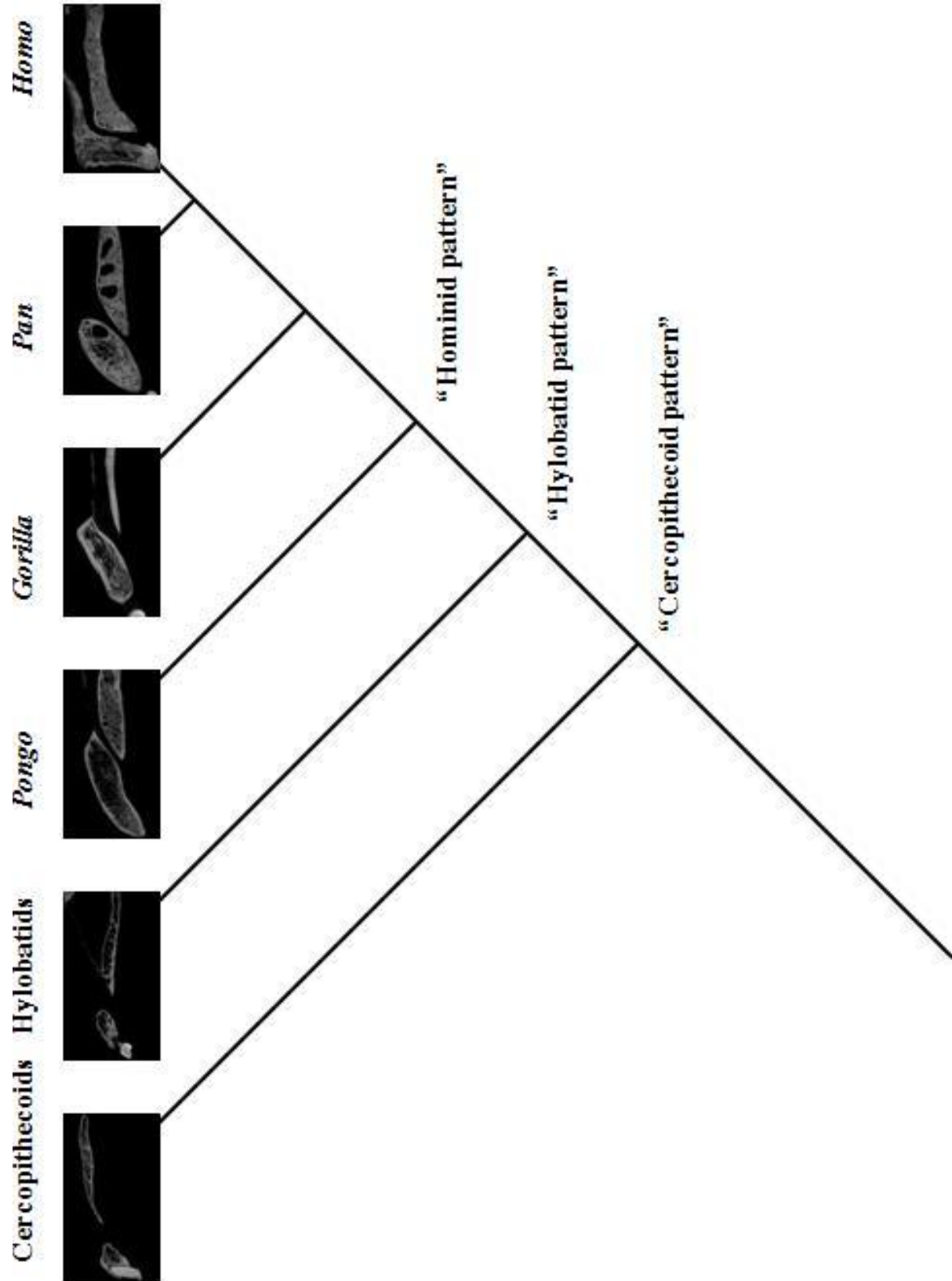
Figure 30 Cladogram of Primate Subnasal Morphological "Patterns" (μ-CT images)

8.1.4   Hominids

All of the adult non-human hominids exhibited an "overlap" of the palatine processes by the premaxillae, unlike the "separation" exhibited by the cercopithecoids and hylobatids, suggesting that an "overlap" of the subnasal elements may be diagnostic of the hominids (see: Figure 30). Thus, an "overlap" of the subnasal elements can be considered to be a derived hominid character, confirming the hypothesis of McCollum et al. (1993) and McCollum and Ward (1997). The adult hominids exhibited an elongation of the premaxillae relative to the hylobatids and cercopithecoids, and thus an elongation of the premaxillae can also be considered to be a derived hominid character, confirming previous observations (Begun, 1992; McCollum et al., 1993; McCollum and Ward, 1997; Brown et al., 2005; Begun, 2007; Bilsborough and Rae, 2007). As the adult non-human hominids exhibited an "overlap" of the subnasal elements, the morphology of the passageway of the subnasal anatomy can be described as an "incisive canal" in these hominids. Hominid taxa exhibit morphological differences in their subnasal anatomies, which are discussed below.

8.1.4.1   Hominines

8.1.4.1.1   *Gorilla*

The adult male *Gorilla* exhibited a large "overlap" of the subnasal elements and a large "step-down" in the nasal cavity floor, confirming the hypothesis of McCollum et al. (1993) and McCollum and Ward (1997), but contrary to Begun (1992; 1994; 2007) and Bilsborough and Rae (2007), who claimed *Gorilla* could also exhibit the more primitive "hominoid pattern" of the subnasal anatomy of no "overlap" of the subnasal elements and/or elevation of the premaxillae above the palatine processes (compare: Figure 10 and Figure 31 and see: Figure 30). However, there was a large degree of individual variation in the "overlap," "step-down," and canal length in the adult male *Gorilla* due to the morphology of the premaxillae and the location of the Posterior Pole, although the adult males exhibited similar angles of the "incisive canal." The adult male *Gorilla* exhibited the absolutely and relatively thinnest palatine processes among the adult hominids, a possibly diagnostic character that differentiates *Gorilla* from other hominids, confirming previous observations (cf. McCollum et al., 1993; McCollum and Ward, 1997;

Bilsborough and Rae, 2007). The thinness of the palatine processes in *Gorilla* is of particular utility in discriminating *Gorilla* from the hominine *Pan*, which in other respects exhibits a similar morphological pattern as *Gorilla*. The premaxillae of adult male *Gorilla* elongates relative to the premaxillary width during ontogeny. The infant *Gorilla* was more similar to the infant *Pongo* and the youngest *Pan* juvenile than it was to the adult male *Gorilla* in the morphology of its subnasal anatomy, suggesting that during the earliest periods of ontogeny, the subnasal anatomy is not of phylogenetic value (compare: Figure 24 and Figure 25).

8.1.4.1.2 *Pan*

Pan exhibited a slightly larger degree of "overlap" and slightly larger "step-down" in the subnasal elements than *Gorilla*. *Pan* also exhibited an elongation of the premaxillae compared with *Gorilla* (see: Figure 26). These results may be diagnostically meaningful, and suggestive that these characters are derived relative to *Gorilla*, although this is uncertain given the small sample size and lack of adult male *Pan* for comparative analysis (see: Figure 30). *Pan* is clearly distinguished from *Gorilla* by the thickness of the palatine processes, which is absolutely and relatively thicker than *Gorilla*, confirming previous observations (cf. McCollum et al., 1993; McCollum and Ward, 1997; Bilsborough and Rae, 2007). The thickness of the palatine processes in the region of the "incisive canal" is likely a derived character in *Pan*, and may be of phylogenetic utility in discriminating the non-human hominines. The premaxillae of *Pan* are also more elongated and robust than *Gorilla*, confirming previous observations (cf. Ward and Kimbel, 1983; Begun, 1992; 1994; 2007Bilsborough and Rae, 2007). However, *Pan* also appears to exhibit a markedly steeper angle of the "incisive canal" than *Gorilla*, contrary to previous observations (cf: Begun, 1992; 1994; 1997; Brown et al., 2005; Bilsborough and Rae, 2007). The degree of "overlap" increased during ontogeny in *Pan*, although the angle of the "incisive canal" decreased with age. It appeared that *Pan* exhibited a derived morphology of the subnasal anatomy relative to *Gorilla*. It is interesting that the oldest male juvenile *Pan*, exhibited quantitative morphological differences in subnasal measurements that were suggestive of sexual dimorphism in *Pan*, although this warrants further investigation.

8.1.4.1.3   *Homo sapiens*

H. sapiens was the only taxon in this analysis to exhibit two distinct morphologies of the subnasal anatomy, exhibiting either a "separation" or an "overlap" of the subnasal elements (compare: Figure 27 and Figure 28). While a number of *H. sapiens* exhibited the "inverted-L pattern" of the anterior alveolar processes (cf. Ward and Kimbel, 1983, McCollum and Ward, 1993; McCollum et al., 1997), the horizontal line of the "inverted-L" was typically formed by the bony nasal septum and was not an extension of the anterior alveolar processes itself (see: Figure 28). The "overlap" in *H. sapiens* was due to the posterior inclination of the anterior alveolar process over the palatine process, analogous to the "overlap" of the subnasal elements in the non-human hominids, but not due to an extension of the "superior plate" of the anterior alveolar process and contrary to previous observations (contra: Ward and Kimbel, 1983; McCollum et al., 1993; McCollum and Ward, 1997).

The "separation" exhibited by other individual *H. sapiens* resulted from the near-vertical orientation of the anterior alveolar process, confirming previous observations regarding the diagnostic orientation of the anterior alveolar processes in *H. sapiens* (see: Figure 27) (McCollum et al., 1993; McCollum and Ward, 1997). *H. sapiens* also exhibited the diagnostic downward deflection of the anterior portion of the premaxillae in the region of the incisive foramina and incisive canals, confirming previous observations (see: Figure 30) (McCollum et al., 1993; McCollum and Ward, 1997). The near-vertical orientation of the anterior alveolar processes formed steeply inclined incisive foramina in those *H. sapiens* that exhibited a "separation" in the subnasal elements. The long and steeply inclined incisive foramina in *H. sapiens* resulted in the large "drop" from the posterior pole of the anterior alveolar process and the palatine processes in *H. sapiens*. Contrary to previous observations, all *H. sapiens* exhibited at least some degree of partitioning of the superior portion of the incisive foramen or "incisive canal" (contra: McCollum et al., 1993; McCollum and Ward, 1997).

Those *H. sapiens* that exhibited an "overlap" of the subnasal elements in the region of the "incisive canal" exhibited a smaller "step-down" in the nasal cavity floor than the other adult hominines, but a larger "step-down" than that of the adult *Pongo*. These individuals also exhibited a markedly steeper angle of the "incisive canal" than the other hominids, diagnostic of

this taxon. The steep angle of the "incisive canal" was due to the anterior alveolar processes being more vertically inclined than those of other hominids, and likely a derived character of *H. sapiens*, confirming earlier observations (cf. McCollum et al., 1993; McCollum and Ward, 1997). *H. sapiens* also exhibited thicker palatine processes and an elongation of the anterior alveolar processes compared with the other hominines, suggesting that these characters are derived in *H. sapiens* and of phylogenetic utility, confirming earlier observations (cf. McCollum et al., 1993; McCollum and Ward, 1997).

There were a number of sexually dimorphic characters in *H. sapiens*, as females exhibited thicker palatine processes, longer premaxillae, and a shallower angle of the "incisive canal" than males, while males exhibited a larger "step-down" in the nasal cavity floor, more robust premaxillae and longer hard palates. It was noteworthy that some *H. sapiens* exhibited a similar canal angle and "drop" as the youngest *Pan* juvenile, suggesting that aspects of the subnasal morphology in *H. sapiens* might represent paedomorphisms (cf. McCollum and Ward, 1997).

8.1.4.2   Pongines

8.1.4.2.1   *Pongo*

Pongo exhibited the most derived subnasal anatomy in the analysis, confirming previous observations (see: Figure 29 and Figure 30) (Ward and Kimbel, 1983; McCollum et al., 1993; McCollum and Ward, 1997; Brown et al., 2005; Bilsborough and Rae, 2007). *Pongo* exhibited the most extreme "overlap" of the subnasal elements in the analysis, suggesting this character is diagnostic of *Pongo* and of great phylogenetic utility confirming earlier observations (cf. Ward and Kimbel, 1983; McCollum et al., 1993; McCollum and Ward, 1997; Begun, 2007; Brown et al., 2005; Bilsborough and Rae, 2007). The extreme "overlap" of the subnasal elements was largely due to the elongation of the premaxillae, which were more elongated than the other non-human hominids, also confirming previous observations (cf. Ward and Kimbel, 1983; McCollum et al., 1993; McCollum and Ward, 1997; Begun, 2007; Brown et al., 2005; Bilsborough and Rae, 2007). The absence of arterial or venous structures in the incisive canal in *Pongo* is a likely explanation for its narrowness (Ward and Kimbel, 1983).

Contrary to previous observations, *Pongo* exhibited a similar angle of the "incisive canal" as *Gorilla* (contra: Brown et al., 2005; Begun, 2007; Bilsborough and Rae, 2007). The angle of the "incisive canal" decreased slightly with age in *Pongo*. It should be noted that the adult male *Pongo* exhibited an invasion of the "incisive canal" by the vomer, partitioning the superior portion of the "incisive canal", confirming the observation of Bilsborough and Rae (2007) and McCollum and Ward, (1997). The adult male and juvenile *Pongo* exhibited the smallest degree of "step-down" in the nasal cavity floor of all the hominids, suggesting that the this character state is derived relative to other hominids, and diagnostic of *Pongo*, confirming previous observations (cf. Ward and Kimbel, 1983; McCollum et al., 1993; McCollum and Ward, 1997; Begun, 2007; Brown et al., 2005; Bilsborough and Rae, 2007). *Pongo* exhibited the thickest palatine processes of the non-human hominoids, confirming the observations of McCollum et al. (1993), but contrary to the description of Bilsborough and Rae (2007). The absolute and relative increase in the thickness of the palatine processes at the incisive foramen in *Pongo* over the other non-human hominids may be of phylogenetic utility in diagnosing *Pongo* from other non-human hominoids.

The unique morphology of the subnasal anatomy of *Pongo* relative to the other non-human hominids is highly diagnostic of this taxon, confirming the "*Pongo* pattern" discussed in the literature (cf. Ward and Kimbel, 1983; McCollum et al., 1993; McCollum and Ward, 1997; Begun, 2007; Brown et al., 2005; Bilsborough and Rae, 2007). However, the infant *Pongo* was more similar to the infant *Gorilla* and the young juvenile *Pan* than it was to the male juvenile or adult *Pongo* in the morphology of its subnasal anatomy, again suggesting that during the earliest periods of ontogeny, the subnasal anatomy is not of phylogenetic value, as previously observed (McCollum and Ward, 1997).

8.2 Comparisons with the Miocene Hominoids and Phylogenetic Implications

The cercopithecoids, hylobatids, and hominids exhibited particular morphological "patterns" of the subnasal anatomy that were diagnostic of each taxon in the analysis (compare: Figure 10 and Figure 31). The cercopithecoids exhibited a "cercopithecoid pattern" that was defined by a "step-up" in the subnasal elements that identified them as a clade (see: Figure 30 and Figure 31).

The hylobatids were defined by a "drop" from the premaxillae to the palatine processes in the nasal cavity floor and a "separation" of these subnasal elements that identified them as a clade. This is the same pattern exhibited by the Early Miocene hominoid *Morotopithecus bishopi*, suggesting the "*Morotopithecus* pattern" could be primitive for extant hominoids and *M. bishopi* most likely exhibits the first evidence of a shared derived hominoid subnasal anatomy (see: Figure 31). However, the hylobatids also exhibited a reduction in the size of the palatal fenestrae, which is said to be absent in *M. bishopi*. The Early Miocene hominoid *Afropithecus turkanensis* exhibits a reduction in the size of the palatal fenestrae, although *A. turkanensis* appears to lack the "drop" in the subnasal elements present in *M. bishopi* (see: Figure 31). The "hylobatid pattern" of the subnasal anatomy thus appears to be derived relative to the Earliest Miocene hominoids, although it is primitive among the extant hominoids (see: Figure 30 and Figure 31). However, it is not until the appearance of the Late Miocene dryopithecines *Rudapithecus hungaricus* and *Hispanopithecus laietanus* does the "hylobatid pattern" of the subnasal anatomy definitively appear in the fossil record (see: Figure 31).

The extant hominids are derived from the "hylobatid pattern" (or possibly the "*Morotopithecus*" or "*Rudapithecus*" patterns) exhibiting a "hominid pattern" of an "overlap" of the subnasal elements and an elongation of the premaxillae that identifies them as a clade (see: Figure 31). The "hominid pattern" was first exhibited by the Middle Miocene hominoid *Nacholapithecus kerioi*, which was also derived relative to the Early Miocene hominoids, indicating that the "hominid pattern" is of phylogenetic utility (see: Figure 30). The "hominid pattern" is also exhibited by the majority of Late Miocene Eurasian hominoids and suggestive that the extant hominines arose from one of these genera, in the absence of fossils of Late Miocene African hominoids. However, it is interesting that the derived "hominid pattern," of *N. kerioi* (14 Ma) and *Pierolapithecus catalaunicus* (12 Ma) may precede the more primitive "hylobatid pattern" of *R. hungaricus* and *H. laietanus* (10 Ma) in the fossil record, depending on interpretations of the subnasal anatomy in *M. bishopi* and *A. turkanensis* (see: Figure 31).
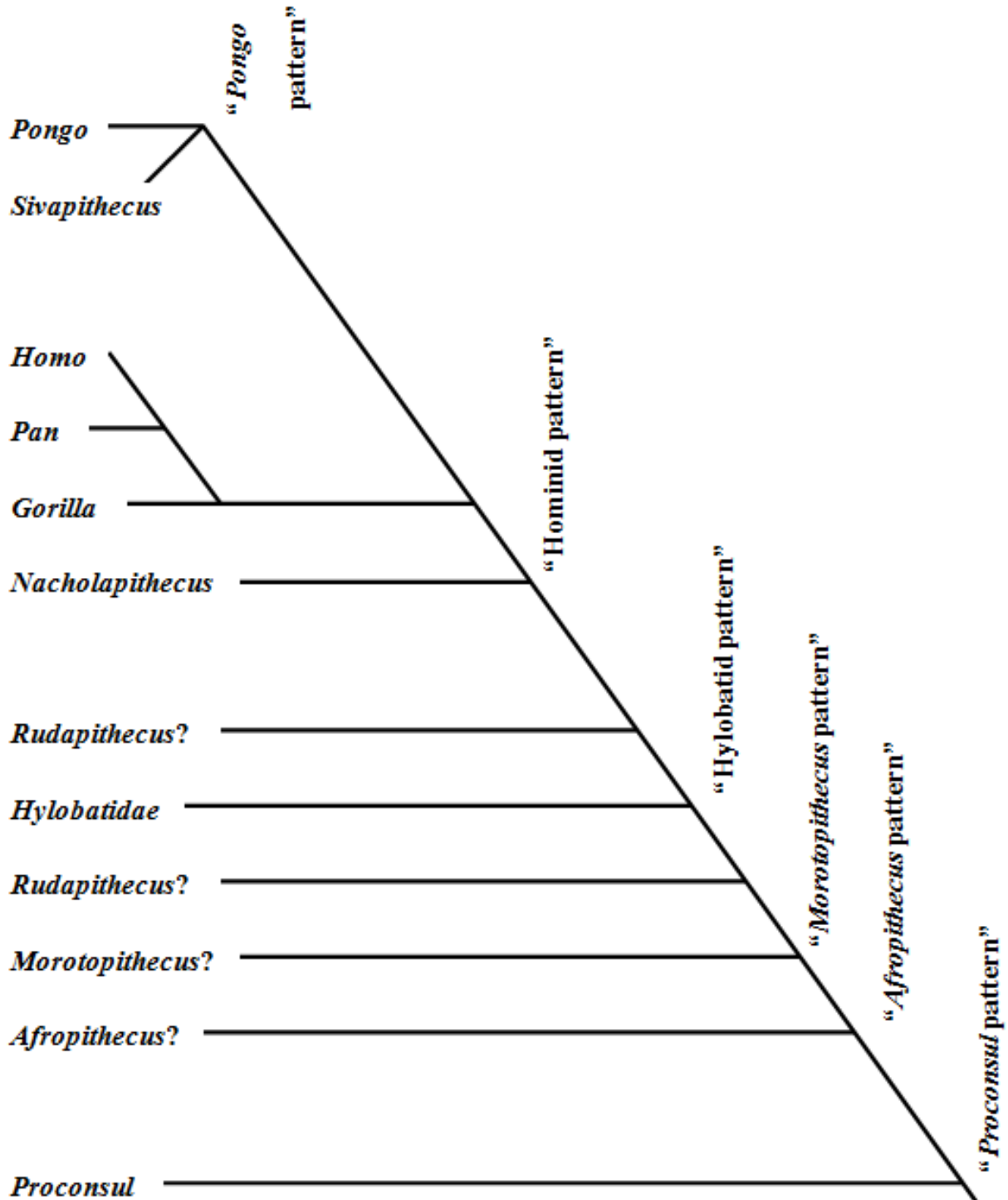
Figure 31 Cladogram of the Hominoid Subnasal Morphology Based on the Results of the Micro-CT Analysis (compared to Figure 9)

The extant hominines all exhibit some variation on this "hominid pattern", although each taxon exhibits its own diagnostic morphological "pattern" of the subnasal anatomy. It is likely that *Pan* is derived relative to *Gorilla* in the increase in the degree of "overlap," the steepness of the "incisive canal", and most of all the discovery that the palatine processes of *Pan* are markedly thicker than *Gorilla* (see: Figure 30 and Figure 31). The subnasal morphology of *Pan* is thus more similar to *Homo sapiens* than *Gorilla* and possibly indicative of a *Pan*/*Homo* clade as suggested by Begun (1992; 1994; 2007). While *H. sapiens* exhibited two morphological patterns of the subnasal anatomy, H. *sapiens* appears to be derived relative to *Pan* in the thickness of the palatine processes, the downward deflection of its anterior portion, and the more vertically inclined anterior alveolar processes, that result from the extreme reduction of the dentition and facial prognathism in *H. sapiens* (see: Figure 30 and Figure 31) (McCollum et al., 1993; McCollum and Ward, 1997; Lieberman, 2011).

Finally, *Pongo* exhibited an easily diagnostic and highly derived pattern of the subnasal anatomy. The "*Pongo* pattern" is defined by an extreme "overlap" of the subnasal elements, the smallest degree of "step-down" in the nasal cavity floor, and the thickest palatine processes of the non-human hominids (see: Figure 30 and Figure 31). The "*Pongo* pattern" appears after the "hominid pattern" in the Miocene fossil record, suggesting that it is indeed derived from earlier hominids. An elongation of the premaxillae and a marked "overlap" of the subnasal elements are exhibited by *S. indicus*, and the later *S. sivalensis* exhibits a further increase in the "overlap," evidence of evolution of the "*Pongo* pattern" within this lineage.

It should be reiterated that in earliest stage of ontogeny the hominoid subnasal anatomy is not a reliable phylogenetic indicator, as infants and young juveniles exhibit a primitive morphological pattern, which might lead to a misdiagnosis of these fossil specimens. The morphology of the subnasal anatomy of *Lufengpithecus* is largely based on a young juvenile cranium of *L. kalakolensis*, and as such, the subnasal morphology of this taxon, and others based on infant or young juvenile specimens, could be open to revision.

9   Conclusions

This micro-CT analysis examined the morphology of the hominoid subnasal anatomy to confirm its phylogenetic utility as a character complex. The analysis confirmed the hypothesis of McCollum et al. (1993) and McCollum and Ward (1997) that the extant hominoids *Hylobates*, *Gorilla*, *Pan*, *Homo*, and *Pongo* exhibit diagnostic morphological "patterns" of the subnasal anatomy and that these patterns are phylogenetically informative. However, this thesis expanded on the patterns described by McCollum et al. (1993) and McCollum and Ward (1997) with the discovery that cercopithecoids exhibited a "step-up" in the topography of the nasal cavity floor. Finally, it also confirmed the hypothesis of McCollum and Ward (1997) that in the earliest stages of ontogeny the morphology of the subnasal anatomy is not phylogenetically informative. These infants and juveniles exhibited a "primitive hominoid" or "hylobatid pattern" of the subnasal morphology, and were more similar to one another than they were to adults of their own taxon.

This thesis provided a unique quantitative methodology to analyse the morphology of the hominoid subnasal anatomy that clearly defines the terminology of the subnasal elements and the measurements employed, avoiding ambiguities of previous analyses. The utilization of micro-CT imaging permitted precise measurements, reproductions, and descriptions of the morphology of the hominoid subnasal anatomy, that surpass those of previous analyses.

A future analysis of the morphology of the hominoid subnasal anatomy using a statistically valid sample size should be undertaken to verify the conclusions of this micro-CT analysis. Finally, it is suggested that the subnasal anatomy of the Miocene fossil hominoids be subjected to a re-analysis following a methodology similar to that outlined in this thesis in order to clarify the morphology of the Miocene hominoid subnasal anatomy and improve the understanding of their evolution.

Bibliography

Alba DM. 2012. Fossil apes from the Vallès-Penedès Basin. Evol Anthropol 21:245-269.

Alpagut B, Andrews P, Fortelius M, Kappelman J, Temizsoy I, Celebi H, Lindsay W. 1996. A new specimen of *Ankarapithecus meteai* from the Sinap Formation of central Anatolia. Nature 382:349-351.

Alpagut B, Andrews P, Martin L. 1990. New Miocene hominoid specimens from the Middle Miocene site at Paşalar, Turkey. J Hum Evol 19:397-422.

Andrews PJ, Cronin J. 1982. The relationship of *Sivapithecus* and *Ramapithecus* and the evolution of the orang-utan. Nature 297:541-546.

Andrews PJ, Simons EL. 1977. A new Miocene gibbon-like genus *Dendropithecus* (Hominoidea, Primates) with distinctive postcranial adaptations: its significance to origin of Hylobatidae. Folia Primatologica 28:161-169.

Andrews PJ. 1974. New species of *Dryopithecus* from Kenya. Nature 249:188-190.

Andrews PJ. 1982. Hominoid evolution. Nature 295:185-186.

Andrews PJ. 1992. Evolution and environment in the Hominoidea. Nature 360:641-646.

Andrews PJ. 1996. Palaeoecology and hominoid palaeoenvironments. Biol Rev 71:257-300.

Begun DR, Güleç E, Geraads D. 2003. Dispersal patterns of Eurasian hominoids: implications from Turkey. Deinsea 10:23-39.

Begun DR, Güleç E. 1995. Restoration and reinterpretation of the facial specimen attributed to *Sivapithecus meteai* from Sinap Tepe (Yassiören), Central Anatolia, Turkey. Am J Phys Anthropol S20:63-64.

Begun DR, Güleç E. 1998. Restoration of the type and palate of *Ankarapithecus meteai*: taxonomic and phylogenetic implications. Am J Phys Anthropol 105:279-314.

Begun DR, Kordos L. 1993. Revision of *Dryopithecus brancoi* Schlosser, 1901 based on the fossil hominoid material from Rudabánya. J Hum Evol 25:271-285.

Begun DR, Nargolwalla MC, Kordos L. 2012. European Miocene hominids and the origins of the African ape and human clade. Evol Anthrop 21:10-23.

Begun DR, Nargolwalla MC. 2004. Late Miocene hominid biogeography: some recent perspectives. Evol Anthropol 13:234-238.

Begun DR, Ward CV, Rose MD. 1997. Events in hominoid evolution. In: Begun DR, Ward CV, Rose MD, editor. Function, phylogeny and fossils: Miocene hominoid evolution and adaptations. New York: Plenum Publishing Co. p 389-415.

Begun DR, Ward CV. 2005. Comment on *Pierolapithecus catalaunicus*, a new Middle Miocene great ape from Spain. Science 308:203c.

Begun DR. 1992. Miocene fossil hominoids and the chimp-human clade. Science 257:1929-1933.

Begun DR. 1994. Relations among the great apes and humans: new interpretations based on the fossil great ape *Dryopithecus*. Yrbk Phys Anthropol 37:11-63.

Begun DR. 2002. European hominoids. In: Hartwig W, editor. The primate fossil record. Cambridge: Cambridge University Press. p 339-368.

Begun DR. 2007. Fossil record of Miocene hominoids. In: Henke W, Rothe H, Tattersall I, editors. Handbook of paleoanthropology. Vol 2: Primate evolution and human origins. Berlin: Springer-Verlag. p 921-977.

Begun DR. 2010. Miocene hominids and the origins of the African apes and humans. Annu Rev Anthropol 39:67-84.

Benefit BR, McCrossin ML. 1991. Ancestral facial morphology of Old World higher primates. Proc Natl Acad Sci USA 88:5267-5271.

Benefit BR, McCrossin ML. 1997. Earliest known Old World monkey skull. Nature 388: 368-371.

Benefit BR, McCrossin ML. 2002. The Victoriapithecidae, Cercopithecoidea. In: Hartwig W, editor. The primate fossil record. Cambridge: Cambridge University Press. p 241-253.

Bernor RL. 2007. New apes fill the gaps. Proc Natl Acad Sci USA 104(50):19661-19662.

Bilsborough A, Rae TC. 2007. Hominoid cranial diversity and adaptation. In: Henke W, Rothe H, Tattersall I, editors. Handbook of paleoanthropology. Vol 2: Primate evolution and human origins. Berlin: Springer-Verlag. p 1031-1105.

Bonis L de, Koufos G. 1993. The face and mandible of *Ouranopithecus macedoniensis*: description of new specimens and comparisons. J Hum Evol 24:469-491.

Bräuer G. 2007. The origin of modern humans. Handbook of paleoanthropology. Vol 3: Phylogeny of hominids. Berlin: Springer-Verlag. p 1749-1779.

Brown B, Kappelman, Ward S. 2005. Lots of faces from different places: what craniofacial morphology does(n't) tell us about hominoid phylogenetics. In: Lieberman DE, Smith RJ, Kelley J, editors. Interpreting the past: Essays on human, primates and mammal evolution. Boston: Brill Academic Publishers, Inc. p. 167-188.

Brunet M, Guy F, Pilbeam D, Mackaye HT, Likius A, Ahounta D, Beauvilian A, Blondel C, Boschernes H, Boisserie JR, de Bonis L, Coppens Y, Dejax J, Denys C, Duringer P, Eisenmann V, Fanone G, Fronty P, Geraads D, Lehmann T, Lihoreau F, Louchart A, Mahamat A, Merceron G, Mouchelin G, Otero O, Pelaez Campomanes P, Ponce de Leon M, Rage JC, Sapanet M, Schuster M, Sudre J, Tassy P, Valentin X, Vignaud P, Viriot L, Zazzo A, Zollikofer C. 2002. A new hominid from the Upper Miocene of Chad, Central Africa. Nature 418:145-151

Casanovas-Vilar I, Alba DM, Garcés M, et al. 2011. Updated chronology for the Miocene hominoid radiation in Western Eurasia. Proc Natl Acad Sci USA 108:5554-5559.

Chaimanee Y, Yamee C, Tian P, Khaowiset K, Marandat B, Tafforeau P, Nemoz C, Jaeger JJ. 2006. *Khoratpithecus piriyai*, a Late Miocene hominoid of Thailand. Am J Phys Anthropol 131:311-323.

Cote SM. 2004. Origins of the African hominoids: an assessment of the paleobiogeographical evidence. C R Palevol 3:323-340.

Dean D, Delson E. 1992. Second gorilla or third chimp? Nature 359:676-677.

Fleagle JG, Simons EL. 1978. *Micropithecus clarki*, a small ape from the Miocene of Uganda. Am J Phys Anthropol 49:427-440.

Gebo DL, MacLatchy L, Kityo R, Deino A, Kingston J, Pilbeam D. 1997. A hominoid genus from the Early Miocene of Uganda. Science 276:401-404.

Ginter JK. 2001. Dealing with unknowns in a non-population: the skeletal analysis of the Odd Fellows series. Faculty of Graduate Studies. Western University: London, Ontario.

Groves CP. 2001. Primate Taxonomy. Washington: Smithsonian Institute.

Harrison T, Rook L. 1997. Enigmatic anthropoid or misunderstood ape? The phylogenetic status of *Oreopithecus bambolii* reconsidered. In: Begun DR, Ward CV, Rose MD, editor. Function, phylogeny and fossils: Miocene hominoid evolution and adaptations. New York: Plenum Publishing Co. p 327-362.

Harrison T. 1981. New finds of small fossil apes from the Miocene locality of Koru in Kenya. J Hum Evol 10:129-137.

Harrison T. 1986. New fossil anthropoids from the middle Miocene of East Africa and their bearing on the origin of the *Oreopithecidae*. Am J Phys Anthropol 71:265-284.

Harrison T. 1988. A taxonomic revision of the small catarrhine primates from the early Miocene of East Africa. Folia Primatologica 50:59-108.

Harrison T. 1989 A new species of *Micropithecus* from the middle Miocene of Kenya. J Hum Evol 18:537-557.

Harrison T. 2002. Late Oligocene to middle Miocene catarrhines from Afro-Arabia. In: Hartwig W, editor. The primate fossil record. Cambridge: Cambridge University Press. p 311-338.

Harrison T. 2010. Apes among the tangled branches of human origins. Science 327:532-534.

Heizmann E, Begun DR. 2001. The oldest Eurasian hominoid. J Hum Evol 41:463-481.

Hürzeler J. 1960. The significance of *Oreopithecus* in the genealogy of man. Triangle 4:164-174.

Ishida H, Kunimatsu Y, Takano T, Nakano Y, Nakatsukasa M. 2004. *Nacholapithecus* skeleton from the Middle Miocene of Kenya. J Hum Evol 46:69-103.

Kappelman J, Kelley J, Pilbeam D, Sheikh KA, Ward S, Anwar M, Barry JB, Brown B, Hake P Johnson NM, Raza SM, Shah SMI. 1991. The earliest occurrence of *Sivapithecus* from the Middle Miocene Chinji Formation of Pakistan. J Hum Evol. 21:61-73.

Kay RF, Ungar PS. 1997. Dental evidence for diet in some Miocene catarrhines with comments on the effects and phylogeny on the interpretation of adaption. In: Begun DR, Ward CV, Rose MD, editor. Function, phylogeny and fossils: Miocene hominoid evolution and adaptations. New York: Plenum Publishing Co. p 131-151.

Kelley J, Alpagut B. 1999. Canine sexing and species number in the Paşalar large hominoid sample. J Hum Evol 36:335-341.

Kelley J, Qinghua X. 1991. Extreme sexual dimorphism in a Miocene hominoid. Nature 352:151-153.

Kelley J, Ward S, Brown B, Hill A, Downs W. 2000. Middle Miocene hominoid origins. Science 287:2375a.

Kelley J. 2002. The hominoid radiation in Asia. In: Hartwig W, editor. The primate fossil record. Cambridge: Cambridge University Press. p 369-384.

Kordos L, Begun DR. 1997. A new reconstruction of RUD 77, a partial cranium of *Dryopithecus brancoi* from Rudabánya, Hungary. Am J Phys Anthropol 103:277-294.

Kordos L, Begun DR. 2001. A new cranium of *Dryopithecus* from Rudabánya, Hungary. J Hum Evol 41:689-700.

Kordos L, Begun DR. 2002. Rudabánya: a Late Miocene subtropical swamp deposit with evidence of the origin of the African ape and human clade. Evol Anthropol 11:45-57.

Koufos GD. 1995. The first female maxilla of the hominoid *Ouranopithecus macedoniensis* from the late Miocene of Macedonia, Greece. J Hum Evol 29:385-389.

Koufos GD. 2007. Potential hominoid ancestors for Hominidae. In: Henke W, Rothe H, Tattersall I, editors. Handbook of paleoanthropology. Vol 3: Phylogeny of hominids. Berlin: Springer-Verlag. p 1347-1377.

Kunimatsu Y, Ishida H, Nakatsukasa M, Nakano Y, Sawada Y, Nakayama K. 2004. Maxillae and associated gnathodental specimens of *Nacholapithecus kerioi*, a large-bodied hominoid from Nachola, northern Kenya. J Hum Evol 46:365-400.

Kunimatsu Y, Nakatsukasa M, Sawada Y, Sakai T, Hyodo M, Hyodo H, Itaya T, Nakaya H, Saegusa H, Mazurien A, Saneyoshi M, Tsujikawa H, Yamamoto A, Mbua E. 2007. A new Late Miocene great ape from Kenya and its implications for the origins of African great apes and humans. Proc Natl Acad Sci USA 104(49):19220-19225.

Le Gros Clark WE, Leakey LSB. 1950. Diagnoses of East African Miocene Hominoidea. Quarterly Journal of the Geological Society of London 105:260-263.

Leakey M, Walker A. 1997. *Afropithecus*: function and phylogeny. In: Begun DR, Ward CV, Rose MD, editor. Function, phylogeny and fossils: Miocene hominoid evolution and adaptations. New York: Plenum Publishing Co. p 225-239.

Leakey REF, Leakey MG, Walker AC. 1988a. Morphology of *Afropithecus turkanensis* from Kenya, Am J Phys Anthropol 76:289-307.

Leakey REF, Leakey MG, Walker AC. 1988b. Morphology of *Turkanapithecus kalakolensis* from Kenya. Am J Phys Anthropol 76:277-288.

Leakey REF, Leakey MG. 1986a. A new Miocene hominoid from Kenya. Nature 324:143-148.

Leakey REF, Leakey MG. 1986b. A second new Miocene hominoid from Kenya. Nature 324:146-148.

Lieberman DE. 2011. The evolution of the human head. Cambridge: Belknap press.

MacLatchy L, Gebo D, Kityo R, Pilbeam D. 2000. Postcranial functional morphology of *Morotopithecus bishopi*, with implications for the evolution of modern ape locomotion. J Hum Evol 39:159-183.

MacLatchy L. 2004. The oldest ape. Evol Anthropol 13:90-103.

Madar SI, Rose MD, Kelley J, MacLatchy L, Pilbeam D. 2002. New *Sivapithecus* postcranial specimens from the Siwaliks of Pakistan. J Hum Evol 42:705-752.

Mai LL, Owl MY, Kersting MP. 2005. The Cambridge dictionary of human biology and evolution. Cambridge University Press: New York.

Manser J, Harrison T. 1999. Estimates of cranial capacity and encephalization in *Proconsul* and *Turkanapithecus*. Am J Phys Anthropol 108(S28):189.

McBrearty S, Jablonski NG. 2005. First fossil chimpanzee. Nature 437: 105-108.

McCollum MA, Grine FE, Ward SC, Kimbel WH. 1993. Subnasal morphological variation in extant hominoids and fossil hominids. J Hum Evol 24: 87-111.

McCollum Ma, Ward SC. 1997. Subnasoalveolar anatomy and hominoid phylogeny: evidence from comparative ontogeny. Am J Phys Anthropol 102:377-405.

Moyà-Solà S, Alba DM, Almecija S, Casanovas-Vilar I, Köhler M, De Esteban-Trivigno S, Robles JM, Galindo J, Fortuny J. 2009a. A unique Middle Miocene European hominoid and the origins of the great ape and human clade. PNAS 106(24):9601-9606.

Moyà-Solà S, Köhler M, Alba DM, Casanovas-Vilar I, Galindo J. 2004. *Pierolapithecus catalaunicus*, a new Middle Miocene great ape from Spain. Science 306:1339-1344.

Moyà-Solà S, Köhler M, Alba DM, et al. 2009b. First partial face and upper dentition of the Middle Miocene hominoid *Dryopithecus fontani* from Albocador de Can Mata (Vallès-Penedès Basin, Catalonia, NE Spain): taxonomic and phylogenetic implications. Am J Phys Anthropol 139:126-145.

Moyà-Solà S, Köhler M. 1995. New partial cranium of *Dryopithecus* Lartet, 1863 (Hominoidea, Primates) from the upper Miocene of Can Llobateres, Barcelona, Spain. J Hum Evol 29:101-139.

Moyà-Solà S, Köhler M. 1996. A *Dryopithecus* skeleton and the origins of great-ape locomotion. Nature 379:156-159.

Moyà-Solà S, Köhler M. 1999. The phylogenetic relationships of *Oreopithecus bambolii* Gervais, 1872. CR Acad Sci Paris 324: 141-148.

Nakatsukasa M, Yamanaka A, Kunimatsu Y, Shimizu D, Ishida H. 1998. A newly discovered *Kenyapithecus* skeleton and its implications for the evolution of positional behaviour in Miocene East African hominoids. J Hum Evol 34:657-664.

Oates JF, Groves CP, Jenkins PD. 2009. The type locality of *Pan troglodytes vellerosus* (Gray, 1862), and implications for the nomenclature of West African chimpanzees. Primates 50:78-80.

Parish JM. 2000. The Stirrup Court cemetery: an examination of health in nineteenth-century Ontario. Faculty of Graduate Studies. Western University: London, Ontario.

Pérez de los Ríos M, Moyà-Solà S, Alba DM. 2012. The nasal and paranasal architecture of the middle Miocene ape *Pierolapithecus catalaunicus* (Primates: Hominidae): phylogenetic implications. J Hum Evol 63:497-506.

Pickford M, Senut B, Gommery D, Musiime E. 2003. New catarrhine fossils from Moroto II, early middle Miocene (ca. 17.5 Ma) Uganda. CR Palevol 2:649-662.

Pilbeam DR, Young N. 2004. Hominoid evolution: synthesizing disparate data. CR Palevol 3:305-321.

Pilbeam DR. 1982. New hominoid skull material from the Miocene of Pakistan. Nature 295:232-234.

Pilbeam DR. 1996. Genetic and morphological records of the Hominoidea and hominid origins: a synthesis. Mol Phylogen Evol 5:155-168.

Pilbeam DR. 1997. Research on Miocene hominoids and hominid origins: the last three decades. In: Begun DR, Ward CV, Rose MD, editor. Function, phylogeny and fossils: Miocene hominoid evolution and adaptations. New York: Plenum Publishing Co. p 13-28.

Pilbeam DR. 2002. Perspectives on the Miocene Hominoidea. In: Hartwig W, editor. The primate fossil record. Cambridge: Cambridge University Press. p 303-310.

Raza SM, Barry JC, Pilbeam D, Rose MD, Shah SMI, Ward S. 1983. New hominoid primates from the middle Miocene Chinji Formation, Potwar Plateau, Pakistan. Nature 306:52-54.

Reinhart C. 2008. Industrial computer tomography—a universal inspection tool. 17th World Conference on Nondestructive Testing, 25-28 Oct 2008, Shanghai, China.

Robinson JT. 1953. *Telanthropus* and its phylogenetic significance. Am J Phys Anthropol 11:445-501.

Robinson JT. 1954. The genera and species of the Australopithecinae. Am J Phys Anthropol 12:181-200.

Rook L, Bondioli L, Köhler M, Moyà-Solà S, Macchiarelli R. 1999. *Oreopithecus* was a bipedal ape after all: evidence from the iliac cancellous architecture. Proc Natl Acad Sci USA 96:8795-8799.

Rose MD 1984. Hominoid postcranial specimens from the middle Miocene, Chinji Formation, Pakistan. J Hum Evol 13:503-516.

Rose MD. 1997. Functional and phylogenetic features of the forelimb in Miocene hominoids. In: Begun DR, Ward CV, Rose MD, editor. Function, phylogeny and fossils: Miocene hominoid evolution and adaptations. New York: Plenum Publishing Co. p 79-100.

Ross C, Henneberg M. 1995. Basicranial flexion, relative brain size, and facial kyphosis in *Homo sapiens* and some fossil hominids. Am J Phys Anthropol 98:575-593.

Ross CF, Ravosa MJ. 1993. Basicranial flexion, relative brain size, and facial kyphosis in nonhuman primates. Am J Phys Anthropol 91:305-324.

Scally A, Dutheil JY, Hillier LW, Jordan GE, Goodhead I, Herrero J, Hobolth A, et al. 2012 Insights into hominid evolution from the gorilla genome sequence. Nature 483:169-175.

Schwartz JH. 2007. Skeleton Keys, second edition. Oxford University Press: New York.

Senut B, Pickford M, Gommery D, Mein P, Cheboi K, Coppens Y. 2001. First hominid from the Miocene (Lukeino Formation, Kenya). C R Acad Sci Paris 332:137-144.

Shea BT. 1985. On aspects of skull form in African apes and orangutans, with implications for hominoid evolution. Am J Phys Anthropol 68:329-342.

Smith H, Crummett TL, Brandt KL. 1994. Ages of eruption of primate teeth: a compendium for aging individuals and comparing life histories. Yrbk Phys Anthropol 37:177-231.

Smith H. 1994. Patterns of dental development in *Homo*, *Australopithecus*, *Pan*, and *Gorilla*. Am J Phys Anthropol 94:307-325.

Suwa G, Kono RT, Katoh S, Asfaw B, Beyene Y. 2007. A new species of great ape from the late Miocene epoch in Ethiopia. Nature 488:921-924.

Swindler DR, Curtis LE. 1998. Introduction to the Primates. University of Washington Press: Washington.

Teaford MF, Beard KC, Leakey RE, Walker AC. 1988. New hominoid facial skeleton from the early Miocene of Rusinga Island, Kenya and its bearing on the relationship *Proconsul nyanzae* and *Proconsul africanus*. J Hum Evol 17:461-477.

Thinh VN, Mootnick AR, Geissmann T, Li M, Ziegler T, Agil M, Moisson P, Nadler T, Walter L, Roos C. 2010. Mitochondrial evidence for multiple radiations in the evolutionary history of small apes. BMC Evolutionary Biology 10:74.

Ulhaas L. 2007. Computer-based reconstruction: technical aspects and applications. In: Henke W, Rothe H, Tattersall I, editors. Handbook of paleoanthropology. Vol 1: Principles, methods, and approaches. Berlin: Springer-Verlag. p 787-813.

Volume Graphics. 2012. Possibilities with VGStudio MAX. Volume Graphics GmbH.

Walker A. 1997. *Proconsul*: function and phylogeny. In: Begun DR, Ward CV, Rose MD, editor. Function, phylogeny and fossils: Miocene hominoid evolution and adaptations. New York: Plenum Publishing Co. p 209-224.

Walker AC, Falk D, Smith R, Pickford M. 1983. The skull of *Proconsul africanus*: reconstruction and cranial capacity. Nature 305:525-527.

Walker AC, Rose MD. 1968. Fossil hominoid vertebra from the Miocene of Uganda. Nature 217:980-981.

Walker AC, Teaford MF, Martin L, Andrews P. 1993. A new species of *Proconsul* from the early Miocene of Rusinga/Mfangano Islands, Kenya. J Hum Evol 25:43-56.

Ward CV, Walker AC, Teaford MF, Odhiambo I. 1993. Partial skeleton of *Proconsul nyanzae* from Mfangano Island, Kenya. Am J Phys Anthropol 90:77-111.

Ward CV. 1997a. Functional anatomy and phyletic implications of the hominoid trunk and hindlimb. In: Begun DR, Ward CV, Rose MD, editor. Function, phylogeny and fossils: Miocene hominoid evolution and adaptations. New York: Plenum Publishing Co. p 101-130.

Ward S, Brown B, Hill A, Kelley J, Downs W. 1999. *Equatorius*: a new hominoid genus from the Middle Miocene of Kenya. Science 285:1382-1386

Ward S, Kimbel W. 1983. Subnasal morphology and the systematic position of *Sivapithecus*. Am J Phys Anthropol 61:157-171.

Ward S. 1997b. The taxonomy and phylogenetic relationships of *Sivapithecus* revisited. In: Begun DR, Ward CV, Rose MD, editor. Function, phylogeny and fossils: Miocene hominoid evolution and adaptations. New York: Plenum Publishing Co. p 269-290.

Ward SC, Duren DL. 2002. Middle and late Miocene African hominoids. In: Hartwig W, editor. The primate fossil record. Cambridge: Cambridge University Press. p 385-397.

White TD, Asfaw B, Beyene Y, Haile-Selassie Y, Lovejoy CO, Suwa G, WoldeGabriel G. 2009. *Ardipithecus ramidus* and the paleobiology of early hominids. Science 326:75-86.

White TD, Folkens PA. 2000. Human Osteology, second edition. Academic Press: San Diego.

Whitehead PF, Sacco WK, Hochgraf SB. 2005 A photographic atlas for physical anthropology. Morton Publishing Co: Englewood.

Wiley EO, Lieberman BS. 2011. Phylogenetics: theory and practice of phylogenetic systematic. 2nd ed. Hoboken: Wiley- Blackwell.

Wood B, editor. 2013. Wiley-Blackwell Encyclopedia of Human Evolution. Blackwell Publishing Ltd: West Sussex.

Young N, MacLatchy L. 2004. The phylogenetic position of *Morotopithecus*. J Hum Evol 46:163-184.

Zollikofer CPE, Ponce De Leon MS, Martin RD. 1998. Computer-assisted paleoanthropology. Evol Anthrop 6(2):41-54.

Appendix A: Micro-CT Sections of the Primate Subnasal Anatomy

The following sections of primate subnasal anatomy were taken from micro-CT (μ-CT) reconstructions of primate crania generated using VGStudio MAX imaging software.
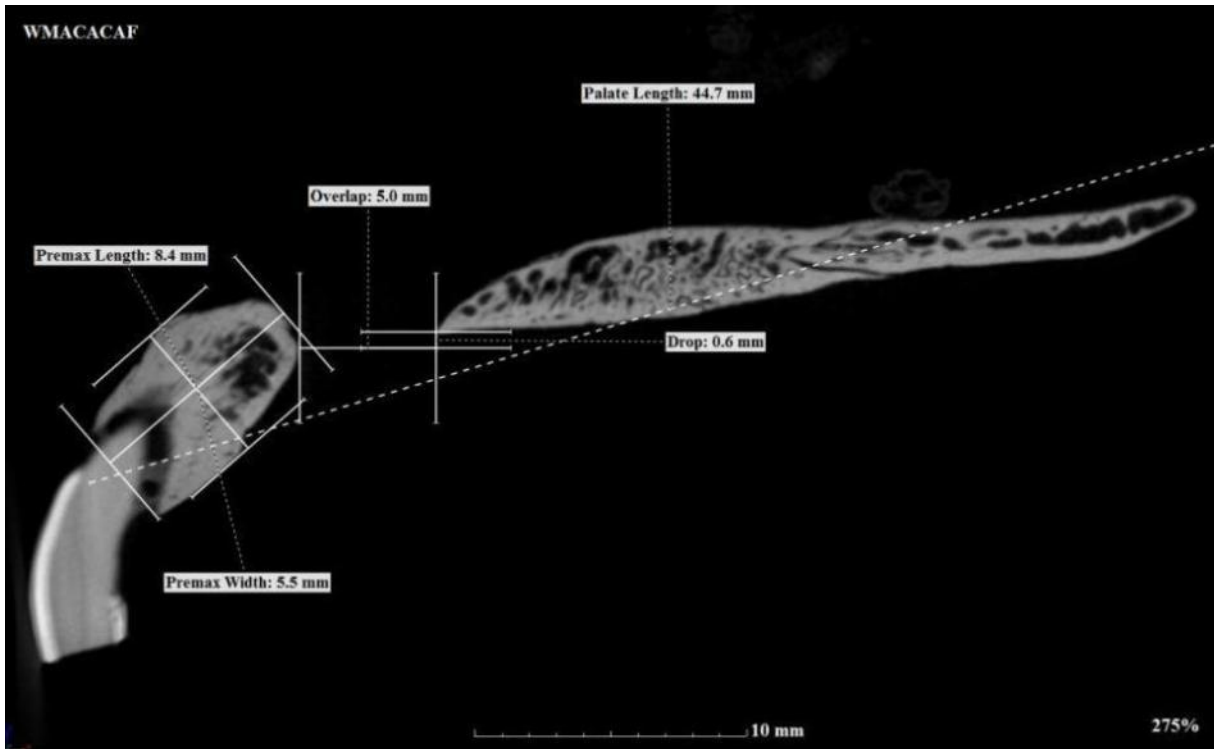
Figure 32 μ-CT of *Macaca mulatta* adult female (WMACACAF), lateral view
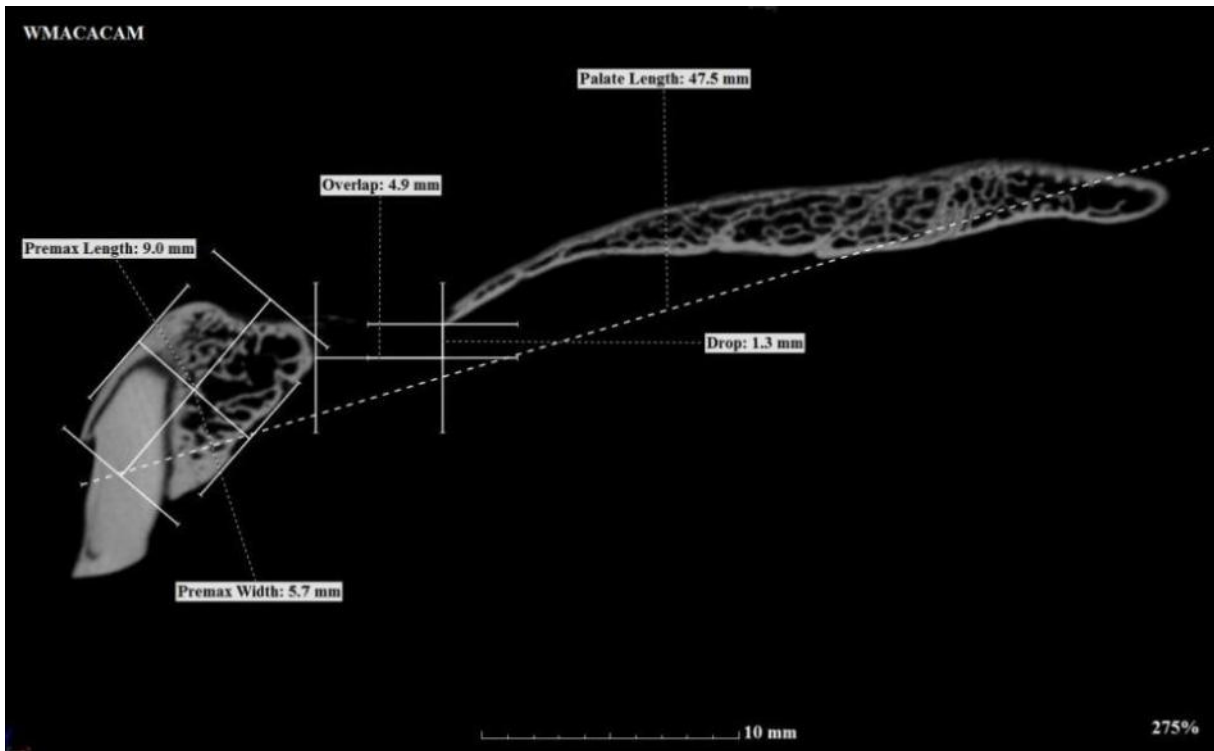
Figure 33 μ-CT of *Macaca mulatta* adult male (WMACACAM), lateral view
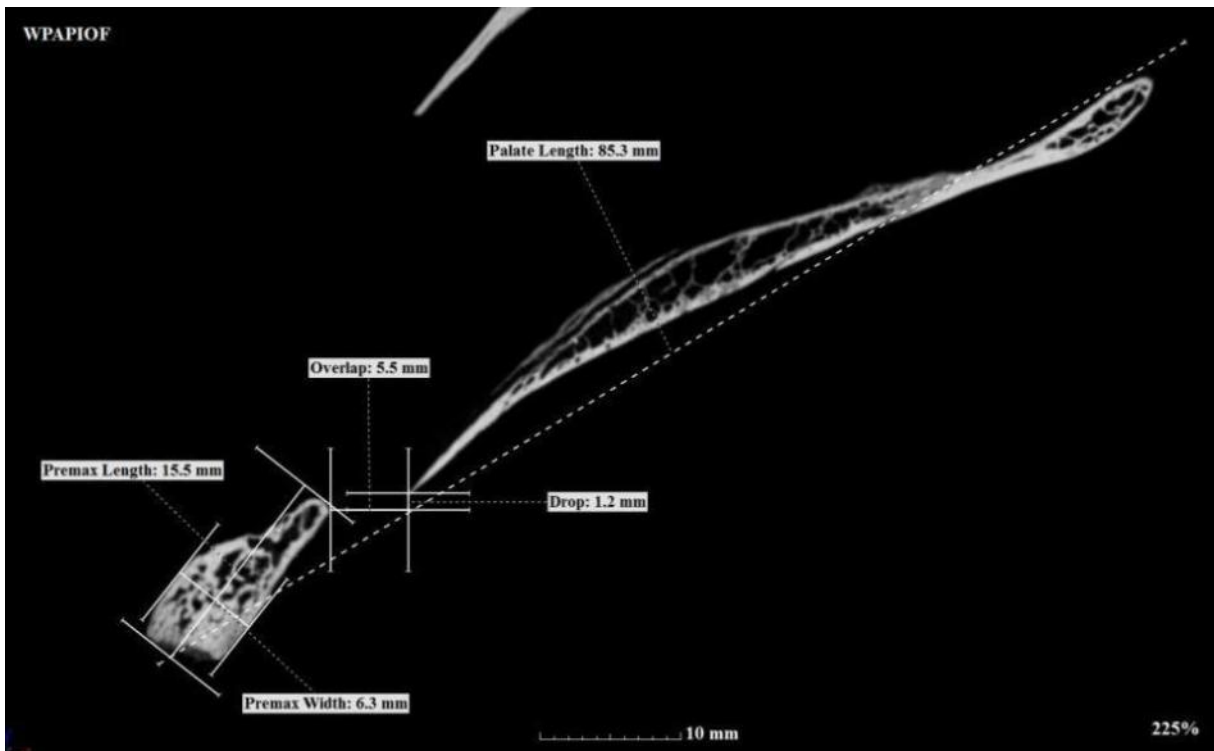
Figure 34 μ-CT of *Papio ursinus* adult female (WPAPIOF), lateral view
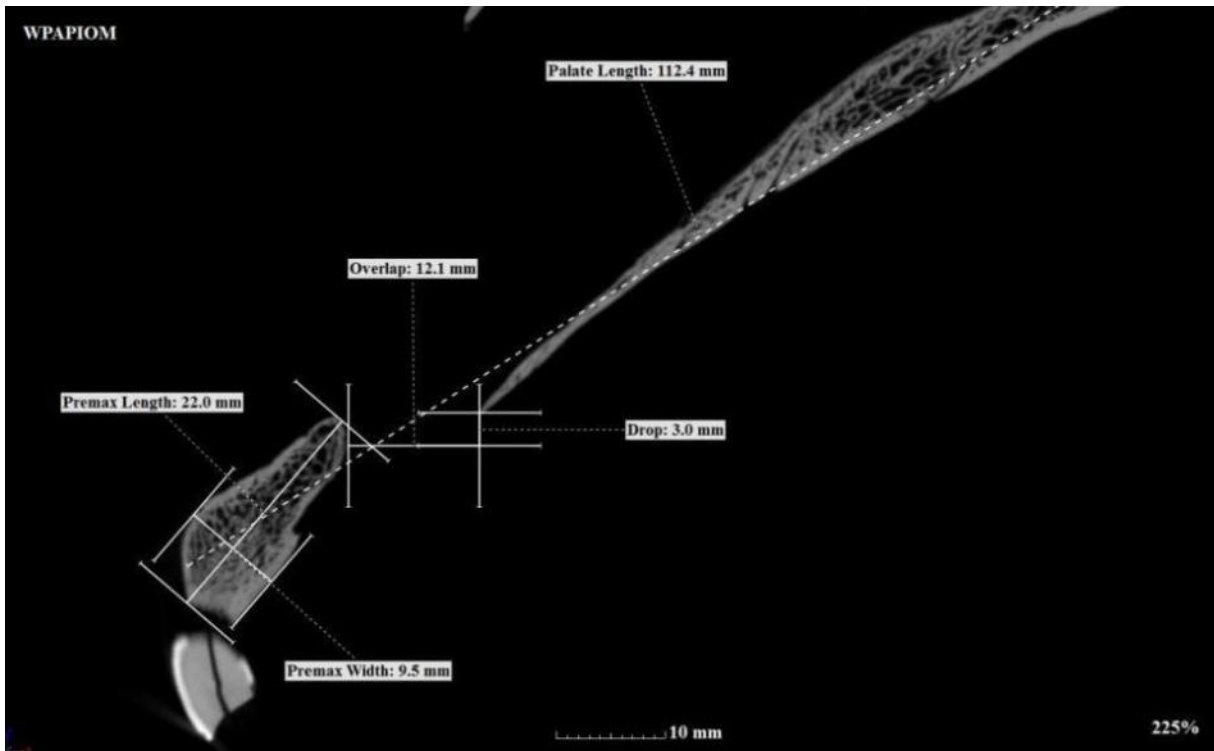
Figure 35 μ-CT of *Papio ursinus* adult male (WPAPIOM), lateral view
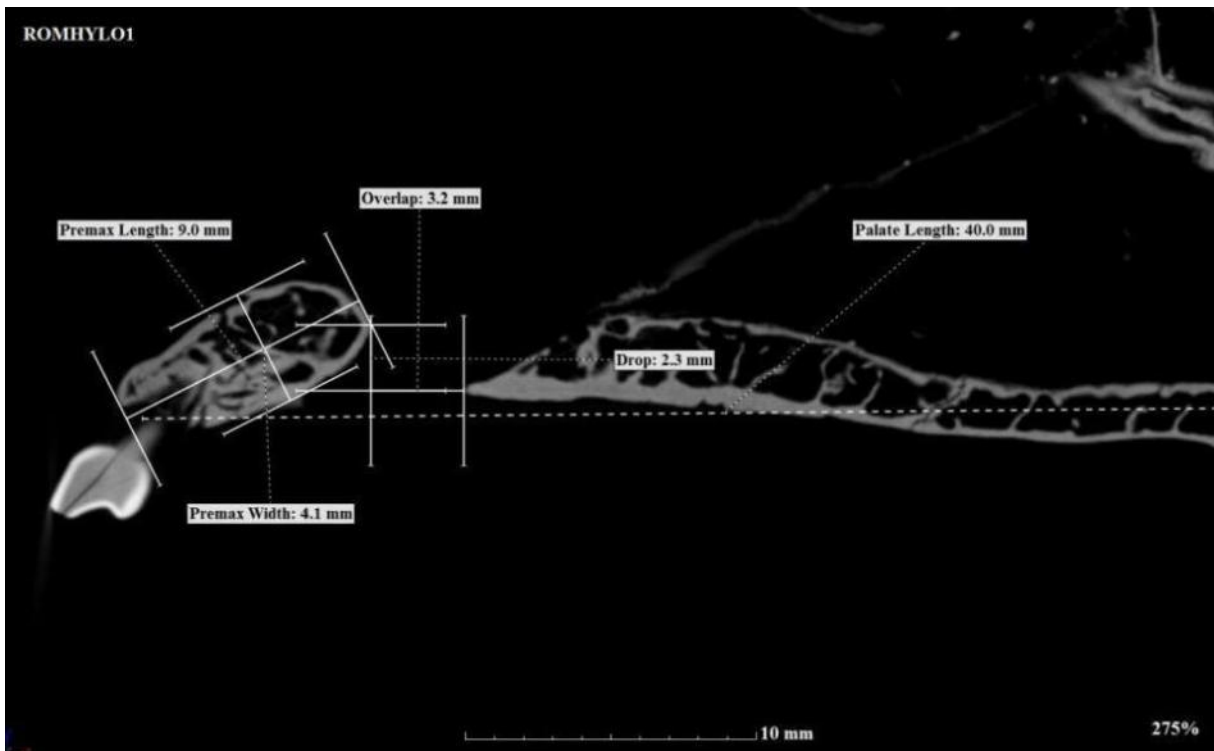
Figure 36 μ-CT of *Hylobates lar* adult (ROMHYLO1), lateral view
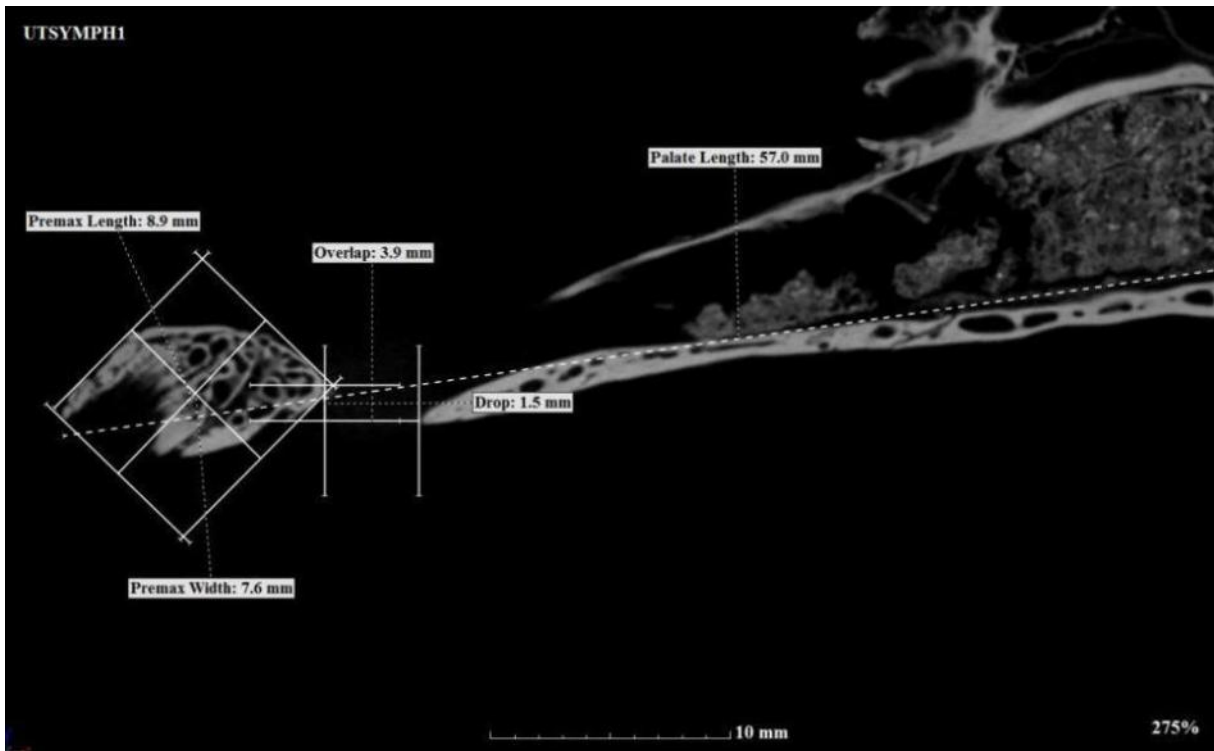
Figure 37 μ-CT of *Symphalangus syndactylus* adult (UTSYMPH1), lateral view
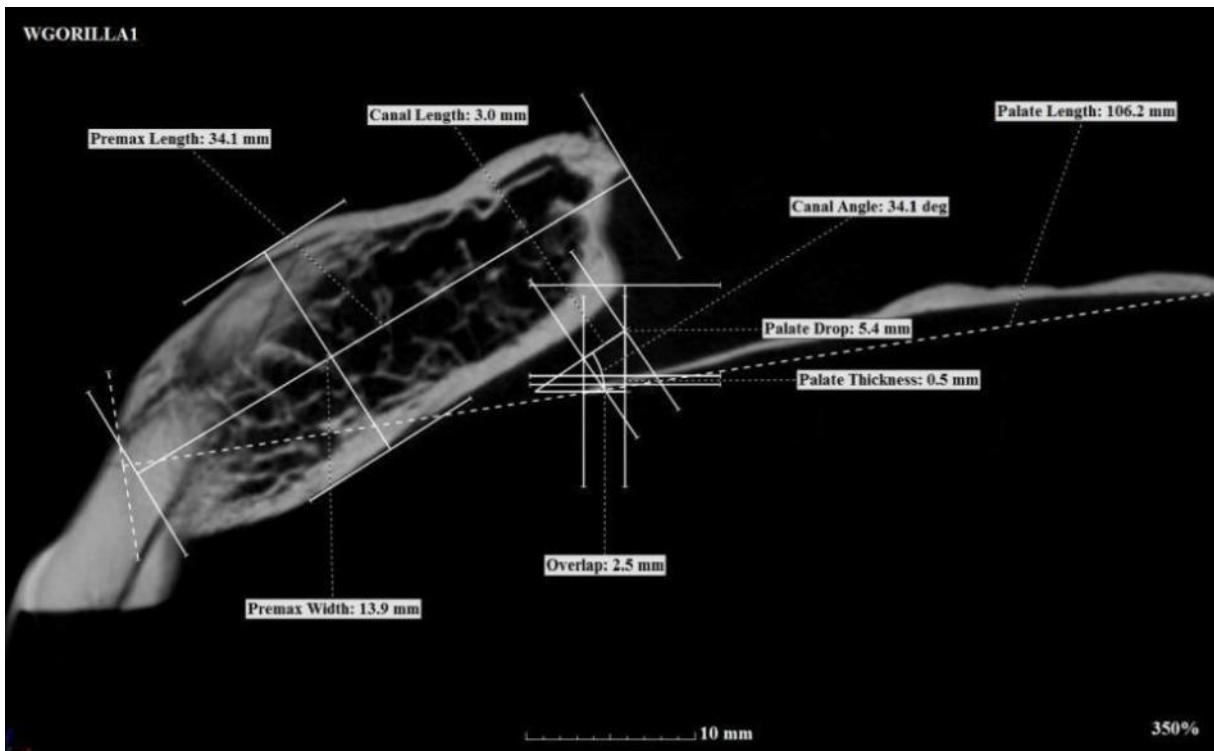
Figure 38 μ-CT of *Gorilla gorilla* adult male (WGORILLA1), lateral view
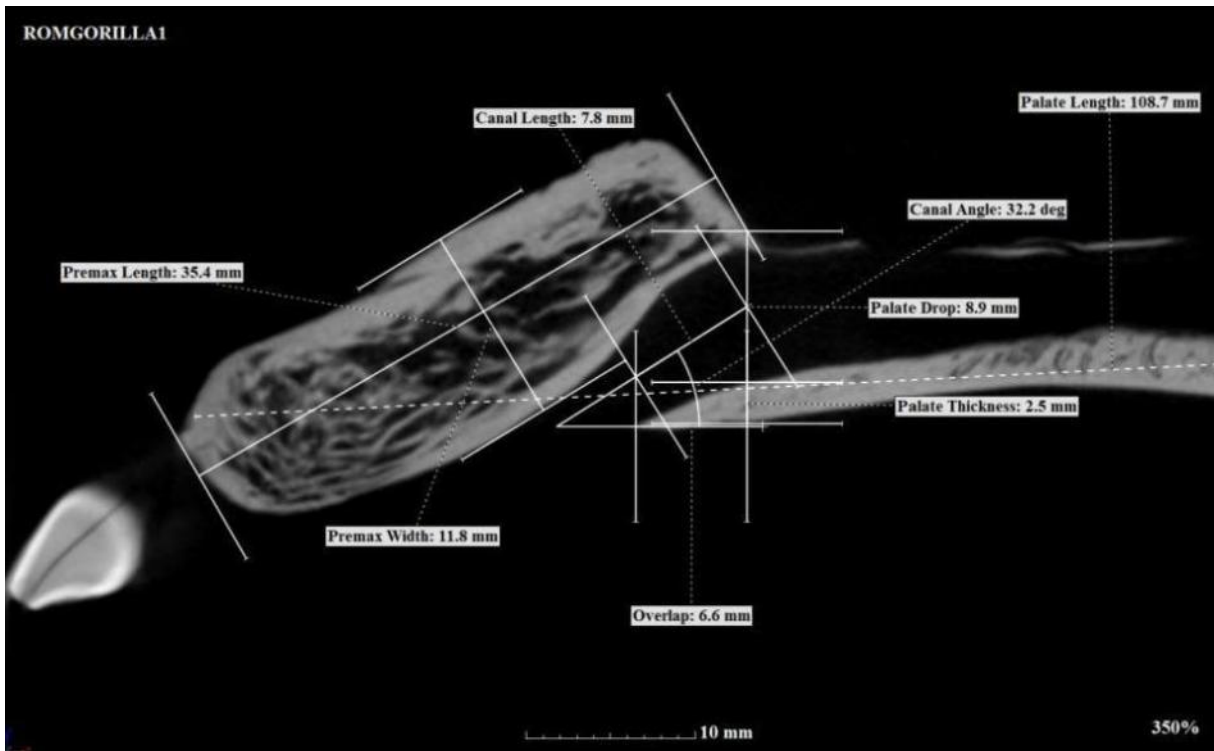
Figure 39 μ-CT of *Gorilla gorilla* adult male (ROMGORILLA), lateral view
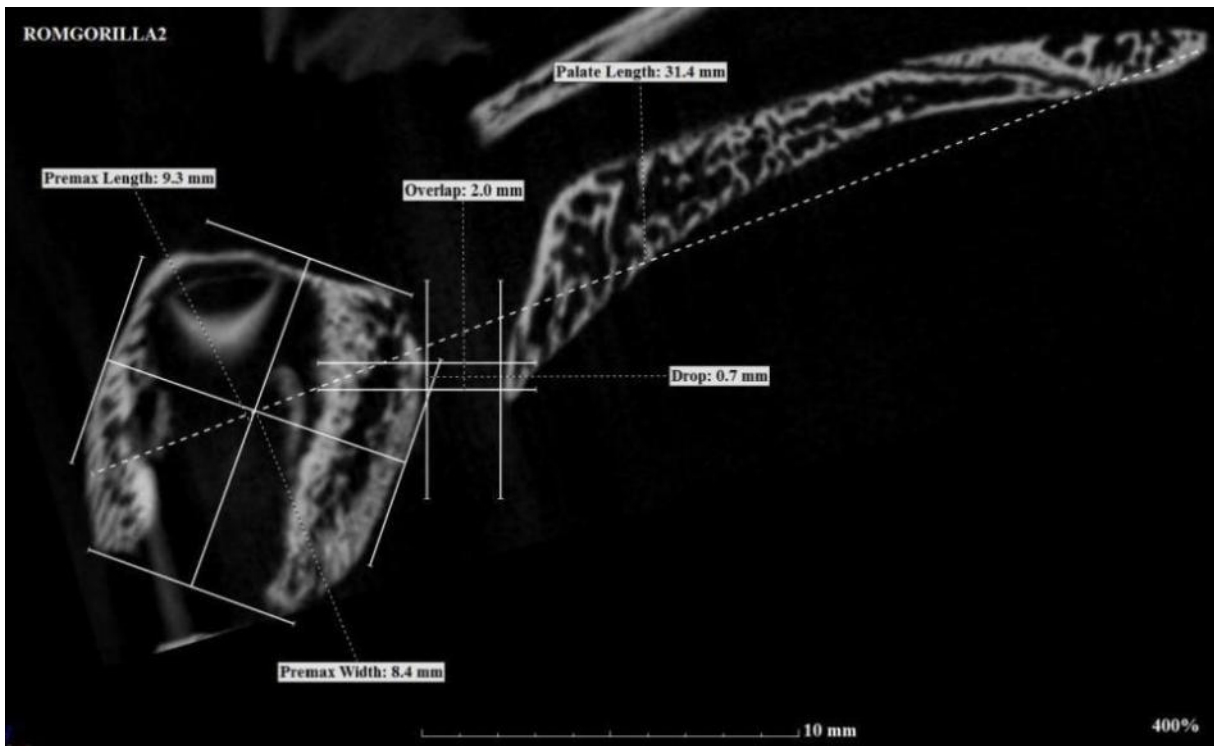
Figure 40 μ-CT of *Gorilla gorilla* infant (ROMGORILLA2), lateral view
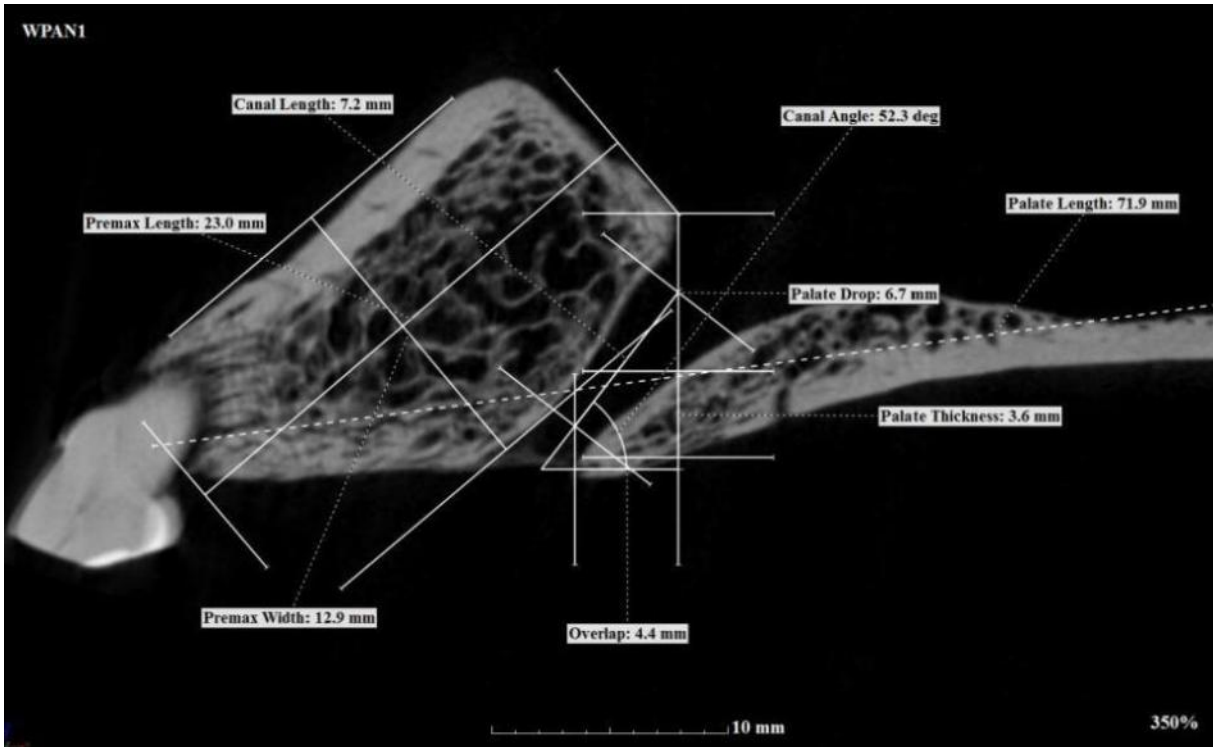
Figure 41 µ-CT of *Pan troglodytes* adult female (WPAN1), lateral view
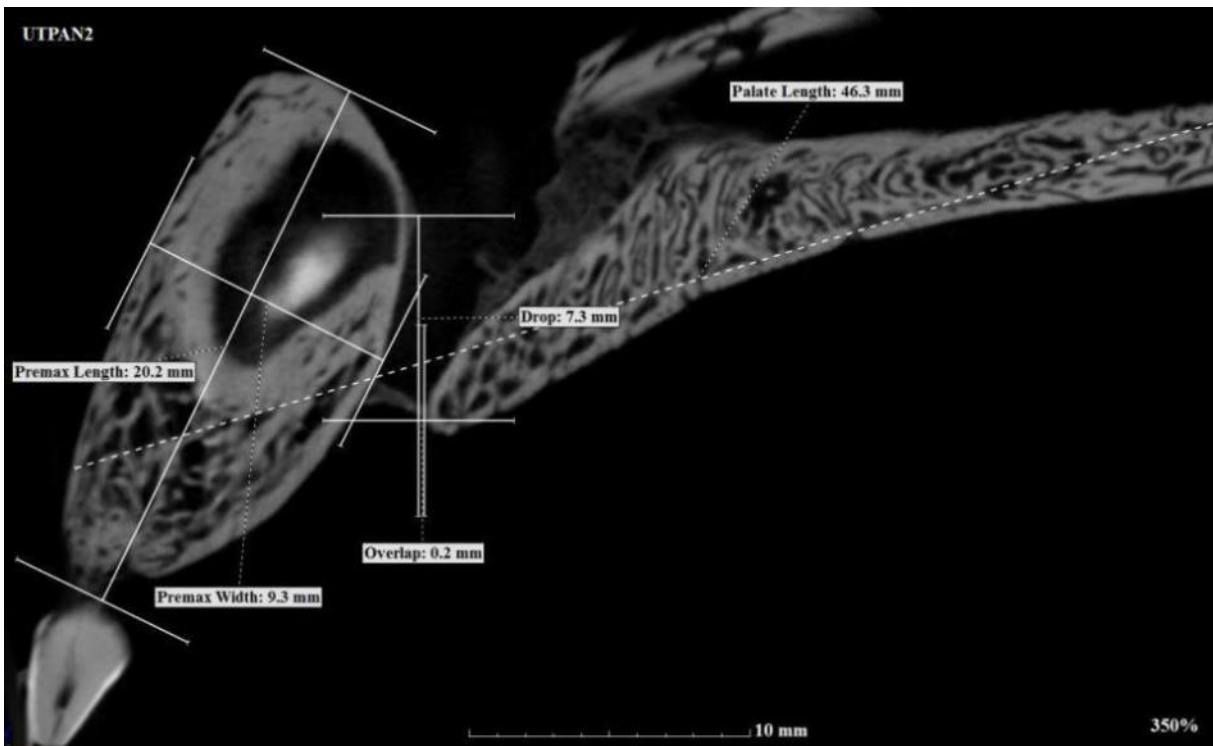
Figure 42 µ-CT of *Pan troglodytes* juvenile (UTPAN2), lateral view
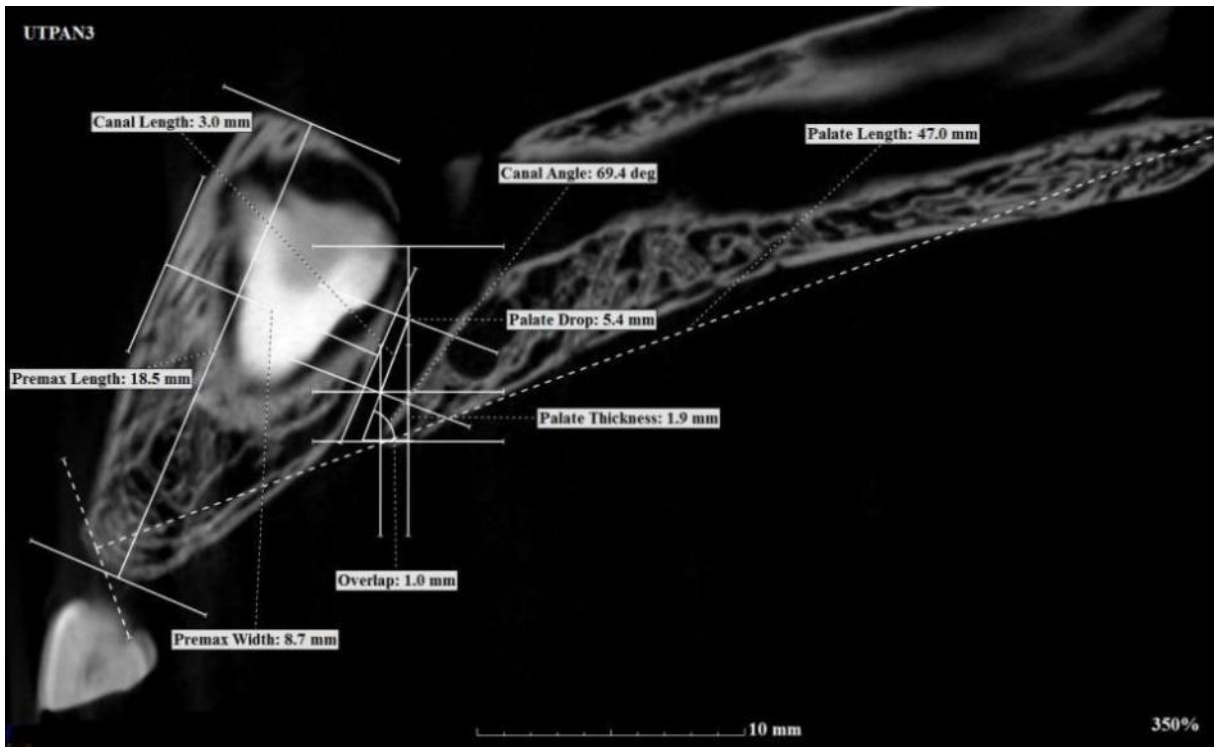
Figure 43 μ-CT of *Pan troglodytes* juvenile (UTPAN3), lateral view
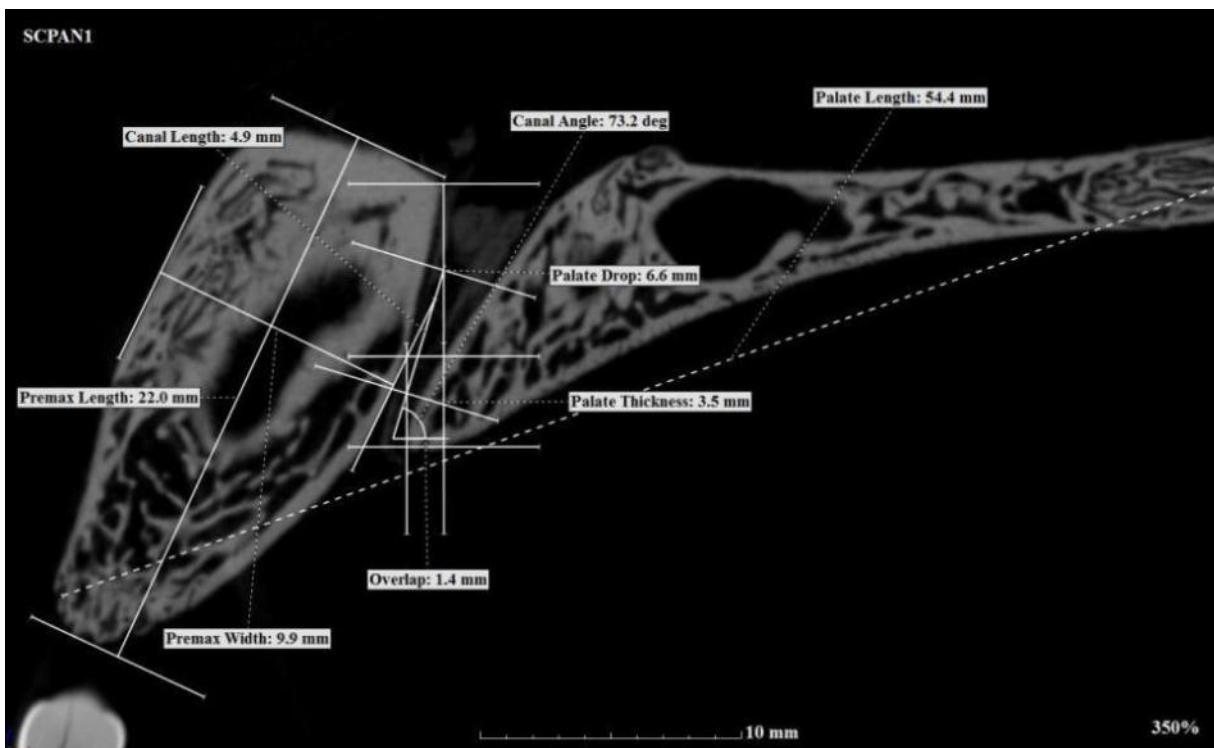
Figure 44 μ-CT of *Pan troglodytes* juvenile (SCPAN1), lateral view
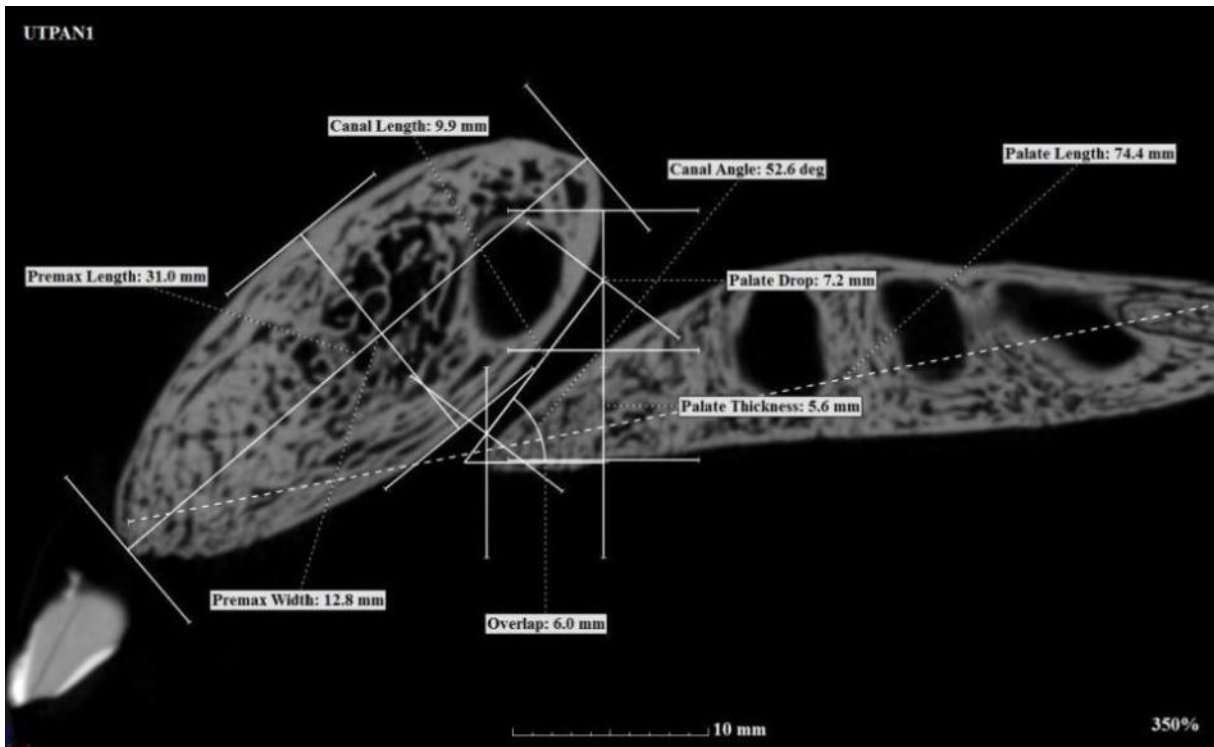
Figure 45 μ-CT of *Pan troglodytes* juvenile male (UTPAN1), lateral view
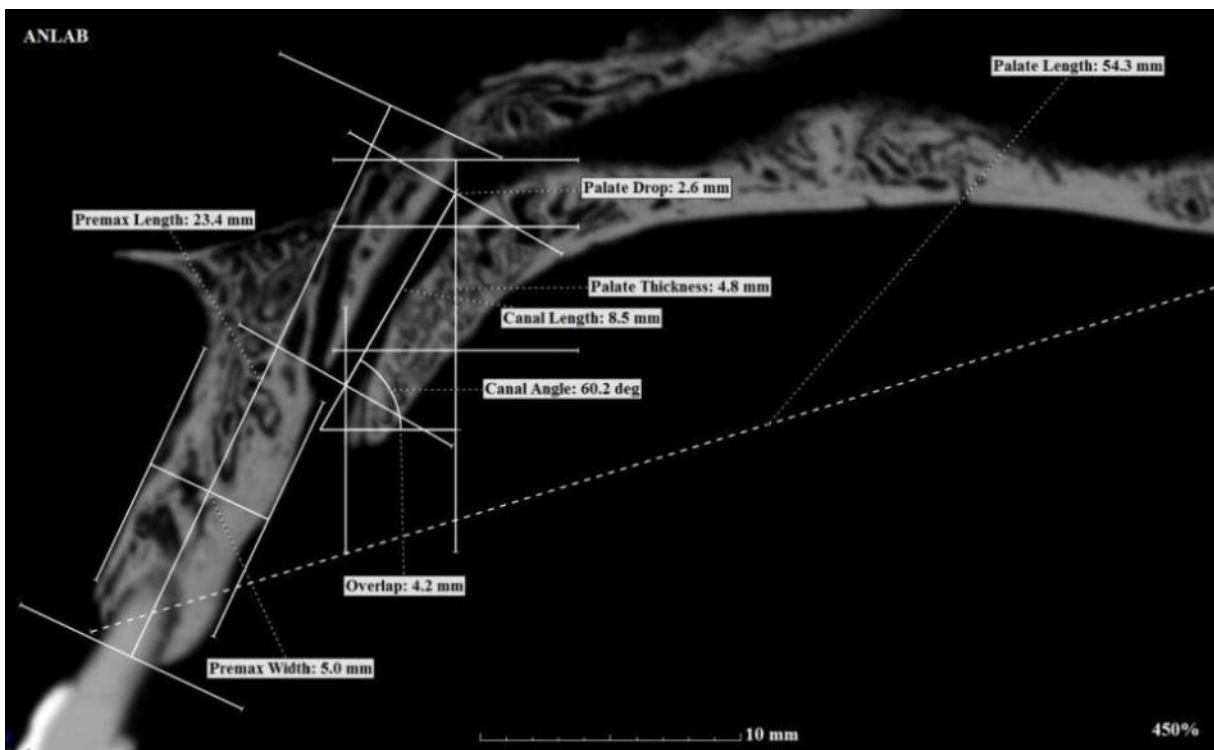
Figure 46 μ-CT of *Homo sapiens* adult female (ANLAB), lateral view
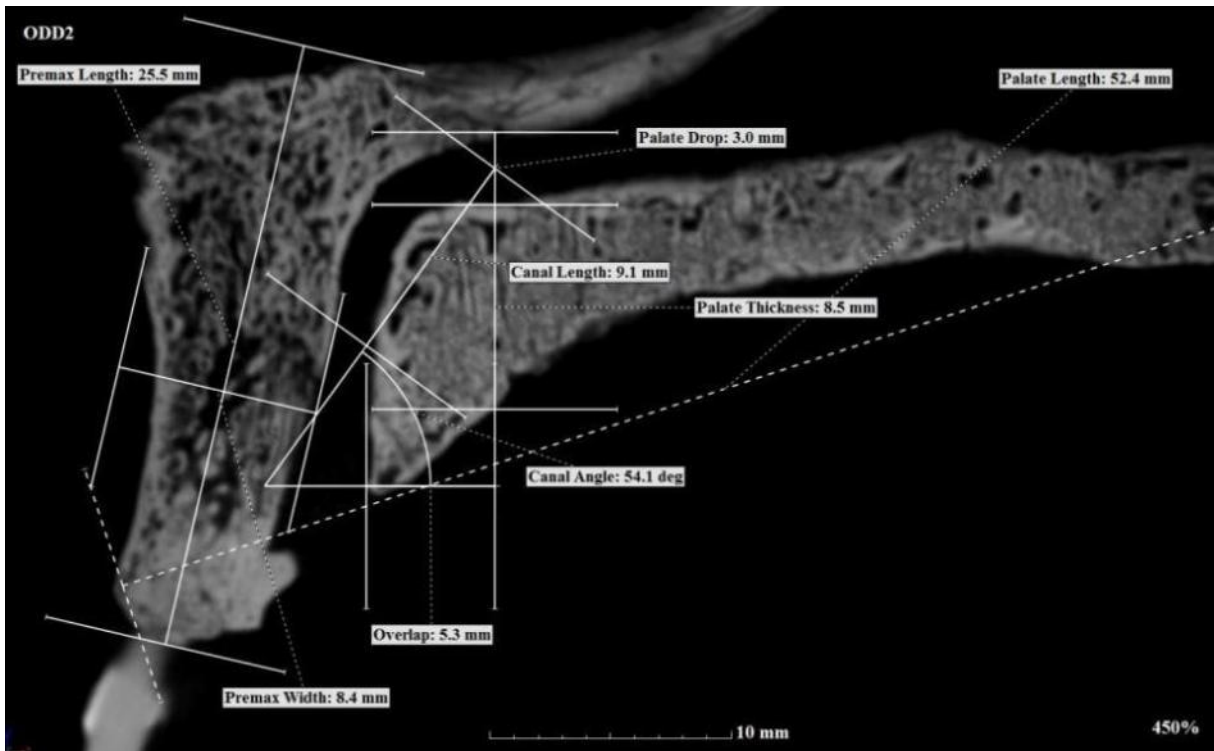
Figure 47 μ-CT of *Homo sapiens* adult female (ODD2), lateral view
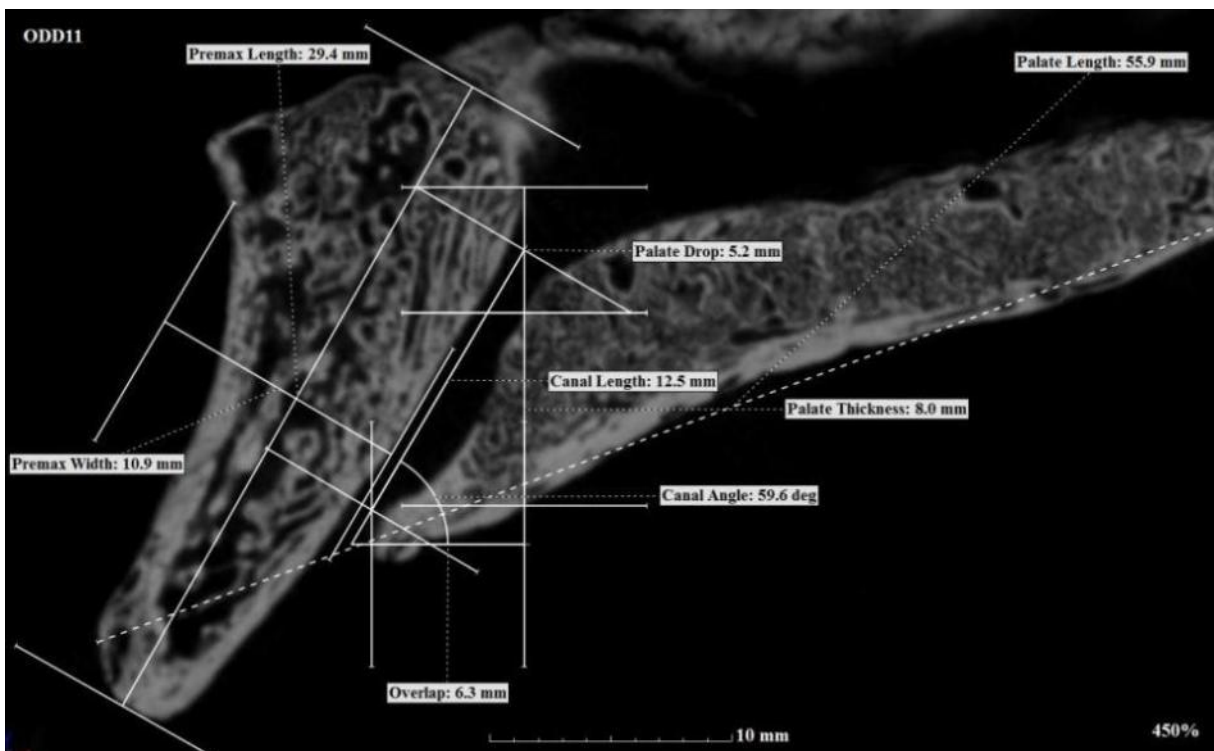
Figure 48 μ-CT of *Homo sapiens* adult female (ODD11), lateral view
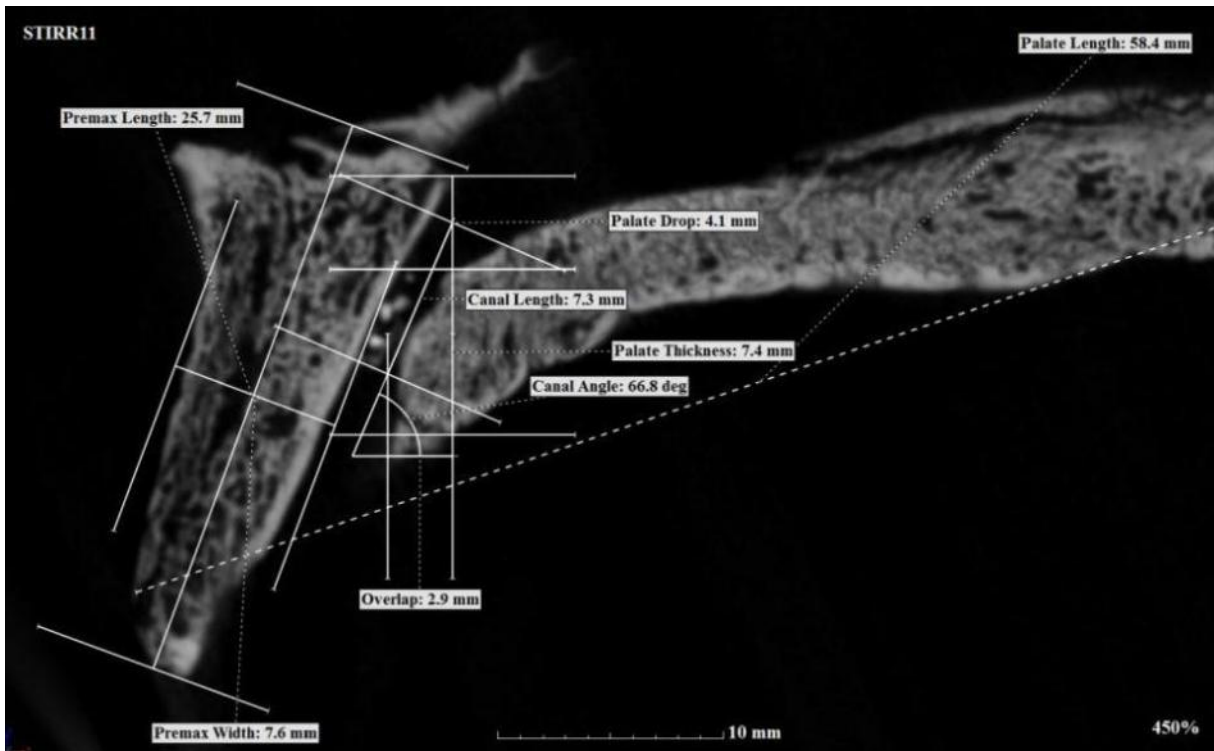
Figure 49 μ-CT of *Homo sapiens* adult male STIRR11), lateral view
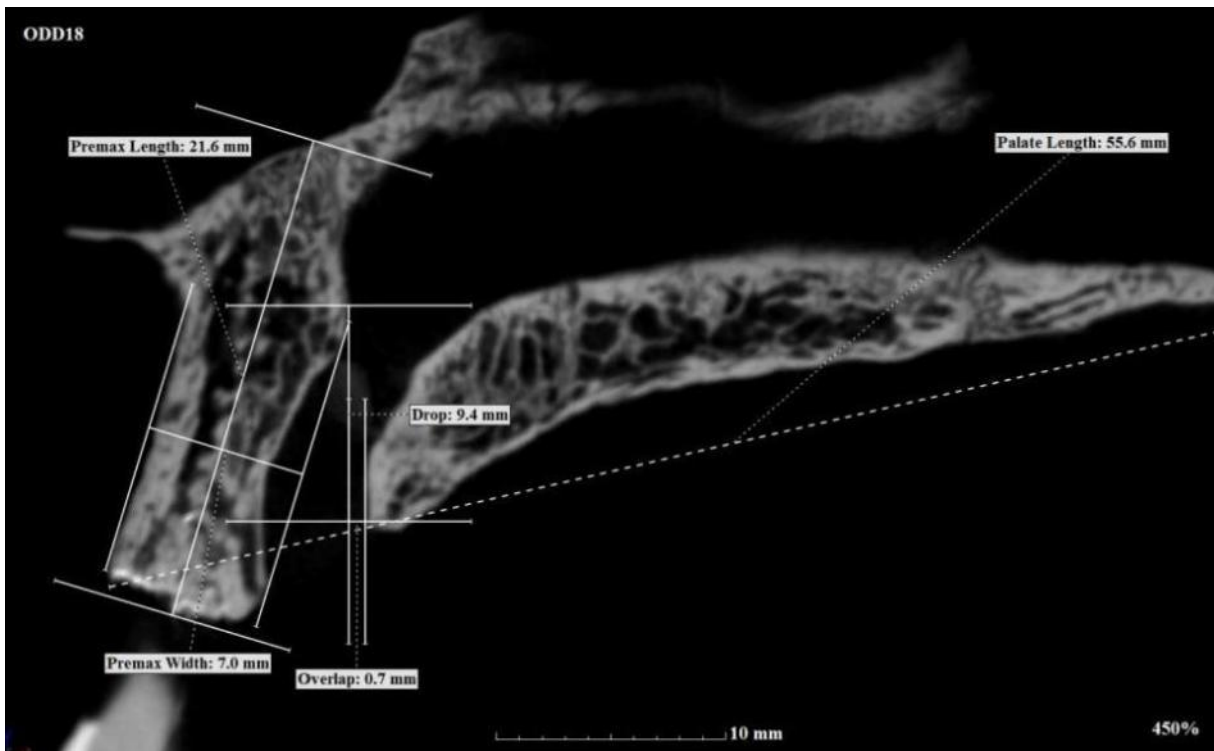
Figure 50 μ-CT of *Homo sapiens* adult male (ODD18), lateral view
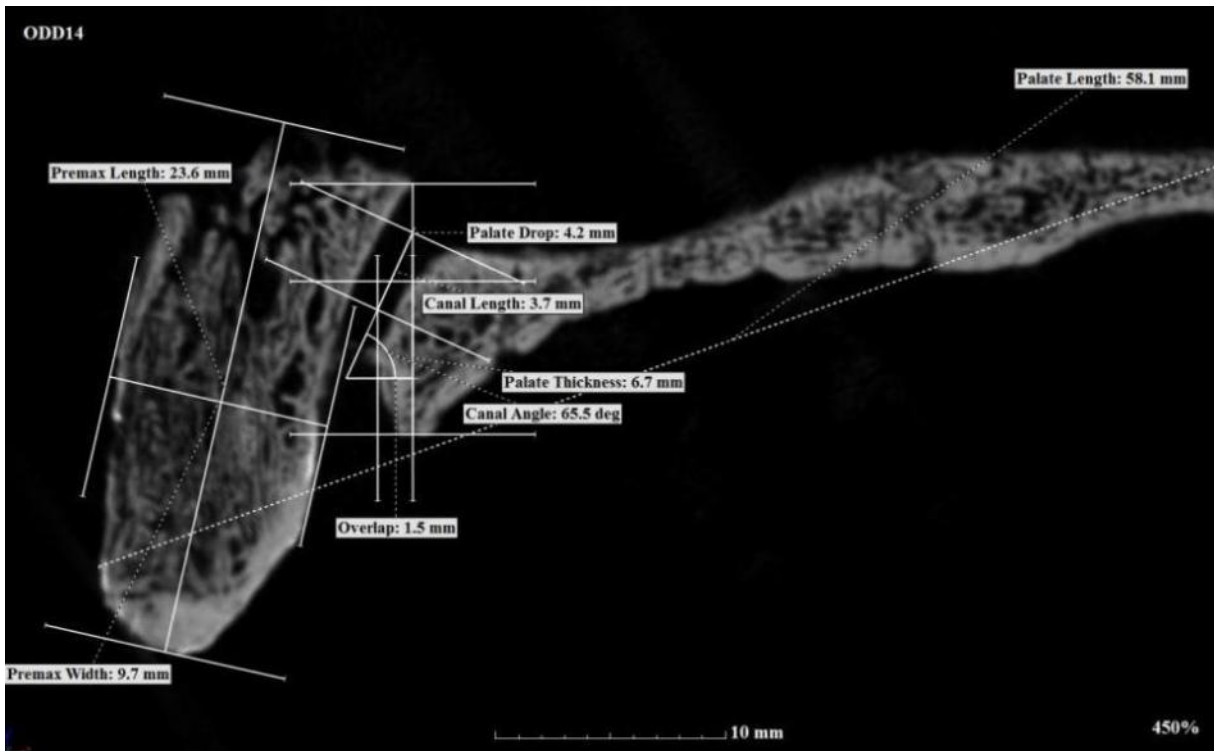
Figure 51 μ-CT of *Homo sapiens* adult male (ODD14), lateral view
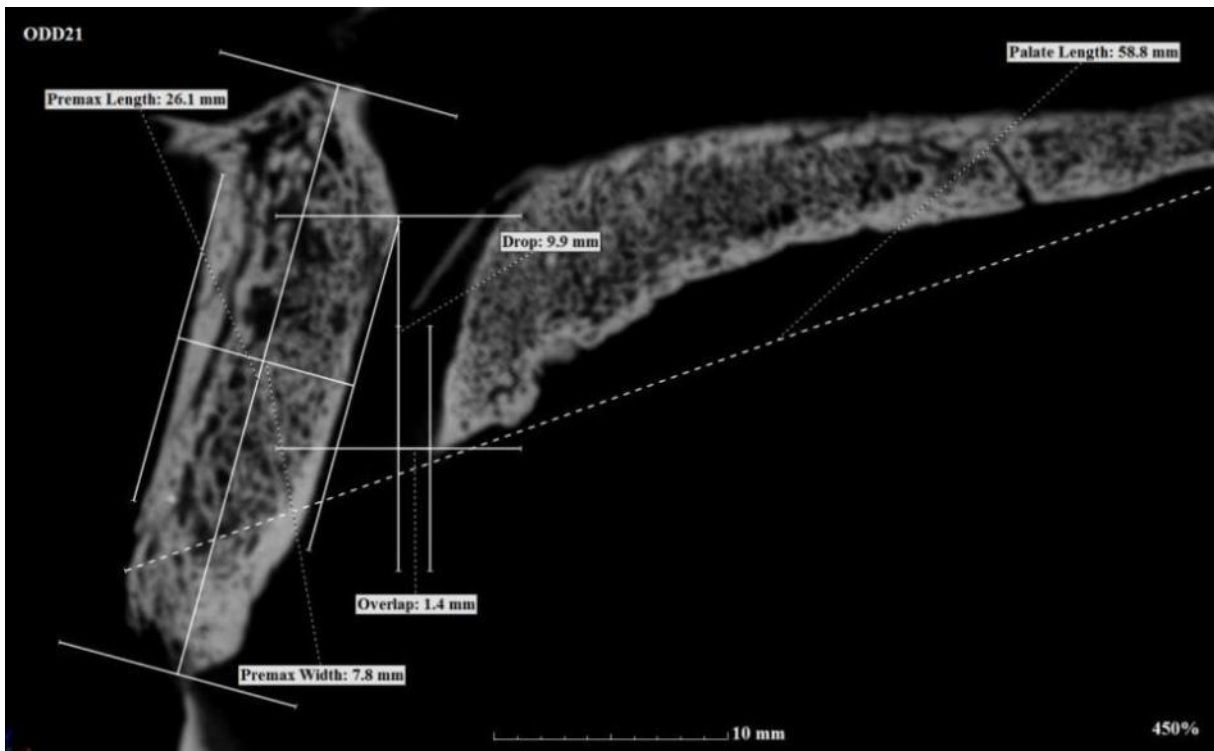
Figure 52 μ-CT of *Homo sapiens* adult male (ODD21), lateral view
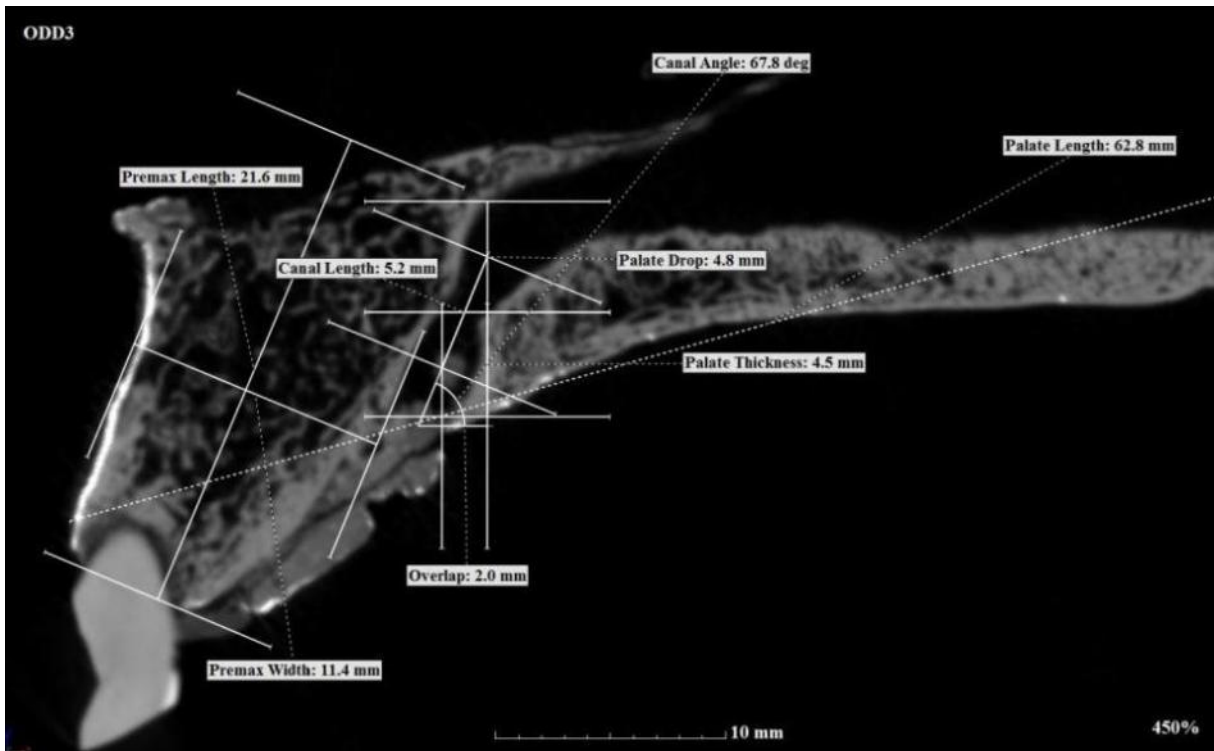
Figure 53 μ-CT of *Homo sapiens* adult male (ODD3), lateral view
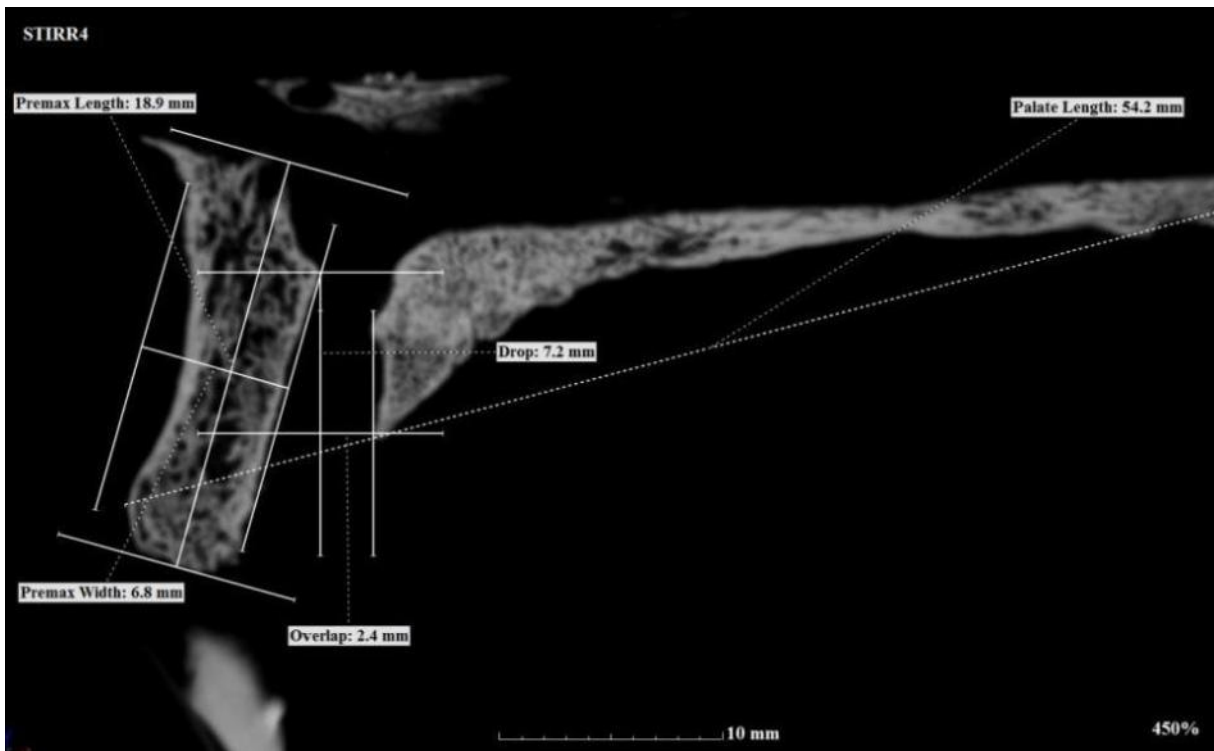
Figure 54 μ-CT of *Homo sapiens* adult male (STIRR4), lateral view
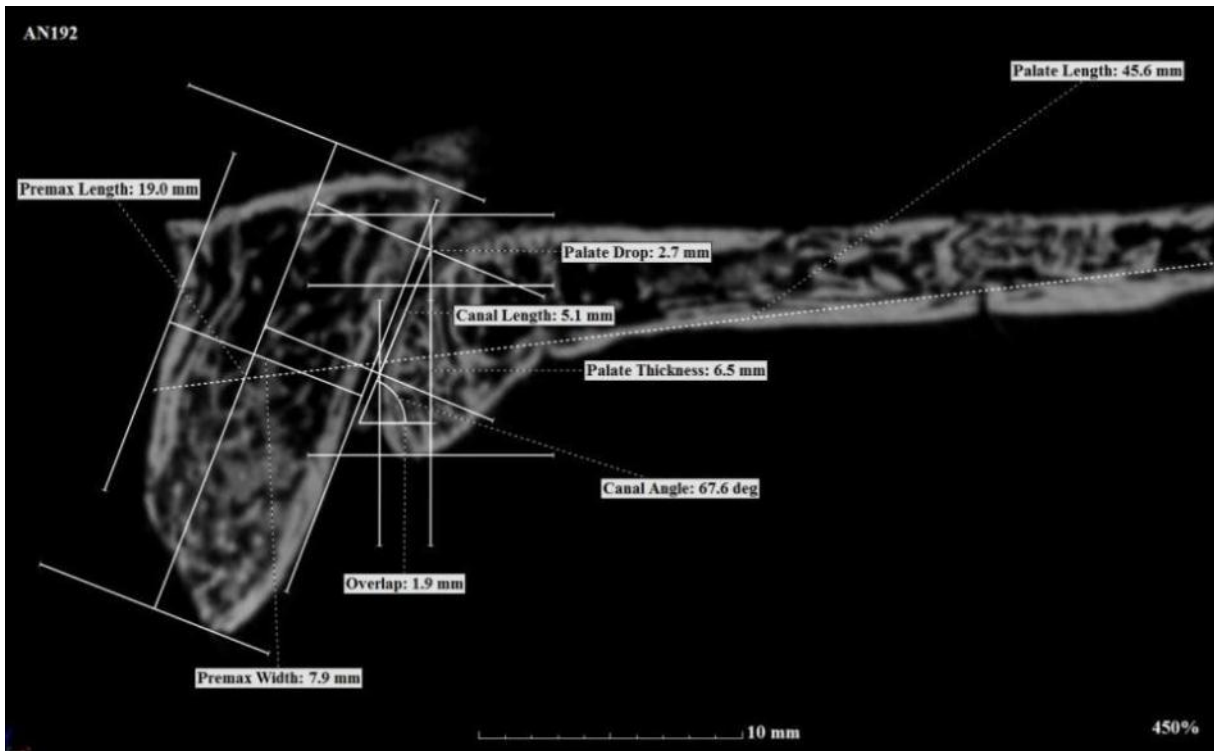
Figure 55 μ-CT of *Homo sapiens* juvenile female (AN192), lateral view
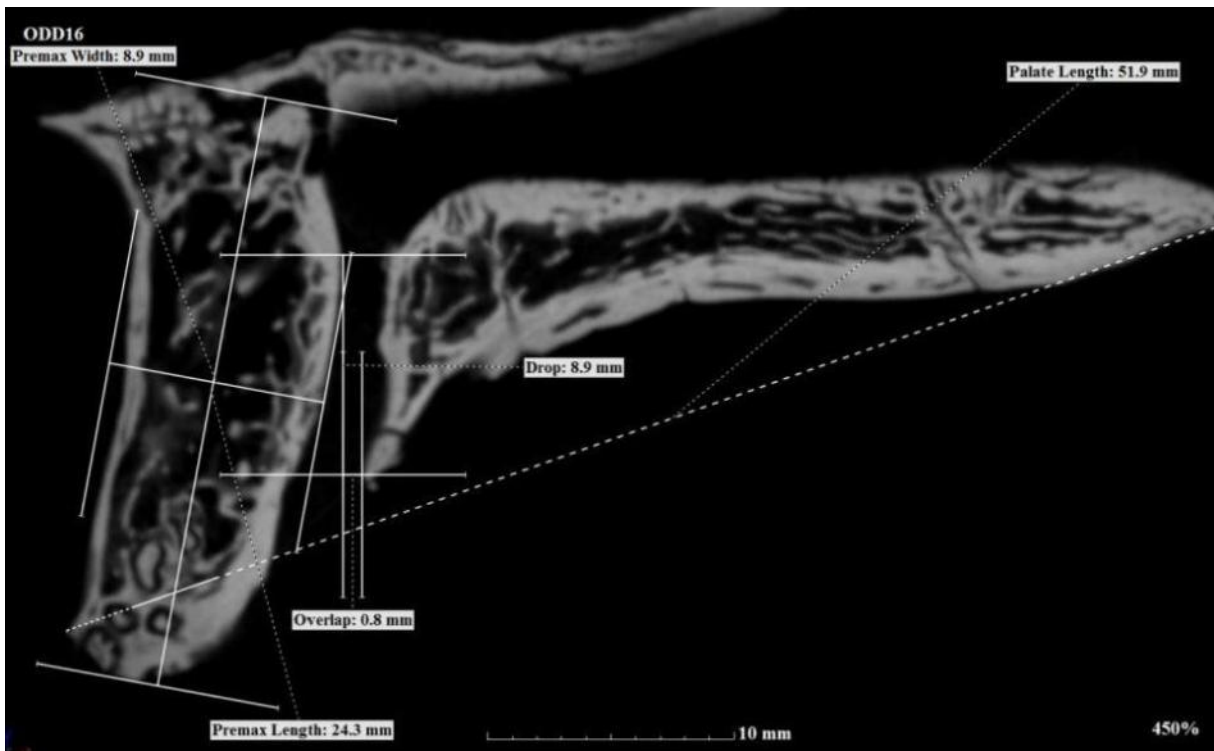
Figure 56 μ-CT of *Homo sapiens* juvenile female (ODD16), lateral view
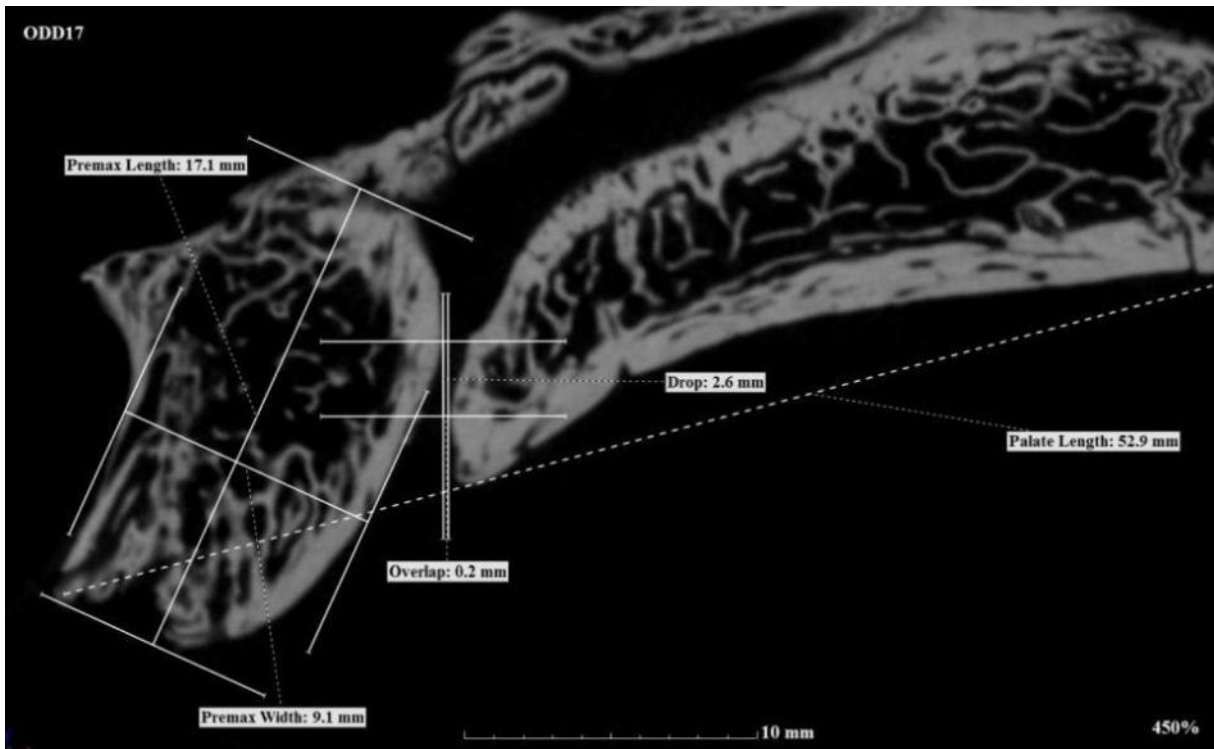
Figure 57 μ-CT of *Homo sapiens* juvenile female (ODD17), lateral view
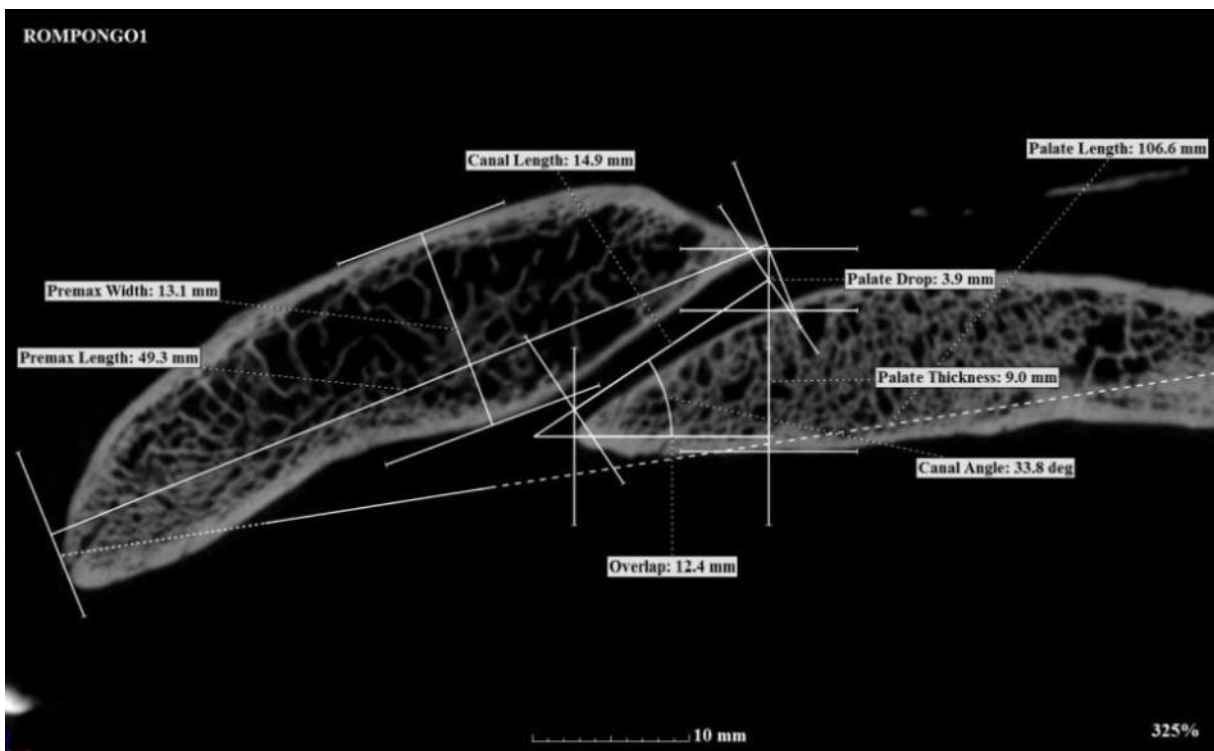
Figure 58 μ-CT of *Pongo abelii* (ROMPONGO1), lateral view
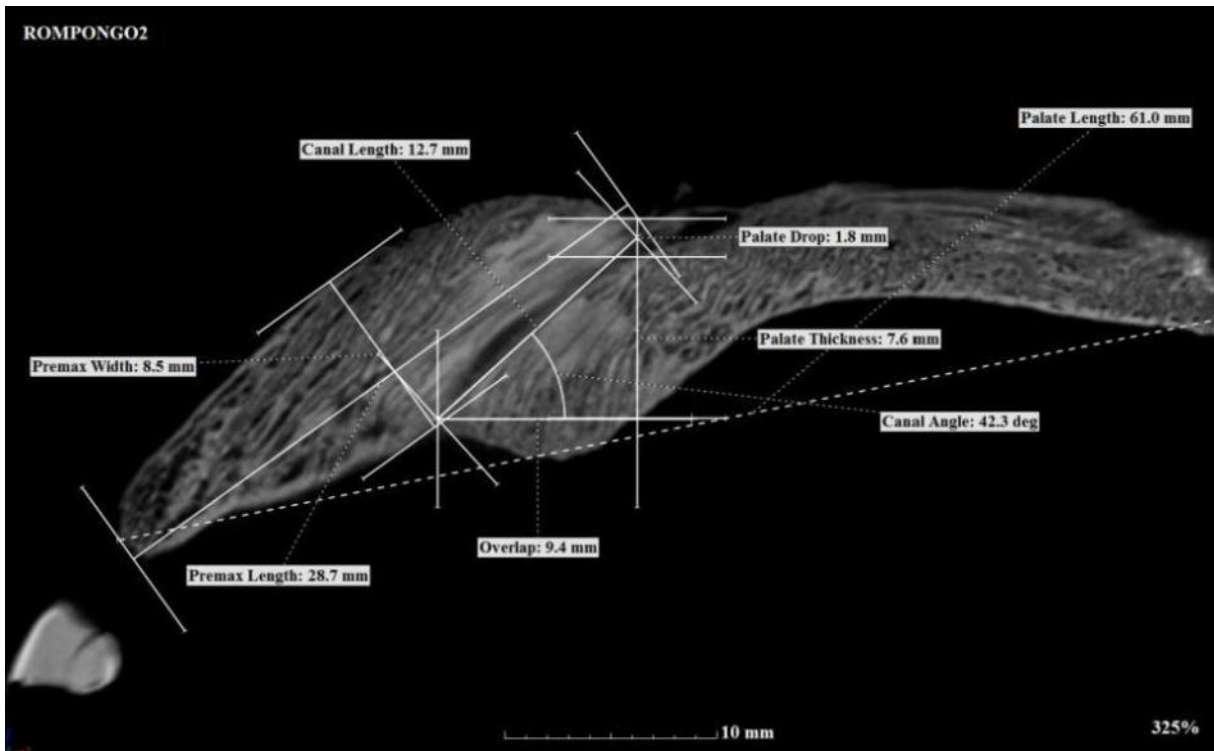
Figure 59 μ-CT of *Pongo abelii* juvenile male (ROMPONGO2), lateral view
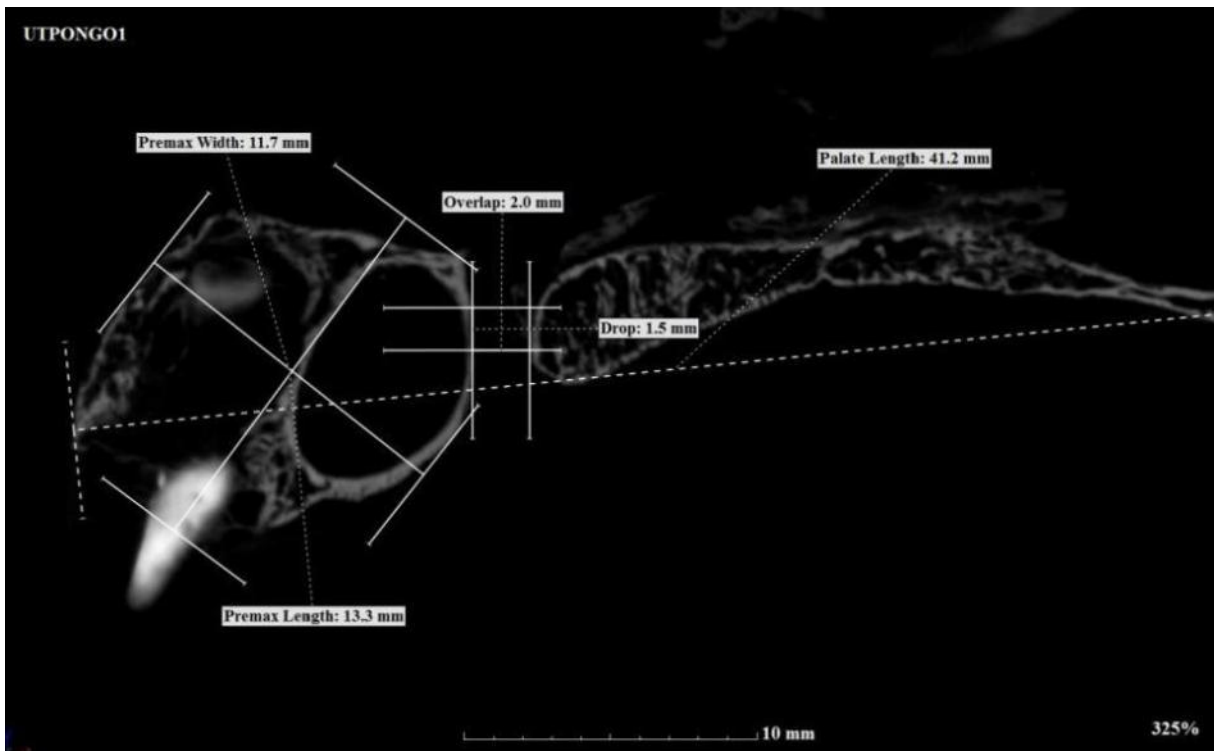
Figure 60 μ-CT of *Pongo abelii* infant (UTPONGO1), lateral view

Appendix B: Primate Subnasal Measurements and Ratios

Macaca mulatta **Subnasal Measurements (mm)**

Individual	Sex	Age	Palate Length	Premax Length	Premax Width	Drop	Overlap
Adults							
WMACACAF	**F**	**Adult**	**44.7**	**8.4**	**5.5**	**-0.6**	**-5.0**
WMACACAM	**M**	**Adult**	**47.5**	**9.0**	**5.7**	**-1.3**	**-4.9**
Mean			*46.10*	*8.70*	*5.60*	*-0.95*	*-4.95*
SD			1.98	0.42	0.14	0.49	0.07

Macaca mulatta **Subnasal Ratios**

Individual	Premax L/ Premax W	Premax L/ Palate L	Overlap/ Palate L	Overlap/ Premax L	Drop/ Palate L	Drop/ Premax L
Adults						
WMACACAF	**1.53**	**0.19**	**-0.11**	**-0.60**	**-0.01**	**-0.07**
WMACACAM	**1.58**	**0.19**	**-0.10**	**-0.54**	**-0.03**	**-0.14**
Mean	*1.55*	*0.19*	*-0.11*	*-0.57*	*-0.02*	*-0.11*
SD	0.04	0.00	0.01	0.04	0.01	0.05

Papio ursinus Subnasal Measurements (mm)

Individual	Sex	Age	Palate Length	Premax Length	Premax Width	Drop	Overlap
Adults							
WPAPIOF	**F**	**Adult**	**85.3**	**15.5**	**6.3**	**-1.2**	**-5.5**
WPAPIOM	**M**	**Adult**	**112.4**	**22.0**	**9.5**	**-3.0**	**-12.1**
Mean			*98.85*	*18.75*	*7.90*	*-2.10*	*-8.80*
SD			19.16	4.60	2.26	1.27	4.67

Papio ursinus Subnasal Ratios

Individual	Premax L/ Premax W	Premax L/ Palate L	Overlap/ Palate L	Overlap/ Premax L	Drop/ Palate L	Drop/ Premax L
Adults						
WPAPIOF	**2.46**	**0.18**	**-0.06**	**-0.35**	**-0.01**	**-0.08**
WPAPIOM	**2.32**	**0.20**	**-0.11**	**-0.55**	**-0.03**	**-0.14**
Mean	*2.39*	*0.19*	*-0.09*	*-0.45*	*-0.02*	*-0.11*
SD	0.10	0.01	0.03	0.14	0.01	0.04

Hylobates lar **and** *Symphalangus syndactylus* **Subnasal Measurements (mm)**

Individual	Sex	Age	Palate Length	Premax Length	Premax Width	Drop	Overlap
Adults							
ROMHYLO1	**NA**	**Adult**	**40.0**	**9.0**	**4.1**	**2.3**	**-3.2**
UTSYMPH1	**NA**	**Adult**	**57.0**	**8.9**	**7.6**	**1.5**	**-3.9**
Mean			*48.50*	*8.95*	*5.85*	*1.90*	*-3.55*
SD			12.02	0.07	2.47	0.57	0.49

Hylobates lar **and** *Symphalangus syndactylus* **Subnasal Ratios**

Individual	Premax L/ Premax W	Premax L/ Palate L	Overlap/ Palate L	Overlap/ Premax L	Drop/ Palate L	Drop/ Premax L
Adults						
ROMHYLO1	**2.20**	**0.23**	**-0.08**	**-0.36**	**0.06**	**0.26**
UTSYMPH1	**1.17**	**0.16**	**-0.07**	**-0.44**	**0.03**	**0.17**
Mean	*1.68*	*0.19*	*-0.07*	*-0.40*	*0.04*	*0.21*
SD	0.72	0.05	0.01	0.06	0.02	0.06

Gorilla gorilla Subnasal Measurements (mm)

Individual	Sex	Age	Palate Length	Premax Length	Premax Width
Adults					
WGORILLA1	**M**	**Adult**	**106.2**	**34.1**	**13.9**
ROMGORILLA1	**M**	**Adult**	**108.7**	**35.4**	**11.8**
Mean			*107.45*	*34.75*	*12.85*
SD			1.77	0.92	1.48
Infants					
ROMGORILLA2	**NA**	**0-0.174**	**31.4**	**9.3**	**8.4**

Gorilla gorilla Subnasal Measurements (mm and degrees)

Individual	Drop	Palate Drop	Overlap	Canal Angle	Canal Length	Palate Thickness
Adults						
WGORILLA1		**5.4**	**2.5**	**34.1**	**3.0**	**0.5**
ROMGORILLA1		**8.9**	**6.6**	**32.2**	**7.8**	**2.5**
Mean		*7.15*	*4.55*	*33.15*	*5.40*	*1.50*
SD		2.47	2.90	1.34	3.39	1.41
Infants						
ROMGORILLA2	**0.7**		**-2.0**			

Gorilla gorilla **Subnasal Ratios**

Individual	Premax L/ Premax W	Premax L/ Palate L	Overlap/ Palate L	Overlap/ Premax L
Adults				
WGORILLA1	**2.45**	**0.32**	**0.02**	**0.07**
ROMGORILLA1	**3.00**	**0.33**	**0.06**	**0.19**
Mean	*2.73*	*0.32*	*0.04*	*0.13*
SD	0.39	0.00	0.03	0.08
Infants				
ROMGORILLA2	**1.11**	**0.30**	**-0.06**	**-0.22**

Gorilla gorilla **Subnasal Ratios**

Individual	Drop/ Palate L	Drop/ Premax L	Palate D/ Premax L	Palate D/ Palate T	Palate T/ Palate L
Adults					
WGORILLA1			**0.16**	**10.80**	**0.00**
ROMGORILLA1			**0.25**	**3.56**	**0.02**
Mean			*0.20*	*7.18*	*0.01*
SD			0.07	5.12	0.01
Infants					
ROMGORILLA2	**0.02**	**0.08**			

***Pan troglodytes* Subnasal Measurements (mm)**

Individual	Sex	Age	Palate Length	Premax Length	Premax Width
Adults					
WPAN1	**F**	**Adult**	**71.9**	**23.0**	**12.9**
Juveniles					
UTPAN2	**NA**	**3.3**	**46.3**	**20.2**	**9.3**
UTPAN3	**NA**	**3.3-5.6**	**47.0**	**18.5**	**8.7**
SCPAN1	**NA**	**3.3-5.6**	**54.4**	**22.0**	**9.9**
UTPAN1	**M**	**11.3**	**74.4**	**31.0**	**12.8**
Mean			*55.53*	*22.93*	*10.18*
SD			13.11	5.57	1.82

***Pan troglodytes* Subnasal Measurements (mm and degrees)**

Individual	Drop	Palate Drop	Overlap	Canal Angle	Canal Length	Palate Thickness
Adults						
WPAN1		**6.7**	**4.4**	**52.3**	**7.2**	**3.7**
Juveniles						
UTPAN2	**7.3**		**-0.2**			
UTPAN3		**5.4**	**1.0**	**69.4**	**3.0**	**1.9**
SCPAN1		**6.6**	**1.4**	**73.2**	**4.9**	**3.5**
UTPAN1		**7.2**	**6.0**	**52.6**	**9.9**	**5.6**
Mean		*6.40*	*2.05*	*65.07*	*5.93*	*3.67*
SD		0.92	2.72	10.96	3.56	1.86

Pan troglodytes **Subnasal Ratios**

Individual	Premax L/ Premax W	Premax L/ Palate L	Overlap/ Palate L	Overlap/ Premax L
Adults				
WPAN1	**1.78**	**0.32**	**0.06**	**0.19**
Juveniles				
UTPAN2	**2.17**	**0.44**	**0.00**	**-0.01**
UTPAN3	**2.13**	**0.39**	**0.02**	**0.05**
SCPAN1	**2.22**	**0.40**	**0.03**	**0.06**
UTPAN1	**2.42**	**0.42**	**0.08**	**0.19**
Mean	*2.24*	*0.41*	*0.03*	*0.08*
SD	0.13	0.02	0.04	0.09

Pan troglodytes **Subnasal Ratios**

Individual	Drop/ Palate L	Drop/ Premax L	Palate D/ Premax L	Palate D/ Palate T	Palate T/ Palate L
Adults					
WPAN1			**0.29**	**1.81**	**0.05**
Juveniles					
UTPAN2	**0.16**	**0.36**			
UTPAN3			**0.29**	**2.84**	**0.04**
SCPAN1			**0.30**	**1.89**	**0.06**
UTPAN1			**0.23**	**1.29**	**0.08**
Mean			*0.27*	*2.00*	*0.06*
SD			0.04	0.78	0.02

Homo sapiens **Subnasal Measurements (mm)**

Individual	Sex	Age	Palate Length	Premax Length	Premax Width
Adult females					
ANLAB	**F**	**>20.5**	**54.4**	**23.4**	**5.0**
ODD2	**F**	**26-38**	**52.4**	**25.5**	**8.4**
ODD11	**F**	**32-36**	**55.9**	**29.4**	**10.9**
Mean			*54.23*	*26.10*	*8.10*
SD			1.76	3.04	2.96
Adult males					
STIRR11	**M**	**35-40**	**58.4**	**25.7**	**7.6**
ODD18	**M**	**28-50**	**55.6**	**21.6**	**7.0**
ODD14	**M**	**38-48**	**58.1**	**23.6**	**9.7**
ODD21	**M**	**40-55**	**58.8**	**26.1**	**7.8**
ODD3	**M**	**45-55**	**62.9**	**21.6**	**11.4**
STIRR4	**M**	**76**	**54.2**	**18.9**	**6.9**
Mean			*58.00*	*22.92*	*8.40*
SD			3.00	2.75	1.78
All adults					
Mean			*56.74*	*23.98*	*8.30*
SD			3.15	3.10	2.05
Juveniles					
AN192	**F**	**11.95**	**45.6**	**19.0**	**7.9**
ODD16	**NA**	**11-20.5**	**52.0**	**24.3**	**8.9**
ODD17	**F**	**20.5**	**52.9**	**17.2**	**9.1**
Mean			*50.17*	*20.17*	*8.63*
SD			3.98	3.69	0.64

Homo sapiens **Subnasal Measurements (mm and degrees)**

Individual	Drop	Palate Drop	Overlap	Canal Angle	Canal Length	Palate Thickness
Adult females						
ANLAB		**2.6**	**4.2**	**60.2**	**8.5**	**4.8**
ODD2		**3.0**	**5.3**	**54.1**	**9.1**	**8.5**
ODD11		**5.2**	**6.3**	**59.6**	**12.5**	**8.0**
Mean		*3.60*	*5.27*	*57.97*	*10.03*	*7.10*
SD		1.40	1.05	3.36	2.16	2.01
Adult males						
STIRR11		**4.1**	**2.9**	**66.8**	**7.3**	**7.4**
ODD18	**9.4**		**-0.7**			
ODD14		**4.2**	**1.5**	**65.5**	**3.7**	**6.7**
ODD21	**9.9**		**-1.4**			
ODD3		**4.8**	**2.0**	**67.8**	**5.2**	**4.5**
STIRR4	**7.2**		**-2.4**			
Mean	*8.83*	*4.37*	*0.32*	*66.70*	*5.40*	*6.20*
SD	1.44	0.38	2.11	1.15	1.81	1.51
All adults						
Mean	*8.83*	*3.98*	*1.97*	*62.33*	*7.72*	*6.65*
SD	1.44	1.01	3.03	5.29	3.10	1.66
Juveniles						
AN192		**2.7**	**2.0**	**67.6**	**5.1**	**6.5**
ODD16	**8.9**		**-0.8**			
ODD17	**2.6**		**-0.2**			
Mean	*5.75*		*0.33*			
SD	4.45		1.47			

***Homo sapiens* Subnasal Ratios**

Individual	Premax L/ Premax W	Premax L/ Palate L	Overlap/ Palate L	Overlap/ Premax L
Adult females				
ANLAB	**4.68**	**0.43**	**0.08**	**0.18**
ODD2	**3.04**	**0.49**	**0.10**	**0.21**
ODD11	**2.70**	**0.53**	**0.11**	**0.21**
Mean	*3.47*	*0.48*	*0.10*	*0.20*
SD	1.06	0.05	0.02	0.02
Adult males				
STIRR11	**3.38**	**0.44**	**0.05**	**0.11**
ODD18	**3.09**	**0.39**	**-0.01**	**-0.03**
ODD14	**2.43**	**0.41**	**0.03**	**0.06**
ODD21	**3.35**	**0.44**	**-0.02**	**-0.05**
ODD3	**1.89**	**0.34**	**0.03**	**0.09**
STIRR4	**2.74**	**0.35**	**-0.04**	**-0.13**
Mean	*2.81*	*0.40*	*0.00*	*0.01*
SD	0.58	0.04	0.04	0.09
All adults				
Mean	*3.03*	*0.42*	*0.04*	*0.07*
SD	0.77	0.06	0.06	0.12
Juveniles				
AN192	**2.41**	**0.42**	**0.04**	**0.11**
ODD16	**2.73**	**0.47**	**-0.02**	**-0.03**
ODD17	**1.89**	**0.33**	**0.00**	**-0.01**
Mean	*2.34*	*0.40*	*0.01*	*0.02*
SD	0.42	0.07	0.03	0.07

Homo sapiens Subnasal Ratios

Individual	Drop/ Palate L	Drop/ Premax L	Palate D/ Premax L	Palate D/ Palate T	Palate T/ Palate L
Adult females					
ANLAB			**0.11**	**0.54**	**0.09**
ODD2			**0.12**	**0.35**	**0.16**
ODD11			**0.18**	**0.65**	**0.14**
Mean			_0.14_	_0.51_	_0.13_
SD			0.04	0.15	0.04
Adult males					
STIRR11			**0.16**	**0.55**	**0.13**
ODD18	**0.17**	**0.44**			
ODD14			**0.18**	**0.63**	**0.12**
ODD21	**0.17**	**0.38**			
ODD3			**0.22**	**1.07**	**0.07**
STIRR4	**0.13**	**0.38**			
Mean	_0.16_	_0.40_	_0.19_	_0.75_	_0.10_
SD	0.02	0.03	0.03	0.28	0.03
All adults					
Mean	_0.16_	_0.40_	_0.16_	_0.63_	_0.12_
SD	0.02	0.03	0.04	0.24	0.03
Juveniles					
AN192			**0.14**	**0.42**	**0.14**
ODD16	**0.17**	**0.37**			
ODD17	**0.05**	**0.15**			
Mean	_0.11_	_0.26_			
SD	0.09	0.15			

Pongo abelii Subnasal Measurements (mm)

Individual	Sex	Age	Palate Length	Premax Length	Premax Width
Adults					
ROMPONGO1	**M**	**Adult**	**106.6**	**49.3**	**13.1**
Juveniles					
ROMPONGO2	**M**	**5.0-6.0**	**61.0**	**28.7**	**8.5**
Infants					
UTPONGO1	**NA**	**0.704**	**41.2**	**13.3**	**11.7**

Pongo abelii Subnasal Measurements (mm and degrees)

Individual	Drop	Palate Drop	Overlap	Canal Angle	Canal Length	Palate Thickness
Adults						
ROMPONGO1		**3.9**	**12.4**	**33.8**	**14.9**	**9.0**
Juveniles						
ROMPONGO2		**1.8**	**9.4**	**42.3**	**12.7**	**7.6**
Infants						
UTPONGO1	**1.5**		**-2.0**			

Pongo abelii **Subnasal Ratios**

Individual	Premax L/ Premax W	Premax L/ Palate L	Overlap/ Palate L	Overlap/ Premax L
Adults				
ROMPONGO1	**3.76**	**0.46**	**0.12**	**0.25**
Juveniles				
ROMPONGO2	**3.38**	**0.47**	**0.15**	**0.33**
Infants				
UTPONGO1	**1.14**	**0.32**	**-0.05**	**-0.15**

Pongo abelii **Subnasal Ratios**

Individual	Drop/ Palate L	Drop/ Premax L	Palate D/ Premax L	Palate D/ Palate T	Palate T/ Palate L
Adults					
ROMPONGO1			**0.08**	**0.43**	**0.08**
Juveniles					
ROMPONGO2			**0.06**	**0.24**	**0.12**
Infants					
UTPONGO1	**0.04**	**0.11**			

Appendix C: Primate Subnasal Data Tables

Primates Subnasal Data Tables (mm)

Individual	Sex	Age Years	Palate Length	Premax Length	Premax Width	Drop	Palate Drop	Overlap
Macaca								
WMACACAF	**F**	**Adult**	**44.7**	**8.4**	**5.5**	**-0.6**		**-5.0**
WMACACAM	**M**	**Adult**	**47.5**	**9.0**	**5.7**	**-1.3**		**-4.9**
Papio								
WPAPIOF	**F**	**Adult**	**85.3**	**15.5**	**6.3**	**-1.2**		**-5.5**
WPAPIOM	**M**	**Adult**	**112.4**	**22.0**	**9.5**	**-3.0**		**-12.1**
Hylobates								
ROMHYLO1	**NA**	**Adult**	**40.0**	**9.0**	**4.1**	**2.3**		**-3.2**
UTSYMPH1	**NA**	**Adult**	**57.0**	**8.9**	**7.6**	**1.5**		**-3.9**
Gorilla								
WGORILLA1	**M**	**Adult**	**106.2**	**34.1**	**13.9**	**6.3**	**5.4**	**2.5**
ROMGORILLA1	**M**	**Adult**	**108.7**	**35.4**	**11.8**	**11.6**	**8.9**	**6.6**
ROMGORILLA2	**NA**	**0-0.174**	**31.4**	**9.3**	**8.4**	**0.7**		**-2.0**
Pan								
WPAN1	**F**	**Adult**	**71.9**	**23.0**	**12.9**	**10.8**	**6.7**	**4.4**
UTPAN1	**NA**	**11.3**	**74.4**	**31.0**	**12.8**	**12.9**	**7.2**	**6.0**
UTPAN2	**NA**	**3.3**	**46.3**	**20.2**	**9.3**	**7.3**		**-0.2**
UTPAN3	**NA**	**3.3-5.6**	**47.0**	**18.5**	**8.7**	**7.3**	**5.4**	**1.0**
SCPAN1	**NA**	**3.3-5.6**	**54.4**	**22.0**	**9.9**	**9.8**	**6.6**	**1.4**
Pongo								
ROMPONGO1	**M**	**Adult**	**106.6**	**49.3**	**13.1**	**12.0**	**3.9**	**12.4**
ROMPONGO2	**M**	**5.0-6.0**	**61.0**	**28.7**	**8.5**	**9.5**	**1.8**	**9.4**
UTPONGO1	**NA**	**0.704**	**41.2**	**13.3**	**11.7**	**1.5**		**-2.0**

Primates Subnasal Data Tables (mm and degrees)

Individual	Palate Rise	Half-Palate Drop	Half-Palate Rise	Canal Angle	Canal Length	Palate Thickness	Incisive Foramen
Macaca							
WMACACAF							**R**
WMACACAM							**R**
Papio							
WPAPIOF							**R**
WPAPIOM							**R**
Hylobates							
ROMHYLO1							**R**
UTSYMPH1							**R**
Gorilla							
WGORILLA1	**3.9**	**2.7**	**2.0**	**34.1**	**3.0**	**0.5**	**R**
ROMGORILLA1	**5.9**	**4.5**	**2.8**	**32.2**	**7.8**	**2.5**	**R**
ROMGORILLA2							**R**
Pan							
WPAN1	**3.7**	**3.3**	**1.8**	**52.3**	**7.2**	**3.7**	**R**
UTPAN1	**3.0**	**3.6**	**1.5**	**52.6**	**9.9**	**5.6**	**R**
UTPAN2							**R**
UTPAN3	**3.6**	**2.7**	**1.8**	**69.4**	**3.0**	**1.9**	**R**
SCPAN1	**3.5**	**3.3**	**1.7**	**73.2**	**4.9**	**3.5**	**R**
Pongo							
ROMPONGO1	**3.4**	**2.0**	**1.7**	**33.8**	**14.9**	**9.0**	**R**
ROMPONGO2	**NA**	**0.9**	**NA**	**42.3**	**12.7**	**7.6**	**M**
UTPONGO1							**R**

Human Subnasal Data Tables (mm)

Individual	Sex	Age Years	Palate Length	Premax Length	Premax Width	Drop	Palate Drop	Overlap
Homo								
AN192	F	11.95	45.6	19.0	7.9	7.9	2.7	2.0
ANLAB	F	>20.5	54.4	23.4	5.0	10.4	2.6	4.2
ODD2	F	26-38	52.4	25.5	8.4	14.7	3.0	5.3
ODD3	M	45-55	62.9	21.6	11.4	9.8	4.8	2.0
ODD11	F	32-36	55.9	29.4	10.9	14.8	5.2	6.3
ODD14	M	38-48	58.1	23.6	9.7	8.5	4.2	1.5
ODD16	F	12-20.5	52.0	24.3	8.9	8.9		-0.8
ODD17	F	20.5	52.9	17.2	9.1	2.6		-0.2
ODD18	M	28-50	55.6	21.6	7.0	9.4		-0.7
ODD21	M	40-55	58.8	26.1	7.8	9.9		-1.4
STIRR4	M	76	54.2	18.9	6.9	7.2		-2.4
STIRR11	M	35-40	58.4	25.7	7.6	12.4	4.1	2.9

Human Subnasal Data Tables (mm and degrees)

Individual	Palate Rise	Half-Palate Drop	Half-Palate Rise	Canal Angle	Canal Length	Palate Thickness	Incisive Foramen
Homo							
AN192	**3.8**	**1.4**	**1.9**	**67.6**	**5.1**	**6.5**	**L**
ANLAB	**3.4**	**1.3**	**1.7**	**60.2**	**8.5**	**4.8**	**R**
ODD2	**11.6**	**1.5**	**5.8**	**54.1**	**9.1**	**8.5**	**R**
ODD3	**5.0**	**2.4**	**2.5**	**67.8**	**5.2**	**4.5**	**L**
ODD11	**2.9**	**2.6**	**1.4**	**59.6**	**12.5**	**8.0**	**R**
ODD14	**6.0**	**2.1**	**3.0**	**65.5**	**3.7**	**6.7**	**L**
ODD16							**R**
ODD17							**R**
ODD18							**R**
ODD21							**R**
STIRR4							**L**
STIRR11	**7.3**	**2.1**	**3.7**	**66.8**	**7.3**	**7.4**	**R**

Appendix D: Primate Micro-CT Scanning Values

Primate Micro-CT Scanning Values

Individual	File Size (GB)	Resolution (μm)	Penetrance kV	Intensity μA
Macaca				
WMACACAF	**2.82 GB**	**79.7**	**140**	**35**
WMACACAM	**2.90 GB**	**84.1**	**140**	**35**
Papio				
WPAPIOF	**2.39 GB**	**125.7**	**140**	**35**
WPAPIOM	**2.29 GB**	**163.1**	**140**	**35**
Hylobates				
ROMHYLO1	**2.78 GB**	**74.5**	**130**	**40**
UTSYMPH1	**3.18 GB**	**90.4**	**135**	**40**
Gorilla				
WGORILLA1	**4.83 GB**	**163.1**	**140**	**35**
ROMGORILLA1	**5.78 GB**	**163.1**	**135**	**40**
ROMGORILLA2	**2.07 GB**	**83.6**	**130**	**40**
Pan				
WPAN1	**4.12 GB**	**116.8**	**140**	**37**
UTPAN1	**2.47 GB**	**141.1**	**135**	**40**
UTPAN2	**3.09 GB**	**98.3**	**135**	**35**
UTPAN3	**2.64 GB**	**103.2**	**135**	**35**
SCPAN1	**3.19 GB**	**105.7**	**130**	**40**
Pongo				
ROMPONGO1	**4.79 GB**	**163.1**	**135**	**40**
ROMPONGO2	**2.90 GB**	**120.7**	**130**	**40**
UTPONGO1	**2.97 GB**	**87.3**	**135**	**35**

Human Micro-CT Scanning Values

Individual	File Size (GB)	Resolution (µm)	Penetrance kV	Intensity µA
Homo				
AN192	**2.58 GB**	**134.7**	**135**	**45**
ANLAB	**2.68 GB**	**136.1**	**135**	**45**
ODD2	**2.42 GB**	**146.8**	**135**	**45**
ODD3	**2.48 GB**	**153.6**	**135**	**45**
ODD11	**2.60 GB**	**146.4**	**135**	**45**
ODD14	**2.67 GB**	**153.9**	**135**	**45**
ODD16	**2.19 GB**	**143.6**	**135**	**45**
ODD17	**3.30 GB**	**121.1**	**135**	**45**
ODD18	**2.60 GB**	**154.2**	**135**	**45**
ODD21	**2.71 GB**	**151.3**	**135**	**45**
STIRR4	**2.48 GB**	**158.8**	**135**	**45**
STIRR11	**2.23 GB**	**157.3**	**135**	**45**

Appendix E: Description of Primates

Cercopithecoids

Macaca mulatta

WMACACAM

WMACACAM is an adult male cranium (T49) from the Biology Department at Western University. The adult upper third molars were fully erupted.

WMACACAF

WMACACAF is an adult male cranium (T46) from the Biology Department at Western University. The adult upper third molars were fully erupted but are missing.

Papio ursinus

WPAPIOM

WPAPIOM is an adult male cranium (T18) from the Biology Department at Western University. The adult upper third molars were fully erupted.

WPAPIOF

WPAPIOF is an adult male cranium (T220) from the Biology Department at Western University. The adult upper third molars were fully erupted.

Hylobatids

Hylobates lar

ROMHYLO1

ROMHYLO1 is an adult cranium and mandible (R1187) from the Department of Vertebrate Paleontology at the Royal Ontario Museum. The adult upper third molars were fully erupted.

Symphalangus syndactylus

UTSYMPH1

UTSYMPH1 is an adult cranium (CO11.V.K.) from the Anthropology Department at the University of Toronto. The adult upper third molars were fully erupted.

Hominids

Hominines

Gorilla gorilla

WGORILLA1

WGORILLA1 is an adult male cranium (T265) from the Biology Department at Western University. The adult upper third molars were fully erupted.

ROMGORILLA1

ROMGORILLA1 is an adult male cranium missing the parietals (R8118) from the Department of Vertebrate Paleontology at the Royal Ontario Museum. The adult upper third molars were fully erupted.

ROMGORILLA2

ROMGORILLA2 is an infant cranium (R2323) from the Department of Vertebrate Paleontology at the Royal Ontario Museum. Only deciduous upper teeth are present and are only beginning to erupt from the alveolar process. The deciduous upper first incisor crowns are fully formed and the root has begun formation but they have not, or have only just begun eruption. In *Gorilla*, the deciduous teeth have not yet begun to erupt at birth and the first teeth to erupt are the deciduous upper incisors (0.174 years) (Smith et al. 1994). ROMGORILLA2 was between 0 and 2 months old.

Pan troglodytes

WPAN1

WPAN1 is an adult female cranium (T266) from the Biology Department at Western University. The adult upper third molars were fully erupted.

UTPAN1

UTPAN1 is a juvenile (female?) cranium (PA/260 PC1) from the Anthropology Department at the University of Toronto. The upper third adult molar is approximately three-quarters erupted and has not reached the occlusal plane although the roots are almost fully formed. In *Pan* the upper adult third molars begin to erupt at 11.33 years in females and 11.36 in males (Smith et al., 1994). UTPAN1 was at least, but not significantly older than, 11.3 years old.

UTPAN2

UTPAN2 is a juvenile cranium (no accession #) from the Anthropology Department at the University of Toronto. The adult upper first molar is beginning to erupt, although the cusps are still even with the surface of the alveolar process and the roots are approximately half-formed. In *Pan* the upper adult first molar begins to erupt at 3.27 years in females and 3.38 in males (Smith et al., 1994). UTPAN2 was approximately 3.3 years old.

UTPAN3

UTPAN3 is a juvenile cranium (PA/275a 9) from the Anthropology Department at the University of Toronto. The adult upper first molar is fully erupted but the roots are still completing formation. The adult upper first incisor crowns are fully formed but they have not begun eruption. In *Pan* the adult upper first molar begins eruption at 3.27 years in females and 3.38 years in males and the adult upper first incisor begins eruption at 5.63 years in females and 5.62 years in males (Smith et al., 1994). UTPAN3 was between 3.3 and 5.6 years.

SCPAN1

SCPAN1 is a juvenile cranium (no accession #) from the Anthropology Department at the University of Toronto, Scarborough. The adult upper first molar was fully erupted and the roots are approximately one-half formed. The adult upper first incisor crowns are fully formed and the roots have begun formation but they have not erupted. In *Pan* the adult upper first molar begins eruption at 3.27 years in females and 3.38 years in males and the adult upper first incisor begins

eruption at 5.63 years in females and 5.62 years in males (Smith et al., 1994). SCPAN1 was between 3.3 and 5.6 years.

Homo sapiens

AN192

AN192 is a probable juvenile cranium (192) from the Bioarchaeology Lab at Western University. The adult upper first premolar was half erupted and the root is half formed. The adult upper second premolar was beginning to erupt, but to less a degree than the adult first upper premolar. The adult upper second molar was just beginning to erupt, to less a degree than the adult second upper premolar and the root did not begin formation. Based on the dental eruption sequences in Smith et al. (1994) the dental eruption pattern fits that of a female. In female *H. sapiens* the adult second molar begins to erupt at 11.95 years (Smith et al., 1994). AN192 was approximately 11.95 years old.

ANLAB

ANLAB is an adult cranium (no accession #) from the Bioarchaeology Lab at Western University. The adult upper third molar is fully erupted. In female *H. sapiens* the adult upper third molar begins eruption at approximately 20.5 years (Smith et al., 2004). ANLAB was at least 20.5 years old

ODD2

ODD2 is an adult female cranium (Odd Fellows 2i), aged 26-38, of possible European ancestry from the Odd Fellows Series at the Anthropology Department, Western University (Ginter, 2001). The adult upper third molar is fully erupted. The third molar is identifiable by size, crown morphology and position. The adult upper first molars are missing and their dental alveoli have been fully resorbed.

ODD3

ODD3 is an adult male cranium (Odd Fellows 3i), aged 45-55, of possible African ancestry from the Odd Fellows Series at the Anthropology Department, Western University (Ginter, 2001). The adult upper third molars are missing but the rest of the adult dentition is fully erupted.

ODD11

ODD11 is an adult female cranium (Odd Fellows 11i), aged 32-36, of possible African ancestry from the Odd Fellows Series at the Anthropology Department, Western University (Ginter, 2001). The adult upper third molars are fully erupted.

ODD14

ODD14 is an adult (male) cranium (Odd Fellows 14i), aged 38-48, of possible African or European ancestry, from the Odd Fellows Series at the Anthropology Department, Western University (Ginter, 2001). The adult upper third molar is fully erupted. The adult second molars are missing and the dental alveoli are fully resorbed.

ODD16

ODD16 is a juvenile female cranium (or adult who has lost molars) (Odd Fellows 16ai), aged 20-30, of possible European or African ancestry from the Odd Fellows Series at the Anthropology Department, Western University (Ginter, 2001). The adult second molars are fully erupted but the adult first molars are missing and the dental alveoli have been fully resorbed. The adult third molar crowns are fully formed and the roots are one-third formed but the teeth have not erupted. All other teeth are fully erupted. In *H. sapiens* females the second last tooth to erupt is the upper second molar at 11.95 years and in males the second last tooth to erupt is the upper canine at 11.29 years (Smith et al., 1994). In *H. sapiens* the upper third molar erupts at approximately 20.5 years. ODD16 was between 12 to 20.5 years old.

ODD17

ODD17 is a juvenile female cranium (Odd Fellows 17ai), aged 18-20, of possible European or South Asian ancestry from the Odd Fellows Series at the Anthropology Department, Western University (Ginter, 2001). The adult third molar has only begun to erupt through the alveolar

process and the roots are not fully formed. In *H. sapiens* the adult upper third molar begins eruption at approximate 20.5 years old (Smith et al., 2004).

ODD18

ODD18 is an adult male cranium (Odd Fellows 18i), aged 28-50, of possible European or Japanese ancestry from the Odd Fellows Series at the Anthropology Department, Western University (Ginter, 2001). The adult third molar is fully erupted but missing.

ODD21

ODD21 is an adult male cranium (Odd Fellows 21ai), aged 40-55, of possible European or Chinese ancestry from the Odd Fellows Series at the Anthropology Department, Western University (Ginter, 2001). The adult third molar is fully erupted.

STIRR4

STIRR4 is an adult male cranium (Stirrup Court 4), aged 76, from the Stirrup Court Series at the Anthropology Department, Western University (Parish, 2000). The adult third molars are fully erupted but missing from the dental alveoli.

STIRR11

STIRR11 is an adult male cranium (Stirrup Court 11), aged 35-40, from the Stirrup Court Series at the Anthropology Department, Western University (Parish, 2000).

Pongines

Pongo abelii

ROMPONGO1

ROMPONGO1 is an adult male cranium and mandible (R1190) from the Department of Vertebrate Paleontology at the Royal Ontario Museum. The upper third molars were fully erupted.

ROMPONGO2

ROMPONGO2 is a juvenile male cranium (R1189) from the Department of Vertebrate Paleontology at the Royal Ontario Museum. The adult upper first and second molars are fully erupted. The adult upper first and second premolars and the adult upper first and second incisor crowns are fully formed but none of the teeth have yet erupted. The adult upper first premolar is just beginning to push out the upper deciduous first premolar.

In *Pongo* the adult upper second molar begins eruption at 5.0 years and while the adult upper first incisor and the adult upper first premolar begin erupting at 6.0-7.0 years. ROMPONGO2 was between 5.0 to 6.0 years old and most likely closer to 6.0 years old.

UTPONGO1

UTPONGO1 is an infant cranium (FA429-1) from the Anthropology Department at the University of Toronto. Only deciduous teeth have erupted. The deciduous upper first incisor is mostly erupted and the root is approximately half formed. The deciduous upper first premolar crown is fully formed and half erupted. The deciduous upper second incisor crown is fully formed and has just begun eruption and the root has not begun formation. In *Pongo* the deciduous upper first premolar begins eruption at 0.625 years and the deciduous upper second incisor begins eruption at 0.704 years. UTPONGO1 was approximately 8.5 months old.

Appendix F: Subnasal Measurement Intra-Observer Error Test

Intra-Observer Error Tests (April 16, July 24, and August 9, 2013)

Hylobates lar **Subnasal Measurements (mm)**

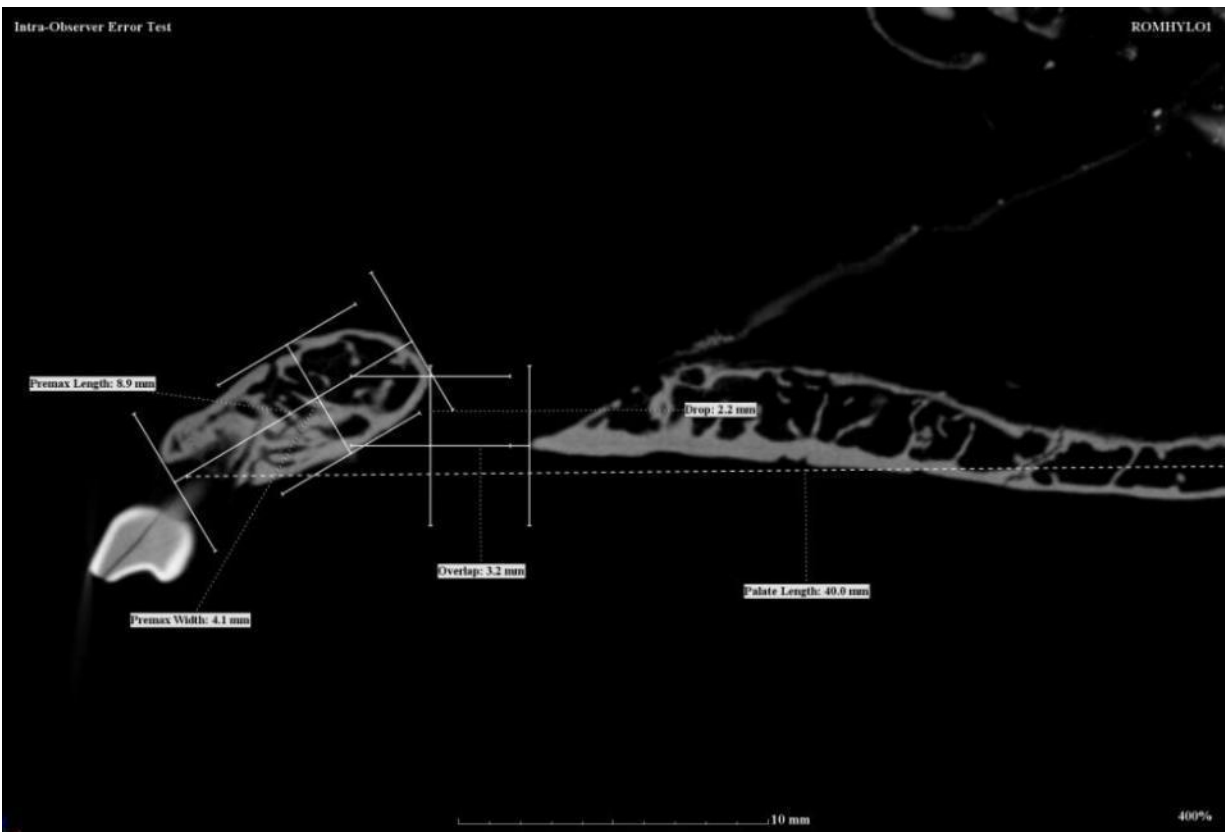| Individual	Date Measured	Palate Length	Premax Length	Premax Width	Drop	Overlap
ROMHYLO1	**Apr-16**	**40.0**	**9.0**	**4.1**	**2.3**	**-3.2**
ROMHYLO1	**Jul-24**	**40.0**	**8.9**	**4.1**	**2.2**	**-3.2**
ROMHYLO1	**Aug-09**	**40.0**	**9.0**	**4.1**	**2.3**	**-3.2**
Mean		*40.00*	*8.97*	*4.10*	*2.27*	*-3.20*
SD		0.00	0.06	0.00	0.06	0.00

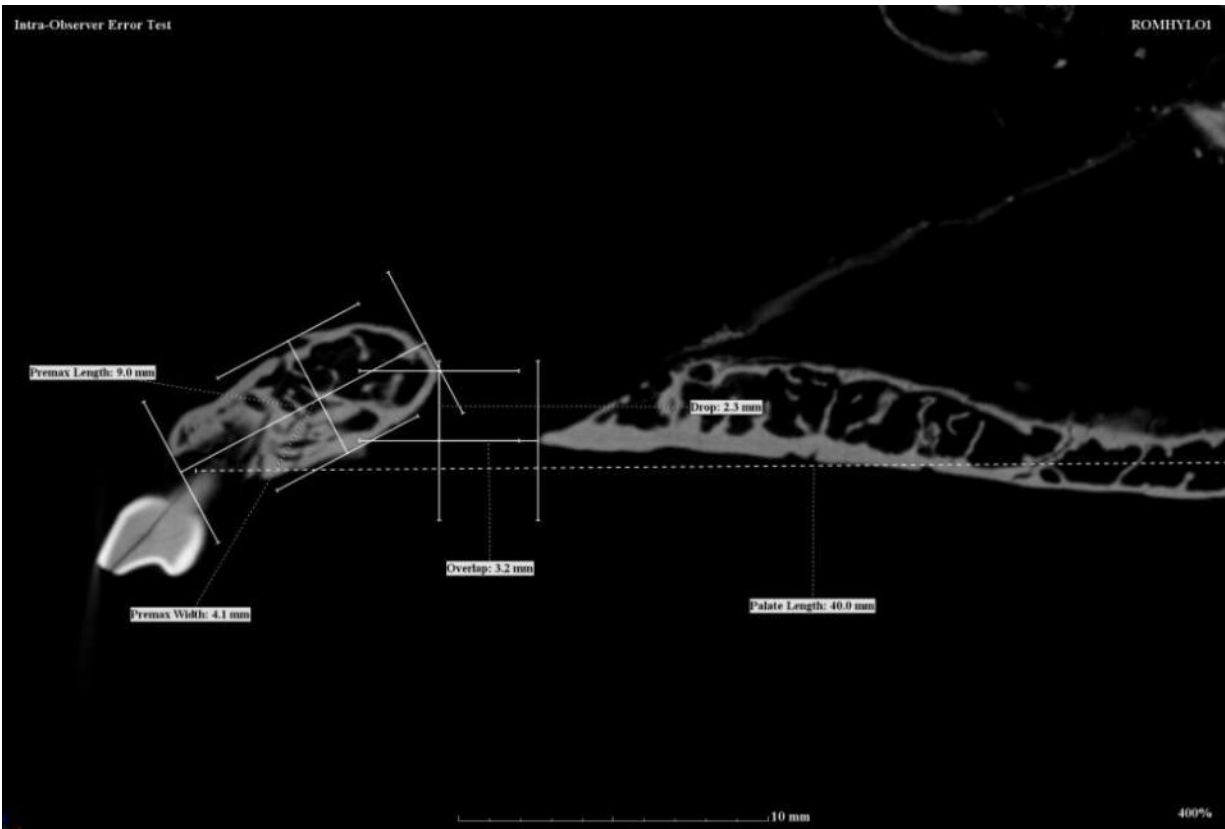**Figure 61 ROMHYLO1 Subnasal Measurements, July 24, 2013**

Figure 62 ROMHYLO1 Subnasal Measurements, August 9, 2013

Appendix G: Specimen Mounting For Micro-CT Scanning

To optimize the scanning of cranial specimens a specially designed Styrofoam mounting box was constructed for each individual specimen. The mounting box was designed with a number of goals in mind. The mounting box was to raise the specimen clear of the manipulator, to hold the specimen stable, to maximize the resolution of the scan and to minimize the effects of beam hardening.

The mounts were open-ended boxes constructed out of one-half-inch thick Styrofoam. Styrofoam is ideal for specimen mounting as the X-rays fully penetrate the material and the Styrofoam holds the specimen securely, while providing protection against damage (see: Figure 63). The specimens could easily be transported and stored in their mounts.
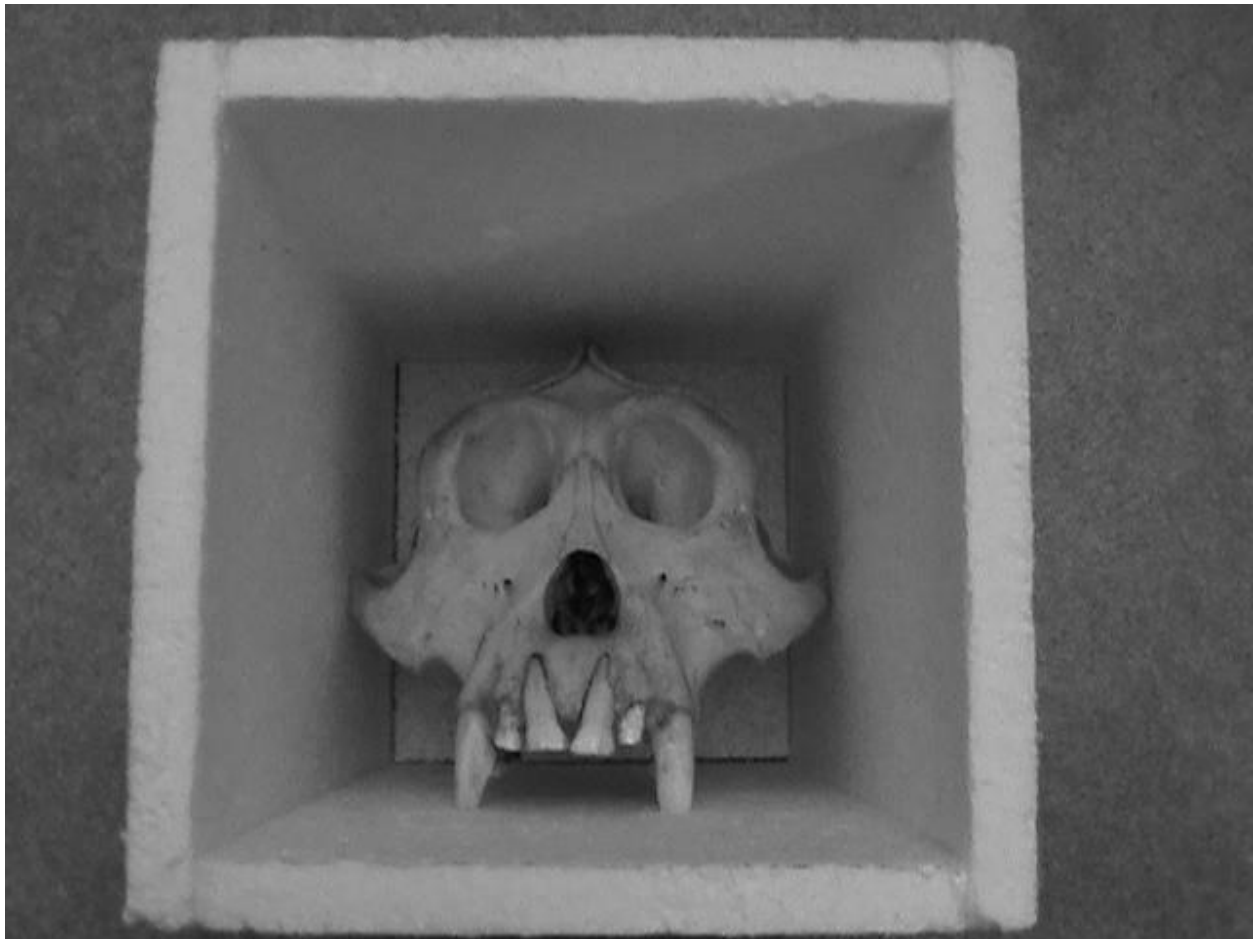

Figure 63 ROMPONGO1 in Styrofoam Mounting Box (adult male *P. abelii*)

The simplest method of mounting crania would be to place in flat on a Styrofoam block, approximating its normal orientation, with the long axis of the crania horizontal. However, this is not the most efficient method of scanning the subnasal anatomy. In order to maximize the resolution of the scanner, a specimen should be mounted in such a way that it fills up the largest area of the imaging panel as possible. The imaging panel is square, measuring (2000 x 2000 pixels) while the majority of the non-human primate crania are sub-rectangular or oblong in shape. This requires them to be mounted on a diagonal—approximately 60 degrees from the vertical, if the image resolution is to be maximized. Mounting the crania in this way, the crania could be brought closer to the source of the x-rays while staying within the imaging panel, maximizing geometric magnification.

The adult male *Gorilla* and *Pongo* specimens had to be mounted with the long-axis oriented towards the vertical as they were too long to fit inside the imaging panel. Even with the optimized orientation mounting described above, they were still too large to fit completely inside the imaging panel. At no time can an image be allowed to rotate outside the imaging panel on the horizontal axis, or perpendicular to the axis of rotation, as this will result in a disruption of the reconstructed specimen. However, portions of a specimen can rotate outside of the imaging panel along the vertical axis, or parallel to the axis of rotation as this will have no effect on image reconstruction.

The appropriate angle of a specimen was determined by the following: The specimen was held in a lateral view, face pointing vertically. Appropriate angle was found by tilting the specimen away from the vertical until the height and width of the specimen, measured with a square, were equal. Thus, the specimen was oriented in such a way it would maximize the area covered within the square scanning panel in a lateral view. In essence the long axis of the skull was titled at 45 degrees from the vertical. However, as the cranium is a three dimensional object, it rotates outside of this defined square. As such, the crania needed to be tilted more towards the vertical and through trial and error it was determined an angle of approximately 30 degrees from vertical would optimize the mounting of cranium, although it would vary for each specimen. It should be noted that increasing the resolution of the scans also results in larger files sizes.

After initial scanning, it was determined that beam hardening was an issue on some crania. Beam hardening is an artifact of the scanning process and results from the rapid transition from a high to a low density surface, in this case the boundary between bone or tooth enamel and air. It is most prominent parallel to the direction of the x-ray beam. As such, a specimen should not be oriented in a manner where large flat surfaces lie in a plane parallel to the x-ray beam. Once the orientation that optimized scanning resolution was determined, the orientation of the specimen was further adjusted to minimize beam hardening. Often this would result in a compromise between the desire to maximizing resolution and minimizing beam hardening. With smaller specimens more effort was given to minimizing beam hardening, while for large specimens, the optimization of resolution was given priority. After scanning the first samples of non-human primates it was determined that by mounting the specimens with the teeth facing upwards minimized the effects of beam hardening in the face and all later specimens were scanned with this orientation.

Once the correct angle of orientation was discovered, the dimensions of the mounting base could be determined. The measurements for the base size were the horizontal length of the above square by the width of the cranium at its widest point. The actual size of the base was made 1 to 2 mm smaller than this size in order to keep the crania held securely within the mount. The length or height of the mounting box was then determined. The vertical length of the defined square constituted the distance required for box height. However, to ensure that the skull sat above the manipulator, a one inch thick square of Styrofoam was added to the base, and this was added to the box height.

A hot glue gun was used to join the boxes together, but as the glue is opaque to x-rays and would be visible in the reconstruction no glue was used in any part of the box that would appear within the imaging panel. An additional three inches of length was added to the box height in order to provide surface for gluing the box together, one inch for a buffer and two inches for gluing surface to join the ends of the box. Thus, only the base of the Styrofoam box and the four upper corners were glued together. The lack of glue along the length of the box allowed an unobstructed image to be generated while allowing expansion of the box along the long axis. This enabled the box to be made slightly smaller than the actual dimensions of the crania, and allowed the specimen to be firmly pressed into the box, ensuring a secure mounting.

It is necessary to have as little movement of the specimen during scanning as possible, to ensure that the last image taken matches the first image and there is no displacement of the specimen. Any displacement results in a lower resolution of the scan and a large displacement results in a warning from the imaging software. By mounting the images using the above method, minimal displacement in the specimen was obtained throughout the scanning process.

Curriculum Vitae

Name: Arthur Klages

Post-secondary   University of Western Ontario

Education and   London, Ontario, Canada

Degrees: 2013 M.A. Bioarchaeology

University of Western Ontario

London, Ontario, Canada

2010 B.A. Honours Anthropology

Wilfrid Laurier University

Waterloo, Ontario, Canada

1999 B.A. History

Honours and   Western Graduate Thesis Research Fund (GTRF)

Awards: Western University, London, ON

2013

Queen Elizabeth Scholarship for Science and Technology (QESST)

Province of Ontario

2011

Faculty of Social Science Dean's Scholarship

Western University, London ON

2011

Related Work   Bioarchaeology Lab Manager

Experience: Western University

2013

Teaching Assistant

Western University

2011-2012

Publications:

Klages, Arthur. (2011). A critical analysis of hominin morphology: the partial skeleton of *Ardipithecus ramidus*. Totem: The University of Ontario Journal of Anthropology, Vol 19 (1), article 11.

Klages, Arthur. (2010). Triage: conserving primates and competing interests. Totem: The University of Ontario Journal of Anthropology, Vol 18 (1), article 12.

Klages, Arthur. (2008). *Sahelanthropus tchadensis*: an examination of its hominin affinities and possible phylogenetic placement. Totem: The University of Ontario Journal of Anthropology, Vol 16 (1), article 5.